TRANSACTIONS
AMERICAN GEOPHYSICAL UNION

Volume 30 OCTOBER 1949 Number 5

WILLIAM BOWIE AS AN ISOSTASIST AND AS A MAN

W. Heiskanen

I had the honor to be in intimate correspondence with William Bowie from 1923 until his death in 1940. Because Bowie's letters to me--40 in all--dealing with scientific and other questions of mutual interest will throw clear and pleasant light on Bowie's personality as a scientist and as a man, I shall include some quotations taken from these letters.

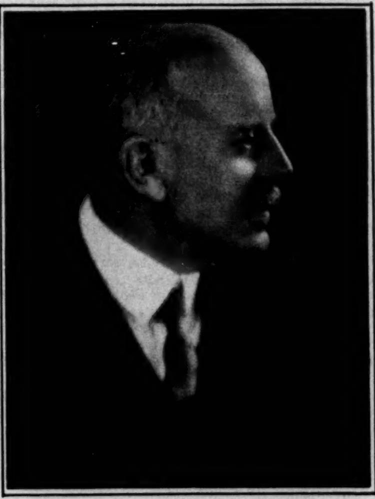

William Bowie, May 6, 1872 - August 28, 1940

It was fortunate for the geodetic science of the United States of America and of the whole world that there were as chiefs of the Division of Geodesy of the United States Coast and Geodetic Survey such far-seeing scientists as J. F. Hayford and later William Bowie. Their scientific interest and high authority resulted in the fact that this large and well-established institution was not content with the practical results of the geodetic operations, such as the computing of the coordinates of the fixed points and the heights of the points of the precise leveling, but it tried also to draw conclusions of a purely scientific character and also to use the time of the staff for such purposes. As a result of this endeavor we have now, for instance, the "International Earth Ellipsoid" of Hayford, the "Bowie reduction" of the gravity anomalies, and the Hayford-Bowie isostatic system.

Still more, without Hayford and Bowie and without the trained staff they had at their disposal, the systematic and exact geodetic study of isostatic problems would hardly have been begun or would at least have been postponed. This study requires large tables, the computing of which is rather laborious, and the topographic-isostatic reduction itself of the gravity values and still more of the deflections of vertical is such a time-consuming job that a staff of several persons is necessary. Especially the computing of tables for the effect of topography in the form which Hayford chose has taken much time. And without these reduction tables and systematic isostatic reduction work, the study of isostasy would be based too much on some geological guesswork.

It was this isostatic work of Hayford and Bowie which brought the study of isostasy from the realm of qualitative guessing into the realm of mathematical computing. F. R. Helmert in Germany, Ilmari Bonsdorff in Finland, and some others, also took this exact mathematical line, but Helmert's staff was more interested in other important porblems, especially in the computing of the European system of the deflection of vertical, so that there was hardly time for detailed isostatic studies, and Bonsdorff had not yet any staff at his disposal.

Nor has there been in British India, the birthplace of the principal isostatic assumptions of Pratt and Airy, any great enthusiasm for isostasy. Rather some geodesists in India have been eager to seek weak points in the isostatic principle.

In this way Hayford, and after him Bowie, has been the founder of modern isostatic study. In the time of Hayford and perhaps still more later, when Bowie was the leading personality in isostasy, there were many pre-eminent men in the world of science who disbelieved in the isostatic principle and fought against it. Therefore it was very good that Bowie, perhaps the strongest defender of isostasy, was so well-known an authority in the United States as well as internationally. His position as president or honorary president of a number of leading American scientific organizations and as President of the International Association of Geodesy (IAG) and later as President of the International Union of Geodesy and Geophysics (IUGG) greatly helped isostatic study to advance, to develop from a dubious hypothesis to a well-established principle.

Bowie had never any doubts on the isostatic principle, and it is evident that anyone who studies gravity anomalies as much as Bowie did, can come to no other conclusion than that the isostatic equilibrium, at least in general, prevails in the Earth's crust. Since isostatic reduction can explain about 90 per cent of the deflections of the vertical and of the observed gravity anomalies of the mountainous regions as Bowie was able to show, the isostatic principle must be a very good one. And the normal gravity, observed in the oceans, in spite of the light water layer about 5000 m depth, made him still more convinced of the reality and importance of isostasy.

Bowie was an enthusiastic supporter of the Pratt-Hayford dough hypothesis. According to this hypothesis, expressed first by Archdeacon Pratt in India in 1855, the mountains have uplifted from the under layer like a fermenting dough, the density of which will become the smaller the higher it rises. In this way the mountains are no mass-addition areas, nor the ocean basins mass-deficient regions, but the mass-plus of the mountain will be compensated by the invisible mass layers of smaller density and the mass-minus of the ocean basins by the underlying mass of larger density. This rather vague assumption of Pratt has been made precise by Hayford in the following way: At a sufficient depth in the Earth's interior the mass unit is under the same pressure, regardless of whether it is under mountain, level land or ocean. This depth has been called the depth of compensation and the first of these levels of equal pressure is the surface of compensation. According to Hayford:

(1) The isostatic compensation is complete, so that each surface unit of this surface of compensation lies under the same pressure.

(2) The compensation is uniform, which means that the compensating density is equal at each depth between the Earth's surface and the surface of compensation.

(3) The compensation is local, that is, the topography, such as a mountain, hill, or valley, will be compensated vertically by masses just beneath the topography.

(4) The compensating layers begin from the physical Earth's surface, not from sea level. On this assumption the depth of compensation reckoned from sea level is under a three-kilometer high mountain higher by three-kilometer, and under a five-kilometer deep ocean five-kilometer deeper than under the level land with the elevation zero.

For this Hayford system, Hayford and Bowie [Spec. Pub. No. 10, U. S. C. and G. S., 1912] have computed reduction tables for the depth of compensation D = 113.7 km. These tables give the effect of the topography and of the isostatic compensation in each of the lettered Hayford zones A to O and the sum of the effects of the topography and of the compensation in the numbered Hayford zones 18 to 1. Later on, [Spec. Pub. No. 17] Bowie computed factors by which the effect, corresponding to the D-value 113.7 km, is to be multiplied in order to get the effect corresponding to the other D-values. These D-values were: 42.6 km, 56.9 km, 60.0 km, 85.3 km. 113.7 km, 127.9 km, 156.25 km, and 184.6 km.

All these tables have been the principal tool of Bowie and of many other isostasists, and they have been used very much. By the aid of these tables it has been possible for instance to determine the most plausible depth of compensation.

A masterpiece of isostatic study is Bowie's book Investigations of gravity and isostasy [Spec. Pub. No. 40, U. S. C. and G. S., 1917]. In this work, Bowie studies the residual isostatic anomalies with accuracy and carefulness which hardly can be surpassed. On the basis of 219 isostatically reduced gravity anomalies of the United States, reduced in his office, and partly on the basis of 42 Canadian, 73 Indian, 40 European, and other stations, he investigated the relation between the isostatic anomalies and the geologic formations and between these anomalies and the areas of erosion and sedimentation. He studied the local compensation versus regional compensation and the dependence of the isostatic anomalies on the height of the stations and on the distance of the ocean coasts. He also derived as good a gravity formula as it was possible to determine from this material.

Especially he spent much time in determining the best-fitting depth of compensation. He realised that the level land stations or the stations of high plateaus can hardly be used for this purpose, for the effect of the isostatic compensation in such regions is nearly independent of the depth of compensation D. Consequently he regarded as the best value for D that obtained by the aid of the high mountains with rough topography. This view has been, I believe, adopted by all isostasists.

In this way Bowie obtained for the depth of compensation the value 95 km as compared with the value 97 km obtained by Hayford from the deflections of the vertical. He regarded the mean of these values, 96 km, as the most plausible value. That this value for the depth of compensation has not been used very much in practical reduction work is due to the fact that all the reduction tables were computed for the value 113.7 km, and to the circumstance that the floating hypothesis of Airy has had more and more defenders.

Later [Spec. Pub. No. 99, p. 13] Bowie explained the idea of the Hayford-Bowie isostatic assumption by the aid of a figure, which is republished here (see Fig. 1) and which presents the matter so clearly that it hardly leaves anything more to hope. It shows that the higher a prism rises in a vessel partly filled with mercury, the smaller is its density. The lower surfaces of the prisms define the depth of compensation. If the mountains have been caused by vertical movements of the crustal material, the manner of their formation must have been similar.

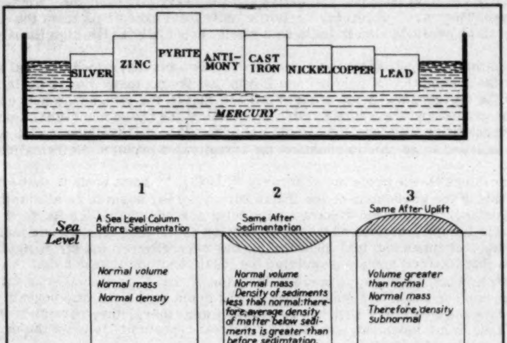
PYRITE
ZINC
ANTI-MONY
CAST IRON
SILVER
NICKEL
COPPER
LEAD
MERCURY
1
2
3
Same After Uplift
Sea Level
A Sea Level Column Before Sedimentation
Same After Sedimentation
Normal volume
Normal mass
Normal density
Normal volume
Normal mass
Density of sediments less than normal: therefore, average density of matter below sediments is greater than before sedimtation.
Volume greater than normal
Normal mass
Therefore, density subnormal
Depth of

Fig. 1--Bowie illustration of isostasy

Bowie realized that the topographic isostatic reduction of gravity, in which the topographic masses will be thought of as transferred from the continents to the layers below the sea level and the mass deficiency of the oceans will be filled by masses taken from the Earth's crust under the ocean bottom, will therefore change the geoid surface downward under the continents, and upward under the oceans. Because of this change of the geoid the gravity anomalies must also change, so that they must be reduced from the actual geoid to the altered one. This correction, or indirect effect will be called the Bowie correction. In Bowie's office, Walter D. Lambert and F. W. Darling have calculated tables for computing this Bowie reduction [Spec. Pub. No. 199].

Bowie, in his investigations and in his papers, fought strongly for isostasy. Some American scientists, for instance, thought that because in the neighborhood of Seattle the isostatic residual anomaly is as large as -93 mgal, isostatic equilibrium could not prevail. Bowie answered that Seattle lies in a level plain, where the effect of isostatic reduction is very small, and that there is a local thick, light-sediment mantle, which is the cause of this local anomaly. As the Coast and Geodetic Survey later made new gravity measurements in the neighborhood of Seattle, it became evident that there is, in fact, only a very small region with large negative gravity anomaly. About 30 km west of Seattle the gravity anomaly was only -25 mgal, about 40 km south of Seattle -12 mgal, and 40 km north of Seattle, +2 mgal. Bowie's view was therefore right.

It was also said that in the West Indies isostatic equilibrium does not prevail, because at many stations there the isostatic gravity anomalies are remarkable, whether positive or negative. Then in in 1935 Bowie published in *Bulletin* of the Geological Society of America a paper entitled Significance of gravity anomalies at stations in the West Indies. This is a very clear document, in which he indisputably showed that even in the West Indies, very active tectonically, the isostatic principle prevails on broad lines. He divided the West Indies region into 15 squares of about 200,000 sq km, about 4° by 4°, and determined the mean isostatic and Bouguer gravity anomalies for each square. The resul was certainly surprising to all anti-isostasists. The mean isostatic anomalies of these 15 areas wer between +41 and -47 mgal, but the mean of the corresponding Bouguer anomalies were from +24 to +395 mgal. The mean anomaly of the whole of this region, for isostatic compensation, was only + two mgal, but without isostatic equilibrium it was +171 mgal. The conclusion, in Bowie's own words, was, "It is believed that this analysis of the gravity data now available in the West Indies region justifies the conclusion that the area as a whole, involving approximately one million square miles of the Earth's surface, is underlaid by crustal material that is very closely in isostatic equilibrium."

In a similar way he replied to some Indian geodesists, who were of the opinion that, because in the Ganges Plain isostatic anomalies are remarkable negative and south of this Plain strongly positive, isostasy does not exist in India. Bowie said that the light-sediment layers of the Ganges Plain cause the negative residual isostatic anomalies and the heavy layers of the "Hidden Range" region the positive ones. They are, according to Bowie, only local exceptions from the isostatic equilibriu which on broad lines prevails also in India as a whole, especially in the high Himalayan mountain.

Many scientists--among them also some geodesists--misunderstood the real meaning of isostas and especially the assumption of Hayford and Bowie that the compensation is quite local and perfectl vertical below the topography. Some of them laughed that if, for instance, a new house has been buil somewhere, the ground and the whole Earth's crust below the house must sink, because--according t Bowie--the compensation was local. They did not understand that the assumption of a local isostasy was used only in order to be able to consider the complicated problem mathematically.

About these things Bowie wrote me [February 9, 1933], "I must confess that I do not quite understand the attitude of the geodesists of the Indian Survey. They seem to be attempting, in every way, to discredit isostasy. They seem to have a particular animus against the Hayford isostasy; that is, the one that calls for the locations of the compensation under each topographic feature. I have written them a number of times and told them that no one subscribes to the strict Hayford idea. I have informed them that Hayford merely postulated the ideal condition in order that the computations mig be readily made and that Hayford, in some of his papers, and I, in a number of mine, had indicated clearly that the compensation of a small ridge or hill could not be directly beneath the feature. In spite of all of this and in spite of writings by yourself and others, they persist in the attack on the H ford isostasy and, in my judgment, are missing a great opportunity to show the degree to which isostasy really exists in India."

On April 14, 1933 he wrote, "I agree with you that . . . . seems to have wrong conception about isostasy but I predict that, if he continues his investigations on this subject, he will become a very good isostasist before long. Nearly every one who started out to fight the idea has eventually become one of its strongest advocates."

As these quotations in themselves show, Bowie was strong in his criticism but at the same time positively constructive.

On the other hand every success of isostasy made him deeply glad. So he wrote on August 4, 1933, "I may say that isostasy seems to be gaining popularity in my country and a number of geologists are now interested in the gravity anomalies and their relation to geological structure."

In many letters we discussed whether the isostasy of Hayford was nearer to the truth, as Bowie thought, or that of Airy, which I began to use in 1924 in explaining gravity anomalies, and which I preferred.

Bowie did not want to admit that the principal cause of mountain building could be a horizontal movement, the assumption of Airy. He definitely was of the opinion that mountains must have been built by vertical movements produced by thermal, physical, and chemical forces. As the material in a place, where there is now a mountain, has extended, its density has become smaller and the smaller the density, the higher the mountain.

As Bowie's letters throw light on his view I shall set forth some quotations here. On March 17th 1927, he wrote, "You have made a real contribution to isostatic literature by setting forth the merits of the Airy hypothesis. I am thoroughly convinced that isostasy is true but I must say that I am still in the dark as to whether the character of isostasy is that of Airy or of Pratt. Neither, as far as I know, can be proved. I have tried to analyze the two types, as far as practicable, and it appears to me that there are mechanical difficulties in the Airy hypothesis that make it seem most improbable. At the same time, there is the difficulty in the Pratt hypothesis of having changes of density due to some phyiscal or chemical action aside from normal thermal expansion and contraction and this seems to be most improbable. Briefly, we have improbable phases of both the Pratt and the Airy ideas of isostasy but I am inclined to think that the objections to the Pratt theory are not so insurmountable as those in the Airy hypothesis. It will probably be many years before there is any unanimity of opinion as to which of the isostatic ideas is the better. In the meantime, it is well to make all of the tests that we can and to try to throw some light on this very important matter. A tremendous step forward in geophysical science was taken when isostasy was proved. Now we shall try to find out more about this very important subject."

October 27, 1927, he claimed among other things, "I am strongly of the opinion that the irregular surface (of the Earth) is due to the heterogeneous densities rather than that the latter are due to the irregular surface. The varying densities are the causes and the irregularities in the surface are the effects."

Bowie defended the Hayford system also in his many papers, as in his presidential address The part played by isostasy in geophysics and geology [J. Wash. Acad. Sci., v. 17, no. 5, 1927]. After a long discussion he comes to the following conclusion [p. 115], "It is my belief that as much evidence, probably more, could be collected in the field in favor of the vertical-uplift theory as may be obtained in support of the view that the horizontal movement is the predominating one."

On April 11, 1930, he stated in his letter, "There are many small problems connected with isostasy that are still outstanding. One is to discover whether the solid crust, in which compensation can occur, extends to a fairly uniform depth or whether it has great variations in depth--in other words, whether we have the Pratt or the Airy conception of isostasy.

"I have worked on this problem to some extent and am rather convinced from my studies that we cannot have large masses of crustal material extending far down into subcrustal space. I believe that the temperature below the crust is such that, if any crustal matter enters that region, it will become heated and take on the characteristics of subcrustal material. In other words, I believe that temperature and pressure conditions limit the depth to which the crustal material can extend downward."

As these quotations show, we both were strongly in favor of the isostatic principle, but we could not agree on the mode of isostatic compensation. Bowie was quite convinced that the Hayford assumption was better in accord with the physical and chemical conditions of the Earth's crust, while I held my course as a defender of the Airy floating theory.

His attitude towards me clearly shows the greatness of Bowie as a man. Although a great part of my scientific work was intended to seek new evidence for the Airy theory, and was in a way against Bowie's assumption, he used his whole great influence in America and in the IAG to facilitate my work. In 1930 he proposed me as his successor as Reporter on Isostasy to the IAG, a job which involves writing a general report for every Assembly of the Association on the advances of isostatic study in various countries since the former Assembly. And as the IAG at its Assembly in Edinburgh in 1936 established an Isostatic Reduction office, which later, under the name of the Isostatic Institute of IAG, has worked at Helsinki, Bowie tried to promote its work as much as possible.

He encouraged me at the end of 1938 to write an application to the Rockefeller Foundation for an annual grant-in-aid, and he himself recommended me to the Foundation very strongly. As this application was not approved, he sent recommendations to the Executive Officer of the American Philosophical Society, to the Head of the Carnegie Corporation, and to the Chairman of the Division of

Geology and Geography of the American National Research Council. It was no fault of Bowie's that these recommendations, perhaps because of the War, brought no positive result. Characteristic of Bowie's gentlemanly nature is the closing of his letter of April 26, 1939, in which he told about his efforts: "Whether anything will come, no one can say, but in any event it gives me great pleasure to continue the effort to secure support for your fine office." When, after the war, in 1946, the Isostatic Institute received a grant for a year, from the Rockefeller Foundation, Bowie could no more rejoice with me on account of this.

Bowie's attitude toward the scientific collaborators of his own office is to be seen best in W. D. Lambert's address, read at the festival in honor of Bowie on his retirement from the Coast and Geodetic Survey held on January 4, 1937. Lambert said, among other things, "In the so-called good old times it was the general practice to attribute all the work done by an outfit to the head man and to publish everything in his name. This practice may still prevail here and there in the Government service but not in the Division of Geodesy. Major Bowie has been too wise and too generous for that. Too wise, for he well knew that the public interested in the work of this Survey were too shrewd to swallow the fiction of official omniscience concentrated in a single person . . . Major Bowie was also too generous for he believes in giving every man credit for his own accomplishments and has gone out of his way to see that credit was given where credit was due. It is his philosophy that more reputation is to be gained by being known as the head of an organization composed of men capable of achievement each in his own right than by appropriating to himself--if that were possible--that product of other men's efforts and brains. By putting this philosophy into practice, he himself has gained, those under him have gained, and the Survey has gained."

What has been said above has shown that Bowie was not only a private scientist studying isostasy but also an international promoter, who forwarded the isostatic study of other countries through wide correspondence as well as through his activity in the IAG and as director of his office. He, for instance, understood sooner than other scientists in America the high importance of the gravity measurements undertaken at sea by Vening Meinesz, and he was one of the first in planning the American gravity expeditions at sea for measuring the gravity in the tectonically interesting West Indies. He encouraged the officials of his institution in Washington to carry out in their own time the isostatic reduction of gravity anomalies of other countries; for example, of Spain and Holland and of gravity anomalies at sea.

In his international activity Bowie was far seeing. When he was president of the IAG, there was much political difficulty resulting from World War I. The representatives of many nations were of the opinion that all countries should have the right to adhere to the Union, but some were strongly of the opposite opinion. Bowie did his best to try at least to have invitations sent to scientific men of non-adhering countries, but it was ruled that invitations would be sent only to those scientists who made a personal request for such an invitation. This rule meant, in fact, that nobody would come from the Central Powers, because no one likes to invite himself to a social or official meeting. If one wants to go to such a place, one usually appeals to some friend who will arrange the necessary invitation.

On this subject Bowie wrote on July 7, 1930, about two months before the Stockholm Assembly, "I have made several requests upon Professor Lallemand, President of our Union, to send official invitations to certain scientific men in non-adhering countries who have expressed their willingness to attend the Stockholm meeting but, up to the present time, Professor Lallemand has insisted that no invitations will be sent until he receives personal requests for them from the individual scientific men.

"This is a matter of so much importance that I am writing to you and to several friends in other countries, suggesting that you or the proper authority in your country in scientific matters write to Professor Lallemand and express the view that it would be to the best interests of scientific co-operation if every effort were made on our part to have invitations sent to the scientific men in non-adhering countries and not to let technicalities interfere with so doing. If several such letters are sent to Professor Lallemand, I think that within a very short time he will be able to send out the invitation in question."

Lambert claimed in his address, mentioned earlier, "This Postwar organization (IUGG) had its share of Postwar troubles and as President of IAG in 1919 until 1933, and then as President of the entire Union from 1933 through the Edinburgh meeting of 1936, Major Bowie had abundant opportunity to display his diplomatic talents in reconciling conflicting views, his cheerfulness in the face of obstacles, and at times his firmness." I think that every one who attended the meetings of the Union in Prague, Stockholm, Lisbon, Edinburgh, and Washington, is willing to confirm this statement of Lambert.

As Bowie's reaction to the efforts of his friends to have him elected the President of the entire Union is characteristic of his generous and noble nature, I shall take a quotation. On December 16, 1932, he wrote, among other things, "I have heard my name mentioned frequently in connection with the presidency of the Union but I shall not, in any way, seek the office and would accept it only if no one else can be found and then only on condition that my selection should be unanimous. If there should be any opposition whatever I shall not be willing to have my name considered . . . . As stated above, I am hoping that some one in Europe will be the next president and I certainly shall not give authority to any one to start a campaign in my favor. I do appreciate very deeply the sentiments expressed by you and by others regarding my possible election as President of the Union. I feel that I have very many friends among the geodesists and also geophysicists of the world and any expression of friendship on their part pleases me very much but that does not mean that I should want to be the President of the Union unless it is absolutely necessary to insure harmonious conditions in the affairs of the Union."

In connection with the General Assembly of IUGG during September 1939, I had the privilege with some other geodesists and geophysicists to be the guest of Dr. and Mrs. Bowie in their home. As scientists we were keen to talk of scientific problems. Bowie proposed, that I should derive a new gravity formula by the aid of the level land stations only. The purpose of his proposition was evident. Using only level land stations, far from mountains, oceans, and tectonically active regions we can expect to get a formula of "normal gravity," as free as possible from the influence of various disturbing layers.

I am glad to be able to announce that this hope and testament of Bowie was fulfilled seven years later. My assistant, E. Niskanen, published as No. 16 of the Publications of the Isostatic Institute of IAG a paper entitled Gravity formula derived by the aid of the level land stations.

The Finnish Geographical Society elected Bowie unanimously as its honorary member in the fall of 1939, but unfortunately the War began some days after the election, and because of slowness of the post, Bowie did not receive the Diploma of this honorary membership before his death.

I am very happy to have had the opportunity in these lines to honor William Bowie, an eminent and enthusiastic scientist, the leading personality of the isostatic study for two decades, a distinguished international promoter of science, a generous, warm-hearted and noble man. Men like Bowie are, in a small country, an irreplaceable treasure, but even in a world-power he was a personality, the like of whom is not often born.

Isostatic Institute,
Helsinki, Finland

(Communicated manuscript received March 10, 1949;
open for formal discussion until March 1, 1950)

Transactions, American Geophysical Union Volume 30, Number 5 October 1949

ON HYDRODYNAMIC EARTHQUAKE EFFECTS

P. Wilh. Werner and K. J. Sundquist

Abstract--This study deals with the hydrodynamic effect of horizontal earthquake action. The theory is developed assuming harmonic motion, also taking the compressibility of the water into consideration. The possibility of resonance is discussed. Solutions are deduced for the most common types of hydraulic vessels. The solutions contain expressions both for the dynami water pressure and for the displacements in the fluid. The dynamic water pressure on the walls is calculated, and the result presented in diagrams.

Introduction

Both from a geophysical and from an engineering point of view it is of value to know the hydrodynamic earthquake effects in basins with free water surface. It is of special importance to find the corresponding dynamic water pressure on the walls of the basin (such as sea shores, dams, tanks, and lighthouse towers).

Although, apparently, with no reference to earthquake action, the vibration of water vessels attracted the attention of scientists at least as early as in the middle of the Nineteenth Century. In a paper entitled On Waves, RAYLEIGH [1876] investigated, on the basis of the theory of velocity potentials, the waves occurring in certain enclosed water bodies due to vibrations. RAYLEIGH in his paper also referred to some practical tests, which showed an excellent agreement with the general theory. With special reference to Earth shocks WESTERGAARD [1933] has treated the two-dimensional case of frontal horizontal vibrations of a straight rigid dam with vertical upstream face placed at one end of an infinitely long reservoir of uniform depth. In a discussion of Westergaard's paper, BRAHTZ and HEILBRON [1933] have indicated, in principle, a solution pertaining to a reservoir of finite length.

(After the completion of the present paper, the writers' attention has been called to some very interesting tests executed by HOSKINS and JACOBSEN [1934], which show a satisfactory verification of the theory. Moreover, JACOBSEN [1949] has placed at our disposal a theoretical investigation, pertaining to the impulsive hydrodynamics of an imcompressible fluid inside a cylindrical tank and outside a cylindrical pier, thus corresponding to the Cases 6 and 7 treated below.)

In the following the problem of horizontal earthquake action will be treated on the basis of the general differential equation for the dynamic pressure, and solutions will be given for some importan cases, both two- and three-dimensional. Some of the solutions involve the use of Bessel functions [WATSON, 1944] and spherical surface-harmonics [FRANK and v. MISES, 1930], which however may be rather conveniently evaluated by means of available tables. In the case that the compressibility of the water can be neglected, the two-dimensional flow will be investigated also by means of a graphical procedure, valid for any arbitrary section.

Following the procedure of WESTERGAARD [1933] it is assumed that the earthquake manifests itself as a harmonic motion, and that the walls of the basin are rigid and, except where otherwise expressly stated, move as a whole with the ground. For the purpose of the investigation and using the terminology given in Appendix this movement may be given by the expression

$$\epsilon_o = -(\alpha g T^2/4\pi^2)(\cos 2\pi t/T) \qquad (1)$$

The water is considered as an ideal fluid, and the problem is closely related to the theory of sound [RAYLEIGH, 1926]. Under the assumption that the displacements in the water body are small, the general Eulerian equations [LAMB, 1932] may be simplified as follows; namely, in rectangular coordinates

$$\left.\begin{aligned} \frac{\partial \sigma}{\partial x} &= \frac{\gamma}{g} \cdot \frac{\partial^2 \xi}{\partial t^2} \\ \frac{\partial \sigma}{\partial y} &= \frac{\gamma}{g} \cdot \frac{\partial^2 \eta}{\partial t^2} \\ \frac{\partial \sigma}{\partial z} &= \frac{\gamma}{g} \cdot \frac{\partial^2 \zeta}{\partial t^2} \end{aligned}\right\} \tag{2}$$

with the condition of continuity for a compressible fluid in simple harmonic motion,

$$\frac{\partial \xi}{\partial x} + \frac{\partial \eta}{\partial y} + \frac{\partial \zeta}{\partial z} = \frac{\sigma}{E} \tag{3}$$

In polar-cylindrical coordinates the corresponding equations are

$$\left.\begin{aligned} \frac{\partial \sigma}{\partial r} &= \frac{\gamma}{g} \cdot \frac{\partial^2 \rho}{\partial t^2} \\ \frac{1}{r} \frac{\partial \sigma}{\partial \varphi} &= \frac{\gamma}{g} \cdot r \cdot \frac{\partial^2 \theta}{\partial t^2} \\ \frac{\partial \sigma}{\partial z} &= \frac{\gamma}{g} \cdot \frac{\partial^2 \zeta}{\partial t^2} \end{aligned}\right\} \tag{4}$$

with the condition of continuity

$$\frac{1}{r} \cdot \frac{\partial (\rho \cdot r)}{\partial r} + \frac{\partial \theta}{\partial \varphi} + \frac{\partial \zeta}{\partial z} = \frac{\sigma}{E} \tag{5}$$

In spherical coordinates the equations read

$$\left.\begin{aligned} \frac{\partial \sigma}{\partial r} &= \frac{\gamma}{g} \cdot \frac{\partial^2 \rho}{\partial t^2} \\ \frac{1}{r} \cdot \frac{\partial \sigma}{\partial \varphi} &= \frac{\gamma}{g} \cdot r \cdot \sin^2 \phi \cdot \frac{\partial^2 \theta}{\partial t^2} \\ \frac{1}{r} \cdot \frac{\partial \sigma}{\partial \phi} &= \frac{\gamma}{g} \cdot r \cdot \frac{\partial^2 \omega}{\partial t^2} \end{aligned}\right\} \tag{6}$$

with the condition of continuity

$$\frac{1}{r^2} \cdot \frac{\partial (\rho r^2)}{\partial r} + \frac{\partial \theta}{\partial \varphi} + \frac{1}{\sin \phi} \cdot \frac{\partial (\omega \sin \phi)}{\partial \Psi} = \frac{\sigma}{E} \tag{7}$$

Differential equations

Using the expression

$$k = \sqrt{gE/\gamma} \tag{8}$$

and (2) and (3), we obtain, after some transformations, the following general differential equation for the pressure ; namely, for three-dimensional flow,

$$\frac{\partial^2\sigma}{\partial x^2}+\frac{\partial^2\sigma}{\partial y^2}+\frac{\partial^2\sigma}{\partial z^2}=\frac{1}{k^2}\cdot\frac{\partial^2\sigma}{\partial t^2} \quad \ldots\ldots\ldots\ldots\ldots\ldots (9)$$

and for two-dimensional flow

$$\frac{\partial^2\sigma}{\partial x^2}+\frac{\partial^2\sigma}{\partial y^2}=\frac{1}{k^2}\cdot\frac{\partial^2\sigma}{\partial t^2} \quad \ldots\ldots\ldots\ldots\ldots\ldots (10)$$

The corresponding equations in polar-cylindrical coordinates are obtained by applying (4) and (8). They read, for three-dimensional flow

$$\frac{\partial^2\sigma}{\partial r^2}+\frac{1}{r}\cdot\frac{\partial\sigma}{\partial r}+\frac{1}{r^2}\cdot\frac{\partial^2\sigma}{\partial\varphi^2}+\frac{\partial^2\sigma}{\partial z^2}=\frac{1}{k^2}\cdot\frac{\partial^2\sigma}{\partial t^2} \quad \ldots\ldots\ldots\ldots (11)$$

and for two-dimensional flow

$$\frac{\partial^2\sigma}{\partial r^2}+\frac{1}{r}\cdot\frac{\partial\sigma}{\partial r}+\frac{1}{r^2}\cdot\frac{\partial^2\sigma}{\partial\varphi^2}=\frac{1}{k^2}\cdot\frac{\partial^2\sigma}{\partial t^2} \quad \ldots\ldots\ldots\ldots\ldots (12)$$

In spherical coordinates the differential equation reads

$$\frac{\partial}{\partial r}\left(r^2\cdot\frac{\partial\sigma}{\partial r}\right)+\frac{1}{\sin^2\phi}\cdot\frac{\partial^2\sigma}{\partial\varphi^2}+\frac{1}{\sin\phi}\cdot\frac{\partial}{\partial\phi}\left(\sin\phi\cdot\frac{\partial\sigma}{\partial\phi}\right)=\frac{r^2}{k^2}\cdot\frac{\partial^2\sigma}{\partial t^2} \quad \ldots\ldots\ldots\ldots (13)$$

The problem is now to find the solution of the differential equation which at the same time satisfies given boundary conditions. The solutions given in the following presume an enforced (earthquake) motion according to (1). Concerning the boundary conditions the following general considerations are worth noting.

As the displacements are small, the dynamic water pressure at the undisturbed surface may be assumed to be zero.

Referring, for instance, to the two-dimensional case in Figure 1, the displacement of the fluid at the wall of the vessel may be written as follows.

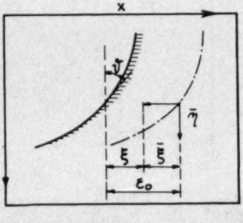

Fig. 1--Displacement of fluid relative to wall, two-dimensional case

$$\xi=\epsilon_0-\bar{\xi} \quad \ldots\ldots\ldots\ldots\ldots (14)$$

$$\eta=\bar{\eta} \quad \ldots\ldots\ldots\ldots\ldots\ldots (15)$$

in which the top indices refer to the movement of the fluid relative to the wall. As the wall is a streamline of this relative motion, the displacement component perpendicular to the wall is zero, resulting in the following equation

$$\xi+\eta\tan\vartheta=\epsilon_0 \quad \ldots\ldots\ldots\ldots (16)$$

in which ϑ denotes the angle between the vertical and the tangent to the wall at the point in question as shown in Figure 1.

As already mentioned, the theory presumes that the displacements in the water body are small. This also holds true for the solutions obtained in the following, except at certain singular points. It may be shown that this singularity does not impair the validity of the results, because the large values of the displacement extend only over an infinitesimal area.

From a physical point of view the resonance, that is, the condition when the frequency of the earthquake coincides with that of the free vibration of the water body, is of great interest. When resonance occurs, the pressure and the displacement at the free water surface becomes theoretically infinite. As WESTERGAARD [1933] has shown, resonance in an infinitely long reservoir cannot occur if the depth is less than kT/4.

Analytical solutions

Case 1: Two-dimensional flow in a basin with square section, the whole section moving in phase in the direction of the x-axis (see Figure 2)--The flow is independent of z, and thus differential (10) applies. The boundary conditions are as follows.

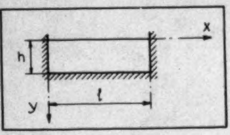

Fig. 2--The elements of Case 1

$$\sigma \Big|_{y=0} = 0 \quad \ldots\ldots\ldots\ldots\ldots (17)$$

$$\xi \Big|_{x=0} = \xi \Big|_{x=l} = \epsilon_0 \quad \ldots (18) \text{ and } (19)$$

$$\eta \Big|_{y=h} = 0 \quad \ldots\ldots\ldots\ldots\ldots (20)$$

Using the series expansion

$$\frac{\pi}{4} = \sum_{0}^{\infty} \frac{1}{2n+1} \cdot \sin(2n+1)\frac{\pi y}{2h} \quad \ldots\ldots\ldots\ldots\ldots (21)$$

it is easily verified that the differential equation and the boundary conditions are satisfied by the following expressions, namely,

$$\sigma = +\frac{8h}{\pi^2}\, \alpha\, \gamma \cos\frac{2\pi t}{T} \sum_{0}^{\infty} \frac{1}{\lambda(2n+1)^2} \cdot \frac{\cosh \varkappa x - \cosh \varkappa(l-x)}{\sinh \varkappa l} \cdot \sin(2n+1)\frac{\pi y}{2h} \quad \ldots\ldots\ldots (22)$$

$$\xi = -\frac{\alpha\, g\, T^2}{\pi^3} \cdot \cos\frac{2\pi t}{T} \sum_{0}^{\infty} \frac{1}{(2n+1)} \cdot \frac{\sinh \varkappa x + \sinh \varkappa(l-x)}{\sinh \varkappa l} \cdot \sin(2n+1)\frac{\pi y}{2h} \quad \ldots\ldots\ldots (23)$$

$$\eta = -\frac{\alpha\, g\, T^2}{\pi^3} \cdot \cos\frac{2\pi t}{T} \sum_{0}^{\infty} \frac{1}{\lambda(2n+1)} \cdot \frac{\cosh \varkappa x - \cosh \varkappa(l-x)}{\sinh \varkappa l} \cdot \cos(2n+1)\frac{\pi y}{2h} \quad \ldots\ldots\ldots (24)$$

in which

$$\varkappa = \lambda\,(2n+1)\,\frac{\pi}{2h} \quad \ldots\ldots\ldots\ldots\ldots (25)$$

and

$$\lambda = \sqrt{1 - \left(\frac{4h}{(2n+1)kT}\right)^2} \quad \ldots\ldots\ldots\ldots\ldots (26)$$

The stability of the flow depends on the value of the denominator $\sinh \varkappa l$, and two cases may be distinguished, according as the parameter λ is real or imaginary. If λ is real, implying that $h < kT/4$, the flow is stable under all conditions. If, on the other hand, λ be imaginary, the denominator becomes zero for certain values of $\varkappa$. Resonance then occurs, resulting in infinite values of σ and η. The roots of the equation

$$\sinh \varkappa \ell = 0 \qquad (27)$$

are

$$\varkappa \ell = \mu \pi i \qquad (28)$$

in which μ is an integer. Introducing this expression in (26), we obtain

$$\left(\frac{4h}{kT}\right)^2 - \left(\frac{2\mu h}{l}\right)^2 = (2n+1)^2 \qquad (29)$$

hence the value of h at which resonance, with n = 0, occurs

$$h = \frac{kT}{4} \cdot \frac{1}{\sqrt{1-\left(\frac{\mu k T}{2l}\right)^2}} \qquad (30)$$

It is seen that the occurrence of resonance is dependent on the length of the reservoir, inasmuch as resonance cannot occur unless

$$\ell > \mu \cdot kT/2 \qquad (31)$$

whereby it is to be noted that the gravest (lowest) value of μ for which σ (and η) becomes infinite is $\mu = 1$. For $\ell = \infty$, (30) gives h = kT/4, that is, the same value as derived by WESTERGAARD [1933] in the limiting case of an infinitely long reservoir.

The dynamical water pressure in the basin may be calculated from (22). The resultant pressure on the end walls is obtained by integrating from y = 0 to y = h, which gives

$$R = \pm \frac{16h}{\pi^3} \alpha \gamma \cos\frac{2\pi t}{T} \sum_0^\infty \frac{1}{\lambda(2n+1)^3} \cdot \tanh\frac{\varkappa l}{2} \qquad (32)$$

Equations (22) and (32) have been evaluated in Figures 3 and 4, respectively, for different ratios between length and depth of the reservoir. In order to show the influence of the compressibility of the

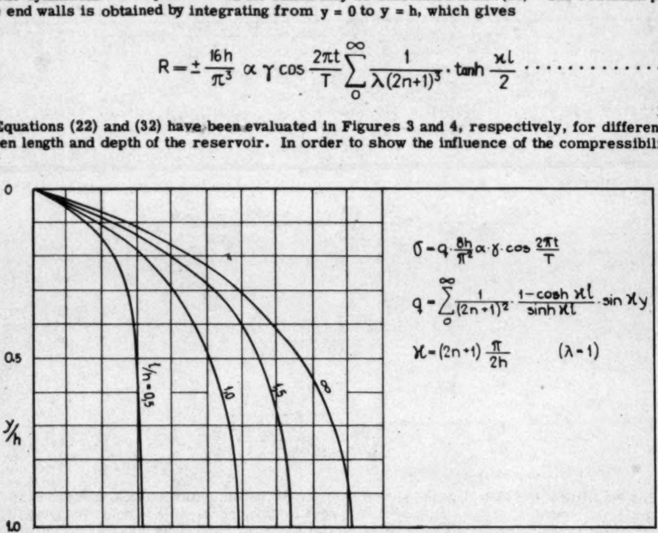

Fig. 3--Evaluation of Eq. (22)

water, (32) has been evaluated for different values of λ while (22) has been evaluated only for $\lambda = 1$.

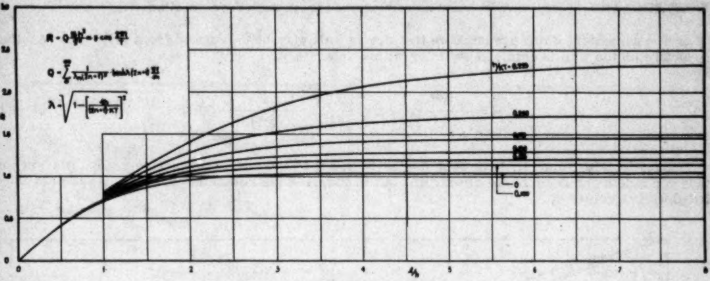

Fig. 4--Evaluation of Eq. (32)

Case 2: Two-dimensional flow in a basin with square section, one end wall moving and the other still (see Fig. 5)--The problem is the same as under Case 1, except that the end wall $x = \ell$ is stationary, the boundary conditions thus being

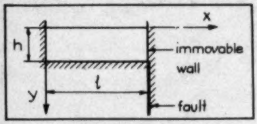

Fig. 5--The elements of Case 2

$$\sigma \Big|_{y = 0} = 0 \qquad (33)$$

$$\xi \Big|_{x = 0} = \epsilon_0 \qquad (34)$$

$$\xi \Big|_{x = \ell} = 0 \qquad (35)$$

$$\eta \Big|_{y = h} = 0 \qquad (36)$$

The solution is

$$\sigma = -\frac{8h}{\pi^2}\,\alpha\,\gamma\,\cos\frac{2\pi t}{T}\sum_{0}^{\infty}\frac{1}{\lambda(2n+1)^2}\cdot\frac{\cosh\varkappa(l-x)}{\sinh\varkappa l}\cdot\sin(2n+1)\frac{\pi y}{2h} \qquad (37)$$

$$\xi = -\frac{\alpha\,g\,T^2}{\pi^3}\cdot\cos\frac{2\pi t}{T}\sum_{0}^{\infty}\frac{1}{(2n+1)}\cdot\frac{\sinh\varkappa(l-x)}{\sinh\varkappa l}\cdot\sin(2n+1)\frac{\pi y}{2h} \qquad (38)$$

$$\eta = +\frac{\alpha\,g\,T^2}{\pi^3}\cdot\cos\frac{2\pi t}{T}\sum_{0}^{\infty}\frac{1}{\lambda(2n+1)}\cdot\frac{\cosh\varkappa(l-x)}{\sinh\varkappa l}\cdot\cos(2n+1)\frac{\pi y}{2h} \qquad (39)$$

in which $\varkappa$ and λ are as given in (25) and (26), respectively. As in the preceeding case the flow is stable under all conditions if λ is real, and resonance, with $n = 0$, occurs for values of h according to (30).

The lowest value of μ to be taken into consideration in this case, however, is zero, thus, according to (31),

$$\ell > 0 \qquad (40)$$

implying that, for the gravest value of μ, the occurrence of resonance in this case is independent of the length of the reservoir. It may be noted in this connection, that the limiting case treated by WESTERGAARD [1933] may be conveniently derived from the above solution.

The dynamical water pressure on the moving wall may be calculated from (37). The resultant pressure on the wall is obtained by integrating, thus,

$$R = -\frac{16h^2}{\pi^3}\,\alpha\,\gamma\cos\frac{2\pi t}{T}\sum_{0}^{\infty}\frac{1}{\lambda(2n+1)^3}\cdot\coth\varkappa l \quad \ldots\ldots\ldots\ldots\ldots (41)$$

Equations (37) and (41) have been evaluated in Figures 6 and 7, respectively, for different ratios between length and depth of the reservoir. As in Figure 4 the resultant pressure has been evaluated for different values of λ.

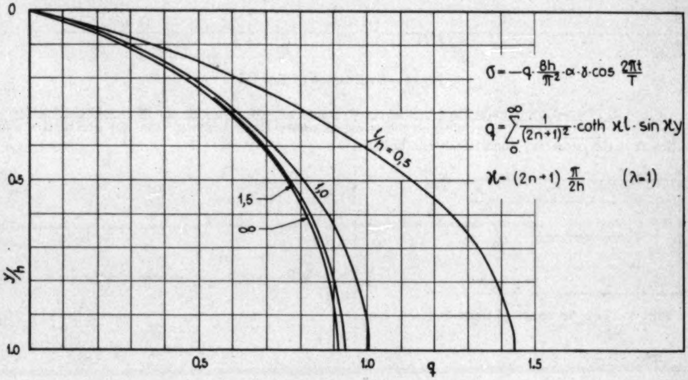

Fig. 6--Evaluation of Eq. (37)

It may be gathered from Figures 4 and 7 that in most practical cases the compressibility of the water may be neglected in calculating the dynamic water pressure. In the cases treated in the following, therefore, the numerical calculations will be carried through only for $\lambda = 1$, corresponding to $k = \infty$.

It is worth noticing that the Cases 1 and 2 may be used also for calculating the dynamic water pressure on dams in a square canyon when the earthquake action is in a direction transverse to the canyon, that is, in the longitudinal direction of the dam axis. For certain parts of the dam Case 2 will then give considerably higher pressures than those obtained in the case treated by WESTERGAARD [1933].

In view of the fact that T, barring exceptional cases, may be taken not less [GEIGER and SCHEEL, 1928], that is, $kT/4 \approx 350$ m, it is seen that resonance need not be feared in basins of ordinary depth, and especially not in artificial hydraulic vessels. It is likewise evident, however, that resonance may be expected along ocean shores with great water depths, and this may at least to some extent explain the heavy flood waves observed during earthquakes in Japan and elsewhere. Case 2 shows that this effect is most pronounced where marked faults in the Earth's crust run along the shores.

Case 3: Three-dimensional flow in a basin with semi-circular section vibrating in the direction of the generating axis (see Fig. 8)--A practical aspect of this problem is obtained for instance, when it is of interest to consider, in principle, the effect of sloping side walls in a canyon.

As the flow is three-dimensional, (11) applies (the z-coordinate being in this case substituted by x). The boundary conditions are as follows.

$$\sigma\Big|_{\varphi=0} = \sigma\Big|_{\varphi=\pi} = 0 \; \ldots\ldots\ldots\ldots\ldots\ldots \quad (42) \text{ and } (43)$$

$$\rho\Big|_{r=r_0} = 0 \; \ldots\ldots\ldots\ldots\ldots\ldots \quad (44)$$

$$\xi\Big|_{x=0} = \xi\Big|_{x=\ell} = \epsilon_0 \; \ldots\ldots\ldots\ldots\ldots\ldots \quad (45) \text{ and } (46)$$

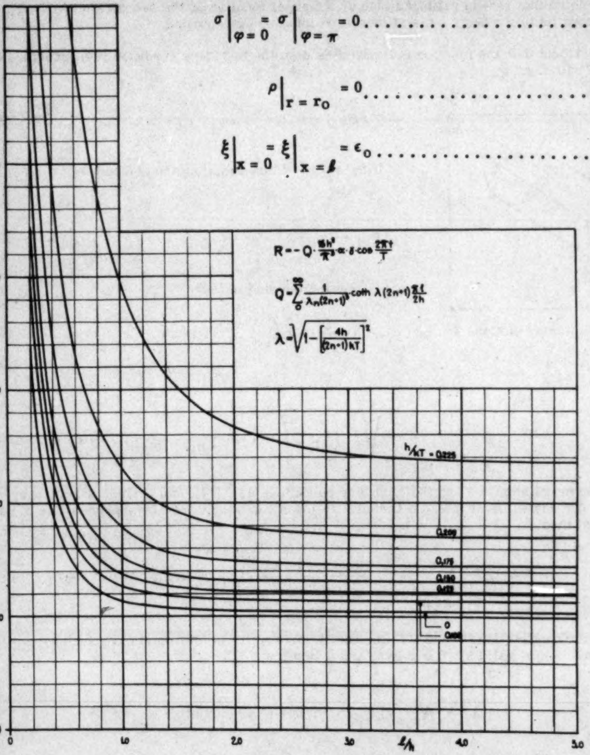

Fig. 7--Evaluation of Eq. (41)

As this case is analogous to Case 1, we build a trial function according to the pattern of (22), thus

$$\sigma = \cos\frac{2\pi t}{T} \cdot A_n \cdot \frac{\cosh \varkappa x - \cosh \varkappa (l-x)}{\sinh \varkappa l} \cdot f(r) \cdot \sin n\varphi \; \ldots\ldots\ldots\ldots \quad (47)$$

in which f(r) is a function of r only. Equation (47) satisfies the boundary conditions (42) and (43). Introducing the expression (47) in the differential equation (11), we receive

$$\frac{d^2 f}{dr^2} + \frac{1}{r} \cdot \frac{df}{dr} + \left[\varkappa^2 + \left(\frac{2\pi}{kT}\right)^2 - \frac{n^2}{r^2}\right] f = 0 \; \ldots\ldots\ldots\ldots \quad (48)$$

Equation (48) is satisfied by a Bessel function f(r) = $J_n(\beta r)$ in which

$$\beta^2 = \varkappa^2 + \left(\frac{2\pi}{kT}\right)^2 \; \ldots\ldots\ldots\ldots\ldots\ldots \quad (49)$$

It may be noted that (48) is satisfied also by a Bessel function of the second kind $f(r) = Y_n$ which, however, becomes infinite when $r = o$ and therefore must be disregarded.

Now it is evident that the function (47) satisfies also the boundary condition (44), provided βr_o is a root of the equation

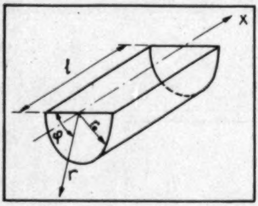

Fig. 8--The elements of Case 3

$$J'_n(\beta r_o) = 0 \qquad (50)$$

If the roots of this equation are denoted $\tau_1, \tau_2, \tau_3, \ldots \ldots {}_m$, thus

$$\beta_m = \tau_m / r_o \qquad (51)$$

we obtain, by introducing in (49)

$$\varkappa = \lambda \cdot \frac{\tau}{r_o} = \lambda\beta \qquad (52)$$

in which

$$\lambda = \sqrt{1 - \left(\frac{2\pi r_o}{\tau k T}\right)^2} \qquad (53)$$

As the differential equation and the boundary conditions (42), (43), and (44) are satisfied by expression (47) for any value of m and n the total solution can be obtained by superposition of particular solutions, thus

$$\sigma = \cos\frac{2\pi t}{T} \sum_m \sum_n A_{m,n} \cdot \frac{\cosh \varkappa x - \cosh \varkappa (l-x)}{\sinh \varkappa l} \cdot J_n(\beta_m r) \cdot \sin n\varphi \qquad (54)$$

To satisfy the conditions (45) and (46) the coefficients $A_{m,n}$ in (54) must have such values that the following condition is valid for $0 \leqq r \leqq r_o$ and $0 \leqq \varphi \leqq \pi$

$$\sum_m \sum_n A_{m,n} \cdot J_n(\beta_m r) \cdot \sin n\varphi = C = \text{constant} \qquad (55)$$

The coefficients $A_{m,n}$ may be determined as follows, according to a method outlined in various handbooks of mathematics [FRANK and v. MISES, 1930]. In the first instance we multiply both sides of (55) by $\sin \mu\varphi$ and integrate between 0 and π. We then obtain

$$\sum_m A_{m,n} \cdot J_{2n+1}(\beta_m r) = C \frac{4}{\pi} \cdot \frac{1}{2n+1} \qquad (56)$$

observing in the operation that the summation sign for n vanishes, as, for all values of μ except $\mu = n$, we have

$$\int_0^\pi \sin nx \cdot \sin \mu x \, dx = 0$$

The next operation is to multiply both sides of (56) by $r \cdot J_{2n+1}(\beta_m r)$ and integrate between 0 and r_o. We then obtain the following expression after some transformations

$$A_{m,n} = C \cdot \frac{4}{\pi} \cdot \frac{1}{2n+1} \cdot \frac{2 \cdot \beta_m^2 \int_0^{r_0} r \cdot J_{2n+1}(\beta_m r)\, dr}{\left(\beta_m^2 \cdot r_0^2 - (2n+1)^2\right) \cdot J_{2n+1}^2(\beta_m r_0)} \qquad \text{(57)}$$

observing in this operation that the summation sign for m vanishes, as, for all values of μ except $\mu = m$, we have

$$\int_0^{r_0} r \cdot J_{2n+1}(\beta_m r) \cdot J_{2n+1}(\beta_\mu r)\, dr = 0$$

The complete solution of the problem may now be written

$$\sigma = +\frac{8}{\pi} \alpha \cdot \gamma\, r_0 \cos\frac{2\pi t}{T} \sum_{m=1}^{\infty} \sum_{n=0}^{\infty} \frac{a_{m,n}}{\lambda(2n+1)\tau_m} \cdot \frac{\cosh \varkappa x - \cosh \varkappa(l-x)}{\sinh \varkappa l} \cdot J_{2n+1}(\beta_m r) \cdot \sin(2n+1)\varphi \qquad \text{(58)}$$

$$\xi = \frac{2\alpha g T^2}{\pi^3} \cos\frac{2\pi t}{T} \sum_{m=1}^{\infty} \sum_{n=0}^{\infty} \frac{a_{m,n}}{2n+1} \cdot \frac{\sinh \varkappa x + \sinh \varkappa(l-x)}{\sinh \varkappa l} \cdot J_{2n+1}(\beta_m r) \cdot \sin(2n+1)\varphi \qquad \text{(59)}$$

$$\rho = -\frac{2\alpha g T^2}{\pi^3} \cos\frac{2\pi t}{T} \sum_{m=1}^{\infty} \sum_{n=0}^{\infty} \frac{a_{m,n}}{\lambda(2n+1)} \cdot \frac{\cos \varkappa x - \cosh \varkappa(l-x)}{\sinh \varkappa l} \cdot J'_{2n+1}(\beta_m r) \cdot \sin(2n+1)\varphi \qquad \text{(60)}$$

in which the coefficients, after some transformations of (57), appear as follows

$$a_{m,n} = \frac{\int_0^{\tau_m} \tau \cdot J_{2n+1}(\tau)\, d\tau}{\left(\tau_m^2 - (2n+1)^2\right) J_{2n+1}^2(\tau_m)} \qquad \text{(61)}$$

The roots of $J'_n = 0$ may be calculated by means of formulas given by McMAHON [1894]. The three first roots of $J'_1 = 0$ and $J'_3 = 0$ are 1.84, 5.33, 8.54 and 4.20, 8.02, 11.34 respectively.

As in Case 1 the occurrence of resonance depends upon the value of the denominator $\sinh \varkappa l$, and (27) and (28) apply. Introducing (28) in (52) we obtain

$$\left(\frac{2\pi r_0}{kT}\right)^2 - \left(\frac{\mu\pi r_0}{l}\right)^2 = \tau^2 \qquad \text{(62)}$$

hence the value of r_0 at which resonance, for the gravest value of τ, occurs

$$r_0 = \frac{1{,}84\, kT}{2\pi} \cdot \frac{1}{\sqrt{1 - \left(\frac{\mu kT}{2l}\right)^2}} \qquad \text{(63)}$$

It is interesting to note that the condition (31) is valid also in this case, but that the resonance occurs for a somewhat larger depth of the reservoir than in the case of a square section.

The dynamic water pressure on the end wall, calculated according to (58) for $l/r_0 = \infty$ and with $\lambda = 1$, is shown in Figure 9. A comparison with Figure 3 shows that the sloping walls of the canyon result in a somewhat lower pressure.

Case 4: Two-dimensional flow in a basin with semi-circular section, vibrating in a direction transverse to the generating axis (see Fig. 10)--Differential equation (12) applies, and the boundary conditions are

$$\sigma \Big|_{\varphi = \pm\pi/2} = 0 \quad \ldots\ldots (64)$$

$$\rho \Big|_{r = r_o} = \epsilon_o \sin\varphi \quad \ldots\ldots (65)$$

A trial function of the form

$$\sigma = \cos\frac{2\pi t}{T}\cdot A_n \cdot f(r)\cdot \sin 2n\varphi \quad \ldots\ldots (66)$$

satisfies the boundary condition (64). Introducing (66) in (12) we obtain

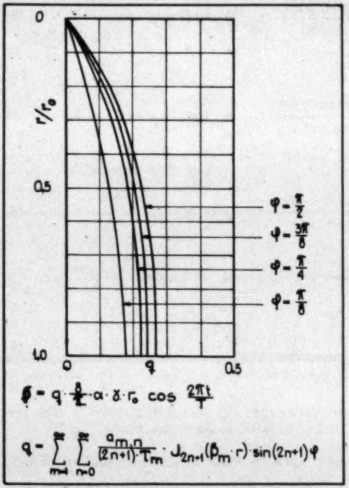

Fig. 9--Dynamic water pressure on end wall in Case 3, $\mathfrak{b}/r_o = \infty$, $\lambda = 1$

$$\frac{d^2f}{dr^2} + \frac{1}{r}\cdot\frac{df}{dr} + \left[\varkappa^2 - \frac{(2n)^2}{r^2}\right] f = 0 \quad \ldots\ldots (67)$$

which is satisfied by a Bessel function $f(r) = J_{2n}(\varkappa r)$ with

$$\varkappa = 2\pi/kT \quad \ldots\ldots (68)$$

Observing the series expansion

$$\sin\varphi = \frac{4}{\pi}\sum_{1}^{\infty}(-1)^{n-1}\cdot\frac{2n}{(2n)^2-1}\cdot \sin 2n\varphi \quad \ldots\ldots (69)$$

it is easily verified that the solution of the problem is given by the following expressions, namely

$$\sigma = \frac{4}{\pi}\alpha\gamma r_o \cdot \cos\frac{2\pi t}{T}\sum_{1}^{\infty}(-1)^{n-1}\cdot \frac{2n}{(2n)^2-1}\cdot\frac{J_{2n}(\varkappa r)}{\varkappa r_o J'_{2n}(\varkappa r_o)}\cdot \sin 2n\varphi \quad \ldots\ldots (70)$$

$$\rho = -\frac{\alpha g T^2}{\pi^3}\cdot \cos\frac{2\pi t}{T}\sum_{1}^{\infty}(-1)^{n-1}\cdot \frac{2n}{(2n)^2-1}\cdot\frac{J'_{2n}(\varkappa r)}{J'_{2n}(\varkappa r_o)}\cdot \sin 2n\varphi \quad \ldots (71)$$

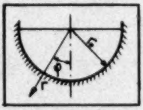

Fig. 10--The elements of Case 4

The stability of the flow depends on the value of the denominator $J'_{2n}(\varkappa r_o)$. Resonance occurs if $\varkappa r_o$ is a root of the equation

$$J'_{2n}(\varkappa r_o) = 0 \quad \ldots\ldots (72)$$

If the roots of this equation are denoted τ_1, τ_2, τ_3, ... , we have

$$\varkappa r_o = \tau \quad \ldots\ldots (73)$$

hence the value of r_0 for which resonance occurs

$$r_0 = \tau kT/2\pi \qquad (74)$$

The roots of (72) may be calculated by formulas cited in Case 3.

The three first roots of $J'_2 = 0$ and $J'_4 = 0$ are 3.05, 6.71, 9.97, and 5.32, 9.31, 12.69 respectively.

If the compressibility of the water can be neglected, that is, if

$$r_0 \ll \tau kT/2\pi \qquad (75)$$

(70) and (71) are simplified as follows

$$\sigma = \frac{4}{\pi}\alpha\gamma r_0 \cdot \cos\frac{2\pi t}{T}\sum_1^{\infty}\frac{(-1)^{n-1}}{(2n)^2-1}\cdot\left(\frac{r}{r_0}\right)^{2n}\cdot\sin 2n\varphi \qquad (76)$$

$$p = -\frac{\alpha g T^2}{\pi^3}\cdot\cos\frac{2\pi t}{T}\sum_1^{\infty}(-1)^{n-1}\cdot\frac{2n}{(2n)^2-1}\left(\frac{r}{r_0}\right)^{2n-1}\cdot\sin 2n\varphi \qquad (77)$$

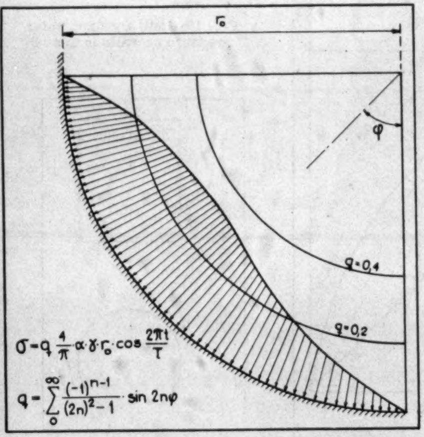

Fig. 11--(left) Dynamic water pressure on walls in Case 4

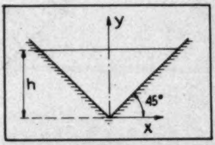

Fig. 12--(above) The elements of Case 5

Figure 11 shows the dynamic water pressure on the walls, as calculated from Equation (76).

Case 5: Two-dimensional flow in a basin with triangular section, the walls sloping 45°, vibrating in a direction transverse to the axis (see Fig. 12)--As far as the writers are aware, a reasonably simple expression for the pressure in this case can be obtained only if the compressibility of the water is neglected.

If $k = \infty$, (12) is simplified to

$$\partial^2\sigma/\partial x^2 + \partial^2\sigma/\partial y^2 = 0 \qquad (78)$$

and the boundary conditions are

$$\sigma\Big|_{y=h}=0 \qquad (79)$$

$$\xi\mp\eta\Big|_{x=\pm y}=\epsilon_o \qquad (80)$$

Observing the series expansion

$$x=\frac{2h}{\pi}\sum_{1}^{\infty}\frac{(-1)^{n-1}}{n}\cdot\sin n\pi\frac{x}{h} \qquad (81)$$

it is easily verified that (78) and the boundary conditions are satisfied by the expression

$$\sigma=\alpha\gamma h\cdot\cos\frac{2\pi t}{T}\cdot\left[\frac{x}{h}-\frac{2}{\pi}\sum_{1}^{\infty}\frac{(-1)^{n-1}}{n\cdot\sinh n\pi}\cdot\left[\sinh n\pi\frac{x}{h}\cdot\sin n\pi\frac{y}{h}+\sin n\pi\frac{x}{h}\cdot\sinh n\pi\frac{y}{h}\right]\right] \qquad (82)$$

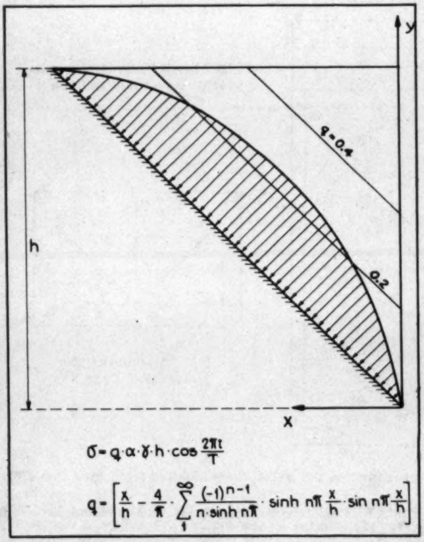

Fig. 13--(left) Dynamic water pressure on walls in Case 5

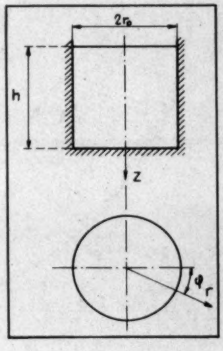

Fig. 14--(above) The elements of Case 6

Figure 13 shows the dynamic water pressure on the walls, as calculated from equation (82).

Case 6: Three-dimensional flow in a vertical cylinder of circular cross section (see Fig. 14). The flow being three-dimensional, (11) applies. The boundary conditions are

$$\sigma\Big|_{z=0}=0 \qquad (83)$$

$$\rho \Big|_{r = r_0} = \epsilon_0 \cos \varphi \qquad (84)$$

$$\zeta \Big|_{z = h} = 0 \qquad (85)$$

A trial function of the form

$$\sigma = \cos\varphi \cdot \cos \frac{2\pi t}{T} \cdot A_n \cdot f(r) \cdot \sin(2n+1) \frac{\pi z}{2h} \qquad (86)$$

satisfies the boundary conditions (83) and (85). Introducing (86) in (11), we obtain

$$\frac{d^2 f}{dr^2} + \frac{1}{r} \cdot \frac{df}{dr} - \left(\varkappa^2 + \frac{1}{r^2}\right) f = 0 \qquad (87)$$

which is satisfied by a Bessel function of purely imaginary argument $f(r) = I_1(\varkappa r)$, in which

$$\varkappa = \lambda \,(2n+1)\, \frac{\pi}{2h} \qquad (88)$$

and

$$\lambda = \sqrt{1 - \left(\frac{4h}{(2n+1)\,kT}\right)^2} \qquad (89)$$

Using the series expansion (21) the complete solution may be written.

$$\sigma = + \frac{8h}{\pi^2} \alpha \gamma \cdot \cos\varphi \cdot \cos \frac{2\pi t}{T} \sum_0^\infty \frac{1}{\lambda\,(2n+1)^2} \cdot \frac{I_1(\varkappa r)}{I_1'(\varkappa r_0)} \cdot \sin(2n+1) \frac{\pi z}{2h} \qquad (90)$$

$$\rho = - \frac{\alpha g T^2}{\pi^3} \cdot \cos\varphi \cdot \cos \frac{2\pi t}{T} \sum_0^\infty \frac{1}{2n+1} \cdot \frac{I_1'(\varkappa r)}{I_1'(\varkappa r_0)} \cdot \sin(2n+1) \frac{\pi z}{2h} \qquad (91)$$

$$\zeta = - \frac{\alpha g T^2}{\pi^3} \cdot \cos\varphi \cdot \cos \frac{2\pi t}{T} \sum_0^\infty \frac{1}{\lambda(2n+1)} \cdot \frac{I_1(\varkappa r)}{I_1'(\varkappa r_0)} \cdot \cos(2n+1) \frac{\pi z}{2h} \qquad (92)$$

If λ is real, the flow is stable under all conditions, the denominator $I_1'(\varkappa r_0)$ then having no zero values. If on the other hand λ becomes imaginary, the function $I_1(\varkappa r)$ changes to $J_1(\varkappa r)$, and resonance occurs for values of $\varkappa r_0$ satisfying the equation

$$J_1'(\varkappa r_0) = 0 \qquad (93)$$

If the roots of this equation are denoted $\tau_1, \tau_2, \tau_3, \ldots\ldots$, we obtain from (88),

$$\left(\frac{4h}{kT}\right)^2 - \left(\frac{2\tau h}{\pi r_0}\right)^2 = (2n+1)^2$$

hence the value of h at which resonance, with n = 0, occurs

$$h = \frac{kT}{4} \cdot \frac{1}{\sqrt{1 - \left(\frac{\tau kT}{2\pi r_0}\right)^2}} \qquad (94)$$

The lowest values of τ are given in Case 3.

From (94) it is seen that the occurrence of resonance is dependent of the radius r_0, and resonance cannot occur unless

$$r_0 > \tau kT/2\pi \quad \ldots\ldots (95)$$

whereby it is to be noted that the gravest value of τ is 1.84.

The dynamic water pressure on the cylinder wall may be calculated from (90). The resultant pressure on the cylinder half is obtained by integrating from $\varphi = -\pi/2$ to $\varphi = +\pi/2$, and from $z = 0$ to $z = h$, thus

$$R = \pm \frac{8h^2 r_0}{\pi^2} \cdot \alpha \cdot \gamma \cdot \cos\frac{2\pi t}{T} \sum_0^\infty \frac{1}{\lambda\,(2n+1)^3} \cdot \frac{I_1(\varkappa r_0)}{I_1'(\varkappa r_0)} \quad \ldots\ldots (96)$$

Equations (90) and (96) have been evaluated, with $\lambda = 1$, in Figures 15 and 16, respectively.

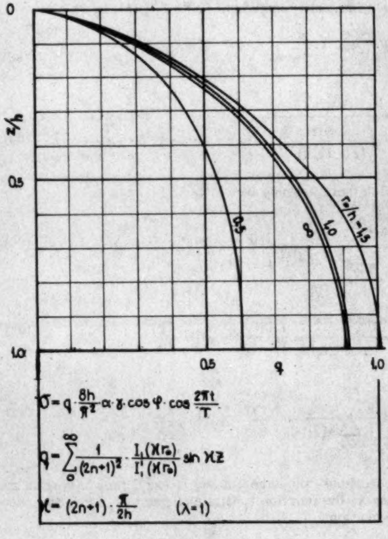

Fig. 15--Evaluation of Eq. (90)

Case 7: Three-dimensional flow around a vertical cylinder of circular cross section, vibrating in a reservoir infinitely extended in a horizontal plane (see Fig. 17)--As this case is of practical importance for the design of lighthouse towers in sea regions subjected to earthquakes, it may be briefly treated in this connection, as follows.

The differential equation and the boundary conditions are the same as in the next foregoing case; the solution, however, must tend to zero when the radius increases. The Hankel function of purely imaginary argument has this property, and thus the solution in this case reads,

$$\sigma = -\frac{8h}{\pi^2} \alpha \gamma \cdot \cos\varphi \cdot \cos\frac{2\pi t}{T} \sum_0^\infty \frac{1}{\lambda (2n+1)^2} \cdot \frac{K_1(\varkappa r)}{K_1'(\varkappa r_0)} \cdot \sin(2n+1)\frac{\pi z}{2h} \quad \ldots\ldots (97)$$

$$\rho = +\frac{\alpha g T^2}{\pi^3} \cdot \cos\varphi \cdot \cos\frac{2\pi t}{T} \sum_0^\infty \frac{1}{2n+1} \cdot \frac{K_1'(\varkappa r)}{K_1'(\varkappa r_0)} \cdot \sin(2n+1)\frac{\pi z}{2h} \quad \ldots\ldots (98)$$

$$\zeta = +\frac{\alpha g T^2}{\pi^3} \cdot \cos\varphi \cdot \cos\frac{2\pi t}{T} \sum_0^\infty \frac{1}{\lambda (2n+1)} \cdot \frac{K_1(\varkappa r)}{K_1'(\varkappa r_0)} \cdot \cos(2n+1)\frac{\pi z}{2h} \quad \ldots\ldots (99)$$

in which $\varkappa$ and λ are as given in (88) and (89).

The dynamic water pressure on the cylinder wall may be calculated from (97). The resultant pressure on the cylinder half is obtained by integrating from $\varphi = -\pi/2$ to $\varphi = +\pi/2$ and from $z = 0$ to $z = h$, thus

$$R = \pm \frac{8h^2 r_0}{\pi^2} \alpha \gamma \cos \frac{2\pi t}{T} \sum_{0}^{\infty} \frac{1}{\lambda (2n+1)^3} \cdot \frac{K_1(\varkappa r_0)}{K_1'(\varkappa r_0)} \quad \ldots\ldots\ldots\ldots\ldots (100)$$

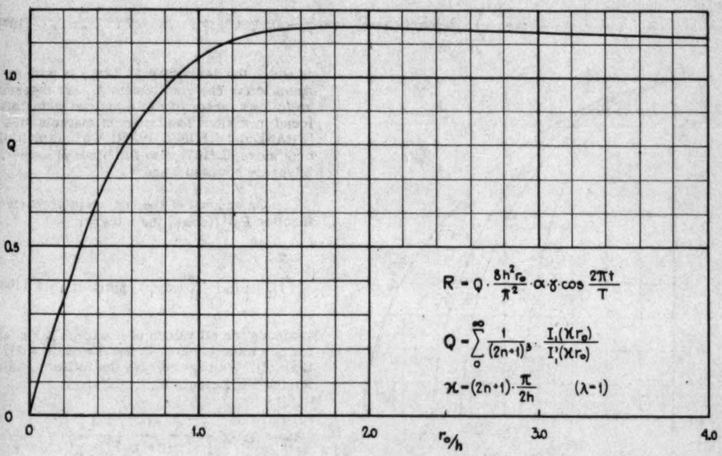

Fig. 16--Evaluation of Eq. (96)

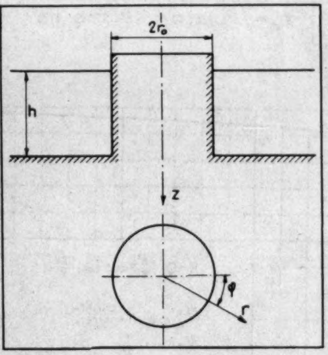

Fig. 17--The elements of Case 7

Equations (97) and (100) have been evaluated, with $\lambda = 1$, in Figures 18 and 19, respectively.

Case 8: Three-dimensional flow in a semi-spherical vessel vibrating in the direction $\varphi = 0$, (see Fig. 20)--Equation (13) applies, and the boundary conditions are

$$\sigma \Big|_{\psi = 0} = \sigma \Big|_{\psi = \pi} = 0 \ldots\ldots (101) \text{ and } (102)$$

$$\rho \Big|_{r = r_0} = \epsilon_0 \cdot \cos\psi \cdot \cos\psi \ldots\ldots\ldots (103)$$

The general solution of (13) can be written [FRANK and v. MISES, 1930; RAYLEIGH, 1926]

$$\sigma = \cos \frac{2\pi t}{T} \cdot \cos\varphi \sum_n A_n \cdot F_n(\varkappa r) \cdot P_n^{(1)}(\cos\phi) (104)$$

in which

$$\varkappa = 2\pi/kT \ldots\ldots\ldots (105)$$

and

$$F_n(\varkappa r) = (1/\sqrt{r}) \cdot J_{n+1/2}(\varkappa r) \dots\dots\dots\dots \quad (106)$$

As the spherical surface-harmonic $P_n^{(1)}(\cos\psi)$ is zero for $\psi = 0$ and $\psi = \pi$, (101) and (102) are satisfied. To satisfy (103), the coefficients A_n must have such values that the following condition is valid

$$\sum_n A_n \cdot F_n'(\varkappa r_o) \cdot P_n^{(1)}(\cos\phi) = \alpha\,\gamma\,\cos\phi \dots\dots\dots\dots \quad (107)$$

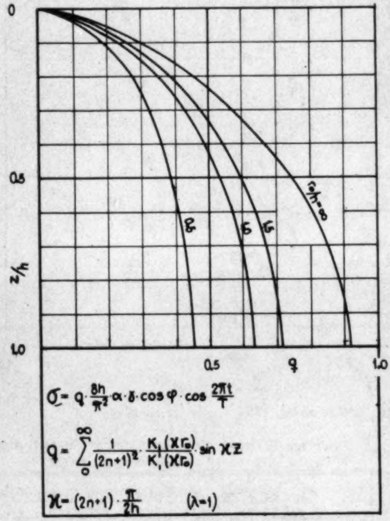

Fig. 18--Evaluation of Eq. (97)

in which the derivative $F'(\varkappa r_o)$ is with respect to r. The coefficients A_n are determined as follows, according to a method which may be found in various handbooks of mathematics [FRANK and v. MISES, 1930]. We thus multiply both sides of (107) with $P\mu^{(1)}(\cos\psi) \cdot \sin\psi$ and integrate between 0 and π.

On account of the conjugate property of th function $P_n^{(1)}(\cos\psi)$ the integral

$$\int_0^\pi P_n^{(1)}(\cos\phi) \cdot P_\mu^{(1)}(\cos\phi) \cdot \sin\phi \cdot d\phi \dots \quad (108)$$

vanishes for all values of μ except $\mu = n$, and for $\mu = n$ the integral is equal to $2n(n + 1)/(2n + 1)$. We thus receive the following value for the coefficients A_n

$$A_n = a_n \cdot \alpha \cdot \gamma \cdot \frac{2n+1}{2n(n+1)} \cdot \frac{1}{F_n'(\varkappa r_o)} \dots \quad (109)$$

in which

$$a_n = \int_0^\pi P_n^{(1)}(\cos\phi) \cdot \cos\phi \cdot \sin\phi \cdot d\phi \dots \quad (110)$$

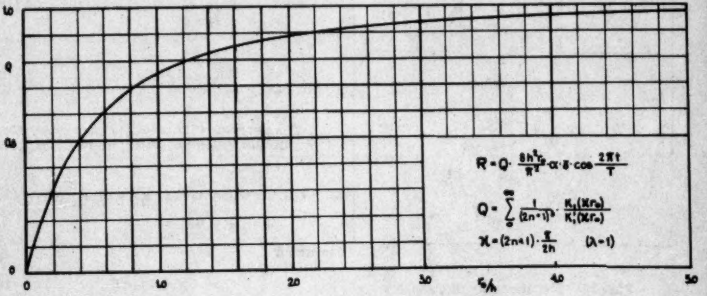

Fig. 19--Evaluation of Eq. (100)

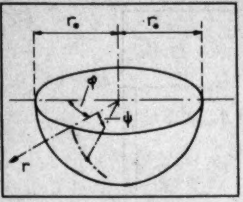

Fig. 20--The elements of Case 8

As $P_n^{(1)}(\cos\psi)$ is an even function when n is an odd integer, the integral in (110) is zero if n is odd.

The complete solution of the problem may now be written.

$$\sigma = \alpha\cdot\gamma\cdot r_o\cdot\cos\varphi\cdot\cos\frac{2\pi t}{T}\sum_1^\infty a_n\cdot\frac{4n+1}{4n(2n+1)}\cdot\frac{F_{2n}(\varkappa r)}{r_o\cdot F'_{2n}(\varkappa r_o)}\cdot P_{2n}^{(1)}(\cos\phi) \quad (111)$$

$$\rho = -\alpha\cdot g\,\frac{T^2}{4\pi^2}\cdot\cos\varphi\cdot\cos\frac{2\pi t}{T}\sum_1^\infty a_n\cdot\frac{4n+1}{4n(2n+1)}\cdot\frac{F'_{2n}(\varkappa r)}{r_o\cdot F'_{2n}(\varkappa r_o)}\cdot P_{2n}^{(1)}(\cos\phi) \quad (112)$$

Resonance occurs if $\varkappa r_o$ is a root of the equation

$$F'_{2n}(\varkappa r_o) = 0 \;\ldots\ldots\ldots\ldots\ldots\ldots\ldots\ldots\; (113)$$

If the roots of this equation are denoted τ_1, τ_2, ..., we have

$$\varkappa r_o = \tau \;\ldots\ldots\ldots\ldots\ldots\ldots\ldots\ldots\; (114)$$

hence the value of r_o for which resonance occurs

$$r_o = \tau kT/2\pi \;\ldots\ldots\ldots\ldots\ldots\ldots\ldots\ldots\; (115)$$

The roots of (113) may be calculated by formulas cited in Case 3. The lowest root is 3.34.

If the compressibility of the water can be neglected, that is, if

$$r_o \ll \tau kT/2\pi \;\ldots\ldots\ldots\ldots\ldots\ldots\ldots\ldots\; (116)$$

(111) and (112) are simplified as follows

$$\sigma = \alpha\cdot\gamma\cdot r_o\cdot\cos\varphi\cdot\cos\frac{2\pi t}{T}\sum_1^\infty a_n\cdot\frac{4n+1}{8n^2(2n+1)}\cdot\left(\frac{r}{r_o}\right)^{2n}\cdot P_{2n}^{(1)}(\cos\phi) \;\ldots\ldots\ldots\; (117)$$

$$\rho = -\alpha\cdot g\cdot\frac{T^2}{4\pi^2}\cdot\cos\varphi\cdot\cos\frac{2\pi t}{T}\sum_1^\infty a_n\cdot\frac{4n+1}{4n(2n+1)}\cdot\left(\frac{r}{r_o}\right)^{2n-1}\cdot P_{2n}^{(1)}(\cos\phi) \;\ldots\ldots\ldots\; (118)$$

Figure 21 shows the dynamic water pressure on the wall, as calculated from equation (117). A comparison with Figure 11 shows that the pressure in a spherical vessel is somewhat lower than in a circular one.

Graphical solution

As mentioned in the Introduction, the dynamic water pressure in the two-dimensional flow can be determined by a graphical procedure when the compressibility of the fluid is neglected. Equation (10) becomes

$$\frac{\partial^2\sigma}{\partial x^2} + \frac{\partial^2\sigma}{\partial y^2} = 0 \;\ldots\ldots\ldots\ldots\ldots\ldots\ldots\ldots\; (119)$$

Considering this equation, it is evident from the general theory of fluid motion that the dynamical water pressure may be obtained by plotting a flow net, that is, two sets of curves, one represent-

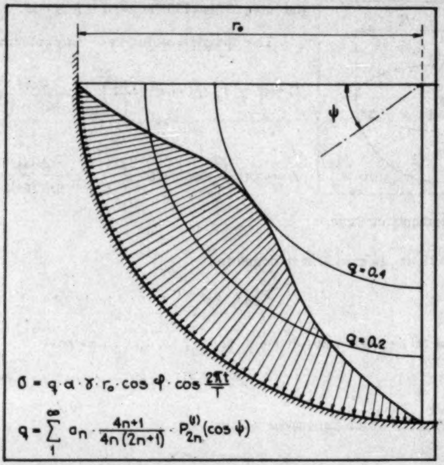
r_0
ψ
$q = a_1$
$q = a_2$
$\sigma = q \cdot \alpha \cdot \gamma \cdot r_o \cdot \cos \varphi \cdot \cos \frac{2\pi t}{T}$
$q = \sum_1^\infty a_n \cdot \frac{4n+1}{4n(2n+1)} \cdot P_{2n}^{(1)}(\cos \psi)$

Fig. 21--Evaluation of Eq. (117)

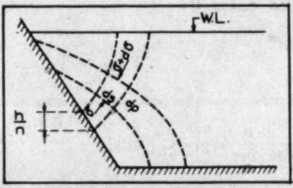
W.L.
$\sigma + d\sigma$
dp
ds
σ
$\frac{h}{n}$

Fig. 22--Elements in a flow net

ing streamlines and the other equipotential lines. The problem is thereby reduced to determining the proper scale of the pressure in the flow net.

If the depth of the reservoir h be divided in n equal parts, it follows from the assumption of rigid walls that the same water quantity must flow through each element. Considering, further, that no water can escape across the streamlines, we obtain by applying the equations of motion and continuity to a square in the flow net (see Fig. 22)

$$d\sigma = \frac{\alpha \cdot \gamma \cdot h}{n} \cdot \frac{dp}{ds} \cdot \cos \frac{2\pi t}{T} \quad \ldots (120)$$

by which the scale of the pressure is determined. If the flow net consists of squares of equal sides, we have dp = ds, and thus for the most important moment with t = T

$$d\sigma = (1/n)\gamma\alpha h \quad \ldots\ldots\ldots\ldots\ldots\ldots\ldots\ldots (121)$$

The graphical method outlined above has been exemplified in three different cases, demonstrated in Figures 23 to 25.

Conclusive remarks

This investigation of the hydrodynamic earthquake effects covers the most common types of artificial hydraulic vessels with rigid walls.

In the case of dams with straight axes, the shape of the canyon walls and of the upstream face of

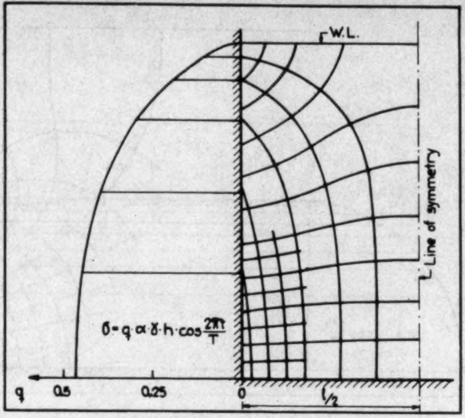
W.L.
Line of symmetry
$\sigma = q \cdot \alpha \cdot \gamma \cdot h \cdot \cos \frac{2\pi t}{T}$
q
0.5
0.25
0
l/2

Fig. 23--Flow net of a square section with $h/l = 1.0$, whole section moving in phase

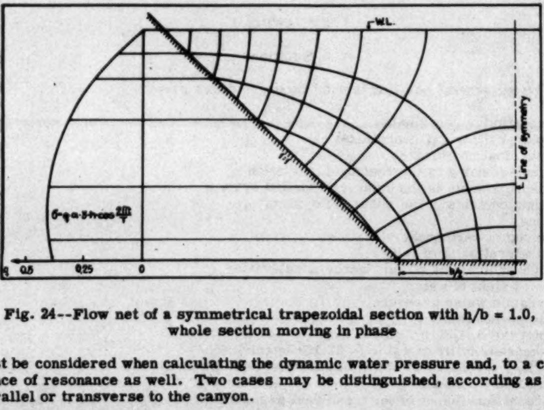
W.L.
Line of symmetry
$\sigma = q \cdot \alpha \cdot \gamma \cdot h \cdot \cos \frac{2\pi t}{T}$
q
0.5
0.25
0
h/2

Fig. 24--Flow net of a symmetrical trapezoidal section with $h/b = 1.0$, whole section moving in phase

the dam must be considered when calculating the dynamic water pressure and, to a certain extent, the occurrence of resonance as well. Two cases may be distinguished, according as the earthquake thrust is parallel or transverse to the canyon.

In the case of parallel action a comparison between a rectangular and a circular canyon shows that the sloping walls of the latter reduces the pressure on the dam by some ten per cent; in most practical cases it is on the safe side to assume a rectangular cross section. In this connection it should be noted that a sloping upstream face of the dam reduces the pressure to a considerable extent. For a sloping or irregular upstream face of the dam the pressure is most conveniently calculated by means of the graphical procedure as given in the foregoing.

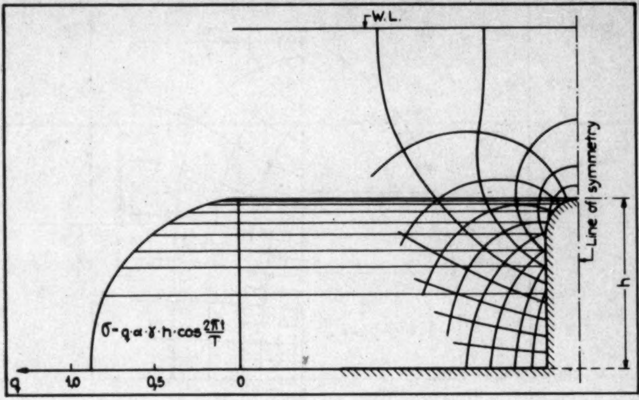
W.L.
Line of symmetry
h
$\sigma = q \cdot \alpha \cdot \gamma \cdot h \cdot \cos\frac{2\pi t}{T}$
q
1.0
0.5
0

Fig. 25--Flow net of a submerged weir

In the case of transverse action the effect of sloping walls in a canyon is very pronounced, as may be seen by a comparison of Figure 3 with Figures 11 and 13. Also the presence of faults at the dam site may considerably influence the pressure on certain parts of the dam, as indicated in Case 2.

APPENDIX 1

Notation

The following general notation is used throughout this paper

xyz	rectangular coordinates
$r\varphi z$	polar-cylindrical coordinates
$r\varphi\psi$	spherical coordinates
$\xi\eta\zeta$	displacements in the rectangular system
$\rho\theta\zeta$	displacements in the polar-cylindrical system
$\rho\theta\omega$	displacements in the spherical system
t	time
T	period of earthquake vibration
g	acceleration of gravity
αg	highest intensity of earthquake acceleration
γ	unit weight of water
σ	dynamic water pressure
R	pressure resultant
n, m, μ	integers 0, 1, 2, 3 . . . . .
E	compressibility of water (= 21.10^7 kg/m^2)
k	$\sqrt{gE/\gamma}$ = velocity of sound in water (= 1 430 m/s)
A	arbitrary constant
J_n	Bessel function of order n and real argument
I_n	Bessel function of order n and purely imaginary argument
K_n	Hankel function of order n and purely imaginary argument
$P_n^{(1)}$	Spherical surface-harmonic function of first order and degree n

It should be noted that the derivatives of the functions J, I, and K used are with respect to the argument.

References

BRAHTZ, H. A., and HEILBRON, C. H., Water pressures on dams during earthquakes, discussion, Trans. Amer. Soc. Civ. Eng., v. 98, pp. 452-460, 1933.

FRANK, PH., and v. MISES, R., Differentialgleichungen der Physik, Vieweg und Sohn, Braunschweig, pp. 385-450, 1930.

GEIGER, H., and SCHEEL, K., Handbuch der Physik, Julius Springer, Berlin, v. 6, p. 596, 1928.

HOSKINS, LEANDER M., and JACOBSEN, LYDIK S., Water pressure in a tank caused by a simulated earthquake, Bull. Seis. Soc. Amer., v. 24, pp. 1-32, 1934.

JACOBSEN, LYDIK S., Impulsive hydrodynamics of fluid inside a cylindrical tank and of fluid surrounding a cylindrical pier, Vibration Research Lab., Technical Rept. 6, under Navy Contract N6-ORI 154, Task Order 1, (processed) 1949.

LAMB, H., Hydrodynamics, University Press, Cambridge, p. 4, 1932.

McMAHON, J., On the roots of the Bessel and certain related functions, Ann. of Math. IX, Univ. of Virginia, Nov. 1894.

RAYLEIGH, LORD, (STRUTT, JOHN W.) On waves, Phil. Mag., London, ser. 5, v. 1, pp. 257-279. April, 1876.

RAYLEIGH, LORD, (STRUTT, JOHN W.) Theory of sound, Macmillan, London, 1926.

WATSON, GEORGE N., A treatise on the theory of Bessel functions, 2nd ed., University Press, Cambridge, 1944.

WESTERGAARD, H. M., Water pressures on dams during earthquakes, Trans. Amer. Soc. Civ. Eng., v. 98, pp. 418-433, 1933.

Vattenbyggnadsbyrån,
29 Humlegårdsgatan,
Stockholm, Sweden

(Communicated manuscript received July 28, 1948;
open for formal discussion until March 1, 1950.)

Transactions, American Geophysical Union Volume 30, Number 5 October 1949

CLIMATOLOGY SINCE THE YEAR 1800

John Leighly

Abstract--Most of the work done in climatology in the past 150 years can be assigned to one of the following classes of investigation or presentation: empirical formulation of climatic data, descriptive climatology, climatologic cartography, organization of observational data by synoptic categories, investigation of the physical bases of climate, definition of climatic types and the delineation of climatic regions, and reconstruction of past climates. Although their relative importance has varied, through much of the period under consideration all these fields have been cultivated simultaneously. Especially in the latter part of the Nineteenth and the early part of the Twentieth Century, climatology has been too strongly dominated by a descriptive approach. Satisfactory physical interpretations of the phenomena recorded have often been impossible, but even the physical insights available at any given time have not always been applied. It would appear that the rational treatment of climatologic data can be attained more readily through synoptic concepts than through a frontal attack with the general formulations provided by physical theory.

> ". . . das arithmetische Mittel, in welchem die allerverschiedensten Zustände zusammen vergraben werden, ist Nichts Wirkliches, sondern eine abstrakte Grösse." W. Köppen, 1874.

Every science has its continuous history, but the continuity is not that of a metal wire, constant in diameter and homogeneous in structure. It resembles, rather, a badly spun or braided cord, made up of strands of varying length and thickness, constituting a fabric that itself varies in bulk. The following brief account traces separately the most important strands in the history of climatology since the early years of the Nineteenth Century, instead of examining cross sections at successive intervals of time. The several themes are discussed in the approximate order in which they become conspicuous in climatologic literature.

The point of view assumed is that climatology is a part of the more inclusive science of meteorology, and inseparable from it. It has been the task of climatology to summarize observations of weather made at specific localities so as to yield some expression of the probability of occurrence of intensities of meteorologic phenomena at given phases of the daily and annual cycles. The arithmetic mean, unsatisfactory as it often is as a representative value, has been by far the most conspicuous element in such summaries. The passage quoted above, uttered halfway through the period covered, is an appropriate motto, since dissatisfaction with means already computed has been the driving force behind all attempts to improve climatology. Dissatisfaction with the mean, indeed, is what led meteorology as a whole out of the bewilderment that afflicted those who concerned themselves with climatic phenomena at the turn of the Nineteenth Century. From the usefulness of the mean as a device for eliminating chance errors in astronomic and physical measurements, it became, for the Eighteenth Century, what the poet Schiller called "den ruhenden Pol in der Erscheinungen Flucht." But the flux of meteorologic phenomena, when reduced to arithmetic means, revealed no fixed pole, no "law," as that term was understood in an age when the physicist imagined that he was discovering the very thoughts of Nature's God. With all its impressive accomplishments, the Eighteenth Century bequeathed to its successor no better tools for investigating climate than the mean and some simple empirical formulas.

Empirical formulation of climatic data

That the mathematical knowledge available at the beginning of the Nineteenth Century was equal to the task of solving difficult problems was amply proven by the contemporary work of Laplace and Gauss; but the observations available for the study of climate presented no formulable problem that might be attacked with the mathematical tools available. In the absence of even hypothetical formulations, simple empirical expressions were all that could be applied. Expressions that represented the distribution of mean annual temperature between the equator and the pole of the Northern Hemisphere as a function of latitude had been set up in the Eighteenth Century; and as new observations were accumulated, new functions of latitude were tried out and new empirical constants computed to fit newly computed means. BREWSTER [1821] assumed that there are two cold poles in the Northern Hemisphere, one in Arctic America and one in northeastern Siberia; and set up equations that expressed the mean annual temperatures of places as a function of angular distance from these poles rather than of latitude. KÄMTZ [1832, pp. 87-109] subjected the earlier formulas to sharp criticism, and set up one of his own, in which the function of latitude was the square of the cosine. He used his expression cautiously, however, computing the numerical constants separately for various meridians and, when the departures from observed values became uncomfortably large, separately for different arcs of the same meridian. He recognized that his formula was a mere device for interpolation, not the expression of a "law" that the distribution of temperature through latitude must be expected to obey. His purpose in computing the constants for a large number of arcs of meridians was to determine where given isotherms intersect those meridians; he used this information to draw a new map of isotherms.

The empirical expression of temperature as a simple function of latitude, even when computed for different meridians, did not have a long life in the Nineteenth Century. Though recognized as a "barren mathematical generalization," it had its uses when subordinated to a physical concept. Thirty years after Kämtz's critical use of it as an interpolation device, FORBES [1861], in an article in which he used the epithet just quoted, derived equations containing trigonometric functions of latitude that represented the distribution of mean annual temperature on hemispheres consisting wholly of water and of land. From these equations he derived one that permitted the expression of the actual mean temperature of any parallel as a function of its latitude and the ratio of land to sea along it. There is thus a continuity between the simple expressions current in the early years of the Nineteenth Century and some of the investigations of "continentality" made in the present century [BROOKS, 1917; SPITALER, 1922]. GORCZYŃSKI'S [1920] well known measure of continentality makes use of an empirical function of latitude as the standard annual range of air temperature over the oceans with which the ranges observed on land are compared.

The early years of the Nineteenth Century provided one additional mathematical tool, the harmonic analysis of periodic phenomena, which was first applied to climatic data (the daily cycle of atmospheric pressure) by BESSEL [1814, 1828]. Bessel's procedure was promptly adopted, with the eagerness that greeted any idea that promised even partial mastery of climatic data. KÄMTZ [1831, 1832] filled page after page of his "Lehrbuch" with harmonic equations and constants of the daily march of pressure, and especially of temperature: temperature of the air at many stations, of the soil, and of water in springs. Though the procedure has remained a standard constituent of the analysis of observations, even Bessel's modest claim for it, that by its use one "goes halfway to meet theory," has been in time nearly abandoned. New concepts of the mechanism of the atmosphere have made it obsolete as a help on the road toward an understanding of physical processes.

Descriptive climatology (climatography)

Older than the summarization of observations by means of empirical formulas, but less distinctly in the main line of development of science in the Nineteenth Century, is the use of words to characterize climate and describe the phenomena of weather. Climatic description has always been a part of geographic and topographic literature. After the invention of the barometer and thermometer in the Seventeenth Century, these instruments were disseminated over the Earth with remarkable speed. The numerical data they yielded became an essential part of climatologic description. Descriptive climatology has, indeed, been the medium by which most climatologic information has been imparted. It is neither desirable nor possible to do more here than call attention to the vast quantity of descriptive climatologic literature that has seen the light in the last century and a half. Much of the Nineteenth Century still fell in the period of climatologic exploration of the Earth, when a set of observations made in a region whose climate was not previously known was eagerly published and read. With time, especially after official meteorologic services were founded in most countries of the Earth, these data became so abundant as to outweigh, sometimes manyfold, verbal discourse on the climates of the regions covered by official networks of observing stations.

Descriptive climatology as a genus of scientific literature is not yet dead, but its best days are probably past. It is therefore worth while, in retrospect, to recall one or two titles. The American can still read with a great deal of pleasure the generous pages of BLODGET [1857]. Blodget had plenty of numerical data at his disposal, but his text and handsome maps are what leave an impression in the memory of the reader. The most tireless collector of climatographic information was Julius Hann, whose parish was the whole Earth. During his long career (1866-1920) as editor of Meteorologische Zeitschrift and its predecessor, the Zeitschrift der Österreichischen Gesellschaft für Meteorologie, he collected and published a vast number of notices, usually brief but always meaty, on the climates of all parts of the Earth. These notices were sometimes extracts from the accounts of travelers, sometimes letters from private persons, sometimes abstracts from formal scientific books or articles. They constituted the store from which he drew most of the material for his deservedly famous "Handbuch" [HANN, 1883, 1897, 1908-11]. The introductory part of this book, in all three editions, was a treatise on general climatology, which emphasized the modifications of climate imposed by the contrasting qualities of the surfaces of land and sea, and by elevation. But the greater part, the climatography, which in the second and third editions occupied the two latter volumes, contains the most skillfully written account of the climates of the Earth that has been published. Hann had enormous quantities of numerical observations to work with, and summary tables compiled from them stud his pages; but in his text he let eye-witnesses speak of their direct, non-instrumental observations, which are often more eloquent than tables or maps. These first-hand accounts are less frequent in the later editions than in the first, but Hann had sufficient literary skill to prevent his numerical tables from becoming tiresome to the reader.

Both the accumulation of observational data and the rise of new interpretations of atmospheric phenomena contribute to the obsolescence of such writings as Hann's "Handbuch." No one could revise his climatography after his death, although the first volume of his "Handbuch" was rewritten [HANN, 1932] so as to become an even better work on general climatology than it had been in Hann's own lifetime. The next and latest attempt to produce a work that might take the place of Hann's was undertaken by W. Köppen in his eightieth year, with the assistance of a younger co-editor [KÖPPEN and GEIGER, 1930 . .]. No longer was it possible for one man to undertake such a task alone. Authors familiar with particular parts of the Earth were recruited to write of the climates of the regions with which they were familiar. A general outline was set up, to be followed by the authors as closely as was practicable. Five massive volumes were planned, the first, as in Hann's "Handbuch," to be devoted to general climatology, the other four to climatography. Only the first two volumes were completed, although several parts of the others were issued separately. Economic depression, political strife, and finally war intervened; the last fragment, prepared by the aged senior editor himself, was published in 1940, the year of his death. The climatographic sections of the work rely more upon tables and maps, and on technical exposition, than did Hann's work. One misses from them the immediacy of observation and the conveyance of personal experience that enlivened Hann's pages.

Climatic maps of the earth

Temperature--The longest step forward in the treatment of climatologic data in the early Nineteenth Century was the publication, in 1817, of Alexander von Humboldt's treatise on the distribution of heat over the globe; and in particular of the map issued with the separate edition of the treatise, which showed by isotherms the distribution of mean annual temperature over the greater part of the Northern Hemisphere. MEINARDUS [1899] has given a good account of the place of this map, the first to use isarithms for representing the distribution of climatic quantities over the surface of the Earth, in the early history of the mapping of temperature. That Humboldt used a map of the Earth to display the results of his critical examination of mean temperature is thoroughly in accord with his habits of thinking. In his earlier reports of his observations in the New World he had made full use of graphic devices: besides excellent maps, he had drawn profiles to display the relief of the countries he visited, and the vertical distribution of their physical attributes. In his essay he remarked: ". . . the use of graphic devices will cast much light on phenomena of the highest importance . . . . . If, instead of maps, we had had only tables containing the coördinates latitude, longitude, and elevation, a great number of noteworthy relations of configuration and relief of the continents would have remained forever unknown."

Humboldt's "beautiful memoir," as David Brewster called it, contained critically selected temperature data from a large number of stations scattered over the Northern Hemisphere, reduced to sea level, and a highly intelligent discussion of these data. This compilation represented, however only a quantitative addition to climatologic lore, and soon became obsolete. It was his discussion of temperature, and particularly his map, that constituted a qualitative advance; that lifted, in Forbes' words, "this part of the science of meteorology [into the domain] of rational physics." Representation on maps, by graphic symbols, of the climatologic observations that accumulated at an increasing rate and with constantly improved comparability among stations, became for the future the characteristic feature of climatology. The isarithm, introduced by Humboldt for displaying the distribution of temperature, became the accepted device for the representation of scalar quantities on maps, while vectorial symbols were easily devised for the plotting of winds. Cartographic array of numerical data, together with the plotting of time series in rectangular coordinates, a device in use before Humboldt, distributes observational data in space and time so that physical problems can be recognized and segregated. It provided the first means for breaking up the amorphous mass of climatologic information into categories that can be attacked rationally.

A full historical account of climatic maps since Humboldt's time would be as long as a comparable account of descriptive climatologic literature, which itself soon became accustomed to depend on maps for the display of illustrative numerical data. It is necessary to limit the present discussion to maps of the entire Earth, although many of the most enlightening climatic maps have covered only small fractions of its surface, and have contributed their content to world maps. HILDEBRANDSSON and TEISSERENC DE BORT [1898-1907, v. 1, chap. 7] have given a good sketch of the history of climatic cartography to the end of the Nineteenth Century, with excellent reproductions of the original documents.

Humboldt did not publish maps of isotherms for the individual months, though from his text one would judge that he drew some. DOVE [1848] published the first maps of mean monthly temperatures, but it was his great memoir [DOVE, 1852] that finally made maps of mean annual temperature obsolete. This memoir included, in addition, maps of thermal anomalies, local departures from the mean temperatures of the parallels of latitude. Maps of anomalies have been prepared from new world maps of temperature as they have been published, and have been a part of the cartographic stock in trade of climatology ever since Dove's time. More attention has been given them, in fact, than they deserve. Dove laid particular stress on the movement of isotherms over the Earth's surface in the course of the year, and so introduced a welcome kinetic element into discussion of the distribution of temperature. The isotherms that Dove thus followed in their annual pendulations represented, it is true, only monthly means; but it requires only a slight further effort of the imagination to extend the same concept to the movements of isotherms from day to day, or even from hour to hour. The details of the annual pendulation of certain critical isotherms northward and southward over Europe were later mapped by HILDEBRANDSSON [1880] and HÖGBOM [1883]. More recently VISHER [1944] has performed the same task for the United States, but in less detail.

Pressure--The first published map of mean pressure [RENOU, 1864] represented only the annual mean, and covered no more than France and adjoining parts of Europe. A Scot, BUCHAN, [1868, pl. 1-3] drew the first maps of mean monthly and annual pressure for the whole Earth: first for January, July, and the year, and soon afterward for all the months [BUCHAN, 1869, pl. 25-27]. His revisions of these maps, made for the Challenger reports [BUCHAN, 1889], and still later for the BARTHOLOMEW and HERBERTSON [1899] Atlas of Meteorology, long remained, as did his maps of mean monthly and annual temperature published in the same places, the standard for the English-speaking world. TEISSERENC DE BORT'S [1883] maps of mean pressure were probably more influential than Buchan's in contributing to a conception of the general circulation of the atmosphere, particularly because of his characterization of the great seasonal cyclones and anticyclones over the continents and oceans as "centers of action" of the atmosphere, his correlation of these centers of action with anomalies of temperature, and his computation of the distribution of pressure in the upper air [TEISSERENC DE BORT, 1887]. Later maps of pressure, such as those by GORCZYŃSKI [1917], have introduced only slight refinements of the maps made in the eighties and nineties of the last century.

Wind--Means or resultants of surface winds observed on land are rarely representative; it is therefore scarcely worth while to compute them, except for the purpose of elucidating local conditions. Winds observed at sea, on the other hand, especially those recorded on sailing ships in the Nineteenth Century, yield useful summaries. MAURY'S [1848-1860] Wind and current charts contained the first compilations of wind observations made at sea. From them stem the many charts of marine climatology that have been issued by official agencies since Maury's time. In the same period COFFIN [1853], another American, compiled wind observations from both land and sea; his collection of data from the Northern Hemisphere was published during his lifetime but his collection from the whole Earth did not appear until after his death, work on it having been completed by others [COFFIN, 1876].

The most convenient graphic device for representing frequencies from the several directions observed, the wind rose, was invented by a Frenchman, L. Brault, in the 1870's. In drawing his maps of seasonal winds over the oceans for the marine atlases of the DEUTSCHE SEEWARTE [1885, pp. 40-41; 1891, pl. 20 and 21; 1896, pl. 18 and 19], Köppen abandoned the wind rose for arrows that show, in addition to predominant direction, the strength and steadiness of the wind by their weight and continuity. Köppen's wind maps, though less useful than wind roses for estimating the probability of winds, undoubtedly give as good a representation of the mean motion of the air at the surface as is obtainable. They have been improved upon only through the use of color in the UNITED STATES WEATHER BUREAU'S [1938] Atlas of climatic charts of the oceans. WERENSKIOLD [1922] went further than Koppen in generalizing marine wind observations, by reducing the data of surface wind over the North Pacific Ocean to rigorous streamlines. It is doubtful, however, whether the original observations are good enough to warrant so precise a treatment. That consideration prompted DEPPERMANN [1935] to limit his reduction of surface winds over the South Pacific and Indian Oceans to the computation of resultants.

Cloudiness--Few compilations of cloudiness over the whole Earth have been made. The first set of maps of cloudiness for each month and the year, a highly creditable one, was made by TEISSERENC DE BORT [1886]. His map of mean annual cloudiness was revised for inclusion in the atlas of BARTHOLOMEW and HERBERTSON [1899, pl. 18], but his monthly maps were included without revision [pl. 17]. Apparently the only later compilation of mean monthly cloudiness over the entire Earth is that done for the maps published by SHAW [1928; ed. 2, 1936, fig. 73-97].

Precipitation--Because of its wide variation from place to place, particularly in rough country, the mapping of precipitation on a small scale presents great difficulty, which is only magnified as data from increasing numbers of stations are accumulated. The most instructive maps of precipitation are therefore those that represent only fractions of the Earth's surface.

The first world map of precipitation was published by BERGHAUS [1845, v. 1, pl. 9]. It did not bear isohyets (although the following plate, 10, is a map of Europe with isohyets of mean annual precipitation at intervals of five Parisian inches), but only shading, graduated in approximate ratio to annual precipitation. It was copied and imitated through a long series of years, even after the first world map of mean annual isohyets [LOOMIS, 1882], was published. Loomis's map was revise by Buchan [MURRAY, 1887], later by LOOMIS [1891] himself, and redrawn for HANN [1887, pl. 11]. At the end of the Nineteenth Century, two men undertook independently the construction of new world maps of precipitation: HERBERTSON [1899], who drew maps for each month and the year, which were also published by BARTHOLOMEW and HERBERTSON [1899, pl. 18 and 20]; and SUPAN [1898a] who prepared a map of mean annual precipitation, one for each of the four seasons, and one showing seasonal distribution.

Direct measurements of amount of precipitation are available only from the lands; routine marine observations record only frequency of occurrence. If a reasonable estimate can be made, from comparable data collected at coastal and insular stations, of the mean amount that falls on a rainy day, observations of frequency can be used for computing estimates of amounts. The first to attempt such computation was SUPAN [1898b], for the Atlantic and Indian Oceans. SCHOTT [1912, pl. 24; ed. 2, 1925, pl. 23] revised Supan's map of the Atlantic. Later SCHOTT [1933] made his own map of mean annual precipitation on the Indian and Pacific Oceans and included it in his Geographie des Indischen und Stillen Ozeans [SCHOTT, 1935, pl. 19]. MEINARDUS [1934] compiled from Schott's maps and the most recent ones showing precipitation on the continents a small-scale map of annual precipitation over the whole Earth, on which the detail is well adjusted to the scale of the map, and between the oceans and the lands. Seasonal maps of frequency of precipitation over the oceans were published by the UNITED STATES WEATHER BUREAU [1938, charts 95-106]. No one has yet attempted to prepare from them maps of seasonal amounts of precipitation on the oceans, though such a task would be no more difficult than Schott's estimation of the annual mean.

The scientific purpose of the never-ending compilation of new maps of means of the climatic elements and the revision of old ones in not always clear. The array of observational data is, of course, desirable. But the means plotted on maps are usually the kind of means castigated by Köppen in the opening quotation, above, "in which the most diverse situations are buried together." The descriptive value of such maps is undeniable, but they lend themselves to no more than the most general physical interpretation. The distribution of mean precipitation over a climatically homogeneous region during a single month, for example, may be the sum of the distributions produced by more than one kind of meteorologic process. It remains for the future to prepare maps of the climatic elements in which meteorologically homogeneous data, the observed results of definable meteorologic processes, are displayed.

Synoptic array of climatic data

If climatic maps of the familiar sort are unsatisfactory to the seeker after a physical understanding of the processes that yield the observations mapped, other ways of organizing the data are available. The segment of time under discussion here has seen the rise of a new kind of conceptual framework for grouping meteorologic facts, intermediate between the raw data of observation and general physical principles. JACOBS [1947] has recently given an outline of the categories, which in the present state of knowledge may be called "synoptic," that may be used for such arrays.

The use of categories of this order is not new. The first such category used as a frame of reference for observations was wind direction. The initial impetus to the association of observed states of the atmosphere with wind direction was given by von BUCH [1820], but it was the indefatigable Dove who pursued the method furthest and most persistently. In his first important publication [DOVE, 1827] he expressed the distribution of pressure, temperature, and vapor pressure at certain stations among the several wind directions by means of harmonic formulas. He developed the theme roundly, on the basis of numerous special investigations, in his Meteorologische Untersuchungen [DOVE, 1837]. In this book, the first part of which, Ueber den innern Zusammenhang der Witterungserscheinungen, is one of the best pieces of popular scientific writing to be found in the literature of meteorology, he uses [p. 18] a homely but effective simile to emphasize the dependence of air temperature on wind direction in the European winter: "Just as hot or cold water flows into the bathtub according to opposite settings of the faucets, so [the wind vane] regulates the temperature of the air bath." At this date Dove had much more evidence of the association of the elements of weather with wind direction than he had had a decade earlier, and Kämtz [1831 and 1832] brought together still more.

Dove's use of surface wind direction as the basis for grouping instrumental observations of weather was of course bound up with his conception of the circulation of the atmosphere in middle and high latitudes as an alternation of shifting currents of air blowing from northeast and southwest, a conception he maintained until his death in 1879. His scheme of circulation was generalized still further by a less cautious follower, **MÜHRY** [1862, 1865]. Mühry, whose copious writings repel the reader by their pretentiousness and dogmatism, thought that "the meteorologic mechanism of the Earth now stands in its entirety before our intellectual eyes," into which conception new facts would fall harmoniously. He traced his conceptual system of the meteorology of the Northern Hemisphere from close and accurate observations of local weather through analyses of weather situations (for which he coined the term "meteoration," a word that might profitably be disinterred) in Europe and North America to a system of radiating currents of air, alternately cold and warm, which flow from and toward poles, "not only poles of cold, but also poles of pressure and wind." The Northern Hemisphere has one such pole in summer, over the Arctic Ocean, but two in winter, as Brewster had argued many years before. The alternating cold and warm currents, arranged like the spokes of a wheel, maintain the exchange of air between low and high latitudes, and by pendulating back and forth produce the familiar changes in weather of the middle latitudes.

Mühry's place in the annals of science is deservedly an obscure one, although we use familiarly a term of his invention which he wrote "Geo-Physik." His accurate observations of the local weather associated with his "polar" and "anti-polar" currents, and particularly with the "boundaries" between them, should reserve that place, however small, for his memory. At the time when he was writing, synoptic meteorology was well under way in the United States, although its progress here was checked in the sixties by the Civil War. On the continent of Europe, Dove's massive influence held back adoption of the American conception of the cyclonic character of the storms of middle latitudes, and the definition of these storms by means of isobars, through the same years. The eclipse of Dove's scheme of circulation made obsolete the organization of observational data for climatologic purposes according to his conflicting currents, so that a paper by **HANN** [1870], which used Dove's interpretation, strikes the modern reader as an anachronism. Recognition of the relation of wind to the distribution of pressure, finally achieved about 1860, and the accumulation of synoptic charts provided new categories of a synoptic order by which observations might be arrayed: the cyclones and anticyclones of the daily weather map.

The first application of these fresh categories was made by **KÖPPEN** [1874], who at the time was a young unsalaried assistant at the Central Physical Observatory, St. Petersburg (now Leningrad). The protest concerning the arithmetic mean cited above is from this memoir. But he was not the first to utter such a protest; **HUMBOLDT** [1817] had protested against lumping together temperatures from all points about a parallel of latitude when there are in fact great differences about the circuit of the Earth. Dove's construction of maps of monthly temperature, motivated by his recognition of differences in the march of temperature through the year, and his sorting out of data by wind direction, were an implicit protest against "burying together" heterogeneous data in an arithmetic mean. From Humboldt on, one sees repeated efforts to group the data of observation into categories that are physically homogeneous, within which the arithmetic mean has representative significance.

Köppen's original intention was to work out the variation of the several climatic elements at St. Petersburg according to wind direction, as Dove and many others had done for nearly a half-century. But on second thought it became evident that the properties of air arriving as wind from a given direction differ, according to whether it has followed a cyclonic or anticyclonic path. "The condition that primarily determines the character of the weather produced by a wind is its trajectory; whence does the air come, over what kind of a route, and how rapidly?" Köppen had only two years of daily synoptic charts to work with, but proceeded to group the morning observations at St. Petersburg during these two years into six classes, depending on whether the station was on a straight, cyclonically curved, or anticyclonically curved isobar; in the center of an anticyclone or a cyclone; or in a region of indeterminate distribution of pressure. He divided the year into two seasons, October to March and April to September, and for each of the two seasons tabulated wind force, departure of pressure and temperature from the normal, relative humidity, cloudiness, and frequency of precipitation and fog, according to direction of surface wind and the relation of the station to the pressure field. "Two years," Köppen commented, "is a very short time, ... but by grouping [the observations] in the manner described the most important source of disturbance is eliminated." Three quarters of a century later we could improve on Köppen's synoptic climatolog only by suggesting that he use gradient winds rather than surface winds as his synoptic categories.

Rejecting the valid features of Dove's conception of atmospheric circulation along with the bad ones, meteorologists postponed for nearly two generations an insight into the structure of cyclones. Cyclones and anticyclones came to be conceived as nearly or quite radially symmetrical. Such a conception dominated the investigations of the distribution of weather phenomena about the centers of cyclones and anticyclones made in Sweden by HILDEBRANDSSON [1883] and under his direction [ÅKERBLOM, 1895; cf. also HILDEBRANDSSON and TEISSERENC DE BORT, 1898-1907, v. 2, pp. 1-144]. It is possible to defend the thesis that when cyclones and anticyclones became, in the minds of meteorologists, radially symmetrical "lows" and "highs" on weather maps, climatology and synoptic meteorology became separated, to the detriment of both. The stimulating essay of KÖPPEN [1874] in which he sought a "clear appreciation of the way in which climatologic means are built up out of individual situations," and of how the mean arises from these situations, was forgotten. Climatology retreated to the familiar and comfortable categories of place, year, month, and hour of the day, oblivious of the heterogeneity of the data averaged. Only in our time have steps been taken to reestablish connections between these two divisions of meteorology [for example, DINIES, 1932; JACOBS, 1947].

The physical basis of climate

That the larger climatic contrasts on the Earth depend on the reception of different daily amounts of radiation from the sun and that insolation is the basis of the diurnal and annual cycles of temperature has been a commonplace since antiquity. Once the physical and mathematical concepts required for obtaining numerical values of insolation in all latitudes and at all times of the day and year were invented, the computations required were largely a matter of mathematical ingenuity and labor. SCHMIDT [1830] attacked the problem by setting up an equation for the gain in heat by a unit area on the Earth's surface when exposed to solar radiation and loss of heat by outward radiation. But he could not evaluate his equation after integrating it over the daily period during which the Sun is above the horizon. Nothing was lost by this failure, since Schmidt had no adequate understanding of the relation between heat content and temperature. He therefore took refuge in an argument, from the form of his equation, that the mean temperature of the year can be expressed as a function of the square of the sine of the co-latitude of a place. He thus arrived at no more than one of the empirical expressions already in use. The most important names associated, during the Nineteenth Century, with the problem of calculating the amount of solar radiation received "at the outer limits of the atmosphere" through the day and year and in all latitudes are MEECH [1857], WIENER [1877] and ANGOT [1885]. These men could arrive at no more than relative values, since the intensity of the solar radiation outside the Earth's atmosphere was not known. When toward the end of the century plausible values of this quantity were determined, the older relative values could be changed into absolute quantities. In the Twentieth Century, the most thorough mathematical work on insolation has been performed by MILANKOVITCH [1920, 1930]; his results are likely to stand for a long time, although to a certain extent they, too, are only relative, since he used a value for the solar constant that is slightly in excess of its most probable value.

The actual amount of solar radiation that reaches the Earth's surface after passing through the atmosphere can not be determined deductively, except in such a rough manner as Angot and Milankovitch computed it, by assuming various coefficients of transmission. It must be found by measurement. Relative measurements of the intensity of solar radiation by means of clear and black-bulb thermometers go back to the very beginning of the Nineteenth Century [LESLIE, 1804]. Absolute measurements became possible only after a sound theory of heat was established and instruments for measuring weak electric currents were perfected. Pyrheliometers suitable for routine use are a technical achievement of the present century. Measurements of incident radiation from Sun and sky at an increasing number of stations have been accumulating for three decades [HAND, 1937]. KIMBALL [1928] has attempted, from the data of measurement and observed cloudiness, to map the distribution of insolation over the entire Earth at critical dates of the year.

Determination of the income of radiant energy from the Sun is only the first step in elucidating the heat economy of the atmosphere at different places on the Earth. The daily and annual cycles of accumulation and transfer of heat in the atmosphere, the water of the oceans, and the soil are as yet only imperfectly known. SIMPSON [1928a, 1928b, 1929] computed the radiation balance of the atmosphere of the Earth by ten-degree squares. The most elaborate investigation of the heat economy of the atmosphere is that by BAUR and PHILIPPS [1934, 1935, 1936]. Their work refers only to the Northern Hemisphere, and their results are broken down only into zones; they thus contribute little toward an understanding of the regime of temperature at any particular place. MILANKOVITCH [1930, p. 100] attempted to derive the daily cycle of temperature in general terms, but under simplifying assumptions. No one has yet derived the annual march of temperature from the numerous factors that determine it at any place.

An exceedingly important factor in the heat economy of the atmosphere and the surficial strata of water and soil is the horizontal transfer of heat and water vapor by the atmospheric circulation. The first conception of a general circulation of the atmosphere was arrived at intuitively [MAURY, 1850] from examination of the distribution of surface winds over the oceans. Maury's "diagram of the winds," and others equally schematic [HILDEBRANDSSON and TEISSERENC DE BORT, 1898-1907, v. 2, pp. 207-212, pl. 25], long afflicted climatologic literature with too simple a conception of an exceedingly complicated mechanism. The only useful role they played was to reduce the complications of the actual circulation to a simplicity that permitted a mathematical analysis of the average motions of the atmosphere. Thus Maury's scheme, defective as it was as a representation of the actual circulation of the atmosphere, provided FERREL [1859-1860] with a mechanical model sufficiently simple to be defined mathematically, and enabled him to start on his far-reaching formulations of atmospheric motions.

Once the physics of the atmosphere was fairly well worked out, it was inevitable that its principles be turned back to mean conditions. Hence the rise, in the thirties of the present century, of the expression "dynamic climatology." It can not be said that the ideas set forth by BERGERON [1930] in the article in which this expression was apparently first used lived up to the promise of its title. The concepts on which Bergeron built his proposals are of a synoptic rather than a dynamic order. His recommendation that air masses and fronts be used as climatologic categories are to be linked with Dove's climatic wind roses and Köppen's investigation of the climatic character of winds from different sources rather than with the main line of physical investigation of the mean state of the atmosphere. The paper by HESSELBERG [1932] on the working methods of a dynamic climatology deserves its title far better than does Bergeron's of 1930. Hesselberg investigated the conditions under which the equations that define instantaneous conditions can be applied to the mean state of the atmosphere, and the modifications that must be made in them if they are to be so applied.

It is scarcely to be expected that the dynamics of the gross mean conditions of the atmosphere will contribute to the understanding of more than a limited range of climatologic phenomena [BJERKNES, 1935]. Only in the upper atmosphere and within restricted areas of the lower atmosphere are the gross means representative. Means of homogeneous arrays of data, such as of typical synoptic situations over parts of the Earth's surface, however, might well be investigated by the procedures Hesselberg has pointed out. In general, climatology is likely to find empirical categories, related to synoptic meteorology, more useful than the general formulations of the dynamics of the atmosphere.

Climatic regions and types

The stage in the history of climatology in which the definition of climatic types and the construction of maps of climatic regions became fashionable coincides in time with the period of refinement of maps of means of the climatic elements and the alienation of climatology from dynamic and synoptic meteorology. To use a hackneyed expression, climatology became "static" after the yeasty middle third of the Nineteenth Century. Whatever may have been the shortcomings of Dove and his followers, they thought of the isarithms they drew on their maps as being constantly in motion; the positions in which they were drawn were only instantaneous. Dove liked to draw isotherms and isanomalous lines for January and July on the same maps, to indicate the extremes of their annual pendulation; and to have as many of his monthly maps as possible printed on the same sheet, so that the changes in position of the isotherms could be followed from one map to the next. In discussing the maps of mean monthly temperature in his memoir of 1852, Dove used, without self-consciousness, verbs that imply motion. The isotherms "sich bewegen," "wandern," "werden steiler," "sich verflachen," "sich zusammendrängen." Areas within closed isotherms expand, contract, merge, vanish. Herbertson, discussing his temperature maps in Bartholomew and Herbertson's "Atlas of Meteorology" at the end of the century, used words that imply fixity; his commonest predicate of "isotherm" is some form of the verb "to be." Perhaps the custom of printing isarithms as extremely thin lines separating solidly colored surfaces contributed toward giving them a stationary character.

The maps by MÜHRY [1862, 1865] of areas within which the seasonal regime of precipitation is approximately constant may have been the first maps of climatic regions. These maps were quickly forgotten, but Köppen's world map of precipitation regions defined in the same way, drawn for HANN

[1887, pl. 12] and revised by BARTHOLOMEW and HERBERTSON [1899, pl. 19] was widely circulated, especially in Bartholomew's general atlases. The first map of temperature regions was devised by SUPAN [1879, pl. 18]; it was widely disseminated in the same author's textbook of physical geography [1884, 1896, 1908]. In this map Supan attempted to rationalize the ancient "zones" by substituting mean annual isotherms of 10° and 20° C. for the tropics and polar circles as boundaries. He then divided each zone thus defined into two parts according to the occurrence of a winter or a summer, defined by mean monthly temperatures of the same values. In his textbook Supan included, in addition, a world map divided into unique climatic regions, each named from the common geographic designation of the area most nearly coincident with it. These climatic regions were defined in various ways, according to local peculiarities of climate; and few of their boundaries were defined and reproducible climatic isarithms. Their definition and extent therefore depended on Supan's subjective judgment.

Supan's map of 1879 was a challenge to Köppen, who in the same year [KÖPPEN, 1884] that saw the publication of Supan's textbook presented a far more sophisticated delineation of temperature zones than Supan had drawn. No criterion can be found in temperature data themselves for the division of the Earth into regions. But, as Köppen [1900, p. 593] wrote later, "by the presence or abse of a certain taxonomic or physiologic group of organisms the predominantly quantitative contrasts recognized by climatologists are transformed into qualitative contrasts." Lest it seem that Koppen was guilty of an innovation in thus drawing into climatologic discussion criteria from a genetically unrelated field, it may be recalled that Humboldt in his time had been stimulated to investigate the distribution of mean temperature vertically and horizontally over the Earth's surface by his observations of the distribution of vegetation. Humboldt's observations, at the time when he constructed his map of isotherms, had been principally in the tropics, where seasonal variations in temperature are of no consequence. To Köppen, whose observations of vegetation had been made in Europe, seasonal changes were the essential element in the delineation of temperature zones. The character of the distinctions he recognized is sufficiently indicated by the precise wording of the title of his article. The temperature values he used in defining his regions, 10° and 20° C., are suspiciously schematic; but his separation of areas in which the mean monthly temperature remains above, between, or below these limits for longer or shorter periods called attention to the actual qualities of temperature seasons.

The next step in the elaboration of climatic classifications was taken by HULT [1892-1893, 1894] Hult's climatic divisions of the Earth are, like Supan's, unique regions, not areas occupied by types of climate that recur in different parts of the Earth; but he grouped them into large classes defined by mean annual temperatures of 10° and 20° C. His divisions of the second order, "realms," are distinguished according to seasonal distribution of precipitation. Some of his smallest divisions, "provinces," are drawn on the basis of seasonal temperatures, some according to a combination of temperature and aridity. For many of his boundaries Hult used definite numerical values.

The term "classification of climates" appears for the first time in the title of the article in which KÖPPEN [1900] returned to the problem of climatic types. The relation to vegetation of the types defined is expressly confessed in that title; most of the types, in fact, are named after some characteristic plant or habit of plant growth. The roots of the classification, in Köppen's article of 1884 and his map of types of seasonal distribution of precipitation are, however, readily recognizable. In Köppen's article of 1900 the concept of the climatic type, an aggregation of defined climatic qualities that recurs in different parts of the Earth, takes form. That form is distinct from the vaguer use of the term to designate such contrasts as those between continental and maritime, mountain and lowland climates, which had long been familiar and which were used in Hann's contemporary *Handbuch*. Köppen's types are defined by numerical values of mean monthly and annual temperature and precipitation, many of which are far from the schematic multiples of five that appeared in his article of 1884. The broad basis of his classification of climates is a classification of vegetation, due to Alphonse de Candolle, according to its requirements or tolerance of temperature and drought. The greatest difficulty Köppen encountered in fitting climatic data to the distribution of vegetation was in the definition of drought; and he here devised the first of the often awkwardly formulated definitions of aridity that he tinkered with almost to the end of his long life. Here, too, the class of dry climates was first raised to a rank coordinate with that of the traditional classes distinguished on the basis of temperature; and a fivefold division of the range of climates on the Earth was introduced: A, the winterless climates; B, the dry climates; C, the climates with only a mild winter; D, the climates with severe winter but a distinct summer; and E, the summerless climates. The capital letters, it may be remarked, were borrowed from de Candolle, to whom they represented classes of plants, not of climates. Köppen's classification of 1900 never came into general use; its principal claim to a place in the history of climatology is as a long step toward the classification he published eighteen years later, which has become known as *the* KÖPPEN [1918] classification of climates.

In 1900, Köppen tried to find an empirical relation between climate and vegetation that could serve in defining climatic types and regions. PENCK [1910] advanced the proposition that climate impresses itself so distinctly on the landscape that a classification of the climates of the lands can be set up even without instrumental observations. The critical question Penck asked was, "What happens to the precipitation that falls on the land?" From this point of view, three major types of climate can be recognized: (1) humid climates, in which more precipitation falls in the average year than is disposed of by evaporation, so that there is an excess that flows off in the form of streams; (2) nival climates, in which more snow falls than can be disposed of by ablation, leaving an excess that flows off in the form of glaciers; and (3) arid climates, in which evaporation from the land surface disposes of all the precipitation that falls, and could dispose of even more, so that the flow of streams that enter arid climates from neighboring humid regions diminishes. It is not necessary to follow Penck into his subdivisions, defined by the seasonal distribution of precipitation and temperature, of these major classes. He drew no map to show the extent and boundaries of the areas occupied by his types on the lands of the Earth, but the insight into the water economy of the land that he provided has become a constituent of all later discussions of climate.

Penck's ideas were eagerly adopted by Köppen, and incorporated into the classification of climates he proposed in 1918. The distinctions Penck made between the nival and humid climates on the one hand, and between the humid and arid climates on the other, were obviously better than the corresponding distinctions Köppen had set up on the basis of poorly defined forms of vegetation in 1900. Hence Köppen was able to make his new classification "more climatologic" than his earlier one. He retained his five major classes, and the first five capital letters as designations of them. He abandoned the designation of types by names of plant forms, for the simple reason that these names had found no acceptance; and substituted instead minuscule letters, except for the divisions of the B and E climates according to the intensity of the distinguishing features of these classes, namely drought and cold respectively. This system of nomenclature was a flexible one, which could be carried to any desired degree of detail. There remained, however, the difficult problem of finding in mean monthly temperature and precipitation, or, for the B (dry) climates, in some combination of the two, critical values that would match the conceptual boundaries of the climatic types. In successive publications, KÖPPEN [1923, 1931, 1936] modified his definitions of the dry climates, without ever finding a satisfactory solution of the problem.

Köppen's classification of 1918 achieved an astonishing popularity, particularly as a pedagogic device. It found its way, either in the form in which it came from its author's hand or in transparent disguise, into many textbooks; and its literal symbols became for many students as familiar as the chemical symbols of common substances. It was applied in detail to restricted areas of the Earth's surface, and often modified to suit the particular conditions found in those areas; and since its author's death his world map has undergone a general revision [ANGERVO, 1944]. The reasons for all this attention are not immediately evident, except for the pedagogic use of the classification. Here it undoubtedly has a value, since, although in many respects arbitrary, it does systematize the characteristics of the climates of the Earth according to an easily remembered scheme.

But if the problem of correlating climate with the inorganic and organic features of the Earth's surface is taken seriously, Köppen's classification falls far short of the ideal. Perhaps it is too much to ask of standardized observations of temperature and precipitation that they yield numerical values that are critical in the physical and chemical processes that go on in the surface layers of the land and in plants. Dissatisfaction with Köppen's classification has found its most conspicuous expression in the formulation of a new classification by THORNTHWAITE [1931, 1933]. Thornthwaite, like Penck, adopted the fate of the water that falls on the Earth as the basis of his classification; and, reversing the tradition of centuries, relegated temperature to secondary rank among the qualities that distinguish climates. He sought a more rational basis for evaluating the data of mean monthly temperature and precipitation as criteria of relative dryness of climates than Köppen had found. The means he devised is based on a comparison of monthly amounts of evaporation from a free water surface with precipitation and mean temperature during the same month. From these three quantities he found an empirical relation between the ratios of precipitation to evaporation and precipitation to temperature in the same months, which yields a measure of the relative "effectiveness" of the precipitation that falls at different temperatures. The scale of "effectiveness" of precipitation is divided empirically according to the coincidence of its distribution over the land with the distribution of vegetation and climatic soil types. The range of mean monthly temperature is divided in an analogous manner. Climatic types are defined by the superposition of the scales of "effectiveness" of precipitation and "efficiency" of temperature.

Thornthwaite's criterion of dryness of climates has been revised both by other hands [SETZER, 1946] and more recently by his own [THORNTHWAITE, 1948]. His measure of relative dryness, when compared with the distribution of physical and organic phenomena of the land surfaces, seems to reflect the actual variation of the moisture factor of climate in so far as it depends on precipitation and temperature, certainly the most important factors. His latest formulation of the classification is still to be tested.

It is evident from the last few paragraphs that the attempts that have been made to classify climates have led climatologists off the main path of meteorologic science. By seeking norms of organization in phenomena other than the atmospheric, the classifiers of climate have passed into the realm of applied climatology, which must adapt its methods to non-atmospheric phenomena, the more accurately the better. Their mistake has probably been that they have attempted to make their classifications all things to all men, in a field where each relation between the independant variable climate and dependent variables - the physiology of plants, the weathering of rocks, or an economic activity - is highly specific. Any formulation broad enough to be applicable to all such relations is so general as to be meaningless in a specific application.

One attempt has been made [MARKUS, 1935] to draw a map of climatic regions of the Earth solely on the basis of the distribution of mean temperature and precipitation in the extreme months of the year. Detailed maps of these quantities display zones in which the rate of change along the surface of the Earth normal to the isarithms is great, and which separate more extensive areas over which change is gradual. Such zones coincide with steep slopes of mountains or plateaus, and with coast lines; or with both along mountainous coasts; and on the surface of the oceans with convergences of cold and warm water masses. Markus used these zones of rapid transition, as far as they go, as boundaries between climatic regions. Since the zones of rapid transition are discontinuous, except along some coast lines, Markus had to help himself over the areas within which transitions are gradual by using selected isotherms and isohyets as connections between the zones of rapid transition. Such boundaries are of course inevitably unconvincing. It is sufficient to recognize sharp transitions where they exist, as CONRAD [1946, p. 149] has done with his emphasis on the climatic incoherence of some neighboring regions.

Climatic history

Folklore concerning changes in climate in historic time, or even within human memory, is apparently ubiquitous and perennial. Ever since instrumental records of climate became long enough to provide perspective, these records have been scrutinized for evidence of secular change. The literature dealing with the question is enormous, and I am neither sufficiently familiar with it to make an intelligent selection nor sufficiently well informed to pass an intelligent judgment on its validity. No account of the recent history of climatology, however, would be complete without some mention of it. The soundest results of investigation of past climates have been achieved in Scandinavia, so that it is not inappropriate to mention first the academic address of EHRENHEIM [1824]. Ehrenheim could make use of a number of long records kept at European stations, and from his examination of them he concluded that since the middle of the Eighteenth Century winters had become milder and summers cooler. As records have become longer, they have been constantly subjected to scrutiny of the same sort that Ehrenheim exercised. Trends such as he discovered have been found in many records; the one that is most conspicuous is a general rise in winter temperature in the high latitudes of the Northern Hemisphere, especially about the North Atlantic [AHLMANN, 1947]. Attempts to find "cycles" in the records, by which future changes might be predicted, have been unsuccessful. Since the period covered by instrumental records is brief, general historical and archeologic records have been searched for evidence of possible changes in climate [for example, BRÜCKNER, 1890; PETTERSSON, 1913; HELLAND-HANSEN, 1920; EASTON, 1928; NORDHAGEN, 1933]. The results obtained by the examination of historical data are more equivocal than those derived by the methods of the natural sciences, but are not without value as evidence.

With the rise of geology in the Nineteenth Century, perspective into past time was enormously lengthened, and new kinds of evidence of past climates became available. In particular, recognition that large parts of Europe and North America, now free of ice, had been covered by glaciers in the not too remote geologic past provided a strong stimulus to the investigation of Pleistocene and Recent climates by geologic methods. The hard-headed geologic principle of explaining the past by what can be observed in the present failed here, since no consistent change in present climates had been observed. Geologic evidence concerning Quaternary climates has been brought together at a symposium held at the Eleventh International Geological Congress [1910], in a more recent symposium of less international character [TROLL, 1944], and in a recent review [ZEUNER, 1945]. Only in northern Europe have the late glacial and postglacial changes in climate been worked out with dependable results; the key to the success of the Scandinavian scientists in this difficult field is their possession of a good chronology [DE GEER, 1940].

Since no grounds have been found in the behavior of the Earth's solid, liquid, or gaseous constituents that are adequate to account for the changes of climate that have occurred in the past, recourse has been had to postulated changes in the rate of reception of radiant energy from the Sun. MILANKOVITCH [1930, 1938] has provided, in the form of curves that show the radiation received by the Earth in all latitudes during the last 600,000 years, the physical canon by which Pleistocene and Recent changes in climate are at present being interpreted.

Much work remains to be done before a definitive climatic history of the Earth through Quaternary times can be written. The investigator of present climates can take a larger share in this work than he has taken in the past, by applying what can be learned about current fluctuations to changes of the same character that are recorded in geologic evidence. From persistent types of weather - cold or mild winters, periods of drought or excessive precipitation - judgments can be derived concerning the nature of the circulation of the atmosphere that must have prevailed when similar departures from present averages persisted through long periods in the past.

References

AHLMANN, H. W:SON, Den nutida klimatfluktuationen och dess utforskande, Norsk Geogr. Tidsskr., v. 11, pp. 290-326, 1947.

ÅKERBLOM, PH., Sur la distribution, à Vienne et à Thorshavn, des éléments météorologiques autour des minima et des maxima barométriques, Sv. Vetensk.-Akad. Handl., Bihang, v. 20, avd. 1, no. 3, 1895.

ANGERVO, J. M., Eine neue Klimakarte der Erde nach der Köppenschen Klassifikation, Mitt. d. Meteor. Zentralanst. (Finland), no. 23, 1944.

ANGOT, ALFRED, Recherches théoriques sur la distribution de la chaleur à la surface du globe, Ann. Bur. Cent. Mét. France, ann. 1883, pt. 1, pp. B121-B169, 1885.

BARTHOLOMEW, J. G., and HERBERTSON, A. J., Atlas of meteorology (Bartholomew's physical atlas, v. 2), Westminster, 1899.

BAUR, F., and PHILIPPS, H., Der Wärmehaushalt der Lufthulle der Nordhalbkugel im Januar und Juli und zur Zeit der Äquinoktien und Solstitien, 1: Die Einstrahlung bei normaler Solarkonstante, Beitr. Geophys., v. 42, pp. 160-207, 1934; 2: Ausstrahlung, Gegenstrahlung und meridionaler Wärmetransport bei normaler Solarkonstante, ibid., v. 45, pp. 82-132, 1935; 3: Zwischenbemerkung, ibid., v. 47, pp. 218-223, 1936.

BERGERON, TOR, Grundlinien einer dynamischen Klimatologie, Met. Zs., v. 47, pp. 246-262, 1930.

BERGHAUS, HEINRICH, Physikalischer Atlas, v. 1, Gotha, 1845.

BESSEL, FRIEDRICH WILHELM, Review of A. F. von KRUSENSTERN, Reise um die Welt . . . (1812), Jenaische Allgemeine Literatur-Zeitung, no. 231, pp. 409 ff., 1814 (not seen; cited after BESSEL, 1828.)

BESSEL, FRIEDRICH WILHELM, Ueber die Bestimmung des Gesetzes einer periodischen Erscheinung, Astr, Nachr., v. 6, pp. 333- , 1828; Abhandl. v. F. W. Bessel, v. 2, pp. 364-372, Leipzig, 1876.

BJERKNES, J., La circulation atmosphérique dans les latitudes sous-tropicales, Scientia, v. 57, pp. 114-123, 1935.

BLODGET, LORIN, Climatology of the United States and of the temperate latitudes of the North American continent, Philadelphia, 1857.

BREWSTER, DAVID, Observations of the mean temperature of the globe, Trans. R. Soc. Edinburgh, v. 9, pp. 201-225, 1821.

BROOKS, C. E. P., Continentality and temperature, Q. J. R. Met. Soc., v. 43, pp. 159-173, 1917.

BRÜCKNER, EDUARD, Klimaschwankungen seit 1700 . . ., Geogr. Abhandl., v. 4, no. 2, 1890.

BUCHAN, ALEXANDER, Handy book of meteorology, ed. 2, Edinburgh and London, 1868.

BUCHAN, ALEXANDER, The mean pressure of the atmosphere and the prevailing winds over the globe. for the months and for the year, part II, Trans. R. Soc. Edinburgh, v. 25, pp. 575-637, 1869.

BUCHAN, ALEXANDER, Report of atmospheric circulation in Report on the scientific results of the voyage of H. M. S. Challenger . . . , Phys. and Chem., v. 2, maps 27-52, 1889.

COFFIN, JAMES H., Winds of the Northern Hemisphere, Smiths. Contrs. Knowl., v. 6, no. 6, 1853.

COFFIN, JAMES H., Winds of the Earth, Smiths. Contrs. Knowl., v. 20, 1876.

CONRAD, VICTOR, Methods in climatology, Cambridge, Mass., 1946.

DEPPERMANN, CHARLES E., The mean transport of air in the Indian and south Pacific Oceans, Comm. Philipp., Weather Bur., Cent. Manila Observ., 1935.

DE GEER, GERARD, Geochronologica suecica. Principles. Sv. Vetensk.-Akad. Handl., ser. 3, v. 18, no. 6, 1940.

DEUTSCHE SEEWARTE, Segelhandbuch für den Atlantischen Ozean, Hamburg, 1885.

DEUTSCHE SEEWARTE, Indischer Ozean; ein Atlas . . . , Hamburg, 1891.

DEUTSCHE SEEWARTE, Stiller Ozean; ein Atlas . . . , Hamburg, 1896.

DINIES, ERWIN, Luftkörper-Klimatologie, Arch. Deutschen Seewarte, v. 50, no. 6, 1932.

DOVE, HEINRICH WILHELM, Einige meterologische Untersuchungen über den Wind, An. Phys. und Chem., v. 11, pp. 545-590, 1827.

DOVE, HEINRICH WILHELM, Meteorologische Untersuchungen, Berlin, 1837.

DOVE, HEINRICH WILHELM, Temperaturtafeln nebst Bemerkungen über die Verbreitung der Wärme auf der Oberfläche der Erde und ihre jährlichen periodischen Veränderungen, Berlin, 1848.

DOVE, HEINRICH WILHELM, Die Verbreitung der Wärme auf der Oberfläche der Erde erläutert durch Isothermen, thermische Isanomalien und Temperaturkurven, Berlin, 1852.

EASTON, C., Les hivers dans l'Europe occidentale, Leyden, 1928.

EHRENHEIM, FREDRIK WILHELM, Om climaternas rörlighet, tal hallet vid presidii nedläggande uti Kongl. Vetenskaps Academie, Stockholm, 1824.

FERREL, WILLIAM, The motions of fluids and solids relative to the Earth's surface, Math. Mon., v. 1, pp. 140-148, 210-216, 300-307, 366-373, 397-406, 1859; v. 2, pp. 89-97, 339-346, 374-390, 1859-1860.

FORBES, JAMES D., Inquiries about terrestrial temperature . . . , Trans. R. Soc. Edinburgh, v. 22, pp. 75-100, 1861.

GORCZYŃSKI, W., Pression atmosphérique en Pologne et en Europe, pls. 28-40, Warszawa, 1917.

GORCZYŃSKI, L., Sur le calcul du degré du continentalisme et son application dans la climatologie, Geogr. An., v. 2, pp. 324-331, 1920.

HAND, IRVING F., Review of United States Weather Bureau solar radiation investigations, Mon. Wea. Rev., v. 65, pp. 415-441, 1937.

HANN, JULIUS, Untersuchungen über die Winde der nördlichen Hemisphäre und ihre klimatologische Bedeutung, SitzBer. Akad. Wiss. Wien, math.-naturw. Kl., v. 60, Abt. 2, pp. 162-228, 1870.

HANN, JULIUS, Handbuch der Klimatologie, Stuttgart, 1883; ed. 2, 3 v., 1897; ed. 3, 3 v., 1908-1911.

HANN, JULIUS, Atlas der Meteorologie (Berghaus' Physikalischer Atlas, v. 3), Gotha, 1887.

HANN, JULIUS, Handbuch der Klimatologie, v. 1, ed. 4, rev. by Karl Knoch, Stuttgart, 1932.

HELLAND-HANSEN, BJØRN, and NANSEN, FRIDTJOF, Temperature variations in the north Atlantic Ocean . . . , Smiths. Inst., Misc. Coll., v. 70, no. 4, 1920.

HERBERTSON, ANDREW J., The distribution of rainfall over the land, London, 1899.

HESSELBERG, TH., Arbeitsmethoden einer dynamischen Klimatologie, Beitr. Phys. freien Atm., v. 19, pp. 291-305, 1932.

HILDEBRANDSSON, H. HILDEBRAND, Marche des isothermes au printemps dans le nord de l'Europe, Nova Acta Soc. Reg. Scient. Upsal., ser. 3, v. 11, no. 3, 1880.

HILDEBRANDSSON, H. HILDEBRAND, Sur la distribution des éléments météorologiques autour des minima et des maxima barométriques, Nova Acta Reg. Soc. Scient. Upsal., ser. 3, v. 12, no. 6, 1883.

HILDEBRANDSSON, H. HILDEBRAND, and TEISSERENC DE BORT, LÉON, Les bases de la météorologie dynamique: historique, état de nos connaissances, Paris, 2 v., 1898-1907.

HÖGBOM, A. G., Marche des isothermes en automne dans le nord de l'Europe, Nova Acta Soc. Reg. Scient. Upsal., ser. 3, v. 12, no. 9, 1883.

HULT, RAGNAR, Jordens klimatområden. Försök till en indelning af jordytan efter klimatiska grönder, Vetenskapl. Med. Georg. Fören., Finland, v. 1, pp. 140-201, 1892-1893.

HULT, RAGNAR, Grunddragen af den allmänna geografin, v. 1, Matematiska geografi och klimatografi, pp. 147-186, pl. 12, Helsingfors, 1894.

HUMBOLDT, ALEXANDER von, Des lignes isothermes et de la distribution de la chaleur sur le globe, Mém, de phys. et de chim. de la Soc. d'Arcueil, v. 3, pp. 462-602, 1817; also separate, with map, Paris, 1817. Eng. transl. by David Brewster, On isothermal lines, and the distribution of heat over the globe, Edinburgh Philos. J., v. 3, pp. 1-20, 256-274, 1820; v. 4, 23-37, 262-281, 1821; v. 5, pp. 29-39, 1821. Germ. transl., Von den isothermen Linien und der Verbreitung der Wärme auf dem Erdkörper, in **HUMBOLDT, ALEXANDER** von, Kleinere Schriften, v. 1, pp. 206-314, Stuttgart u. Tübingen, 1853. Neither translation is accompanied by the map. It has been reproduced a number of times, among other places in the following: **BRUHNS, KARL,** Alexander von Humboldt, eine wissenschaftliche Biographie, v. 3, p. 100, Leipzig, 1872; **HELLMANN, G.,** Neudrucke von Schriften und Karten über Meteorologie und Erdmagnetismus, no. 8, Berlin, 1897; **MEINARDUS, WILHELM,** 1899, op. cit., pl. 1; **HILDEBRANSSON, H. HILDEBRAND, and TEISSERENC DE BORT, LÉON,** Les bases de la météorologie dynamique, v. 1, pl. 23, 1907; **WOOLARD, EDGAR W.,** Historical notes on charts of temperature, pressure, and winds over the surface of the Earth, Mon. Wea. Rev., v. 48, pp. 408-411, 1920; **SHAW, NAPIER,** Manual of meteorology, v. 1, Meteorology in history, pp. 260-261, Cambridge, 1926.

INTERNATIONAL GEOLOGICAL CONGRESS (Eleventh), Die Veränderungen des Klimas seit dem Maximum der letzten Eiszeit, Stockholm, 1910.

JACOBS, WOODROW C., Wartime developments in applied climatology, Met. Monogr., v. 1, no. 1, 1947

KÄMTZ, LUDWIG FRIEDRICH, Lehrbuch der Meteorologie, Halle, v. 1, 1831; v. 2, 1832.

KIMBALL, HERBERT H., Amount of solar radiation that reaches the surface of the Earth on the land and on the sea, and methods by which it is measured, Mon. Wea. Rev., v. 56, pp. 393-399, 1928.

KÖPPEN, W., Über die Abhängigkeit des klimatischen Charakters der Winde von ihrem Ursprunge, Rep. Met., v. 4, no. 4, 1874.

KÖPPEN, W., Die Wärmezonen der Erde, nach der Dauer der heissen, gemässigten und kalten Zeit, und nach der Wirkung der Wärme auf die organische Welt betrachtet, Met. Zs., v. 1, pp. 215-226, pl. 4, 1884.

KÖPPEN, W., Versuch einer Klassifikation der Klimate, vorzugsweise nach ihren Beziehungen zur Pflanzenwelt, Geogr. Zs., v. 6, pp. 593-611, 657-679, pls. 6-7, 1900.

KÖPPEN, W., Klassifikation der Klimate nach Temperatur, Niederschlag und Jahreslauf, Pet. Mitt., v. 64, pp. 193-203, 243-248, pls. 10-11, 1918.

KÖPPEN, W., Die Klimate der Erde, Berlin and Leipzig, 1923.

KÖPPEN, W., Grundriss der Klimakunde, Berlin and Leipzig, 1931.

KÖPPEN, W., Das geographische System der Klimate, in KÖPPEN, W., and GEIGER, R., (ed.), Handbuch der Klimatologie, v. 1, pt. C, Berlin, 1936.

KÖPPEN, W., and GEIGER, R. (ed.), Handbuch der Klimatologie, Berlin, 1930. . .

LESLIE, JOHN, An experimental inquiry into the nature and propagation of heat, pp. 409-471, London, 1804.

LOOMIS, ELIAS, Contributions to meteorology . . . , 16th paper; mean annual rainfall for different countries of the globe, Amer. J. Sci., ser. 3, v. 23, pp. 1-25, map, 1882.

LOOMIS, ELIAS, Contributions to meteorology, Mem. Nat. Acad. Sci., v. 5, pp. 21-109, pl. 33, 1891.

MARKUS, EDUARD, Klimatische Grenzlinien, An. Hydr. u. marit. Met., v. 63, pp. 144-155, 1935.

MAURY, M. F., Wind and current charts, Washington, 1848-1860.

MAURY, M. F., On the general circulation of the atmosphere, Proc. Amer. Assoc. Adv. Sci., v. 3, pp. 126-147, 1850.

MEECH, L. M., On the relative intensity of the heat and light of the Sun upon different latitudes of the Earth, Smiths. Contr. Knowl., v. 9, no. 2, 1857.

MEINARDUS, WILHELM, Die Entwickelung der Karten der Jahres-Isothermen von Alexander von Humboldt bis auf Heinrich Wilhelm Dove, in Wissenschaftliche Beiträge zum Gedächtniss der hundertjährigen Wiederkehr des Antritts von Alexander von Humboldts Reise nach Amerika am 5. Juni 1799, Gesellsch. f. Erdk., Berlin, 1899.

MEINARDUS, WILHELM, Eine neue Niederschlagskarte der Erde, Pet. Mitt., v. 80, pp. 1-4, pl. 1, 1934.

MILANKOVITCH, M., Théorie mathématique des phénomènes thermiques produits par la radiation solaire, Paris, 1920.

MILANKOVITCH, M., Mathematische Klimalehre und astronomische Theorie der Klimaschwangungen, in KÖPPEN, W., and GEIGER, R. (ed.), Handbuch der Klimatologie, v. 1, pt. A, Berlin, 1930.

MILANKOVITCH, M., Astronomische Mittel zur Erforschung der erdgeschichtlichen Klimate, in GUTENBERG, B. (ed.), Handbuch der Geophysik, v. 9, pp. 593-698, Berlin, 1938.

MÜHRY, ADOLF, Klimatographische Uebersicht der Erde . . . , Leipzig and Heidelberg, 1862.

MÜHRY, ADOLF, Supplement zur Klimatologischen Uebersicht der Erde . . . , Leipzig and Heidelberg, 1865.

MURRAY, JOHN, On the total annual rainfall on the land of the globe, and the relation of rainfall to the annual discharge of rivers, Scott. Geogr. Mag., v. 3, pp. 65-77, 1887.

NORDHAGEN, ROLF, De senkvartaere klimavekslinger i Nordeuropa og deres betydning for kulturforskningen, Instituttet for Sammenlignende Kulturforskning, ser. A, no. 12, 1933.

PENCK, ALBRECHT, Versuch einer Klimaklassifikation auf physiogeographischer Grundlage, SitzBer. Akad. Wiss. Berlin, 1910, v. 1, pp. 236-246, 1910.

PETTERSSON, OTTO, Klimatförändringar i historisk och forhistorisk tid. En studie i geofysik, Sv. Vetensk.-Akad. Handl., v. 51, no. 2, 1913.

RENOU, E., Hauteurs moyennes du baromètre en France, Ann. Soc. Mét. France, v. 12, pt. 2, pp. 240-244, pl. 5, 1864.

SCHMIDT, J. C. EDUARD, Lehrbuch der mathematischen und physischen Geographie, v. 2, pp. 351-356, Göttingen, 1830.

SCHOTT, GERHARD, Geographie des Atlantischen Ozeans, Hamburg, 1912; ed. 2, 1925.

SCHOTT, GERHARD, Die jährlichen Niederschlagsmengen auf dem Indischen und Stillen Ozean, An. Hydr. u. marit. Met., v. 61, pp. 1-12, pl. 1, 1933.

SCHOTT, GERHARD, Geographie des Indischen und Stillen Ozeans, Hamburg, 1935.

SETZER, JOSÉ, A new formula for precipitation effectiveness, Geogr. Rev., v. 36, pp. 247-263, 1946.

SHAW, NAPIER, Manual of meteorology, v. 2, Comparative meteorology, Cambridge, 1928, ed. 2, 1936

SIMPSON, G. C., Some studies in terrestial radiation, Mem. R. Met. Soc., v. 2, no. 16, pp. 69-95, 1928a.

SIMPSON, G. C., Further studies in terrestrial radiation, Mem. R. Met. Soc., v. 3, no. 21, pp. 1-26, 1928b.

SIMPSON, G. C., The distribution of terrestrial radiation, Mem. R. Met. Soc., v. 3, no. 23, pp. 53-78, 1929.

SPITALER, R., Klimatische Kontinentalität und Ozeanität, Pet. Mitt., v. 68, p. 113, 1922.

SUPAN, ALEXANDER, Die Temperaturzonen der Erde, Pet. Mitt., v. 25, pp. 349-358, 1879.

SUPAN, ALEXANDER, Grundzüge der physischen Erdkunde, Leipzig, 1884; ed. 2, 1896; ed. 3, 1908.

SUPAN, ALEXANDER, Die Verteilung des Niederschlags auf der festen Erdoberfläche, Pet. Mitt., Erg.-Heft 123, 1898a.

SUPAN, ALEXANDER, Die jährlichen Niederschlagsmengen auf den Meeren, Pet. Mitt., v. 44, pp. 179-182, pl. 13, 1898b.

TEISSERENC DE BORT, LÉON, Cartes des isothermes et isobares à la surface du globe en janvier, mars, juillet, octobre, An. Bur. Cent. Mét., France, ann. 1881, pt. 4, pp. 1-62, 8 maps, 1883.

TEISSERENC DE BORT, LÉON, Étude sur la distribution moyenne de la nébulosité à la surface du globe, d'après les premières cartes d'isonèphes, An. Bur. Cent. Mét. France, an. 1884, pt. 4, pp. 27-66, pls. 2-14, 1886.

TEISSERENC DE BORT, LÉON, Étude sur la circulation générale de l'atmosphère, An. Bur. Cent. Mét. France, an. 1885, pt. 4, pp. 35-44, pls. 6-14, 1887.

THORNTHWAITE, C. W., The climates of North America according to a new classification, Geogr. Rev., v. 21, pp. 633-655, pl. 3, 1931.

THORNTHWAITE, C. W., The climates of the Earth, Geogr. Rev., v. 23, pp. 433-440, pl. 5, 1933.

THORNTHWAITE, C. W., An approach toward a rational classification of climate, Geogr. Rev., v. 38, pp. 55-94, pl. 1, 1948.

TROLL, CARL (ed.), Dilulial-Geologie und Klima, Geol. Rundschau, v. 34, pp. 307-776, 1944.

UNITED STATES WEATHER BUREAU, Atlas of climatic charts of the oceans, Washington, 1938.

VISHER, STEPHEN S., When American seasons begin, Sci. Mon., v. 59, pp. 363-369, 1944.

von BUCH, LEOPOLD, Ueber barometrische Wind-Rosen, Abhandl. d. Akad. d. Wiss. Berlin a. d. J. 1818-1819, pp. 104-110, 1820.

WERENSKIOLD, W., Mean monthly air transport over the north Pacific Ocean, Geofys. Pub., v. 2, no. 9, 1922.

WIENER, CHR., Ueber die Starke der Bestrahlung der Erde durch die Sonne in ihren verschiedenen Breiten und Jahreszeiten, Zs. Math. Phys., v. 22, pp. 341-368, 1877.

ZEUNER, FREDERICK E., The Pleistocene period: its climate, chronology and faunal successions, London, Ray Society, 1945.

University of California,
Berkeley, California

(Communicated manuscript received January 28, 1949; related to the Report of the Committee on Climatology, 1947-1948 [see Trans. June 1949, pp. 439-443]; open for formal discussion until March 1, 1950.)

Transactions, American Geophysical Union Volume 30, Number 5 October 1949

PREDICTION OF SUNSPOT NUMBERS

A. G. McNish and J. V. Lincoln

Abstract--A formula for predicting smoothed annual sunspot numbers is developed. A first approximation to the prediction of a future value in a cycle is the mean of all past values for that part of the cycle. This estimate can be improved by adding to the mean a correction proportional to the departure of earlier values of the cycle from the mean cycle. These correction factors are determined by the method of least squares. Sunspot data for 1834 through 1943 are used, and statistical reasons for rejecting data of earlier years are presented. Reliability of the method is discussed on the basis of the standard deviations of predictions made for each of the years of the ten cycles in question, using all the prediction formulas developed. The prediction of three-month means is also discussed.

Introduction--Since the discovery of the sunspot cycle by Schwabe in 1851, considerable interest in forecasting the trend of future cycles has been exhibited by a number of investigators [YULE, 1927; DURKEE, 1937; CLAYTON, 1939; SCHUSTER, 1906, 1910-1911; STEWART and PANOFSKY, 1938; STEWART and EGGLESTON, 1939, 1940; GLEISSBERG, 1944; LINDER, 1945; SHAPLEY, 1944; WALDMEIER, 1941, p. 120; 1946]. The methods of prediction previously used have covered a wide range, including harmonic analysis, assumption that cycles repeat after a number of years, and numerous empirical relationships between heights of maxima, rate of rise, and other factors. Until recently these predictions were largely of academic interest, but with the discovery of the close relationships which exist between radio propagation conditions and sunspot activity the prediction of sunspot numbers has assumed great practical importance.

It would be desirable to predict the ionospheric conditions directly, but that is not yet possible since ionospheric measurements do not extend much beyond one cycle of solar activity - not enough to be regarded as a fair sample of cyclic phenomena in the statistical sense. However, the Zürich relative sunspot numbers R constitute a highly homogeneous series extending back to 1849, while less reliable data extend the series back to 1749. Since the correlation is very high between relative sunspot numbers and ionospheric phenomena, for the interval during which the latter have been observed, conclusions reached from study of the sunspot data may be assumed to apply to the ionospheric phenomena as well.

The various formulas which have been developed for prediction of the sunspot cycle lead to widely different predictions. The originators of the various prediction methods do not give satisfactory estimates of the reliability of their formulas for the future. In the present paper a method that may be adapted to the prediction of the smoothed annual sunspot-numbers, or any other mean such as a three-month mean sunspot number is given with its reliability estimate.

Method--To develop a satisfactory formula for prediction of sunspots the following assumptions were made: (1) In a time series exhibiting cyclic tendencies an estimate, to a first approximation, of a future value in the series is the mean of all past values for the same part of the cycle; and (2) this estimate can be improved by adding to the mean a correction proportional to the departures of earlier values of the same cycle from their respective means, the factors of proportionality being determined by the method of least squares.

The prediction formula then becomes

$$R'_n = \bar{R}_n + \Delta R'_n = \bar{R}_n + k_{n-1}\Delta R_{n-1} + k_{n-2}\,\Delta R_{n-2} + \cdots\cdots k_{n-i}\Delta R_{n-i} + \cdots\cdots\cdots \quad (1)$$

in which R'_n is the smoothed annual value to be predicted in a particular cycle for the nth year after the minimum, $\bar{R}_n$ is the mean of all the nth values of R in preceding cycles, obtained by superposing past observed cycles with the time of minimum (n = o) coincident, ΔR_{n-i} is the departure of the particular R_{n-i} from $\bar{R}_{n-i}$, and k_{n-i} is a prediction coefficient to be calculated. The values of k_{n-i} are adjusted so that for each particular value of n

$$\sum_{1}^{N} (\Delta R_n - \Delta R'_n)_N^2 = \min \ldots\ldots\ldots\ldots \quad (2)$$

when the summation is taken over N cycles of past data. YULE [1926-1927] had used a somewhat similar regression equation to fit Zürich unsmoothed annual sunspot numbers for 1749-1924. Yule's work led to the following equation

$$R'_n = 1.34254\,R_{n-1} - 0.65504\,R_{n-2} + 13.854$$

In Yule's formula the subscript n refers to any arbitrary origin in the entire series and not to order of the year in a particular cycle. Later in this paper the comparative reliability of Yule's method and that presented here will be discussed. The significant difference in the two methods is that Yule used regression to the grand mean of all observed sunspot numbers while this one uses regression to a mean cycle ordered for the successive years after minimum.

To calculate k_{n-i}, the value of $\Delta R'_n$ computed by (1) is substituted in (2). This expression is differentiated with respect to each k_{n-i}. The results of this differentiation, equated to zero, produce the following array of simultaneous equations which must be solved to obtain the "best" value of each k_{n-i}. They are

$$\begin{aligned}
S_{n-1,n-1}k_{n-1} + S_{n-1,n-2}k_{n-2} + \dots + S_{n-1,n-i}k_{n-i} &= S_{n,n-1}\\
+ S_{n-2,n-2}k_{n-2} + \dots + S_{n-2,n-i}k_{n-i} &= S_{n,n-2}\\
+ \dots\quad &\\
+ S_{n-i,n-i}k_{n-i} &= S_{n,n-i}
\end{aligned}$$

in which $S_{n-j,n-i} = \sum_{1}^{N} (\Delta R_{n-j}\Delta R_{n-i})_N$.

An array of equations was formed for each desired period of the cycle and as many coefficients as were of interest were calculated. By arbitrarily setting any or several k_{n-i} equal to zero, coefficients were obtained for predicting any value from one particular preceding value of the cycle or from any combination of preceding values. Thus, to predict the smoothed annual sunspot number or $\Delta R'$ for the fourth year of the cycle, the coefficients were derived for a prediction based on values of R' for (1) the first, second, and third years, (2) the third year alone, (3) the second year alone, and for other combinations. Naturally, the coefficient for predicting from any given year depends upon what other years are used in the prediction.

Table 1--Years of sunspot minima for cycles 1-18

Cycle no.	Selected for this study	Selected by Zürich
1	1755.8	1755.2
2	1766.5	1766.5
3	1775.6	1775.5
4	1784.6	1784.7
5	1798.8	1798.3
6	1810.6	1810.6
7	1823.2	1823.3
8	1834.1	1833.9
9	1843.6	1843.5
10	1856.3	1856.0
11	1867.3	1867.2
12	1878.8	1878.9
13	1889.5	1889.6
14	1901.8	1901.7
15	1913.4	1913.6
16	1923.6	1923.6
17	1933.8	1933.8
18	1944.2	1944.2

The data employed for the computations were the smoothed twelve-month means of the Zürich relative sunspot numbers from 1834 to 1943. For reasons to be set forth later, data prior to 1834 were rejected. First, the beginning of each cycle to the nearest tenth of year was selected, each cycle being assumed to begin at the point of minimum sunspot number, obtained by passing a smooth curve through the twelve-month smoothed numbers. The times of minimum so selected for the entire series back to 1755 are shown in Table 1 compared with times given by Zürich, selected for being the lowest smoothed annual number for each cycle. The differences, where they exist are slight.

Having selected the minimum, the twelve-month smoothed means were then ordered for the successive years after minimum for all the cycles and their averages for the last ten cycles were obtained. Departures of the smoothed annual numbers from corresponding values for this average cycle were then derived for the first, second, third year, and successive years, after the minimum for each cycle. These departures are shown in Table 2, together with the departures for the earlier cycles from the same mean cycle. These are the values

Table 2--Deviations of observed values of smoothed twelve-month running average of Zürich relative sunspot numbers from mean value of cycles 8-17

Cycle	0	1	2	3	4	5	6	7	8	9	10	11
1	4.4	-0.9	-9.4	-34.1	-32.0	-19.5	-13.2	-0.8	-4.5	-3.6	3.1	32.2
2	6.2	21.4	17.4	25.4	9.6	-4.5	-2.1	-13.4	-1.4	-15.4	5.6	76.1
3	2.7	5.8	48.0	71.1	32.4	-0.3	-3.7	-11.6	-11.1	-12.7	12.6	75.5
4	4.9	10.4	37.0	51.5	38.3	31.3	18.7	17.0	26.7	23.8	27.2	9.8
5	0.2	-8.4	-31.6	-43.1	-46.6	-43.1	-21.3	-10.6	-9.9	-14.6	-3.6	-10.3
6	-5.0	-13.1	-45.5	-67.6	-77.8	-50.6	-23.7	-8.0	-3.0	0.8	3.0	-5.8
7	-4.9	-7.8	-35.2	-53.7	-42.6	-22.7	-6.5	16.0	26.3	10.8	-0.3	-3.8
8	2.8	12.7	49.5	62.0	30.0	-6.7	10.8	-0.2	6.7	-4.4	-0.9	18.4
9	5.6	0.7	-9.4	-18.1	10.8	37.9	22.7	17.4	30.9	30.4	25.2	8.9
10	-1.1	1.8	-1.5	7.2	3.8	-3.3	-6.1	-3.8	13.3	12.6	5.8	-6.3
11	0.2	11.8	19.4	43.5	28.8	14.7	6.3	0.0	-12.8	-9.8	-0.1	-6.9
12	-2.6	-2.7	-10.6	-21.3	-35.2	-13.3	-15.7	-1.6	-16.6	-9.6	-7.0	-5.8
13	1.3	-8.0	-15.4	-9.7	-7.3	-14.5	-6.3	-6.0	-6.7	5.0	-0.6	-1.7
14	-1.4	-7.1	-20.4	-30.3	-32.1	-23.9	-19.6	4.2	2.1	-8.6	-8.9	-8.1
15	-3.4	-7.6	-4.7	-26.1	4.6	0.7	-2.5	-10.4	-6.0	-7.7	-5.9	3.5
16	0.6	1.9	-3.0	-16.4	-22.5	-9.1	-5.1	-15.4	-12.2	-11.4	-7.6	-2.1
17	-1.6	-3.2	-3.6	9.6	19.3	17.3	15.7	15.6	14.4	3.0	-0.2	0.5
Mean, cycles 8 - 17	5.0	15.0	50.0	80.7	91.6	86.3	69.9	49.0	33.3	22.6	12.8	11.5

Table 3--Cross-product summation terms ($S_{n-i,n-j}$) for departures of smoothed annual numbers from mean cycle of smoothed annual numbers

i ($i \leqq j$)	n-j											
	0	1	2	3	4	5	6	7	8	9	10	11
0	65.34	497.57	3726.95	8623.90	5083.16	3049.22	1657.92	962.12	2057.49	1587.69	890.68	624.12
1	....	78.52	1186.49	5202.83	5172.10	2502.20	1985.58	708.26	1038.96	1598.14	1116.31	280.79
2	....	....	147.53	1787.71	3053.28	959.46	2361.47	1083.98	1032.27	733.64	1089.90	293.17
3	....	....	....	221.75	977.12	415.79	1777.87	732.52	1607.63	818.23	569.32	258.74
4	....	....	....	....	213.01	352.59	....	....	....	....	....	....
5	....	....	....	....	....	213.72	....	....	....	....	....	....

of ΔR_n. The values for the sunspot numbers were taken from IRPL-R23 [1945]. After the computations for all the smoothed annual numbers were completed it was noted that a few errors existed in these tables. They were of such magnitude as not to warrant the recomputation of the prediction coefficients and standard deviations for the smoothed annual numbers.

Values calculated for $S_{n-i,\ n=j}$ are given in Table 3. Since $(n - 1) - i = n - (i + 1)$, etc., the number of values of S required for computing a given number of k's is relatively small. From the values in Table 3, 130 k's were computed for the smoothed annual numbers on the assumptions that $\Delta R'_n$ would be calculated (1) from the immediately preceding value of ΔR, (2) from several successive preceding values ΔR, and (3) from other combinations of preceding values of ΔR from which certain values of ΔR were omitted. In the case of the fifth year of the cycle values of k_{n-i} were computed for all values of i up to and including five. By arbitrarily setting certain values of k_{n-i} equal to zero, alternate values of the other values of k_{n-i} were computed which were applicable for computing $\Delta R'_n$ from specific preceding values of ΔR. Thus for the fifth year of the cycle, 15 prediction formulas were obtained based on prediction from the preceding year, the two preceding years, and so on up to the five preceding years, as well as from the fifth, fourth or any other preceding year alone, or any combination of these years. The coefficients are given in Table 4.

Table 4--Prediction coefficients, (k_{n-i}), for values of annual sunspot numbers for the nth year of the cycle (based on years 1843-1944)

$$(R_n = \bar{R}_n + k_{n-1}\Delta R_{n-1} + k_{n-2}\Delta R_{n-2} + \cdots)$$

(coefficients in each column constitute a set)

i	n = 1	n = 2			n = 3					
1	1.2	0.0[a]	2.5	2.4	0.0[a]	0.0[a]	1.0	1.0	0.0[a]	1.4
2	. .	2.3	-0.8	0.0[a]	0.0[a]	3.8	1.2	1.1	3.6	0.0[a]
3	. .	. .	. .	. .	3.4	-1.1	-0.4	0.0[a]	0.0[a]	0.0[a]
4	. .	. .	. .	. .	. .	. .	. .	. .	. .	. .

i	n = 4									
1	0.0[a]	0.0[a]	0.0[a]	0.8	0.7	0.7	0.6	0.0[a]	0.0[a]	0.0[a]
2	0.0[a]	0.0[a]	0.9	0.1	0.0	-0.1	0.0[a]	0.8	0.0[a]	0.8
3	0.0[a]	1.8	-0.4	-1.3	-0.8	0.0[a]	0.0[a]	0.0	2.0	0.0[a]
4	3.3	1.1	1.8	2.1	0.0[a]	0.0[a]	0.0[a]	0.0[a]	0.0[a]	0.0[a]

i	n = 5														
1	0.0[a]	0.0[a]	0.0a	0.0[a]	1.0	1.1	1.0	1.0	0.5	0.0[a]	0.0[a]	0.0[a]	0.0[a]	0.0[a]	0.0[a]
2	0.0[a]	0.0[a]	0.0[a]	0.2	-0.6	-0.7	-0.4	-0.5	0.0[a]	0.1	0.0[a]	0.3	0.0[a]	0.0[a]	0.1
3	0.0[a]	0.0[a]	-0.4	-0.5	-0.6	-0.6	-0.2	0.0[a]	0.0[a]	-0.6	-0.5	-0.3	0.0[a]	0.1	0.0[a]
4	0.0[a]	0.2	1.1	0.9	2.3	2.5	0.0[a]	0.0[a]	0.0[a]	1.7	1.8	0.0[a]	0.7	0.0[a]	0.0[a]
5	3.3	3.0	2.7	2.8	0.6	0.0[a]	0.0[a]	0.0[a]	0.0[a]	0.0[a]	0.0[a]	0.0[a]	0.0[a]	0.0[a]	0.0[a]

i	n = 6						n = 7					
1	0.0[a]	0.0[a]	0.5	0.5	0.0[a]	0.7	0.0[a]	0.0[a]	0.2	0.0	0.0[a]	0.4
2	0.0[a]	0.3	0.2	0.2	0.5	0.0[a]	0.0[a]	0.4	0.3	0.4	0.4	0.0[a]
3	0.2	-0.2	0.0	0.0[a]	0.0[a]	0.0[a]	0.1	-0.1	-0.1	0.0[a]	0.0[a]	0.0[a]

i	n = 8						n = 9					
1	0.0[a]	0.0[a]	0.8	0.9	0.0[a]	1.1	0.0[a]	0.0[a]	0.8	0.9	0.0[a]	0.8
2	0.0[a]	0.0	0.0	0.2	0.6	0.0[a]	0.0[a]	0.5	-0.2	-0.2	0.8	0.0[a]
3	0.5	0.6	0.3	0.0[a]	0.0[a]	0.0[a]	0.6	0.3	0.1	0.0[a]	0.0[a]	0.0[a]

i	n = 10						n = 11					
1	0.0[a]	0.0[a]	0.8	0.8	0.0[a]	0.7	0.0[a]	0.0[a]	0.7	0.7	0.0[a]	0.3
2	0.0[a]	0.5	-0.2	-0.1	0.5	0.0[a]	0.0[a]	0.3	-0.3	-0.3	0.2	0.0[a]
3	0.6	0.0	0.2	0.0[a]	0.0[a]	0.0[a]	0.1	-0.1	-0.1	0.0a	0.0[a]	0.0[a]

[a] Coefficient set equal to zero in computation.

Reliability--To test the reliability of the predictions the differences between observed values and predicted values were formed and their standard deviations were calculated. The predictions were made for each of the years of the ten cycles, 8-17, using all of the combinations of prediction formulas given in Table 4. An estimate of reliability for predictions beyond the observed data requires that the standard deviation

$$\sigma = \sqrt{\Sigma(R' - R)^2/N} \text{ be multiplied by } \sqrt{N/(N-M)}$$

in which N is the number of cases and M is the number of parameters used in the prediction. When the prediction R'_n is made by assigning to R'_n the value obtained for the nth year of the average cycle, M = 1; when the value of R'_n is predicted by correcting this value by k_{n-1} times the departure of one preceding value, M = 2; and if the prediction is made by correcting for the departures of five preceding values, as it may be when n = 5, M = 6. These estimates of σ for the predicted values for each year of the cycle are given in Table 5.

Table 5--Standard deviations of smoothed annual sunspot number predictions for cycles 8-17 using coefficients, k_{n-1}, of Table 4

$$\sigma = \sqrt{\Sigma(\Delta R' - \Delta R_n)^2/(N - M)}$$

Item	Years used in prediction						Year predicted following observed minimum (n)										
	Mean	n-1	n-2	n-3	n-4	n-5	1	2	3	4	5	6	7	8	9	10	11
1	x	..	..	..	..	..	7.4	20.4	31.0	23.8	18.4	13.6	10.3	15.1	13.3	9.9	8.3
2	x	x	..	..	..	..	7.1	10.6	13.0	15.7	15.1	6.8	8.9	10.8	6.6	3.6	8.2
3	x	..	x	..	..	..	..	20.6	16.6	18.0	19.2	8.5	8.6	13.3	11.3	6.3	8.4
4	x	..	..	x	..	..	..	..	31.3	19.9	19.4	4.0	10.4	12.3	11.6	8.3	8.7
5	x	x	x	..	..	..	..	11.1	13.2	16.9	12.4	5.3	9.2	11.3	6.9	3.8	8.5
6	x	..	x	x	..	..	..	..	17.4	19.0	20.3	12.7	9.1	13.2	11.4	6.7	9.0
7	x	x	x	x	..	..	..	..	14.3	21.2	13.3	5.7	9.5	11.7	7.3	3.8	9.3
8	x	..	..	..	x	..	..	..	..	23.4	18.7	..	..	..	..	..	..
9	x	..	..	..	..	x	..	..	..	..	17.1	..	..	..	..	..	..
10	x	..	..	x	x	..	..	..	..	21.0	19.3	..	..	..	..	..	..
11	x	..	..	..	x	x	..	..	..	..	18.2	..	..	..	..	..	..
12	x	..	x	x	x	..	..	..	..	20.1	20.7	..	..	..	..	..	..
13	x	..	..	x	x	x	..	..	..	..	19.3	..	..	..	..	..	..
14	x	x	x	x	x	..	..	..	..	18.5	8.8	..	..	..	..	..	..
15	x	..	x	x	x	x	..	..	..	..	21.0	..	..	..	..	..	..
16	x	x	x	x	x	x	..	..	..	..	9.6	..	..	..	..	..	..

When these values of σ are examined, it is apparent that for most of the years of the cycle the "best" prediction, that is, the prediction for which σ is smallest, is obtained by correcting the mean value by the departure from mean of the preceding year. Inspection of Table 5 reveals that for certain years of the cycle a smaller value of the estimated σ is obtained if the prediction is made using special combinations of years; for example, the value of σ for the fifth year is lowest if the prediction includes corrections for the four preceding years. For this reason one might be inclined to select for the prediction of each year of the cycle that particular combination of years which resulted in the lowest value of σ for that year. This would be an unwise procedure for, due solely to random variations in estimating the values of σ, particular combinations may result in lower values of the estimate. This selection would also imply that different physical principles were believed to be active during different parts of the cycle. For only three years is an improvement in the estimate of R obtained by basing the estimate on any correction for preceding years other than the immediately preceding year, and in two of these cases the apparent improvement so obtained is only slight.

From the foregoing considerations it was decided to employ only the mean, corrected by the departure of the preceding year, for prediction of future smoothed annual sunspot numbers. The mean cycle with its limits of standard deviation are shown in Figure 1. For most practical considerations this procedure is satisfactory for forecasts of propagation conditions. If more advanced predictions are desired, the prediction may be based on the mean, corrected for the departure two years preceding the year to be predicted.

The values of the prediction coefficients, k_{n-1}, exhibited a relatively smooth variation with n, except for n = 7 and n = 8. These two erratic values were regarded as significant. Therefore a smooth curve of k_{n-1} as a function of n was drawn (see Fig. 2) and values of k_{n-1} to be used for prediction were taken from the curve. The curve also serves to supply values of k_{n-1} for non-integral values of n.

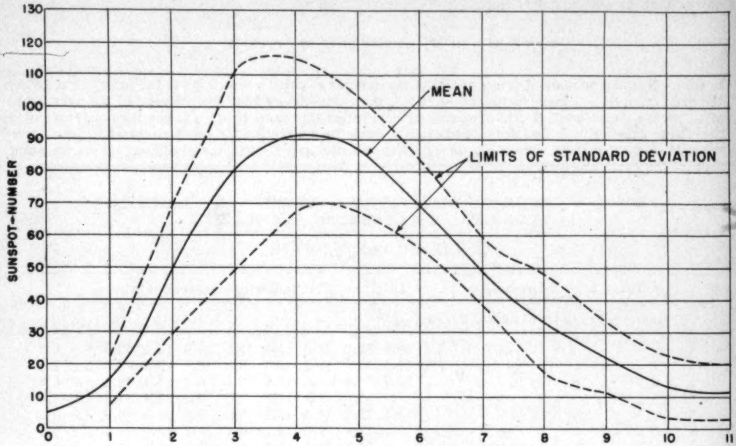

Fig. 1--Mean sunspot-cycle, 1834-1944, from superposed minima and its limits of standard deviation

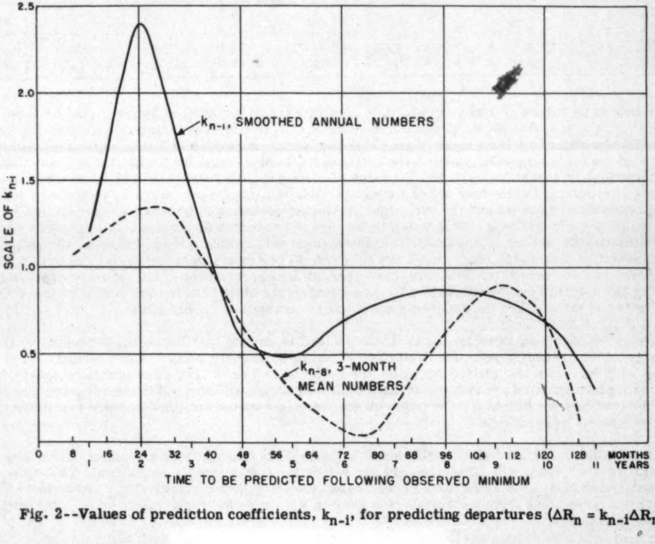

Fig. 2--Values of prediction coefficients, k_{n-i}, for predicting departures ($\Delta R_n = k_{n-i}\Delta R_{n-i}$)

A comparison of the reliability of predictions made by this method and by the regression method of Yule was carried out for the two cycles, 1923-1946. The standard deviation for the observed annual numbers (not the smoothed annual ones) was 34.0 in that interval. This corresponds to the standard deviation of the error of a prediction that a future value will be the grand average of all past values, regardless of the stage of the sunspot cycle at the time for which the prediction is made. For Yule's method the standard deviation of the observed minus predicted values was 14.2 and for the method described in this paper it was 7.3. Thus the improvement in variance was 95 per cent for this method as compared with 83 per cent for Yule's method. It should be stated that statistically the method of this paper was favored in the comparison to the extent that the prediction coefficients used were based in part on the data from 1923-1944. In addition smoothed annual sunspot numbers rather than annual means were used in the present paper. To eliminate this bias the values of k_{n-1} were recomputed using annual means for the first eight cycles of the later series. These values were then used to predict the ninth and tenth cycles so that the tests of reliability were as valid as those applied to Yule's method. The improvement in variance in this case was 93 per cent as compared with the 83 per cent for Yule's method.

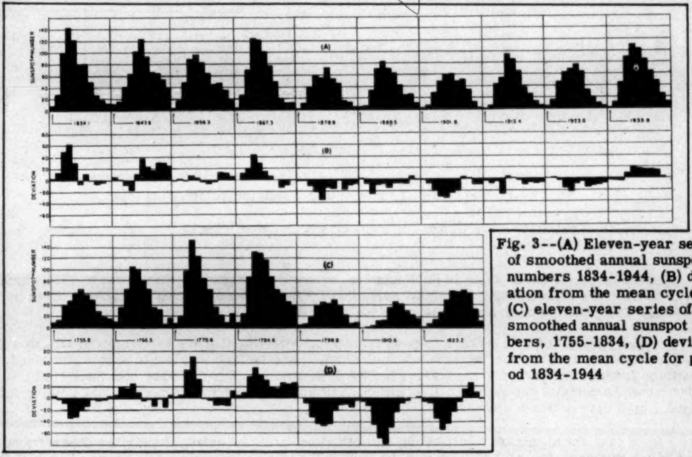

Fig. 3--(A) Eleven-year series of smoothed annual sunspot numbers 1834-1944, (B) deviation from the mean cycle; (C) eleven-year series of smoothed annual sunspot numbers, 1755-1834, (D) deviation from the mean cycle for period 1834-1944

Auto-correlation in the data--The calculations performed for obtaining the prediction coefficients may be employed for studying statistical characteristics of sunspot cycles. A somewhat idealized representation of the data is shown in the upper part of Figure 3 obtained by spacing the minima shown in Table 1 at 11-year intervals and plotting the observed smoothed annual value at these minima and for the ten succeeding years. Deviations of these observed smoothed annual values from the "mean cycle" obtained from the data of the last ten cycles are shown in the lower part of Figure 3. The conservatism of the series is conspicuous from the tendency of adjacent annual deviations to have the same sign and similar magnitudes, the tendency upon which this system of prediction is based. It is also clear that this tendency is less marked for non-adjacent deviations in any given cycle, so that the further in advance a prediction is made the greater is its uncertainty. Prediction of the last few years of a cycle from the first few years seems unwarranted.

These tendencies find numerical expression in the mean auto-correlation coefficients of the series which may be calculated from the S-values by the formula

$$r_i = \sum_{n=1}^{n-i} \left[(S_{n-o,\ n-i})/\sqrt{S_{n-o,\ n-o}\, S_{n-j,\ n-i}}\right]/(n-i) \qquad (j = i)$$

These values are plotted in Figure 4 for values of i up to three for the smoothed annual numbers. It is interesting to note that if the correlation coefficients between each pair of adjacent years in the cycle are multiplied by the ratios of the sunspot numbers of the later year to the earlier year in the same

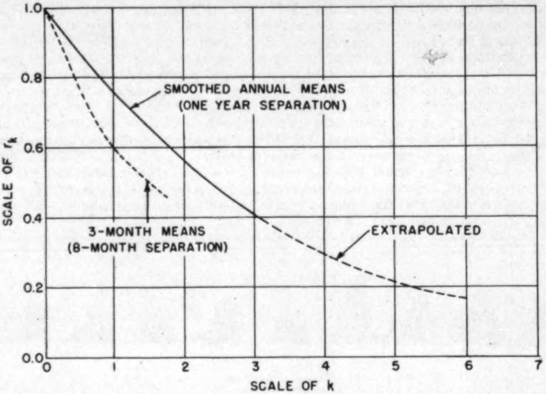

Fig. 4--Correlogram showing auto-correlation coefficients (r_k)

pair, a series of prediction coefficients is obtained which agree closely with those computed above from the values of ΔR alone.

The foregoing remarks apply in particular to the series in Figure 3 subsequent to 1834 which were used in the calculations. It may be noted that the deviations as shown in Figure 3 (B) prior to 1834 are somewhat greater than those subsequent to 1834.

Test for validity of data--There is good reason for believing that the earlier observations are subject to considerable uncertainty because of absence of a uniform system of observations and reductions from one observer to another. Also the data subsequent to 1834 are substantiated by regular measurements of geomagnetic fluctuations, initiated by Gauss and others at that time, which show a high correlation with sunspots.

It is of interest to inquire whether any statistical basis for rejecting the earlier observations can be established. In order to increase the size of the working sample all 11 years of each of the later ten cycles were normalized by expressing the deviations of the smoothed annual numbers from the mean cycle in units of the standard deviation for that part of the cycle thus supplying a sample of 11 x 10 = 110 individuals. Frequencies of occurrence of these deviations in six class intervals wer tested by the chi-squared test, to ascertain the probability that they arose from a normal distribution [degrees of freedom (6 - 3) = 3]. Neglecting the effect of auto-correlation, there was only one chanc in 1000 that the normalized deviations came from a normal distribution. (The distribution could not b expected to be normal since the sunspot numbers have a lower bound of zero.)

The deviations were then fitted by inspection to a type VI Pearsonian curve (see Figure 5), and the chi-squared test (chi-squared = 3.37) showed a probability of 0.19 that the hypothesis of a VI Pearsonian distribution was valid, effects of auto-correlation again being neglected [in this case the degrees of freedom were (6 - 4) = 2]. The observations prior to 1834 were normalized, using the σ from the later series, and tested to ascertain the probability that they came from the same set as the later observations. Chi-squared in this case was 117. In this case the degrees of freedom were (6 - 1) = 5, the mean, the standard deviation, and the skewness having been determined by the data from the later series. Values of chi-squared as great as 117 for five degrees of freedom do not appear in the tables; there is practically zero probability that the deviations obtained for the earlier years of the series came from the same set as those of the later years.

The above calculations were performed on the assumption that there are 110 independent observations in the later series and 77 in the earlier. A difficulty arises in taking into account the equivalent number of independent observations; certainly the numbers cannot be as great as 110 and 77, nor can they be less than 10 and 7. Fortunately it is not necessary to decide on the exact equivalent number of independent observations. Assuming the extreme case that there were ten and seven independent observations, the probability that the later series comes from a VI Pearsonian distribution becomes about 0.85 while the probability that the earlier series comes from the same distribution lies between 0.01 and 0.001. This is equivalent to saying that if we observe sunspot numbers for the next 10,000 years, we would not expect to encounter a series of seven cycles which differed as much from the last ten cycles as the seven preceding them did. Since the first auto-correlation coefficient is 0.73, we may assume that about one-fourth of each observation is independent, and that therefore the number of independent observations in the later and earlier series is 110/4 and 77/4, respectively. These give values of chi-squared equal to 0.84 and 29 which indicate probabilities of about 0.65 and less than 0.001 for the two hypotheses.

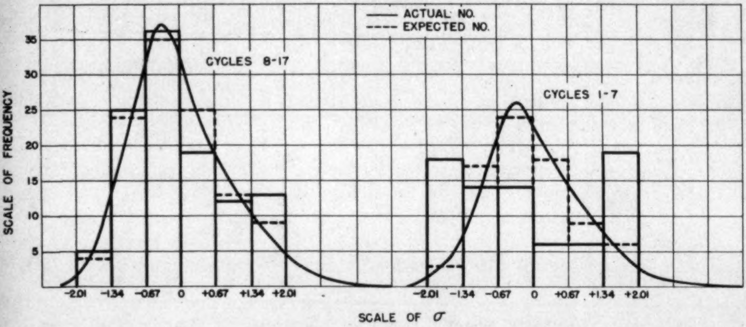

Fig. 5--Pearson VI curve fit to yearly deviations from mean curve for cycles 8-17

For the reasons stated above the earlier data were not employed in deriving the prediction formulas. However, if they had been included, no outstanding change in the coefficients would have resulted but the estimate of reliability of the predictions would have been decreased.

Reliability of empirical methods--One of the faults of most of the methods which have been proposed for predicting the sunspot cycle is that no reliability estimate of the accuracy of the predictions is supplied. Estimation of reliability for certain types of formulas is very difficult. Undoubtedly many formulas can be derived which, when applied to past cycles, give satisfactory predictions, for it is always possible with a sufficiently large number of degrees of freedom to fit satisfactorily any finite group of events to any desired accuracy. In estimating the reliability of future predictions due allowance must be made for the degrees of freedom involved in the prediction formula.

A more subtle consideration is involved in estimating the reliability of a prediction based on an empirical formula. Empirical formulas are usually obtained by trying various relationships and selecting those which worked best in the past. If a large number of relationships were tried it would not be surprising to find that some of them worked very well but allowance must be made for the number of relationships examined. The number implicitly examined but rejected by simple inspection of the data is ordinarily much greater than the number explicitly examined and consequently is difficult to take into account in assessing reliability. Such considerations do not apply if an a priori prediction formula is assumed, even though the parameters of the formula are obtained empirically from past data. But in estimating the reliability of the prediction, allowance must be made for the number of parameters in the formula as was done in computing the standard deviations of the predictions given in Table 5.

Application to present cycle--These prediction methods have been applied to the first part of cycle 18 as shown in Figure 6 (A) in which the mean curve for the last ten cycles, the observed curve to date and the predicted curves are represented for the smoothed annual sunspot numbers. The predictions were made for Figure 6 (A) for one year in advance using only one coefficient, namely, that to correct

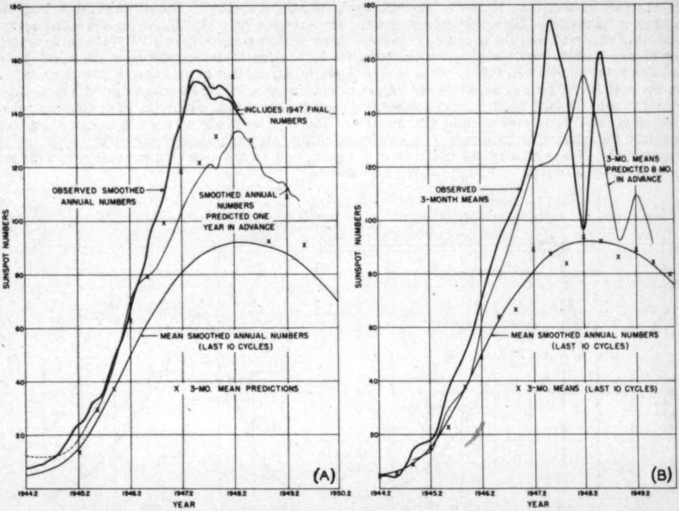

Fig. 6--(A) Comparison of observations and predictions for cycle 18 for smoothed annual sunspot numbers and (B) for 3-month centered mean sunspot numbers

for the preceding year. These coefficients were interpolated from Figure 2 for the non-integral times. Thus, for example, the prediction of the smoothed annual number for one year after the minimum was obtained by subtracting from the observed minimum the value of the minimum for the average cycle (7.5 - 5.0) = 2.5 . This quantity was multiplied by the coefficient relating the zero year to the first year (2.5 x 1.2) = 3.0 (see Fig. 2) and added to the value for the first year in the average cycle giving the predicted value (3.0 + 15.0) = 18.0, etc. Agreement of smoothed annual predictions with the observed curve was extremely satisfactory from February, 1945, until May, 1946, but the exceptional rapid increases to the highest sunspot maximum in 100 years threw the predictions into pronounced disagreement until February, 1948, at which time the predictions were again within the estimates of reliability of the predictions.

Short-term prediction--Some criticism on physical grounds has been voiced regarding the significance of the correlation of monthly ionospheric critical frequencies and smoothed annual sunspot numbers centered on the month in question. To obtain the annual sunspot number applicable to a certain month six months in the future must be observed. Thus the confusion in thought is introduced in that current ionospheric conditions seem to depend on sunspot numbers yet to be observed. This contention is not cogent when it is recongnzed that current ionospheric conditions actually depend on current solar activity, but that the average sunspot number for the 12-month interval centered on the epoch involved is a better measure of this solar activity than the current number of sunspots.

To reduce the time interval involved an extension of the above described technique was made to the prediction of three-month mean sunspot numbers. Analyses have shown that the correlation coefficient of critical frequencies of the ionosphere with three-month mean sunspot numbers is almost as great as that with smoothed annual ones. By use of three-month means only one future month of observing sunspots would be involved in the correlation with ionospheric conditions and the time interval between observation of sunspot numbers and predictions can be shortened. An eight-month interval was selected as being the most practical to test for the use of our laboratory in the preparation of ionospheric frequency predictions.

Table 6--Deviations of observed values of three-month-centered means of Zürich relative sunspot numbers from mean cycle of smoothed annual numbers for cycles 8-17

Cycle	Month after minimum (n)								
	0	8	16	24	32	40	48	56	64
8	5.0	3.9	21.5	41.2	40.9	48.6	28.2	-9.2	-17.2
9	5.6	6.9	-6.7	-18.7	-11.1	-26.6	-32.2	19.0	51.7
10	-2.7	0.0	2.6	-4.3	-5.0	15.4	0.9	-5.0	-3.8
11	0.7	7.2	11.0	15.9	13.8	53.5	58.8	1.4	20.1
12	-1.5	-4.6	-0.9	-3.4	-12.2	-26.6	-24.5	-27.2	4.5
13	1.2	-5.8	-11.9	-0.6	-7.6	-21.0	-4.4	-16.9	-17.9
14	-2.3	-7.8	-11.7	-18.5	-28.5	-21.5	-11.3	-15.5	-2.1
15	-4.7	-6.7	-15.1	-2.3	-27.4	-43.5	9.6	6.6	5.0
16	-0.6	-3.4	-3.1	-8.7	-15.5	-16.7	-35.7	-10.5	-27.0
17	-2.2	3.1	-6.3	-8.2	-6.0	40.9	29.5	18.3	-0.4
Mean, cycles 8-17	5.0	9.5	24.6	50.0	72.5	87.2	91.6	90.3	83.9

Cycle	Month after minimum (n)								
	72	80	88	96	104	112	120	128	136
8	7.7	5.9	12.5	-6.2	2.1	-4.5	-0.5	7.1	32.0
9	3.6	17.4	19.2	18.9	39.1	37.7	32.6	2.1	7.5
10	-16.0	-8.0	-8.4	14.3	19.4	10.7	5.6	-6.8	-6.7
11	4.2	0.5	9.7	-8.5	-11.6	-6.7	3.4	-3.6	-11.5
12	-21.1	19.8	-5.0	23.2	-5.9	-8.8	-5.6	-4.1	-9.6
13	-7.6	-8.5	-0.1	-13.7	9.4	15.4	1.1	0.2	-4.7
14	0.7	-11.8	13.8	17.7	-9.4	-11.3	-9.2	-6.5	-11.4
15	13.8	-8.0	-7.7	-3.9	-6.1	-12.2	-6.7	-7.5	10.3
16	-0.6	-13.8	-10.8	-18.1	-14.6	-8.6	-10.1	-2.5	-3.4
17	32.3	11.7	10.1	24.1	6.8	3.3	-0.4	-7.7	6.6
Mean, cycles 8-17	69.9	54.6	42.7	33.3	25.6	18.0	12.8	10.3	13.3

Table 7--Cross product summation terms $(S_{n-i,n-j})$ for departures of three-month-centered means from mean cycle of smoothed annual numbers

i ($i \leqq j$)	n - j								
	0	8	16	24	32	40	48	56	64
0	100.4	296.4	1191.5	2820.8	4057.3	11607.4	8274.5	2227.0	4486.4
8	. . .	107.8	373.4	1514.8	2953.9	5246.5	7758.9	1100.6	1709.5
16	. . .	. . .	171.3	329.1	2027.0	4365.7	3085.4	1093.8	21.0

i ($i \leqq j$)	n - j								
	72	80	88	96	104	112	120	128	136
0	2083.4	1396.7	1182.9	2635.2	2552.3	2276.9	1370.2	294.9	1662.8
8	310.8	152.5	547.7	913.4	1395.6	2275.2	1605.9	176.2	322.9
16	1464.1	1432.5	682.9	184.8	673.7	1026.3	1658.3	198.8	268.0

To make these predictions of three-month means the same general steps were taken. Using the data from 1834 to 1943 three-month means were calculated for each of the selected minima and at eight-month intervals thereafter. Departures of these means were made from the average cycle of the smoothed annual numbers (see Table 6). The average annual sunspot number cycle was used

Table 8--Prediction coefficients, (k_{n-i}), for values of three-month-centered mean sunspot numbers for the nth month of the cycle i = 8, (based on years 1843-1944)

n	8	16	24	32	40	48	56	64	72
k	1.07	1.26	1.27	1.05	1.29	0.67	0.13	0.77	0.07

n	80	88	96	104	112	120	128	136
k	0.07	0.39	0.77	0.53	0.89	0.71	0.13	1.09

Table 9--Standard deviations of three-month mean predictions for cycles 8-17 using coefficients k_{n-i}, of Table 8

Months used in prediction		Month predicted following observed minimum (n)								
Mean	n - 8	8	16	24	32	40	48	56	64	72
X	. .	5.7	11.5	17.7	21.2	35.9	30.3	15.7	22.3	15.2
X	X	4.7	9.0	10.6	11.3	25.0	19.7	18.3	22.1	16.0

Months used in prediction		Month predicted following observed minimum (n)							
Mean	n - 8	80	88	96	104	112	120	128	136
X	. .	12.5	11.5	17.1	17.1	15.9	12.3	5.7	13.6
X	X	12.4	10.8	15.6	15.9	5.6	5.7	9.5	13.0

since a smooth curve through the three-month mean values (see Figure 6 B) would almost coincide with the smoothed annual number curve. Cross-product summations terms given in Table 7 were used to compute the prediction coefficients k_{n-8}, of Table 8. (In this case n refers to number of months after minimum.) A smooth curve for k_{n-8} as a function of n is presented in Figure 2. Finally the standard deviations for the predicted three-month means for the past ten cycles were computed and are given at eight-month intervals in Table 9.

By forming the ratios of the standard deviations of the predictions to the standard deviation of the mean, the predictions of three-month means can be compared with those of smoothed annual numbers. A ratio of 1.00 would indicate no improvement in the chosen method over that of predicting the mean as a future value. Throughout the cycle the average ratio for the three-month predictions using k_{n-8} was 0.86 and for the smoothed annual numbers using k_{n-1} it was 0.66. The overall reliability of the prediction of smoothed annual numbers was therefore superior to that of the prediction of three-mont mean numbers, demonstrating the superior stability of annual values as compared with three-month values. The auto-correlations for three-month means at eight-month intervals are shown in Figure 4. Though auto-correlation in the data is high it is not quite as high of that of the smoothed annual numbers.

The application of these three-month mean predictions to the present cycle is shown in Figure 6 (B). After February, 1947, the fit of predicted to observed values became erratic. If these three-month mean predictions were considered as approximate smoothed annual predictions, indicated by the crosses in Figure 6 (A), the fit of predicted to observed values from May, 1946, to February, 1947 would have been better than it was for predicted smoothed annual numbers and observed ones. However, though adjusting in a shorter time interval to continually increasing sunspot numbers as soon as the sunspot numbers began to fluctuate, the three-month mean predictions were far more erratic, thereby indicating the lower overall reliability of the prediction method when three-month values are used.

Therefore for prediction of sunspot numbers for use in radio frequency predictions it is recommended that smoothed annual sunspot numbers corrected by departures one year earlier than the time in question be used. This method does not predict the time of maximum but rather month by month the "best" prediction for one year ahead. The apparent maximum in March, 1948, of 133 was obviously known not to be a prediction of maximum since it was based on March, 1947, at which time the observed number was 143.4. Such a prediction did indicate that the true maximum would lie between March, 1947, and March, 1948. The law of averages over a sunspot cycle should favor the statistically based prediction method of this paper with individual predictions having the reliability suggested by the σ's of Table 5.

Acknowledgment--The extension of the method from 12-month smoothed numbers to three-month means was carried out by R. M. Davis, Jr., whose contribution is gratefully acknowledged.

References

CLAYTON H., The sunspot period, Smithsonian Misc. Coll., v. 98, no. 2, 1939.
DURKEE, A., Forecasting sunspot and radio transmission conditions, Bell Lab. Rec., v. 16, pp. 127-129, 1937.
GLEISSBERG, W., Note on the epoch of the next sunspot maximum, Astrophys. J., v. 100, p. 114, 1944.
IRPL-R23, Solar cycle data for correlation with radio propagation phenomena, Interservice Radio Propagation Laboratory, Nat. Bur. Std., Oct. 1945.
LINDER, R. C., Prediction of next sunspot maximum, Pop. Astron., v. 53, p. 250, 1945.
SCHUSTER, A., On the periodicity of sunspots, Phil. Trans. R. Soc. London, v. 206, pp. 69-100, 1906, cont. in Proc. R. Soc. London, v. 85, pp. 50-53, 1910-1911.
SHAPLEY, A. H., An estimate of the trend of solar activity, 1944-1950, J. Terr. Mag. Elec., v. 49, pp. 43-45, 1944.
STEWART, J. and EGGLESTON, F., A prediction of the remaining course of the present sunspot cycle, Phys. Rev., v. 55, p. 1102, 1939.
STEWART, J., and EGGLESTON, F., The mathematical characteristics of sunspot variations II, Astrophys. J., v. 91, pp. 72-82, 1940.
STEWART, J., and PANOFSKY, H., The mathematical characteristics of sunspot variations, Astrophys. J., v. 88, pp. 385-407, 1938.
WALDMEIER, M., Ergebnisse und Probleme der Sonnenforschung, Leipzig, 1941.
WALDMEIER, M., A prediction of the next maximum of solar activity, J. Terr. Mag. Elec., v. 51, p. 270, 1946.
YULE, G. U., On a method of investigating periodicities in disturbed series, with special reference to Wolfer's sunspot numbers, Phil. Trans. R. Soc., v. 226, pp. 267-298, 1926-1927.

Central Radio Propagation Laboratory,
National Bureau of Standards,
Washington, D. C.

(Manuscript received April 26, 1949; presented at the Twenty-Eighth Annual Meeting, Washington, D. C., April 29, 1947; open for formal discussion until March 1, 1950.)

Transactions, American Geophysical Union Volume 30, Number 5 October 1949

PREDICTION OF IONOSPHERIC CONDITIONS FOR ANTIPODAL STATIONS

Gladys R. White and Roy F. Potter

Abstract--Predicted values of F2 critical frequencies for all hours of the day for Watheroo, Western Australia, and for Baton Rouge, Louisiana, were compared with observed values. It was found that predicted values for Baton Rouge, based on data from Watheroo, agreed with observed values almost as well as those predicted from Baton Rouge values. The two stations in question are located at almost antipodal points. Similar tests conducted for other stations in corresponding geographical latitudes, north or south, but not antipodally located showed poorer agreement. It is concluded from this that data observed at any given station may be applied with considerable assurance to antipodal points for which no data are available.

It has been assumed for several years that ionospheric characteristics at a given latitude and longitude and at a given season of the year are simulated at the antipodal point for the corresponding season. This reciprocity, if definitely established, would effectively double the information obtained from each operating ionosphere station and thus supply information for parts of the world where for political, economic, or geographical reasons no data are available. The pair of stations best suited for study of this principle are Watheroo, Western Australia, which has been in operation since May, 1938, and Baton Rouge, Louisiana, which has been in operation since July, 1943.

The relation between ionospheric critical frequency and 12-month running average sunspot number seems approximately linear at all times of day at locations where sufficient data are available to determine well-established trends. Such a relationship has been used for many years in prediction of critical frequencies and maximum usable frequencies for long distance communication. Due to the limited number of ionosphere stations in the world-wide network many gaps occur on a world map of ionosphere conditions. Consequently, data from existing stations have been used to indicate the corresponding conditions expected at antipodal locations. Since the station at Baton Rouge was established in 1943, until recently there were insufficient data to make a quantitative comparison of observed data from the two stations which are at almost antipodal points.

The regression line of critical frequency of the F2 layer versus 12-month running average sunspot number for each hour and month is maintained for all stations in connection with the regular prediction services of the Central Radio Propagation Laboratory of the National Bureau of Standards Smoothed diurnal curves of the zero sunspot number intercepts and the slopes of the regression lines were obtained for each of the three seasons for Baton Rouge and Watheroo. These parameters were used to estimate the critical frequencies at their respective stations at all hours of the day for the pertinent sunspot number for each season of the years 1944-1947. In this way "predicted" diurnal variations of critical frequency were obtained for Baton Rouge from Baton Rouge data and for Watheroo from Watheroo data. Using the parameters obtained from Watheroo data a second set of diurnal variations was computed for Baton Rouge. In carrying out this second "prediction" for Baton Rouge the parameters used to predict the November-February season at Baton Rouge were those obtained from the Watheroo data for the May-August season and vice versa. Thus three sets of predicted curves were obtained for comparison to ascertain the efficiency with which the data from an approximately antipodally located station can be used to predict data for the given station itself.

It is also of interest to inquire how effective the prediction may be when data from one station are used to predict data from another station where the antipodal principle does not apply. Since the Earth's magnetic field plays an important role in the distribution of ions in the F2 region of the ionosphere, the data from two other stations with approximately the same geographic latitude as Watheroo and Baton Rouge but with different geomagnetic latitudes were likewise compared with the Watheroo data. These stations are Brisbane on the eastern side of Australia and Delhi, India. Brisbane is 37° in longitude from Watheroo, whereas Baton Rouge is 27° in longitude from the antipodal point of Watheroo. However, Baton Rouge is only 1° nearer the geomagnetic equator than Watheroo while Brisbane is 6° nearer. Delhi is 39° in longitude from Watheroo but is 23° nearer the geomagnetic equator. Calculations like those described above for Baton Rouge were also carried out for Brisbane and Delhi.

The diurnal curve of observed frequencies was compared with the diurnal curve of estimated frequencies by taking deviations for every other hour of the day. The root mean square deviation was used as a measure of the goodness of fit of the two curves. The root mean square deviations over the four year period for each season and location are given in Table 1. Values in the σ_s column are a measure of the agreement between estimates made from the parameters of a given location and the observed data at that location. The values in the σ_w column are a measure of the agreement between estimates made from the parameters for Watheroo data and the observed data at the location indicated. The number of degrees of freedom used in calculating the deviation σ_s was adjusted to account for the fact that observed data for the years 1944-1947 were used in determining the parameters from which the corresponding estimates were made. Consequently, deviations in the σ_s and σ_w columns are based on 24 and 48 degrees of freedom, respectively.

Table 1--Root mean square deviations of estimated from observed critical frequencies over the four year period, 1944-1947. The σ_s and σ_w deviations are derived from estimates obtained, respectively, from data at the location indicated and from Watheroo data

Season	Station						
	Watheroo	Baton Rouge		Brisbane		Delhi	
	σ_s	σ_s	σ_w	σ_s	σ_w	σ_s	σ_w
	Mc	Mc	Mc	Mc	Mc	Mc	Mc
Summer	0.50	0.53	1.02	0.45	0.82	0.70	1.39
Winter	0.44	0.43	0.55	0.31	0.66	0.46	1.54
Equinox	0.48	0.47	0.52	0.48	0.93	0.59	1.92

Naturally it is important to determine how well estimates of the critical frequency at a given location agree with the data observed there. Referring to the σ_s columns in Table 1, it is seen that at the three locations which are of primary interest the deviations over the four year period are 0.53 Mc or less. The slightly higher values at Delhi may be significant but it is of minor concern in the present study. The four year period covers a range in sunspot number from approximately 10 to 155. The latter number, for 1947 northern summer, is unusually high. Estimates for the lower sunspot numbers in the years 1944 and 1945 are very close to the observed values.

A comparison of the σ_s and σ_w deviations at Baton Rouge shows that Watheroo estimates for the winter and equinoctial seasons agree with Baton Rouge observations nearly as well as do Baton Rouge estimates. The discrepancy in the estimates of the summer season is largely a result of differences of the predicted and observed values during one year 1947. Dirunal curves of average critical frequency observed at Watheroo and at Baton Rouge for summer 1944-1948 are shown in Figures 1 and 2, respectively. The Watheroo curves retain the same shape as the sunspot number changes and are separated at least qualitatively in a regular manner, whereas the shape of the Baton Rouge curves changes rather markedly and the separation in values is somewhat erratic. For example around 14^h00^m to 20^h00^m during 1947 the critical frequencies seem too low and throughout 1948 frequencies are as high or higher than during 1947. The Watheroo curves are above the corresponding Baton Rouge curves during 1944-1947, the differences being more pronounced at hours in the neighborhood of noon and midnight. No corrections for solar distance, local time, or time of sweep of multifrequency recorder were applied since they are of a much lower order of magnitude in general than the observed differences, although at times when the curves are rising or falling rapidly, such corrections would have improved the agreement somewhat.

The Watheroo estimates for Brisbane do not agree with the observed data as well in winter and equinoctial seasons as do Watheroo estimates of Baton Rouge, but approximate somewhat closer the Brisbane summer frequencies. Thus, in general, Watheroo data are as efficient for estimating the critical frequency at Baton Rouge as at Brisbane which is located in the same hemisphere and separated by only 37° in longitude from Watheroo. Since Baton Rouge is separated by 27° in longitude from the antipodal point of Watheroo, some of the discrepancy in the characteristics of Baton Rouge, as calculated from Watheroo data, are no doubt attributable to this longitude difference. On the other hand, Watheroo data can not be used to estimate the critical frequencies for Delhi which is separated by only 39° in longitude from Watheroo but, being in the opposite hemisphere, is 26° nearer the geomagnetic equator.

While the investigation described above was in progress, data for 1948 were becoming available, and at the end of the year it was possible to test further the antipodal hypothesis by comparing the data observed in 1948 with the predictions based on parameters obtained from both Baton Rouge and Wath-

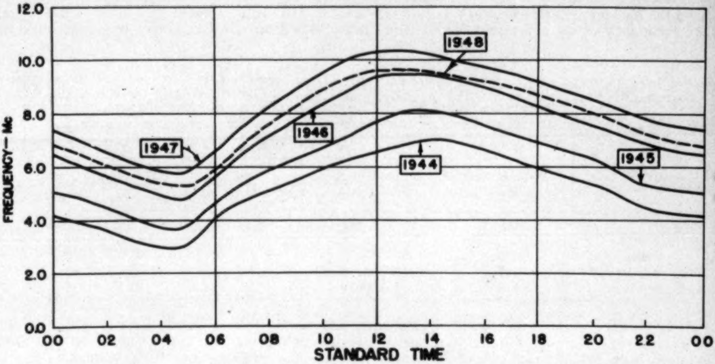

Fig. 1--Average critical frequency observed at Watheroo in summer season, 1944-1948, for corresponding sunspot numbers 12.9, 38.4, 93.0, 143.0 and 132.0 respectively

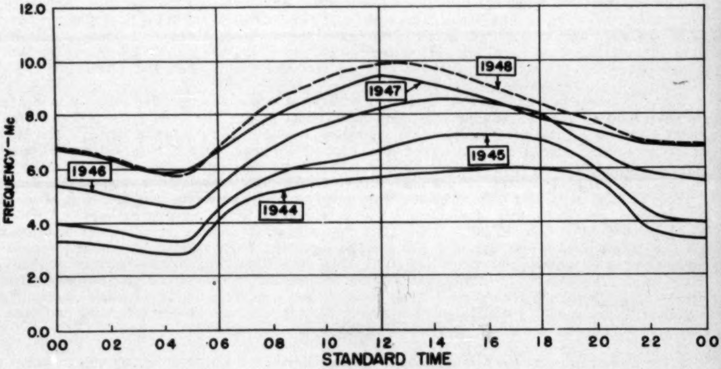

Fig. 2--Average critical frequency observed at Baton Rouge in summer season, 1944-1948, for corresponding sunspot numbers of 9.9, 34.4, 91.4, 155.1, and 133.0, respectively

eroo data observed prior to 1948. Diurnal curves presented in Figures 3, 4, and 5 show the comparison by season of observed and predicted critical frequencies. As was true with the previous estimates, the Watheroo data fail to give a close prediction of summer observations at Baton Rouge but predict winter and equinoctial seasons very well. Again root mean square deviations were calculated as described previously. The number of degrees of freedom was 12 for both sets of data. The standard deviations are 0.41, 0.27, and 0.26 Mc for predictions from Baton Rouge summer, winter, and equinoctial data, respectively, and 0.83, 0.40, and 0.38 Mc for corresponding predictions from Watheroo data.

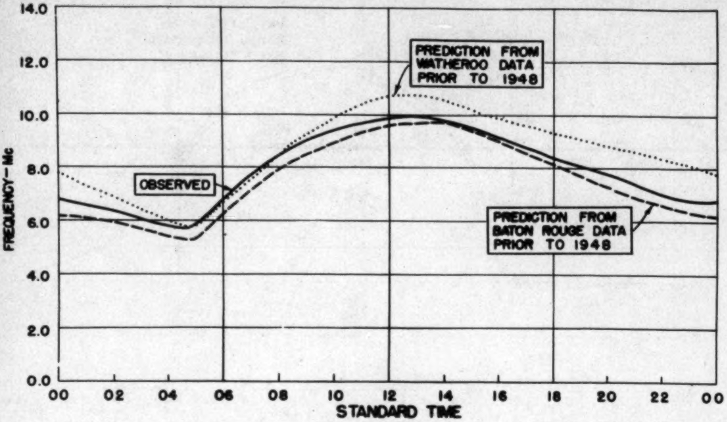

Fig. 3--Observed and predicted diurnal variation in critical frequency at Baton Rouge in summer season for 1948

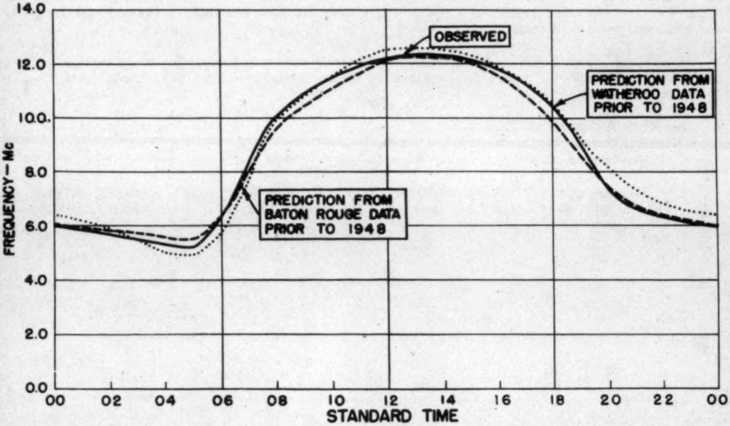

Fig. 4--Observed and predicted diurnal variation in critical frequency at Baton Rouge in equinoctial season for 1948

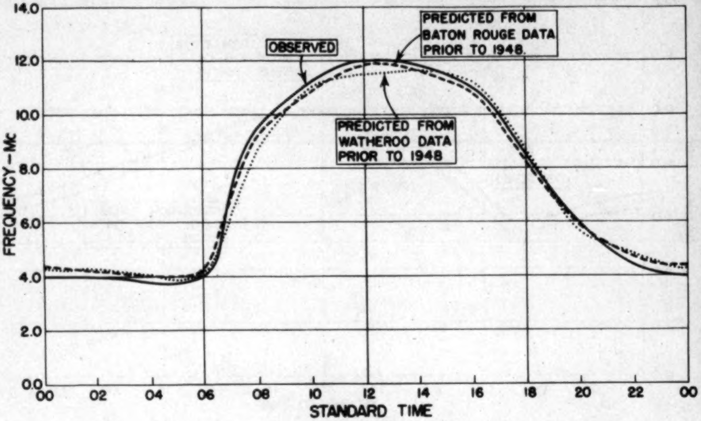

Fig. 5--Observed and predicted diurnal variation in critical frequency at Baton Rouge in winter season for 1948

As mentioned above, some of the discrepancy in the characteristics of Baton Rouge as calculated from Watheroo data are doubtless a result of the separation in longitude between Baton Rouge and the antipodal point of Watheroo.

These almost antipodal stations reflect each other well enough that the more complete picture of worldwide ionospheric conditions obtained by applying observed data to antipodal points seems to be a reliable one.

Central Radio Propagation Laboratory,
National Bureau of Standards,
Washington, D. C.

(Manuscript received March 31, 1949; presented at the Thirtieth Annual Meeting, Washington, D. C., April 22, 1949; open for formal discussion until March 1, 1950.)

Transactions, American Geophysical Union Volume 30, Number 5 October 1949

MEASUREMENT OF OCEAN WAVES

R. G. Folsom

Abstract--Laboratory and field investigations demonstrate that theoretical pressure ratios for pressure wave recorders are correct to within ten to 20 per cent. The theoretically corrected measured wave heights in shallow water are low. The University of California Mark III and Mark V wave recorders are described and typical records from the latter are reproduced. The limitations of the available information on spar buoy damping disc systems for deep water wave measurements are summarized.

Introduction--Investigations of ocean waves require measurements to be made in deep water, shallow-water, and in some cases on the shore. The principal characteristics may be determined by one of three general methods; (a) surface configurations, (b) pressures at a given depth below the mean surface, and (c) velocities at a given position. The first two methods appear to be most practical. Many wave measurments are now being made by means of pressure recorders placed at some depth below the ocean surface. This paper presents the elementary theory of the pressure method and discusses some of the instruments being used in the field.

Since a series of ocean waves usually is irregular in heights and periods, adequate definitions of wave properties are necessary. The following definitions have been accepted:
Wave height is the vertical distance between the crest and the previous trough.
Characteristic height is the average height of the one-third highest waves.
Characteristic period is the average period for the well-defined series of highest waves observed.
Direction is the orientation of the line of travel of the largest well defined waves,

The definitions of the characteristics of height and period are incomplete in that the length of the observation period is not specified. The best information available at the present time indicates that the recording period should be a minimum of about twenty minutes. The present wave forecasting methods specify the defined values.

Pressure depth relationship--One method of recording surface wave heights and periods is to place a pressure-actuated device at some point below the surface and record the pressure variations at that point. In order to express the maximum pressure differences as surface wave heights, the relationships of these values with respect to the pertinent variables must be determined. Theoretical methods and experimental results are available.

The theoretical treatment considers the two dimensional, irrotational motion of an incompressible fluid in a relatively deep channel of constant depth. The fluid motion is assumed to be generated from rest by the action of normal forces; thus a velocity potential ϕ exists and will satisfy the Laplace equation

$$\partial^2\phi/\partial x^2 + \partial^2\phi/\partial Z^2 = 0$$

For two dimensional flow, Euler's equations may be reduced to

$$p/\rho = \partial\phi/\partial t + gZ - [(\partial\phi/\partial x)^2 + (\partial\phi/\partial Z)^2]/2$$

where Z is the vertical dimension measured positive in the downward direction. Surface contours of progressive waves in a long channel with constant width and depth are assumed to be a simple harmonic form of function of the distance x along the surface.

A velocity potential with suitable boundary conditions may be defined as

$$\phi = [ga \cosh k(D - Z) \cos(kx - \sigma t)]/\sigma \cosh kD$$

where

$k = 2\pi/L$ c = wave velocity
$\sigma = 2\pi/T$ t = time

L = wave length
T = wave period
$c = L/T = \sigma/k$
D = depth of water
a = amplitude of wave
g = acceleration of gravity

Substituting and neglecting higher order terms, solve for the pressure change at a given depth Z when transient conditions have been eliminated.

$$(\Delta p)_Z = p_{max} - p_{min}$$

From the velocity potential

$$(\Delta p/\rho)_Z = [2\, ga \cosh k(D - Z)]/\cosh kD = 2\, Kga$$

The pressure equivalent of the wave height is

$$(\Delta p_0/\rho)_Z = 2\, ga$$

Then

$$K = (\Delta p/\Delta p_0)_Z = \cosh[(2\pi D)(1 - Z/D)/L]/\cosh(2\pi D/L)$$

When the Z position is at or near the bottom

$$K = 1/\cosh(2\pi D/L)$$

In usual observations, the wave period T is determined instead of the wave length L. The relationship is given by

$$L = [gT^2 \tanh(2\pi D/L)]/2\pi$$

Suitable graphs and tables are available for solution of this equation [WIEGEL, 1948].

An analysis of the equations presented shows that the pressure variation decreases as the depth of the instrument increases [FOLSOM, 1947]. In the case of short period waves the instrument may be placed at a depth such that the pressure variations due to the surface waves will give no appreciable record of pressure change. By placing the instrument at greater depths, it is possible to damp out the short period or wind waves, thus producing a pressure record providing information with respect to wave heights associated with the swell.

Limited experimental data have been obtained in the laboratory and field to demonstrate the applicability of the theoretical relationships. Field observations in the ocean are difficult to correlate due to the irregular wave pattern usually existing. Laboratory observations may be made under controlled conditions, but difficulty is encountered due to the necessary sensitivity of the pressure measuring equipment. Results obtained by both of these methods demonstrate that the theoretical magnitude of the pressure ratio K is low.

Investigations have been made in laboratory wave tanks at the Waterways Experiment Station, Vicksburg, Mississippi, and at the University of California, Berkeley. Ten random determinations at Vicksburg showed an average-correction factor to the pressure ratio of 1.07. Seventeen calibration tests at Berkeley for D/L range of 0.22 to 0.82 and a Z/D range of 0.21 to 0.63 indicated an average correction factor of about 1.1. Each test consisted of a series of measurements taken from a uniform train of waves. Field observations in shallow water have been reported by Woods Hole Oceanographic Institution [SEIWELL, 1948] and the Department of Engineering at Berkeley [FOLSOM, 1947]. Observations of pressure on the ocean bottom near Cuttyhunk in 75 ft of water and near Bermuda in 120 ft of water are reported to have an average correction factor of 1.35. These field determinations were made by photographing on 16 mm movie film the ocean surface alongside a graduated pole anchored on the sea bottom. The subsurface pressures were determined by suitable instruments developed at Woods Hole. Analysis of the data in the publication concerned shows that the theoretical wave factors were calculated on deep water relationships alone. Although shallow-water conditions prevailed for a portion of the runs, the correction factors were computed from theoretical pressure ratios based on deep water phenomena. The correction factors are lower when expressed on the basis of equations presented here, but the magnitude is still somewhat greater than 1.2.

Field observations by the University of California were made in shallow water along the Pacific Coast. Data for the first tests were obtained from the end of the Standard Oil Pier at Estero Bay.

The pressure element of the recorder system was placed at a depth of 16 ft in water of 20-foot average depth. Data were obtained from the pressure record and from observations of each wave against a staff gage attached to the outermost pile of the pier. The waves were breaking inshore from the pier end. At the end of the pier the characteristic wave height was 3.4 ft and the period eight seconds. On the basis of 22 waves which formed the 1/3 highest waves during the observation period, the correction factor was found to be 1.18. A similar procedure was followed at Princeton Beach, Half Moon Bay [FOLSOM, 1946]. One pressure element was placed at a Z/D of 0.96 and gave a correction factor of 1.08. The other pressure element was placed at Z/D of 0.76 and give a correction factor of 1.06. The average depth of water was 12.5 ft. The characteristics height was 1.31 ft and the period was 14 sec.

University of California field observations have been made in deep water by making use of a floating spar buoy system with a damping disc and a recording pressure gage. Pictures were made of the sea surface elevation changes with respect to the spar buoy with 16 mm movie film and results compared with the corresponding pressure records obtained at the bottom of the spar buoy at a depth of approximately 20 ft. By use of a wave factor calculated on the basis of the pressure reduction from the surface and dynamic characteristics of the floating spar buoy system, the average correction factor obtained was about 1.15.

Laboratory and field data show that a correction factor must be applied to sub-surface pressure measurements in order to obtain surface wave characteristics. The order of magnitude of this correction factor is between 1.1 and 1.2 times the theoretical wave factor. This variation is not surprising in view of the simplified assumptions involved in the determination of the theoretical magnitudes. Further investigations should be made into the effect of D/L, Z/D, and the bottom approach conditions on the correction factor.

Shore wave recorders--In order to investigate wave characteristics near a shoreline, it is desirable to measure heights, periods, and directions in shallow water adjacent to the shore. Of the several possible methods of recording wave heights and periods, the surface profile or surface pressure at a given location has proved to be the most practical. The choice of a given type depends on the purpose for which the wave measurements are being made. If the actual surface contour is of importance the surface profile method is the only suitable one. Applications of this type involve surging in harbors and landing conditions for seaplanes. When it is desired to separate and identify the long period waves or swell, the pressure method possesses advantages since the action of short period waves on sub-surface pressures is small with respect to that of the long period waves.

A standard water-level recorder having proper dynamic characteristics may serve to obtain a record of the water surface. Recorders of this type have been used by the United States Engineers for studies of surface profiles at Monterey Harbor, California. Scripps Institution of Oceanography at La Jolla has used a recorder of this type for a long period. The equipment consists of a float which operates the recording pen or drum position and a time element (electric or spring driven) which controls the recording pen or drum position not connected with the float. Another type of instrument that has been used for obtaining records at the water surface is the step-resistance gage used by the BEACH EROSION BOARD [1948]. The applications of these devices are restricted to locations on piers or other fixed structures.

The United States Naval Electronics Laboratory at San Diego has used an echo-sounding device placed on the bottom in shallow water to determine surface profiles. This electronic method is limited with respect to the depth of water in which a satisfactory surface profile may be obtained. The limiting factor at any water depth is the angle of spread of the beam with respect to the wave length. Although this equipment in its present form is not suitable for routine recording, further development should be carried out due to the possibilities of the system.

Several subsurface pressure recorders have been developed and tried out. In general this type of instrument consists of a pressure head or element placed at or near the bottom of the ocean with a cable to shore for connecting electrically to a recorder. Different principles of operation have been used with a reasonable degree of success.

The University of California wave equipment involves simple electrical measurements. Figure 1 shows a schematic sketch of the University of California Mark III shore wave recorder pressure element. Two resistances of a Wheatstone bridge circuit are formed by a 750-ohm potentiometer and connected to shore by the three conductor cable. The position of the precision potentiometer is controlled by a cantilever beam which is subject to deflections proportional to the difference in the average pressure and the instantaneous pressure due to the passage of a wave. This differential type of instrument provides a pressure record that is independeent of tides and at the same time will

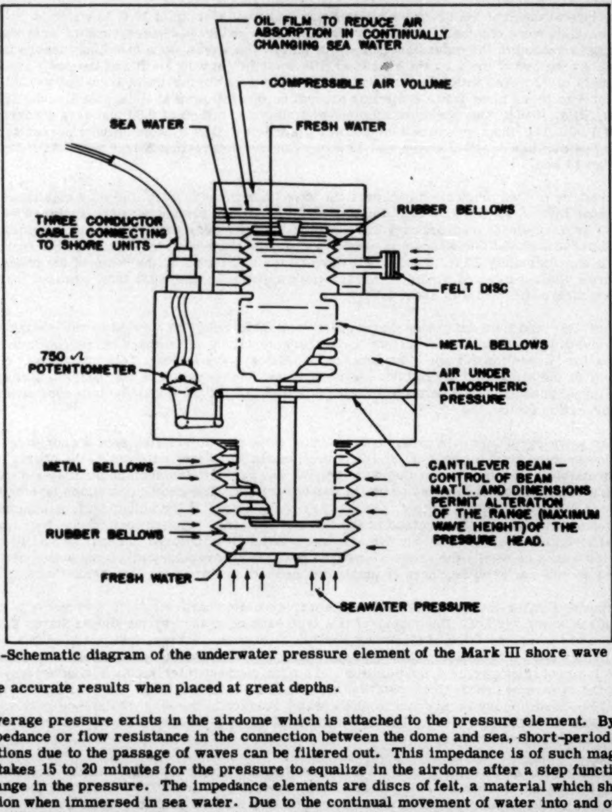
OIL FILM TO REDUCE AIR ABSORPTION IN CONTINUALLY CHANGING SEA WATER
COMPRESSIBLE AIR VOLUME
SEA WATER
FRESH WATER
THREE CONDUCTOR CABLE CONNECTING TO SHORE UNITS
RUBBER BELLOWS
FELT DISC
METAL BELLOWS
750 Ω POTENTIOMETER
AIR UNDER ATMOSPHERIC PRESSURE
CANTILEVER BEAM - CONTROL OF BEAM MAT'L. AND DIMENSIONS PERMIT ALTERATION OF THE RANGE (MAXIMUM WAVE HEIGHT) OF THE PRESSURE HEAD.
METAL BELLOWS
RUBBER BELLOWS
FRESH WATER
SEAWATER PRESSURE

Fig. 1--Schematic diagram of the underwater pressure element of the Mark III shore wave recorder

produce accurate results when placed at great depths.

Average pressure exists in the airdome which is attached to the pressure element. By providing impedance or flow resistance in the connection between the dome and sea, short-period pressure fluctuations due to the passage of waves can be filtered out. This impedance is of such magnitude that it takes 15 to 20 minutes for the pressure to equalize in the airdome after a step function or sudden change in the pressure. The impedance elements are discs of felt, a material which showed no corrosion when immersed in sea water. Due to the continual movement of water into and out of the airdome there is a tendency to absorb the air and remove it from the dome. A thin layer of oil is placed on the water surface inside the dome in order to reduce the absorption of air in the water. The metal bellows are standard brass units and the rubber bellows are used to separate the metal bellows from the sea water.

Using this same basic element which was designed for a maximum pressure of about 125 ft, it is possible to attach equalizer gas containers and safety mechanisms to operate the recorder at 600-ft depths. The design is somewhat more complicated, as illustrated in Figure 2, since it is necessary to lower and raise the instrument rapidly.

Installations with this type of instrument (University of California Mark III) have been made and operated for some periods as shown in Table 1. At the present time Mark III type instruments are being installed at Apra Harbor, Guam. It is of interest to note that the Point Arguello and Heceta Head installations include a wave direction meter, which consists of a Rayleigh disc with angle of disc being recorded on shore by means of a Selsyn telemetering system. In operation this disc aligns itself with the flat surface perpendicular to the direction of wave travel [RAUCH, 1945].

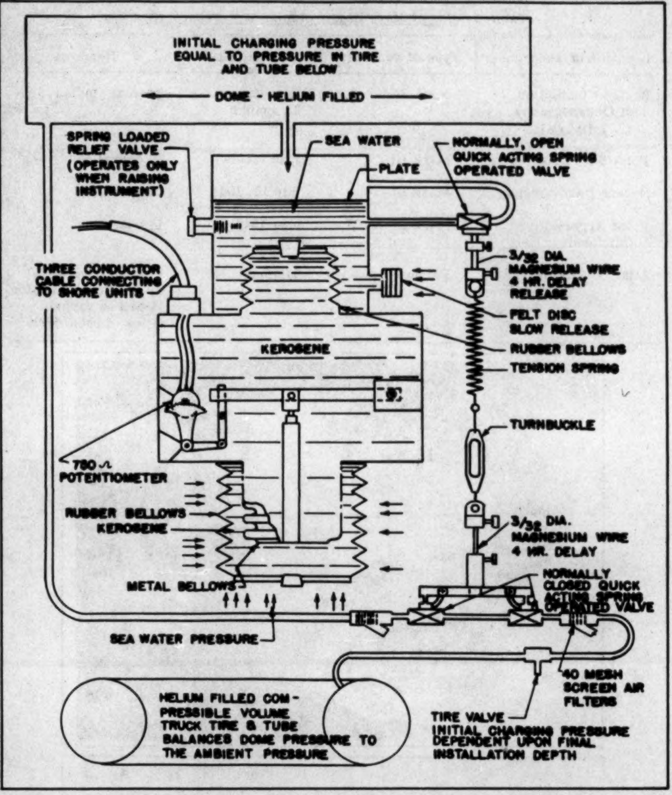
INITIAL CHARGING PRESSURE EQUAL TO PRESSURE IN TIRE AND TUBE BELOW
DOME - HELIUM FILLED
SPRING LOADED RELIEF VALVE (OPERATES ONLY WHEN RAISING INSTRUMENT)
SEA WATER
PLATE
NORMALLY, OPEN QUICK ACTING SPRING OPERATED VALVE
THREE CONDUCTOR CABLE CONNECTING TO SHORE UNITS
3/32 DIA. MAGNESIUM WIRE 4 HR. DELAY RELEASE
FELT DISC SLOW RELEASE
RUBBER BELLOWS
TENSION SPRING
KEROSENE
TURNBUCKLE
750 Ω POTENTIOMETER
RUBBER BELLOWS
KEROSENE
3/32 DIA. MAGNESIUM WIRE 4 HR. DELAY
NORMALLY CLOSED QUICK ACTING SPRING OPERATED VALVE
METAL BELLOWS
SEA WATER PRESSURE
40 MESH SCREEN AIR FILTERS
HELIUM FILLED COMPRESSIBLE VOLUME TRUCK TIRE & TUBE BALANCES DOME PRESSURE TO THE AMBIENT PRESSURE
TIRE VALVE
INITIAL CHARGING PRESSURE DEPENDENT UPON FINAL INSTALLATION DEPTH

Fig. 2--Schematic diagram of the underwater pressure element of the special deep water (600 ft) Mark III shore wave recorder

In order to improve the simplicity and reduce the cost of instruments for shore wave recorders, the University of California Mark V or thermopile wave meter has been developed. The pressure elements of this recorder consists of a thermopile mounted on a copper block inside of a rubber bellows. In operation the rubber bellows is submerged and subjected to pressure variations due to the passage of waves. These pressure variations tend to compress the air inside of the bellows, producing a rise in temperature which may be measured by the emf developed by the thermopile when the copper block temperature remains at water temperature. The thermopile is connected to a suitable automatic balancing recording potentiometer. The deflection recorded on the potentiometer is a function of the initial temperature and pressure, the change in pressure, the wave period, and the heat transfer characteristics of the pressure unit. Calibration has shown a maximum deflection of approximately one-third of the magnitude calculated on the basis of the perfect gas laws and adiabatic compression. Figure 3 shows the pressure element disassembled. This instrument requires a calibration chart which is a function of the location of the instrument and the instrument deflection and response characteristics. These charts may be prepared readily and are convenient to use.

Table 1--Use of Mark III and similar type recorders

Location of recorder	Type of recorder	Date installed	Remarks
Scripps Institution of Oceanography, La Jolla, Calif.	Mark III	Operating 11 months	Special studies
Point Sur, Calif.	Mark III	June 27,1947	In operation
Heceta Head, Oregon	Mark III	July 15, 1947	In operation
Point Arguello, California	Mark III and V	June 1948	In operation
Atlantic City, N. J.	Various types	Summer 1947	Comparative tests by the Beach Erosion Board on various types of recorders

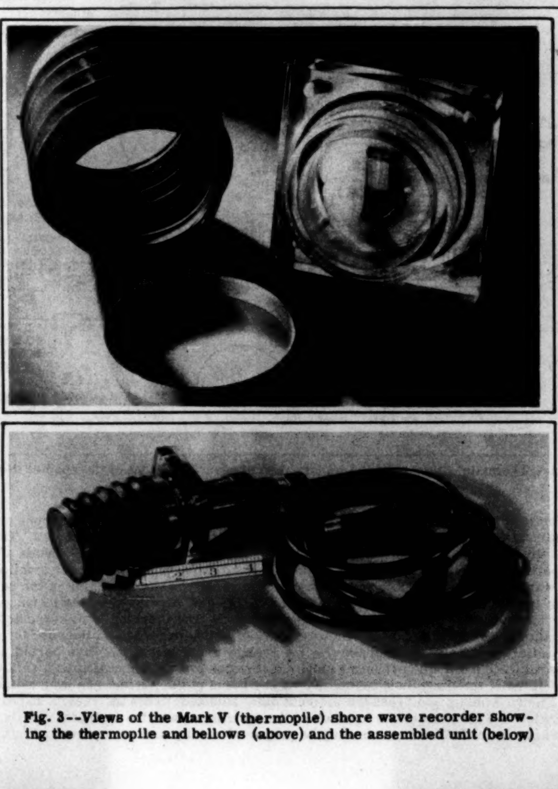

Fig. 3--Views of the Mark V (thermopile) shore wave recorder showing the thermopile and bellows (above) and the assembled unit (below)

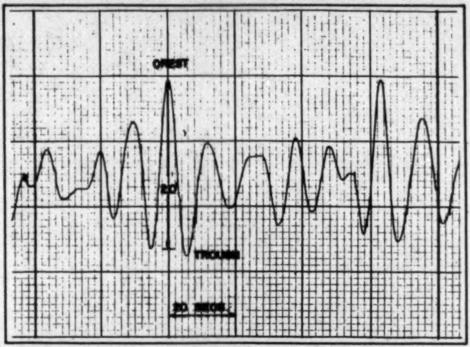

Fig. 4--Chart record from the Mark V (thermopile) shore wave recorder made at Pt. Arguello, Calif., August 31, 1948, 08^{h}15^m PST; note the typical variability of the height and period of ocean waves

A sample of the record obtained on the Point Arguello Mark V wave meter is included in Figure 4, where a deflection of one main division corresponds to about a one foot wave height. This type of instrument has many advantages, including relatively small cost for the pressure unit, the part most subject to loss or damage.

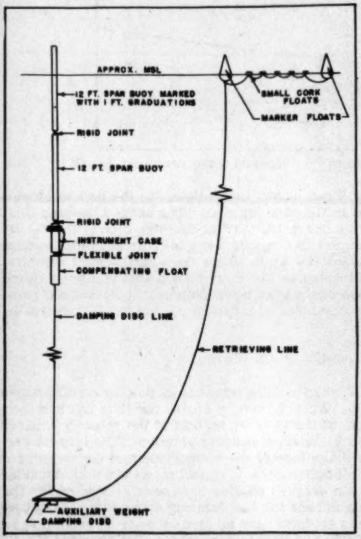
APPROX. MSL
12 FT. SPAR BUOY MARKED WITH 1 FT. GRADUATIONS
SMALL CORK FLOATS
MARKER FLOATS
RIGID JOINT
12 FT. SPAR BUOY
RIGID JOINT
INSTRUMENT CASE
FLEXIBLE JOINT
COMPENSATING FLOAT
DAMPING DISC LINE
RETRIEVING LINE
AUXILIARY WEIGHT
DAMPING DISC

Wave measurements are being obtained on a continuous basis. At present the major problem is one of analysis rather than measurement. A wave analyzer for records obtained on film has been in operation at Woods Hole and Scripps. This analyzer, based on Fourier's Theorem, was originated by the British. In an effort to simplify the interpretation of the records, an investigation was made about three years ago regarding the possibility of using wire recorder equipment. The scheme considered involved recording on the wire at a low speed, then increasing the speed of of the wire so that normal standard sound analyzers could be used. On the basis of preliminary studies, the response characteristics of the available materials and recorders introduced distortion of a magnitude to interfere with proper recording. Due to the rapid strides made in wire recorders and associated equipment, it is possible that another investigation of this system for the purpose of making accurate wave analyses should be made now.

Deep water--In order to make wave measurements in deep water it is necessary to have some datum. It appears possible that one might consider an airplane or airship at some distance above the water, a floating system in the water that has little or no absolute motion, or a float moving with water surface and having suspended from it a recorder that moves through a region in which the pressures are essentially hydrostatic. Attempts at wave measurements have been made on the basis of each one of these methods. The stationary floating platform appears to offer several advantages. Elements of the spar bouy damping disc system are shown in Figure 5. The

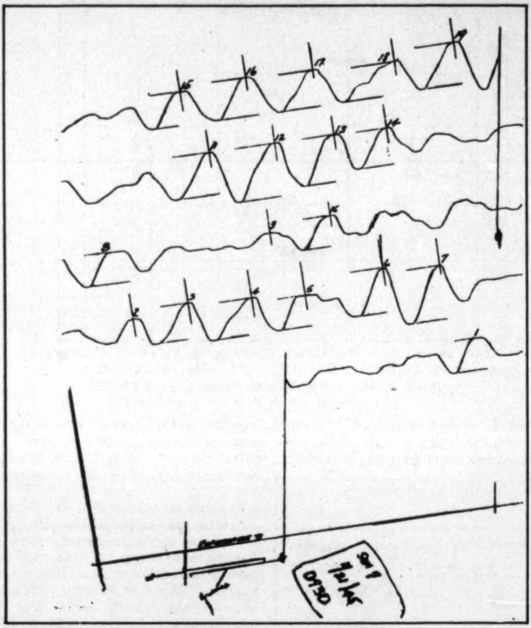

Fig. 6--Photograph of a typical record from the deep-sea wave recorder, Mark I

spar buoy is a long aluminum pole, approximately three inches in diameter, to the bottom of which is attached a pressure recorder and in turn a line to the damping disc. The second line and floats are for the purpose of recovering the equipment. In operation the flat damping disc of three- or four-foot diameter has a virtual mass of about two tons and as a result there is little absolute motion of the complete system when the damping disc is placed at a depth where the water orbital velocities are negligible. A correction factor K′ can be calculated for the spar buoy damping disc system. This correction factor includes the absolute motion of the spar buoy system and the normal pressure ratio variation with depth due to waves. The combined equation of motion for the system is of the type

$$dZ^2/dt^2 + B(dZ/dt)^2 + C\ Z + E = P \sin \omega t$$

This equation assumes surface waves of sinusoidal shapes. The equation is non-linear and approximations are required in order to obtain a solution. When B is very small, the fluid friction damping term may be expressed approximately in terms of the velocity instead of the velocity squared, or successive approximation methods may be used to obtain a suitable solution. The largest error involved appears to be in the determination of the magnitude of the virtual mass of the damping disc. Laboratory experiments on a disc with linear acceleration show a virtual mass which is considerably larger than the theoretical value [LAMB, 1932]. No detailed studies have been conducted for the virtual mass of an oscillatory system. Calibration curves for the damping disc system have been calculated on the basis of laboratory measurements to determine an approximate virtual mass for the disc. When the disc is placed at a distance of 250 to 300 ft in deep water, the standard floating system has a calculated maximum absolute motion of about eight per cent of the wave height.

In order to have a recorder with an outside diameter of the same order as the spar buoy, special units had to be constructed. Records have been obtained with a mechanical pressure recorder and with an echo sounding device which transmitted its readings by radio. A typical record obtained by the mechanical unit is shown in Figure 6.

On the basis of experience at sea with launching and retrieving of spar buoy systems it appears that any system which requires recovery is not practical. In order to obtain a large number of records at sea, a necessary procedure for some types of investigations, it is desirable to develop an expandable radio-sending unit similar to those used for meteorological observations.

Conclusions--Appreciable progress has been made during recent years in obtaining wave measurements. Instruments are now in operation for obtaining a continuous or semi-continuous recording of wave characteristics. Much developmental work remains to be done in the study of basic factors and in the application of suitable instruments.

Acknowledgments--This investigation was part of an extensive series of experiments on waves for the Bureau of Ships, United States Navy, under contracts NObs 16290 and 2490.

References

BEACH EROSION BOARD, An ocean wave measuring instrument, Tech. Memo. no. 6, Washington, D. C., 1948.

FOLSOM, R. G., Field test of shore wave recorders, Half Moon Bay, Navy Wave Proj., Univ. Calif., Rept. HE-116-180, 28 pp., Jan. 15, 1946 (unpublished).

FOLSOM, R. G., Sub-surface pressures due to oscillatory waves, Trans. Amer. Geophys. Union, v. 28, pp. 875-881, 1947.

LAMB, H., Hydrodynamics, 6th ed., p. 166, Cambridge Univ. Press, 1932.

RAUCH, S. E., Preliminary investigations of wave direction indicator, Navy Wave Proj., Univ. Calif., Rept. HE-116-193, 8 pp., Aug. 31, 1945, (unpublished).

SEIWELL, H. R., Evaluation of sea-surface roughness from underwater pressure recordings, Trans. Amer. Geophys. Union, v. 29, pp. 197-201, 1948.

WIEGEL, R. L., Oscillatory waves, Bull. Beach Erosion Board, Spec. Issue No. 1, July 1, 1948.

University of California,
Berkeley, California

(Presented at the First Conference on Geophysics, University of California, Berkeley, California, May 15, 1948; open for formal discussion until March 1, 1950.)

Transactions, American Geophysical Union Volume 30, Number 5 October 1949

AN ANALYSIS OF DATA FROM WAVE RECORDERS ON THE PACIFIC COAST OF THE UNITED STATES

R. L. Wiegel

Abstract--The wave heights and periods from wave recorders installed off Point Sur, California, and Heceta Head, Oregon, have been compared for the period from April 1947 to June 1948. These data, together with some obtained at Point Arguello, California, showed that the ratio of the maximum wave recorded each day to the average of the highest ten per cent for that day was 1.46 and the ratio of the average of the highest ten per cent to the average of the highest one-third of the waves each day was 1.29 for any place along this section of the Pacific Coast. It was also found that the average period of the swells (that is, excluding the local storm "chop") was 12 sec.

Introduction--There are many problems for which the dimensions of ocean waves are necessary. Some of these are in the design of shore-protection structures such as sea walls and jetties for harbor development, in aircraft ditching, and in the design of ship hulls.

Various ways of obtaining these dimensions have been tried [FOLSOM, 1949], the most widely used at the present being the Mark III type of wave recorder. This instrument is placed on the ocean bottom and records the differential pressure fluctuation by means of a bellows linked to a cantilever beam which in turn controls the position of a precision potentiometer. The Wheatstone bridge circuit of which the potentiometer is a part is connected by means of a three-conductor cable to a suitable recorder located on shore.

A number of these instruments have been installed along the Pacific Coast of the United States by the Department of Engineering, University of California, as part of an extensive investigation of surface waves conducted for the Bureau of Ships, United States Navy. Two have operated almost continuously since April 1947. They are located at Point Sur, California, and Heceta Head, Oregon (Fig. 1). In addition, data were obtained from an instrument located at Point Arguello, California, for the period July 1948 through September 1948.

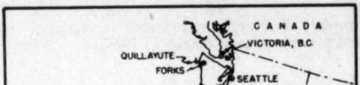

Fig. 1--Location of wave measuring instruments of the University of California along the Pacific Coast

The methods by which ocean waves are forme by normal pressures and tangential stresses durin storms are fairly well known [SVERDRUP and MUNK, 1947; JOHNSON, 1948] as is the change in their dimensions during their travel from the generating area to the coast. However, these theories deal with "significant waves," which are waves with the average height and period of the one-third highest waves of a group. Using the forecasting method developed by SVERDRUP and MUNK [1947] data on significant waves may be found for any location from files of past weather charts. However, the problem of what other waves existed would still remain to be determined. The data shown here should be of help in this regard.

Analysis of records--The records obtained from the Mark III recorders showed the pressure fluctuation on the ocean bottom due to the surface waves. In order to obtain the heights of the surface waves the following equation had to be used.

$$\text{Pressure fluctuation/Wave height} = K = \cosh[(2\pi D/L)(1 - Z/D)]/\cosh(2\pi D/L)$$

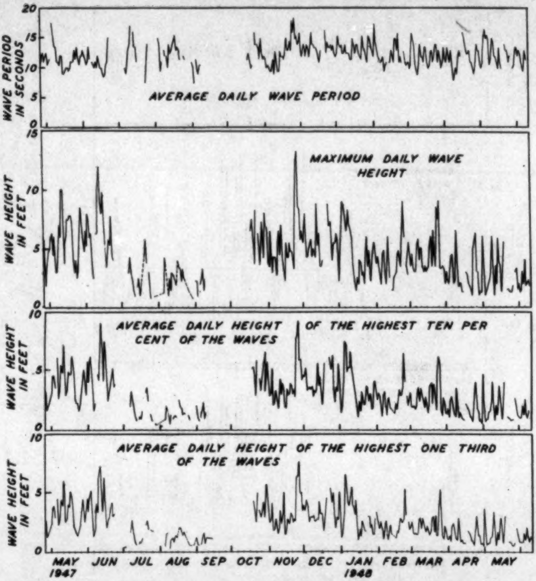

Fig. 2--Data obtained at Point Sur, California from April 26, 1947 through June 10, 1948

This was the equation for the pressure fluctuation at any distance Z below the still water level due to a surface wave where the ocean depth is D and the wave length at that point is L [FOLSOM, 1947]. For an instrument recording on the bottom this equation reduces to

$$K = 1/\cosh(2\pi D/L)$$

As the records from a wave recorder show only the bottom pressure fluctuation and period, an additional equation must be used to determine the wave length from the known depth and the measured period. This equation is

$$L = [gT^2 \tanh(2\pi D/L)]/2\pi$$

which, after combining with other relationships, may be tabulated in the form $2\pi D/gT^2$ versus both $\tanh(2\pi D/L)$ and D/L. Hence L is easily computed from D/L which is found in the tables as a function of $2\pi D/gT^2$ [WIEGEL, 1948].

Wave records were taken almost continuously at the locations mentioned above. For all recorders the charts were operated at two speeds, these being three inches per minute for a period of 20 min out of every eight hours and then at three inches per hour for the remaining time. The highest ten per cent and the highest one-third of the waves recorded during the 20-minute fast speed period were measured and tabulated along with the average period. In addition the maximum wave recorded was tabulated along with the average period. In addition the maximum wave recorded was tabulated. The maximum wave height, the average of the highest ten per cent and the highest one third were determined from those portions of the daily record when the chart was moving at high speed; that is, at three inches per minute. Figures 2 and 3 are examples of the first steps in the analysis of the data.

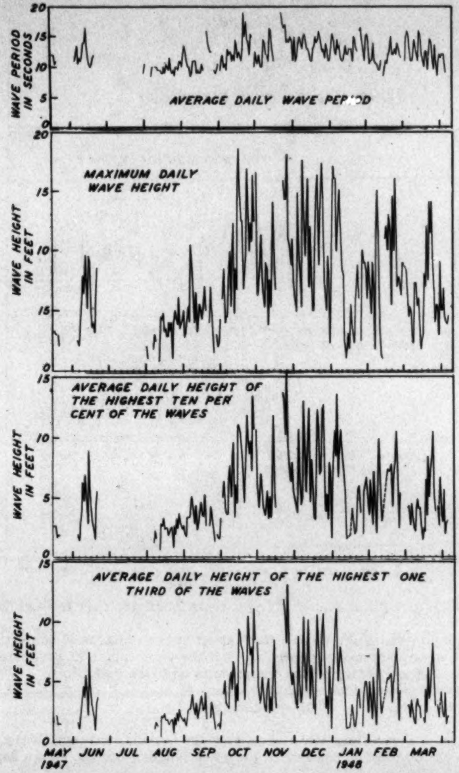

Fig. 3--Data obtained at Heceta Head, Oregon from May 10, 1947 through April 5, 1948

Results--The most interesting results were the excellent correlations between the daily average highest ten per cent and the daily average highest one third. The average ratio for all points at Point Sur was 1.27 (see Fig. 4), for Heceta Head 1.30, and for Point Arguello 1.30, giving an average of 1.29 for the Pacific Coast of the United States. Even more surprising was the fact that almost every point was within plus or minus ten per cent of this value.

Next, it was found that the average ratio of the maximum wave measured each day to the daily average of the highest ten per cent was 1.46 for Point Sur (see Fig. 5), 1.47 for Heceta Head, and 1.42 for the three-month period at Point Arguello. The weighted average of these was 1.46. Almost all the individual points were within plus or minus 20 per cent of the average, which was very good considering the many factors which conceivably could build up a maximum wave.

The next correlation was between the maximum wave measured each day and the daily average of the highest one third. The average ratio for the entire period was found to be 1.85 for Point Sur (see Fig. 6), 1.91 for Heceta Head and 1.85 for the three-month period at Point Arguello. The average of these was 1.87. Again, almost every point was within plus or minus 20 per cent of this average value.

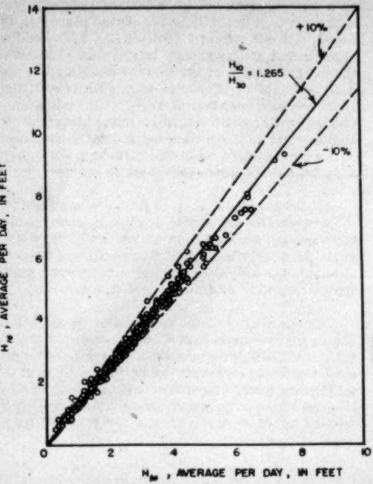

Fig. 4--Comparison of the average of the highest ten per cent of the waves as measured for a day with the highest one third for the same day, Point Sur, California, April 26, 1947-June 10, 1948

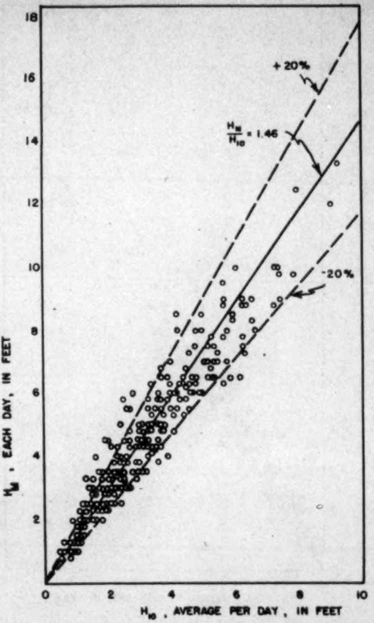

Fig. 5--Comparison of the highest wave measured each day with the average of the highest ten per cent as measured for the same day, Point Sur, California, April 26, 1947-June 10, 1948

The average wave period was computed and found to be 12 sec. This was, of course, of little significance as the individual values varied widely from the average. In addition, the waves of a period less than about seven seconds would not be noticeable on the records owing to the inherent hydrodynamical damping [FOLSOM, 1947] which would have "filtered out" these short periods in depths at which the instruments were installed. Most of these short periods would be of locally generated storm waves rather than of the swell (which become the predominant breakers along the shore).

Little was done on comparing the periods recorded at Point Sur and Heceta Head, because for any good correlation the direction of the waves would be needed and neither of the two stations had, as then, direction recorders. It could be seen, however, that during the winter months, when the predominant swell was from the northwest, the periods at both stations were similar, as would be expected. This did not apply during the summer months when the direction varied considerably.

The comparison of the daily average of the highest ten per cent of the waves at Point Sur and Heceta Head was similar to the comparison of the wave period; for example, in the summer the relationships were not good, but during the winter months the swell at Point Sur varied in a similar manner to the swell at Heceta Head, except for the fact that the swell at Point Sur was of a lower magnitude. Thus, when the swell was high at Heceta Head it was high at Point Sur and when it was low at Heceta Head it was low at Point Sur; there was no constant ratio between the two.

Discussion and conclusions--The implication from the excellent correlation between the maximum waves recorded each day and the average of the highest ten per cent and the average highest one third, along with the correlation between the daily average of the average highest ten per cent with the average highest one third, seems to be that a statistical grouping of waves is generated by a storm. This belief is furthered by the results found in two widely separated places in the western North Atlantic [SEIWELL, 1948] which showed that at Cuttyhunk, Mass., and at Bermuda the average ratio of the highest one-third to the daily average of all waves was, with very little fluctuation, a constant of 1.57. This indicates that a similar ratio would be found along the Pacific Coast, if the data for the daily average of the waves were tabulated, although the constant would not necessarily be the same.

It seems, then, that as far as some fairly large area like the North Pacific is concerned, the waves generated by a storm would have the same or nearly the same distribution of heights, although the magnitude would depend upon the intensity, fetch, and duration of the storm.

These correlations could be of immediate use in that records would only have to be reduced for the highest ten per cent in order to determine the "significant waves," namely, the highest one-third; this would cut analysis time considerably. It should also improve the understanding of the method by which wave groups are formed in a generating area.

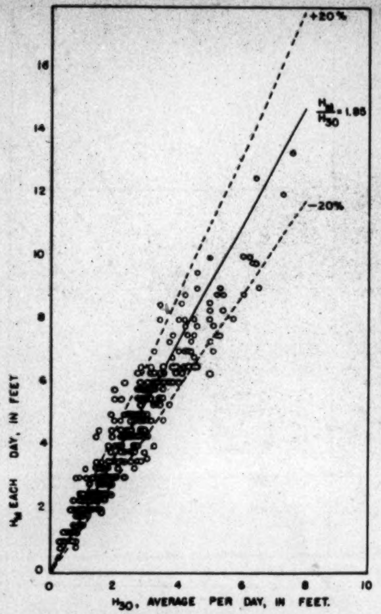

Fig. 6--Comparison of the highest wave measured each day with the average of the highest one third as measured for the same day, Point Sur, California, April 26, 1947-June 10, 1948

References

FOLSOM, R.G., Sub-surface pressures due to oscillatory waves, Trans. Amer. Geophys. Union, v. 28, pp. 875-881, 1947.

FOLSOM, R. G., Measurement of ocean waves, Trans. Amer. Geophys. Union, v. 30, pp., 691-699, 1949.

JOHNSON, J. W., The characteristics of wind waves on lakes and protected bays, Trans. Amer. Geophys. Union, v. 29, pp. 671-681, 1948.

SEIWELL, H. R., Results of research on surface waves of the western North Atlantic, Papers Phys. Ocean. Met., v. 10, no. 4, 56 pp., 1948.

SVERDRUP, H. U., and MUNK, W. H., Wind, sea, and swell; theory of relations for forecasting, Hydrographic Off. Pub. No. 601, Washington, 1947.

WIEGEL, R. L., Oscillatory waves, Bull. Beach Erosion Board, spec. issue no. 1, Washington, 1948.

Fluid Mechanics Laboratory,
University of California,
Berkeley, California

(Manuscript received January 14, 1949; presented at the West Coast Meeting, Los Angeles, California, February 5, 1949; open for formal discussion until March 1, 1950.)

Transactions, American Geophysical Union Volume 30, Number 5 October 1949

DIFFRACTION OF WATER WAVES PASSING THROUGH A BREAKWATER GAP

Frank L. Blue, Jr. and J. W. Johnson

Abstract--Efficient breakwater design requires a knowledge of the behavior of the waves passing the breakwater. Wave diffraction is an important factor in this behavior. Solutions based on the theory of light diffraction have been proposed for water-wave diffraction, but have not previously been experimentally verified for shallow water nor for waves entering breakwater gaps. This investigation found experimentally the wave patterns and comparative wave heights due to diffraction of water waves entering a gap in a breakwater normal to the incident wave direction in water of uniform depth, and compared these experimental results with approximate theoretical solutions. Both deep-water and shallow-water waves were studied. Oblique incidence and varying depths were not investigated experimentally, but approximate methods of considering their effect are suggested.

The experimental results were found to verify the general form of the wave diffraction theory for breakwater gaps with gap width/wave-length ratios as small as 1.41 in water of depth as small as 0.14 wave length.

The theory and computation methods considered in this investigation form a usable basis for estimating the effect of diffraction on waves at a breakwater gap.

Introduction

A knowledge of water-wave diffraction has application in the design and location of harbor breakwaters and structures protected by those breakwaters. The absence of reliable means of estimating in advance the effect of breakwaters on waves has necessitated individual model studies, which, though less costly than improper breakwater design and location, are nevertheless expensive. A reliable method of estimating such effects would enable breakwaters to be safely planned without model studies in many cases, and the model studies to be improved and simplified in other cases.

PENNEY and PRICE [1944] proposed a solution based on the fact that the boundary value problem for waves of small amplitude impinging on a single semi-infinite straight breakwater is the same as the similar problem in light diffraction, which has been rigorously solved by Sommerfeld (BATEMAN [1944] gives a statement in English of the Sommerfeld solution). By applying the solution so obtained to each of the two wings of a breakwater normal to the wave travel direction and containing a gap, combined solutions are obtained which exactly satisfy the conditions for two similar wings. This method is applied to a gap in a rigid breakwater. The two types of breakwaters referred to above are defined as follows. If a breakwater is considered rigid, the normal component of the fluid velocity is zero, but if the breakwater is of the cushion type, the breakwater is assumed to yield with the passage of a wave; hence the pressure remains constant.

PUTNAM and ARTHUR [1948] have checked experimentally the solution for a semi-infinite breakwater in deep water, using waves 2.52 ft and 2.96 ft long. Experimental heights agreed approximately with the theory in the sheltered region, but were considerably less than theoretical in the unsheltered region. So far as in known, the theory has not been previously checked experimentally for shallow water waves nor for breakwater gaps.

The purpose of this investigation was to check experimentally the diffraction theory for a gap in a breakwater normal to the incident wave travel direction, using both deep water and shallow water waves.

Before proceeding with the experimental investigations, a preliminary theoretical investigation was made of the effect of shallow water upon the theory, leading to the tentative conclusion that for proportions similar to those encountered in practical breakwaters, no change in the theory would be required, other than use of the shallow-water wave length rather than the deep water wave length for L in the basic equations.

Notation--In the theoretical treatment to follow, the following symbols are used:

A	A constant in the equation for waves of small amplitude
b	Width of breakwater gap
C	Wave celerity (velocity of wave form) = L/T
d	Depth from still water level to bottom
e	Base of natural logarithms = 2.7183
F	A function of one or more variables, as F(x,y)
f_1, f_2 g_1, g_2	Functions appearing in the Penney-Price solution for a breakwater gap
g	Acceleration of gravity
H	Wave height from trough to crest
i	$\sqrt{-1}$
K'	Diffraction coefficient (ratio of diffracted wave height at point (x,y) to incident wave height at the breakwater)
k	$2\pi/L$
L	Wave length
L_o	Wave length in deep water
r	Distance from end of breakwater to point (x,y)
S	Real part of diffraction function f(-u) = S + iw
t	Time
u	Upper limit of integral term in solution of diffraction problem.
v	Particle velocity in y direction
w	Imaginary part of diffraction function f(-u) = S + iw
x	Horizontal distance perpendicular to y
y	Horizontal distance in direction of incident wave travel
z_s	Elevation of water surface above still water level
θ_o	Angle between breakwater and incident wave direction

Theory

The general problem of progressive waves has been treated by LAMB [1932]. For the case where a barrier is present PUTNAM and ARTHUR [1948] have extended and checked experimentally a solution developed by PENNEY and PRICE [1944]. For this solution with a rigid barrier as shown in Figure 1, PUTNAM and ARTHUR [1948] give the solution

$$F(r, \theta) = (1/\sqrt{2})\, e^{i[(\pi/4) - kr\cos(\theta_0 - \theta)]} \int_{-\infty}^{u_1} e^{-i\pi v^2/2}\, dv$$

$$+ (1/\sqrt{2})\, e^{i[(\pi/4) - kr\cos(\theta_0 + \theta)]} \int_{-\infty}^{u_2} e^{-i\pi v^2/2}\, dv \ldots\ldots\ldots\ldots (1)$$

where

$$u_1 = -\sqrt{4kr/\pi}\,\sin[(\theta_0 - \theta)/2] \text{ and } u_2 = -\sqrt{4kr/\pi}\,\sin[(\theta_0 + \theta)/2]$$

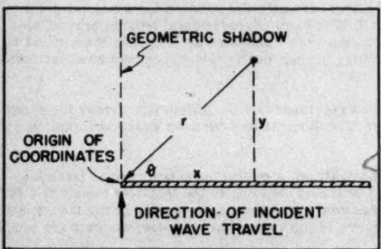

Fig. 1--Nomenclature for wave diffraction analysis at breakwater tip

Using cartesian instead of polar coordinates and noting that $e^{i\pi/4} = (1 + i)/\sqrt{2}$, (1) can be written in the form

$$F(x,y) = (1 + i)\Big[e^{-iky} \int_{-\infty}^{4(r-y)/L} e^{-i\pi u^2/2} du$$

$$+ e^{iky} \int_{-\infty}^{\sqrt{4(r+y)/L}} e^{-i\pi v^2/2} dv\Big]/2 \ldots\ldots (2)$$

For x and y positive (protected region) the signs of the upper limit of both integrals are negative. For x negative and y positive the upper limit of the first integral is positive and that of the second is negative. For x positive and y negative both limits are positive.

When the upper limit is positive, we may use the relation

$$\int_{-\infty}^{u} e^{-i\pi v^2/2}\, dv = \sqrt{2}\, e^{-i\pi/4} - \int_{-\infty}^{-u} e^{-i\pi v^2/2}\, dv \qquad (3)$$

to change (2) into the forms

$$\left.\begin{aligned} F(x,y) &= e^{-iky} - f_1 + g_1 && \text{for } x \leqq 0 \\ &= f_1 + g_1 && \text{for } \begin{cases} x \geqq 0 \\ y \geqq 0 \end{cases} \\ &= e^{-iky} + e^{iky} - f_1 - g_1 && \text{for } \begin{cases} x \geqq 0 \\ y \leqq 0 \end{cases} \end{aligned}\right\} \qquad (4)$$

where f and g are defined as follows

$$\begin{aligned} f = f(r,y) &= (1 + i)(e^{-iky}/2)\int_{-\infty}^{-u} e^{-i\pi v^2/2}\, dv) \\ &= e^{-iky} f(-u) \end{aligned} \qquad (5)$$

$$\begin{aligned} f(-u) &= [(1 + i)/2]\int_{-\infty}^{-u} e^{-i\pi v^2/2}\, dv) \\ &= S + iw \end{aligned} \qquad (6)$$

$$u = \sqrt{4(r - y)/L} \qquad (7)$$

and

$$g = f(r, -y) \qquad (8)$$

In a similar manner, the solution for a cushion type of barrier is

$$\left.\begin{aligned} F(x,y) &= e^{-iky} - f - g && \text{for } x \leq 0 \\ &= f - g && \text{for } \begin{cases} x \geq 0 \\ y \geq 0 \end{cases} \\ &= e^{-iky} - e^{iky} - f + g && \text{for } \begin{cases} x \geq 0 \\ y \leq 0 \end{cases} \end{aligned}\right\} \qquad (9)$$

Solution for gap--Consider a breakwater with a gap as indicated by Figure 2. Suppose the right

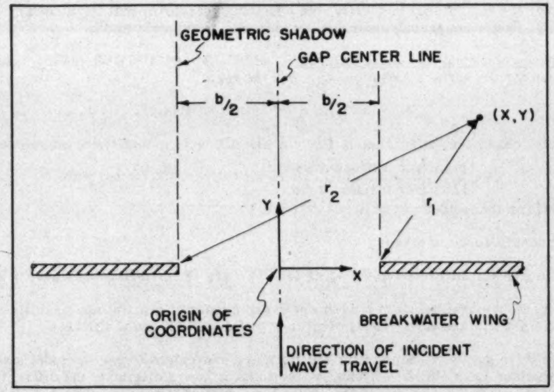
GEOMETRIC SHADOW
GAP CENTER LINE
b/2
b/2
(X,Y)
r_2
r_1
Y
X
ORIGIN OF COORDINATES
BREAKWATER WING
DIRECTION OF INCIDENT WAVE TRAVEL

Fig. 2--Nomenclature for breakwater-gap problem wing is rigid while the left is of the cushion type. Then, since x does not appear directly in (4) and (9), these still apply; and we may take (4), replacing f, g, u, and r by f_1, g_1, u_1, and r_1, as the solution for the left wing acting alone; and (9) with f_2, g_2, u_2, and r_2, as that for the right wing alone. Adding these two solutions and subtracting e^{-iky} (also a solution of the differential equation), we find that the combined solution satisfies the pertinent boundary condition at each barrier; that is, the combined solution for the breakwater with one rigid and one cushion wing is mathematically exact.

When both barriers are of the same type, the boundary conditions at the barriers are not exactly satisfied by a solution formed in this manner. The departure from the exact conditions is small, however, if the gap width is as great as two wave lengths.

Thus in the case of two rigid barriers, the combined solution is as follows

$$\left.\begin{array}{c|c|c}
-f_1+g_1 & & f_1+g_1 \\
+f_2+g_2 & e^{-iky} & -f_2+g_2 \\
\cline{1-1}\cline{3-3}
\text{Rigid barrier} & -f_1+g_1 & \text{Rigid barrier} \\
\cline{1-1}\cline{3-3}
e^{-iky}+e^{iky} & -f_2+g_2 & e^{-iky}+e^{iky} \\
-f_1+g_1 & & -f_1-g_1 \\
-f_2-g_2 & & -f_2+g_2
\end{array}\right\} \dots\dots\dots\dots (10)$$

The boundary condition for rigid barriers has been shown by **PENNEY** and **PRICE** [1944] to be

$$\partial F/\partial y = 0 \dots\dots\dots\dots (11)$$

Considering either side of the right barrier at y = 0, we find from (5), (8), and (11), substituting the asymptotic expression for f(-u)

$$\begin{aligned}\partial F/\partial y &= -2[\partial f_2/\partial y]_{y=0} \\ &= e^{i(\pi/4-4)}[\sqrt{L/r_2}\; e^{i(4r/L+4-\pi)}+1]/\sqrt{2L}\end{aligned} \dots\dots\dots\dots (12)$$

which cannot exceed in absolute value $(\sqrt{L/r_2}+1)/\sqrt{2L}$. This quantity is very small except at the breakwater tip, and there, if b is as great as 2L, it cannot exceed 1.21/L which is less than 1/5 the value of $\partial F/\partial y$ for the incident wave. We conclude, therefore, that the boundary conditions are approximately, though not exactly, satisfied by (10), if b is as great as 2L.

Diffraction coefficient and phase difference--**PUTNAM** and **ARTHUR** [1948] have shown that the expression for the surface elevation, z_s, is of the form,

$$z_s = (AikC/g)\, e^{-ikCt} \cosh kd \cdot F(x,y) \dots\dots\dots\dots (13)$$

The only factor changed by diffraction is F(x,y). The diffraction coefficient therefore is given by

$$K' = \frac{|F(x,y)| \text{ for diffracted wave}}{|F(x,y)| \text{ for incident wave}} = |F(x,y)| \text{ for diffracted wave} \dots\dots\dots\dots (14)$$

since $|F(x,y)|$ for the incident wave is $|e^{-iky}| = 1$.

The phase difference is given by

$$\arg (F \text{ for diffracted wave}) - \arg (e^{-iky}) = \arg (F \text{ for diffracted wave}) + ky \dots\dots (15)$$

In finding these quantities it is convenient to use graphs of arg f(u) and mod f(u) such as that given by **PUTNAM** and **ARTHUR** [1948] or graphs or tables of S and w versus u.

Effect of wave splitters--Since wave splitters are convenient to use in model studies, it is of interest to consider their effect. Physically, the wave splitters eliminate the diffraction influence of the front faces of the breakwater wings, since they prevent the waves reflected by those faces from being diffracted into the path of the portion of the waves which enters the breakwater gap.

Mathematically, this effect appears to be given by the g_1 and g_2 terms of (10), since, as indicated by (4) and (9), these are the only terms affected by the type of breakwater face. It therefore seems reasonable to look for a solution without these terms. No exact solution is know, but a simplified solution, which is approximately the same as (10) for most values of x and y, is obtained by omitting the "g" terms of (10), thus obtaining

$$\left.\begin{array}{c|c|c} f_2 - f_1 & e^{-iky} & f_1 - f_2 \\ \hline \text{Rigid barrier} & & \text{Rigid barrier} \\ \hline & -f_1 \cdot -f_2 & \\ \text{Wave splitter} & & \text{Wave splitter} \end{array}\right\} \cdots\cdots\cdots \quad (16)$$

The solution (16) approximately fits the boundary condition $\partial F/\partial x = 0$, along the face of the wave splitter, (the maximum error being less than $1/\sqrt{2L}\, b$) but is less satisfactory along the back of the breakwater. The complete solution, on the other hand, fits approximately along the breakwater, but not along the wave splitter. Since the wave amplitudes along the back face of the breakwater are very small, both physically and by the approximate equations, failure to fit the boundary conditions is less important there than along the wave splitter, where the waves are large. The simplified approximate solution (16) therefore is considered more appropriate than the complete solution when the wave splitters are present.

Examples of the diffraction coefficients resulting from the complete and this simplified solution are given below in the summary of experimental results. (Figs. 3 to 7).

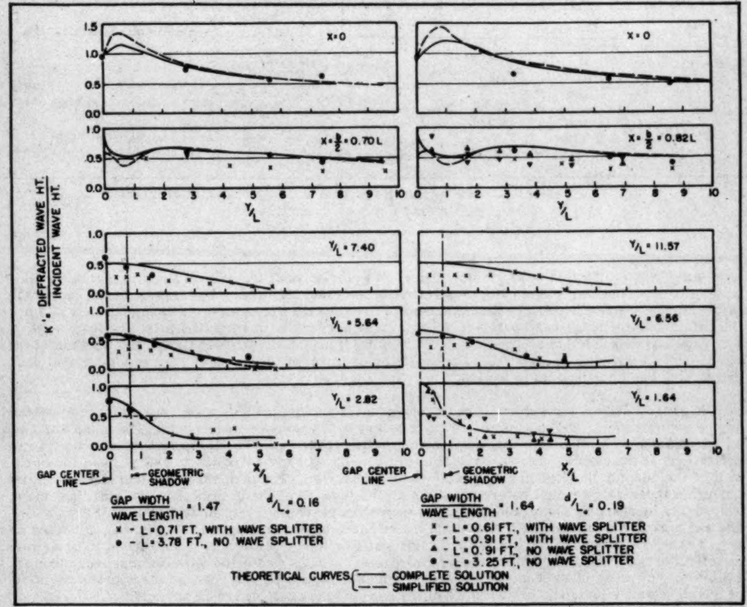

Fig. 3--Comparison between theoretical and experimental diffraction coefficients for shallow water waves

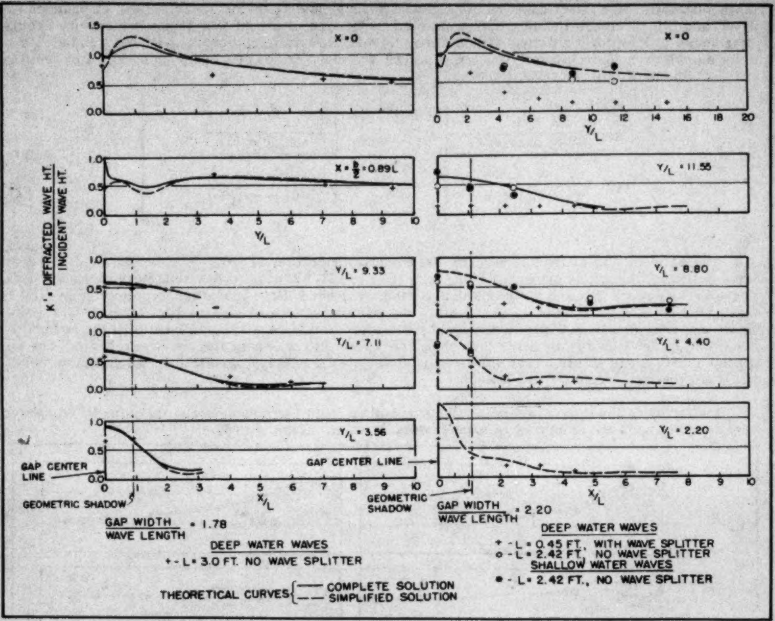

Fig. 4--Comparison between the theoretical and experimental diffraction coefficients for deep water waves

Experiments

Wave basins--To test the foregoing theory of water-wave diffraction at a gap in a rigid breakwater, an experimental investigation was made in the Fluid Mechanics Laboratory at the University of California. Measurements included those required for the diffraction coefficient as well as for the determination of the wave pattern. Studies first were made in a small 6 ft by 12 ft basin one foot deep and then later in a larger basin 64 ft by 65 ft in plan by two feet deep. The bottoms of the basins were horizontal in all tests. The direction of travel of the incident wave was normal to the gap in both the small and large basins.

Figure 8a shows, for the small basin, the general arrangement of wave generator, breakwater gap, wave absorbers, and ranges where wave height measurements were made. The basin was used as a half model, one side representing the center line at the gap. To eliminate the existence of wave reflections at the barrier and the wave plunger, a guide wall was provided to extend from the back wall of the tank for the distance of three feet to the barrier. The incident wave, therefore, traveled through a three-foot channel before passing into the leeward of the breakwater. This arrangement was varied by changing the width of the approach channel (or half-gap) to represent full gaps of one, one and a half, and two feet. To determine the effect of using these approach channels, a limited number of check runs were made without the guide walls or wave splitters in place. Also, to determine the effect of the wall along the gap center line one set of runs was made with the approach channel shifted to the center of the basin. The arrangement of Figure 8a was changed for another set of runs by adding a wall to extend from the edge of the gap into the protected area at angles of 60° and 45° with the incident wave direction, thus representing a symmetrical breakwater with inclined wings. Other variations were the wave period (0.26 sec and up), the water depth, and the elevation and am-

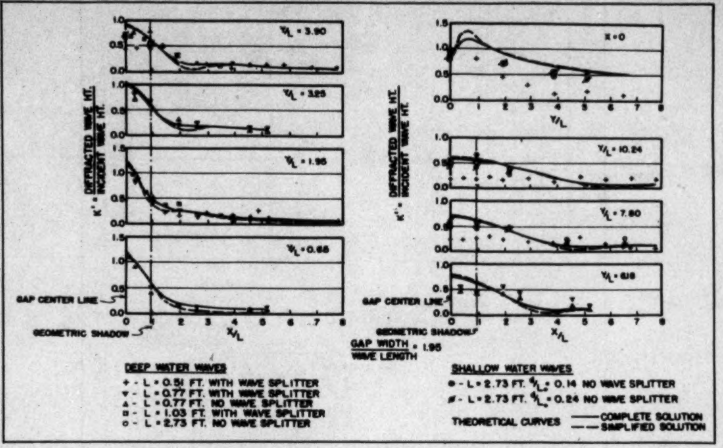

Fig. 5-- Comparison between theoretical and experimental diffraction coefficients for both deep water and shallow water waves with a gap width of 1.95 wave lengths

plitude of the wave plunger. A wedge-shaped plunger was used for water depths of 0.4 to 0.6 ft, while a curved plunger was used for depths of 0.135 to 0.3 ft.

In the large basin (see Fig. 8b) all runs were made with a centrally located gap, 5.33 ft long, without wave splitters. The edges of the gap consisted of 1/4-inch sheet metal plates which extended 6 1/2 inches beyond the ends of the wooden walls forming the breakwater. Waves of constant amplitude and period were generated by a machine consisting of a flap hinged at the bottom of the basin and moved back and forth with a crank mechanism driven by a direct-current motor. Variations here included the wave period (0.64 to 0.94 sec), the water depth (0.48 to 1.5 ft), and the wave amplitude.

Wave-height measurement--Wave heights were measured in both basins by means of electrical resistance elements, each consisting of two 0.033 inch diameter steel piano wires placed 0.5 inch apart. These were subjected to constant alternating current voltages adjusted by a combination of fixed and variable transformers to produce the desired current range, and the resulting currents, which varied with the immersion of the wires in the water with each wave passage, were recorded on an oscillograph. (see Fig. 9). To determine wave heights from the oscillograph record, calibration curves showing element immersion versus record width were plotted for each resistance element, using calibration records made immediately prior to each set of runs.

Experimental procedure (wave heights)--As previously mentioned, wave heights in these tests were obtained by resistance elements. In the small wave basin one element was mounted in the approach channel (see Fig. 8a) to obtain the incident wave height, while three to five others were mounted on an aluminum angle which could be moved into various positions in the lee of the breakwater. In the large wave basin, 13 resistance elements connected in parallel were mounted on point gage holders at the stations indicated on Fig. 8b. Diffraction coefficients were found by dividing the station wave heights by the incident wave heights recorded at the same time.

Experimental procedure (wave patterns)--Although it would have been possible to determine phase differences from the oscillograph records and to compute the wave patterns from these in the same way that they were computed from the theoretical phase differences by using enough observation stations, it was more expendient to trace the patterns from vertical photographs. Figures 10 and 11 are typical photographs showing the diffraction pattern.

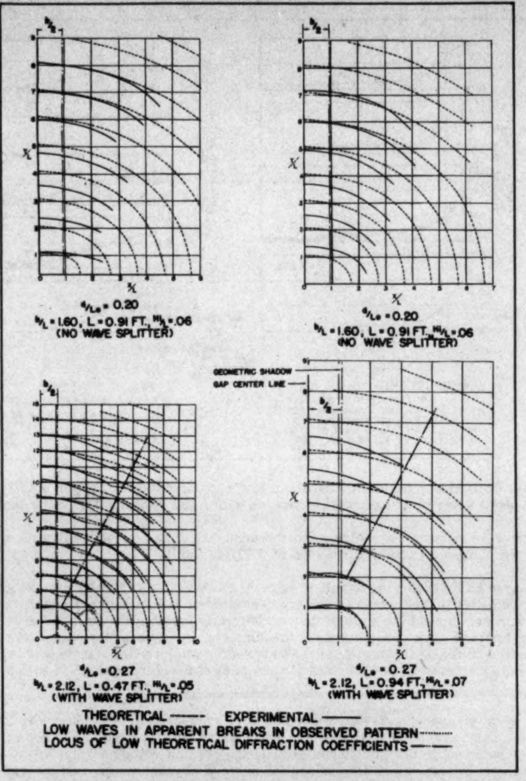

Fig. 6--Wave patterns for shallow water waves

Experimental results--The averaged experimental results are summarized in Figures 3 to 7. The quantities used for comparison are the wave pattern and the diffraction coefficient K' = diffracted wave height/incident wave height. Theoretical curves for the diffraction coefficients are given in most cases for both the simplified (Eq. 16) and the complete solutions (Eq. 10). As indicated by Figure 2 the origin of coordinates is at the center of the breakwater gap.

Comparison of experiment with theory

Diffraction coefficients--Experimental and theoretical diffraction coefficients are shown in Figures 3 to 5. The experimental points represent averages of several individual runs. The various data show that for waves as long as three feet, experimental K', while low or high for individual stations, agrees fairly well with the theory throughout the area investigated. For shorter waves and small y/L, the observed diffraction coefficients, though scattering considerably, tend to agree with the theoretical values. As y/L increases, however, observed K' in the vicinity of the gap center line, where theoretical K' is greatest, falls below theoretical K'. This dropping off is most rapid for shorter waves and less rapid for longer waves. Considering the graphs of K' along the

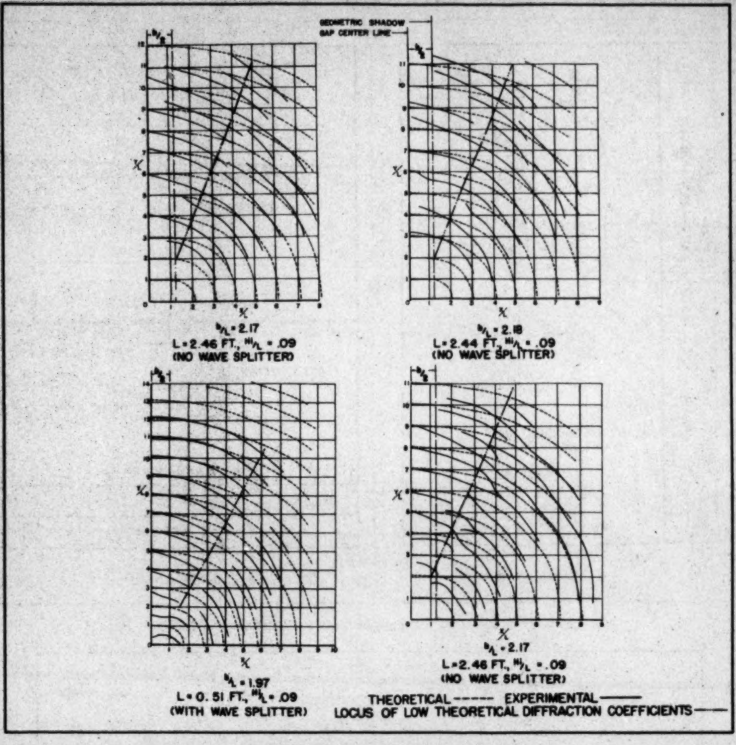

Fig. 7--Wave patterns for deep water waves

lines x = 0 and x = b/2, it appears that as the waves become longer, experimental K' approaches theoretical K' as an approximate limit.

In areas more distant from the center line, this dropping off of K' is less evident. In fact there is a distinct tendency for experimental K' to exceed theoretical K'. This is regarded as due to the increased curvature of the wave crests in the regions of steepest waves, as later explained in the discussion of wave patterns.

Considering the whole width of the observed area, both the region near the center line and the regions distant therefrom, the trend is for the average experimental diffraction coefficient to drop below the average theoretical coefficient as y/L increases, the drop being rapid for short waves and less rapid for longer waves. That is, an energy loss occurs which is relatively large for waves as short as 0.5 ft but unimportant for waves as long as three feet traveling distances up to ten wave lengths.

To check the effect of wave steepness on diffraction coefficients, plots were made showing experimental K' for several waves or groups of waves of different steepnesses made under otherwise similar conditions. These plots indicated no definite trend resulting from the differences in steepness.

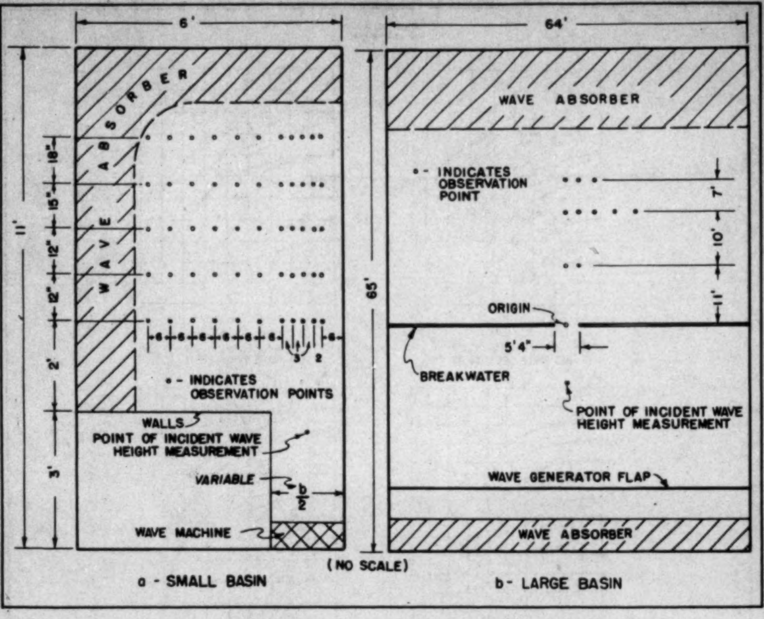
6'
64'
11'
18"
15"
12"
12"
2'
3'
WAVE ABSORBER
• - INDICATES OBSERVATION POINTS
6
3
2
WALLS
POINT OF INCIDENT WAVE HEIGHT MEASUREMENT
VARIABLE
b/2
WAVE MACHINE
(NO SCALE)
65'
WAVE ABSORBER
• - INDICATES OBSERVATION POINT
7'
10'
11'
ORIGIN
5'4"
BREAKWATER
POINT OF INCIDENT WAVE HEIGHT MEASUREMENT
WAVE GENERATOR FLAP
WAVE ABSORBER

a - SMALL BASIN

b - LARGE BASIN

Fig. 8--Model basin arrangements for diffraction studies

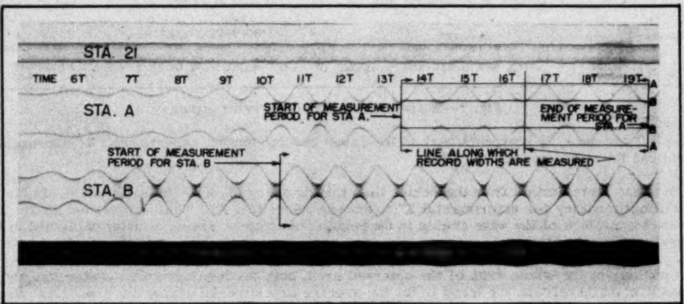

Fig. 9--Typical oscillograph record showing simultaneous wave height measurements at four stations in the large model basin

The possibility of the difference between experimental and theoretical diffraction coefficients obtained in the small wave basin being due to friction at the wall located along the gap center line of the half-model was checked by comparing runs of the same wave length in the half and full model. No consistent difference due to the half model was observed. In these comparisons the wave steepnesses differed, but since the effect of steepness was found to be negligible, the comparisons were considered valid.

The possibility of results beingmeasureably affected by the use of wave splitters may be checked from the separate plots of runs with and without wave splitters shown in Figure 6. Where the triangular symbols for K' are shown in pairs, point down and point up, they correspond to pairs of runs made with and without the removable wave splitter, but otherwise identical. This comparison reveals no important difference due to the wave splitters. As indicated previously the complete theoretical solution applies to the runs with wave splitters; while the simplified solution is considered more appropriate for those without, but this difference is too small to be apparent in the experimental results, and it does not greatly affect the average wave heights.

Fig. 10--Photograph of continuous diffraction pattern in shallow water

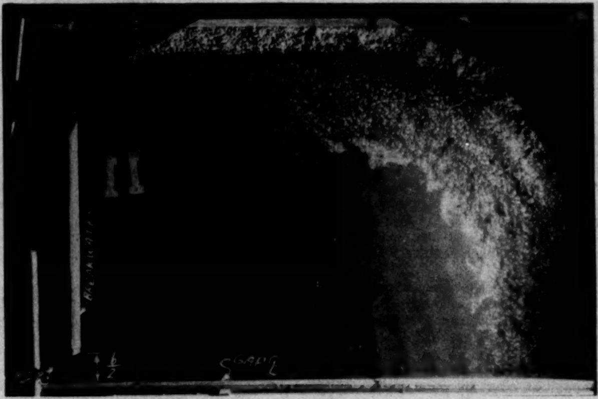

Fig. 11--Photograph of diffraction pattern in shallow water
showing breaks along a narrow zone

The failure of Eq. (4) to meet the exact boundary conditions along the breakwater becomes more important as the ratio of gap width to wave length decreases. PENNEY and PRICE [1944] estimated that this solution would be satisfactory for b/L ratios as small as 2.0. The experiments show results for b/L from 1.41 to 4.87, all of which behave in the same general way. The waves for b/L = 1.41 behave as nearly in accordance with the theory (as modified by the friction effects) as any other. The waves for b/L greater than 2.50 are all short waves made in the small basin, and their experimental diffraction coefficients are much smaller than the theoretical for large y, but this relation is about the same as that which occurs for the short waves for smaller b/L.

An analysis showed that the only modification of the theory required for shallow water would be the use of shallow-water wave lengths instead of deep-water wave lengths in Eq. (7). Theoretical K' was computed accordingly for the cases of uniform shallow-water depths covered in this investigation, the results being compared with expermental K' in Figures 3 to 5. Agreement is as good as for the deep water waves, confirming the conclusion of the preliminary study.

The d/L_o ratios of the waves studied in the experiments included values as small as 0.14, approaching the corresponding ratios for natural waves at real breakwaters. These were mostly relatively flat waves, but since wave steepness has no noticeable effect on diffraction coefficients in deep water, the same is probably true in moderately shallow water. It is concluded, therefore, that the theory gives usable diffraction coefficients for d/L_o as small as 0.14, and very probably for considerably smaller values.

The effect of non-uniform depths was beyond the scope of this investigation. Pending a thorough investigation of the subject, the following comments are offered. If the bottom contours are not normal to the wave directions, refraction as well as diffraction must be considered; in fact, after the first few wave lengths beyond the barrier, refraction may be more important than diffraction. One way of handling the combined effect of refraction and change in wave length and velocity when the bottom contours are not normal to the wave direction would be to divide successive wave crests into increments of equal wave energy (based on wave height), connecting the dividing points by lines which might be considered as "stream lines" of energy flow. Then the corresponding diagram for the uneven bottom could be approximately obtained by changing the distance between crest positions in proportion to the changed wave length due to depth variation, drawing in the energy "stream lines" at the same angles to the wave crests as before. The wave heights could be computed from this diagram based on the wave energy for the measured crest length between "stream lines." It should be noted that the refractive effects of irregular bottom contours can be considerable, and might cause the best gap opening to be at a location different from that indicated by diffraction alone.

Although this study was concerned primarily with straight breakwaters, one set of runs was obtained comparing symmetrical breakwaters with the wings each inclined at angles of 90° (straight breakwater), 60°, and 45° with the gap center line. While all three cases show lower than theoretical diffraction coefficients, due to the friction loss, no significant difference was apparent which may be attributed to the tested inclination of the breakwater wings. This is consistent with the finding of PUTNAM and ARTHUR [1948] wherein for a single breakwater the affect of angle between the breakwater and the incident wave direction is fairly small as long as the angle exceeds about 20°.

Wave patterns--Typical photographs for obtaining wave patterns are shown in Figures 10 and 11, and typical examples of patterns of shallow water waves are shown in Figure 6 and of deep water waves in Figure 7. In general the experimental wave patterns resemble the theoretical patterns in general form, but differ in some details. The successive crest positions (one cycle apart) shown by the patterns tend to be more widely spaced than the theoretical along the gap center line ($x = 0$), the difference decreasing rapidly as x increases, and less rapidly as y increases. That is, the actual wave crests are ahead of the theoretical along the gap center line, resulting in a more sharply convex crest shape there than results from the theory.

The more widely spaced crests, corresponding to greater wave lengths and greater wave velocity, occur in the areas where the diffracted waves are steepest, indicating that the effect is related to wave steepness. This is further indicated by the fact that this effect is most pronounced for the steepest incident waves.

An interesting feature of the wave patterns is the existence of zones of wave crest discontinuity. From this point of view, the wave-pattern photographs may be divided into several types. Figure 10 shows waves which are continuous and of apparently gradually changing height. Figure 11 shows waves containing breaks along a narrow zone, the crests on the side of this zone away from the gap center line being appreciably ahead of the crests on the side nearest the center. Other photographs show waves in which this effect is less pronounced; in fact, close inspection reveals that the waves are really continuous but are of reduced height across the apparent break. Some photographs show waves which do not contain a narrow break zone like those in the other examples, but which do suddenly decrease in apparent amplitude along a line at about the same location, continuing to the flanks at reduced amplitude (in some pictures the continuation is not visible, so discontinuities in pattern may occur for some of this type).

On most of the photographs only one, if any, zone of discontinuity can be identified; however, as many as three definite breaks were visually observed for some of the shorter waves diffracted by comparatively wide gaps with wave splitters.

Figures 10 and 11 were made in the small tank, as were the majority of the pattern photographs. Well defined zones like those of Figure 11 do not appear in any of the waves made without wave splitters in the small basin; however, such zones were generally observed in the large basin where no wave splitters existed.

These zones are believed to be due to the effect of steepness on wave length and wave velocity, combined with the existence of zones of small theoretical diffraction coefficients at about the same locations as the pattern discontinuities (see Fig. 3-5). The wave steepness decreases rapidly from the gap center line to these zones, causing the wave lengths to decrease and the wave crests to bend sharply back from the advanced positions near the center line to the calculated positions in the zones of small amplitude. To the flanks, the amplitudes increase slightly, so the wave crests again advance beyond the positions calculated without regard for steepness. This causes kinks in the wave crests in the zone where the wave heights are very small, resulting in apparent wave crest breaks which are easily converted into actual breaks by slight irregularities of the wave motion.

If the area considered is sufficiently wide, several zones of small diffraction coefficient will be included. The above-described action is repeated to some extent at each of these, accounting for the occasional observation of several break zones.

As may be seen from the graphs of theoretical K', the depressions in values of K' are more marked for the simplified solution than for the complete solution. This is believed to explain the fact that the crest discontinuity zones are more pronounced for the runs with wave splitters than for those without, since the simplified solution is considered more appropriate for the runs with wave splitter.

In tracings of wave patterns made from the photographs, definite zones of apparent crest breaks, like those of Figure 11, have been indicated by dashed crest lines (see Fig. 6 and 7). The approximate location of the first zones of small wave heights has also been shown. In every case these zones are in the same general vicinity.

For the steeper waves, the observed crest break zone tends to lie to the flank of the theoretical small K' zone. This is believed to be due to the sharper than theoretical curvature of the waves at the gap center line. If diffraction did not exist, the wave energy would be transmitted in directions perpendicular to the wave crests; and pairs of orthogonals to the wave crests would each inclose zones through which the amount of energy transmitted would be constant, the wave heights increasing as the orthogonals converged, decreasing as they diverged. Near the gap center line, the theoretical wave patterns (disregarding the effect of steepness) have a convex curvature which causes the orthogonals to diverge and the wave heights to be reduced; that is, the wave energy tends to flow outward from the gap center line. The increased actual curvature caused by differences in wave steepnesses increases this divergence of the orthogonals near the gap center line; that is, the tendency of the wave energy to flow outward from the center line is greater than indicated by the theory. This results in decreased wave energy per foot of crest and consequently decreased wave heights and K' values near the gap center line, and increase in these quantities toward the flanks. The increased heights encroach on the zones of low K', shifting them also to the flanks and decreasing their sharpness. Diffraction, in addition to causing this wave crest curvature and the consequent wave height reduction, probably also causes the direction of energy transmission to be slightly inclined to the flank (away from the greatest amplitudes) of the perpendiculars to the wave crests. This causes energy transmission lines to differ slightly from the orthogonals to the crests. This difference is probably about the same for the actual crest lines (as affected by relative wave steepness) as for the theoretical crest lines (disregarding relative steepness), so the effect of the increased crest curvature remains as stated above, causing the crest break zone to be shifted to the flanks as observed.

Conclusions

This investigation leads to the following conclusions:

(1) The experimental results verify the general form of the wave diffraction theory for breakwater gaps with b/L ratios as small as 1.41 and d/L_0 ratios as small as 0.14.

(2) The theoretical wave pattern and diffraction coefficients are modified by the relative steepnesses of waves in different areas. The waves in areas of great steepness are longer than results from application of the theory without regard for steepness. This causes the crests to be more sharply curved and the diffraction coefficients to be smaller than given by the basic theory for such areas, while the diffraction coefficients are increased in the adjacent areas.

(3) The wave crests tend to develop discontinuities along the zones of small theoretical diffraction coefficients. This tendency is increased by the use of wave splitters.

(4) The diffraction coefficients are not greatly affected by incident wave steepness, wave splitters, nor use of a half-model.

(5) Symmetrical breakwaters with wings inclined at 45° to 90° to the gap center line are not greatly affected by the angle of inclination.

Acknowledgments

This paper is a condensation of a PhD Thesis completed by the senior author at the University of California, Berkeley, in September, 1948. The assistance of personnel from the University of California Wave Project sponsored by the Bureau of Ships, U. S. Navy, in reducing the experimental data is acknowledged with gratitude.

References

BATEMAN, H., Partial differential equations of mathematical physics, Dover, 1944.

LAMB, H., Hydrodynamics, Cambridge University Press, 1932.

PENNEY, W. G., and PRICE, A. T., Diffraction of sea waves by breakwaters, Directorate, Misc. Weapons Development Technical History 26, Artificial Harbors, Sec. 3D, 1944.

PUTNAM, J. A. and ARTHUR, R. S., Diffraction of water waves by breakwaters, Trans. Amer. Geophys. Union, v. 29, pp. 481-490, 1948.

Office of Chief of Engineers (F.L.B.),
Engineer Historical Division,
Baltimore, Md.

University of California (J.W.J.),
Berkeley, California

(Manuscript received March 14, 1949; presented at the Thirtieth Annual Meeting, Washington, D. C., April 21, 1949; open for formal discussion until March 1, 1950.)

Transactions, American Geophysical Union Volume 30, Number 5 October 1949

VOLCANIC ACTIVITY ON UMNAK AND GREAT SITKIN ISLANDS, 1946-1948

F. M. Byers, Jr. and W. W. Brannock

(Published by permission of the Director, U. S. Geological Survey)

Abstract--As part of the United States Geological Survey's volcano program in the Aleutian volcanic arc during 1946-1948, the volcanoes and thermal areas on Umnak and Great Sitkin Islands were studied. In addition to observation of the volcanoes, temperatures of fumaroles were measured and some products of the volcanic activity were collected and analyzed.

After an eruption in 1945, Cone A in Okmok Caldera on northeastern Umnak Island remained relatively quiet during the period 1946-1948. The fumarole gases contained water vapor, carbon dioxide, and sulfur dioxide. The incrustations associated with the sulfur dioxide fumaroles are the sulfate minerals halotrichite, gypsum, and soda alum. Temperatures of lava fumaroles at the source of the December, 1945 lava flow from Cone A dropped from an average of 320°C on July 19, 1946, to 90°C on September 5, 1946. With exception of the large central fumarole which reached red heat in 1947, the extra crater fumaroles of Cone A ranged from 96° to 98° C in temperature.

Cone C, another cone in Okmok Caldera was in the solfataric stage and emitted water vapor, hydrogen sulfide, and probably carbon dioxide. Incrustations associated with fumaroles on this cone consisted of sulfur, pyrite, and aragonite. The temperatures of the fumaroles ranged from 95° to 96°C and were probably kept within this narrow range partly by the heat supplied during condensation of steam.

Sixteen large thermal springs emerging from the base of Cone D in Okmok Caldera had an aggregate discharge of approximately 115 cfs and gave off approximately 21,000 kcal of heat per second on September 7, 1946.

Water samples of thermal springs on Umnak Island contained as high as 159 ppm of boron expressed as B_2O_3 and a few parts per million of arsenic and antimony. Several of the thermal springs in southwestern Umnak Island were slightly superheated with respect to the boiling point of water and behaved as small geysers. As has been found elsewhere, the discharge, temperature, and composition of the emanations from a spring is modified by surface conditions of topography and drainage.

Thermal springs and fumaroles on Great Sitkin Island occurred at an altitude of about 2000 ft near the head of the west fork of Big Fox Creek. All the fumaroles were at or near a temperature of 100°C. The large crater fumarole in the center of the 1945 crater dome was unapproachable. No change in the activity of Great Sitkin volcano was observed between 1946 and August 1948.

Introduction

During the summers of 1946, 1947, and 1948 several volcanic areas of the Aleutian Islands were studied in connection with a broad program of Aleutian research of the United States Geological Survey. Field parties on Umnak from 1946 to 1948 and on Great Sitkin in 1946 observed the volcanoes, making temperature and pH measurements and sampling thermal spring waters and fumarole gases (see Fig. 1). (Thermal spring is used in this paper to designate any spring whose temperature is above the annual mean temperature of the area and whose excess heat is believed to have been derived from a volcanic source.)

Temperatures were measured using maximum thermometers for temperatures up to 200°C and a chromel-alumel thermocouple with potentiometer for temperatures above 200°C. The maximum thermometers were checked in boiling water at sea level and all registered 100°C within limits of reading the scale. Maximum thermometers had to be held or supported upright or nearly so in a fumarole, because the mercury would run past the constriction above the bulb if the maximum thermometers struck the wall of the fumarole while upside down. The potentiometer and thermocouples were checked on return from the field and found to be accurate to within 2.5°C in the range used. In measuring the temperature of a fumarole it was the authors' experience that no observable change of temperature could be detected in a series of measurements extending from a point approximately six inches below the orifice of the fumarole down to a depth of about two feet, which was generally

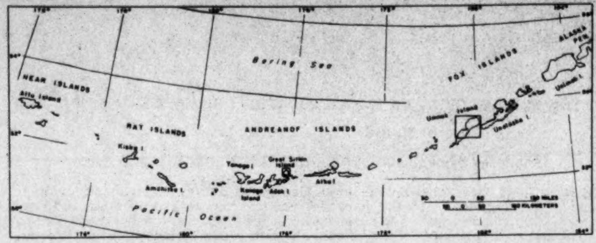
Bering Sea
NEAR ISLANDS
Attu Island
RAT ISLANDS
Kiska I
Amchitka I
ANDREANOF ISLANDS
Tanaga I
Great Sitkin Island
Kanaga Island
Adak I
Atka I
FOX ISLANDS
Umnak Island
Unalaska I
Unimak I
ALASKA PEN.
Pacific Ocean

Fig. 1--Aleutian Islands showing areas of geochemical investigations in 1946

the maximum possible depth of measurement.

Fumarole gases were sampled by using a gas-sampling train and pyrex sampling tubes. Two collections of fumarole gases were made by means of a sampling train consisting of an intake tube, a gas-absorption bottle containing potassium hydroxide solution, and an aspirator bottle. The volume percentage of acid gases was later computed from analyses of the potassium hydroxide solutions and the volume of non-absorbable gases was determined during the run by measuring the volume of displaced water from the aspirator bottle. Blank potassium hydroxide solutions and those used in the sampling train were shipped from the field in wax-lined containers. Fumarole gases were also collected by displacement of air in a 250-cc gas-sampling tube with stopcocks and in 25-cc pyrex pipettes, which were sealed shut by blowtorch immediately after collecting the gases. Gases collected in this manner were analyzed by mass spectrometer at the National Bureau of Standards. Water was not determined in any of the analyses of fumarole gases, but one attempt was made to estimate water content using the physical data obtained at the time of sampling.

Fumarolic incrustations were collected in air-tight, screw-cap vials. Water samples were collected in one-gallon bottles and in one-quart bottles with porcelain clamp stoppers. The latter are far more satisfactory for collecting water samples in difficultly accessible areas.

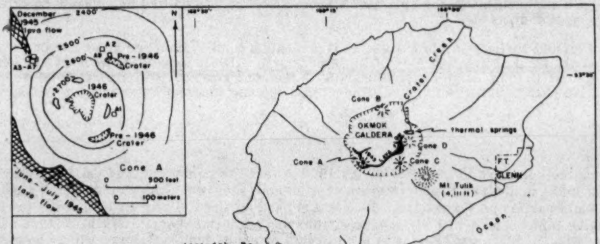
December 1945 lava flow
2400'
2500'
2600'
2700'
A2
A3
A3-A7
Pre-1946 Crater
1946 Crater
A4
Pre-1946 Crater
Cone A
0 300 feet
0 100 meters
June-July 1945 lava flow
Crater Creek
Cone B
OKMOK CALDERA
Thermal springs
Cone D
Cone A
Cone C
FT GLENN
Mt Tulik (4,111 ft)
Pacific Ocean
Inanudak Bay
Hot Springs Cove
Geyser Bight
Bering Sea
fig 4
fig 5
Mt Recheschnoi (6,510 ft)
Vsevidof Volcano (6,920 ft)
N
0 5 10 miles
0 5 10 kilometers
□ fumarole
○ thermal springs
● volcanic vent that contained fumaroles in 1946
Crater Creek
1100'
1200'
1300'
1400'
a b c d e f g h i j k l m n o p q
Thermal springs north of Cone D
0 1000 feet
0 300 meters

Fig. 2--Part of Umnak Island showing location of areas discussed in text

Volcanic activity in Okmok Caldera

Cone A --Geological Survey work in the Aleutian volcanic arc was begun in 1945 following an eruption of Cone A in Okmok Caldera on northeastern Umnak Island (see Fig. 2). Cone A is approximately ten miles west of Fort Glenn, an Army air base on the eastern shore. The most active phases of this eruption lasted from June 4 to July 22, 1945, with a minor outbreak the following December. The eruption was observed on different days by ROBINSON [1948], WILLIAMS [1945], and WILCOX [1945 and 1946].

During 1946 Cone A was considerably more quiet, although it was still the most active cone in Okmok Caldera. It contained both primary fumaroles such as A1, A2, and A8, and secondary or lava fumaroles, such as A3-A7 (see Fig. 2, upper inset). Primary fumaroles as defined by PERRET [1924, p. 105] are those which are associated with the main crater vent of a volcano and which are almost certainly receiving gaseous emanations from an underlying magma. Secondary or lava fumaroles, according to Perret, are those associated with superficial igneous masses, generally lava flows.

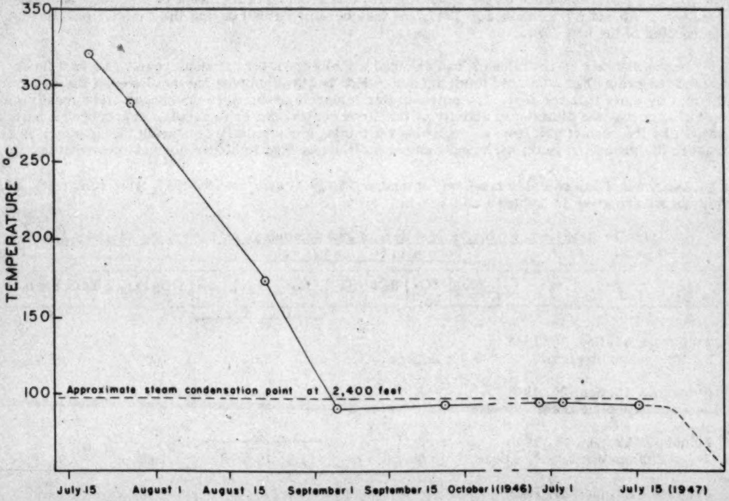

Fig. 3--Change in temperature of fumaroles A3 to A7 on Cone A, July 19, 1946 to July 16, 1947

Primary fumaroles occurred both inside and outside the crater of Cone A. They were characterized by the pungent odor of sulfur dioxide. Because of the steepness of the crater walls, the largest fumaroles, which were at the lowest point within the crater, could not be reached. The primary fumaroles outside the crater occurred in the vicinity of two older crater remnants north and south of the present crater. These fumaroles were small and numerous because of the porous, unconsolidated character of the basaltic ash, and their orifices ranged from less than a millimeter to about five centimeters in diameter. Nearly all the fumaroles had a very narrow range in temperature - from 96° to 98°C, which is near the boiling point of water at an altitude of 2600 ft (749 meters), indicating that the fumarole gases were saturated with steam. This phenomenon was noted by DAY and ALLEN [1925, pp. 104 and 173] in their study of fumaroles of Lassen Peak, California, and probably has been observed by others. On June 30, 1946, the largest extra-crater primary fumarole, A2, was emitting a considerable quantity of steam and SO_2. A temperature of 110°C was recorded at a depth of four feet from the orifice, but the writers question this reading because the maximum thermometer may have struck the walls of the fumarole while upside down. Temperature readings at later dates were consistently 97°C.

Lava fumaroles were still active during the summer of 1946 within the area of the 1945 lava flow (see Fig. 2), and most of them had cooled below 100°C by the end of the summer. Fumaroles A3-A7, although situated at one of the 1945 lava vents, are believed to have been secondary in character because they emitted only odorless gas, and, as will be brought out later, existed for only a short period.

During the summer of 1947, the activity at the crater of Cone A was decidedly greater than in 1946. Steam was escaping with a deafening roar from a three- to six-foot orifice in the bottom of the crater. The walls near the orifice glowed with a cherry-red incandescence, equivalent to a temperature of roughly 800°C. The jet of steam did not condense until it reached a point 50 to 100 ft above the orifice. The inside walls of the crater, especially on the east side, had slumped inward so that the rim was lowered as much as ten feet. No change in intensity of the activity of the large crater fumarole was noted from June 28 to September 9, 1947. Unfortunately, the large crater vent was inaccessible for temperature measurements and gas sampling. The small primary fumaroles outside the crater of Cone A had diminished somewhat in number, although some new fumaroles had come into existence. Fumarole A2 was partly caved in 1947, but a new fumarole, designated A8, had come into existence on the same fissure, and about 50 ft southeast of A2. Only two lava fumaroles, A6 and A7, remained in 1947, and they became extinct during the summer paralleling the cooling of the lava flow.

In the summer of 1948 Cone A had changed slightly from the previous year. The east inner wall of the crater had continued to slump somewhat, but the slumping had not lowered the east part of the rim by more than ten feet. The extra-crater fumarole areas were unchanged. The most significant change was the diminished activity of the large central crater fumarole. It produced a hollow sound like the rush of gas from an open pipe containing a column of gas beneath the opening. In contrast to the preceding year, the sound was not sufficiently loud to hinder normal conversation.

Analyses of gas samples taken on September 26, 1946, and June 28, 1947, from fumaroles A1, A2, and A8 are given in Tables 1 and 2.

Table 1--Analyses, exclusive of water, of gas samples from fumaroles A1 and A2, cone A in volume per cent

Item	CO_2	SO_2	HCl	HF	N_2	O_2	A	$CO_2:SO_2$	Temperature
									°C
Fumarole A1, Sep. 26, 1946 gas-sampling train	7	8	a	a	85			0.87	96.5
Fumarole A2, Sep. 26, 1946 gas-sampling train	43	22	a	a	35			1.95	97.0
Fumarole A2, Sep. 26, 1946 gas-sampling tube[b]	15.5	9.3	a	a	61.9	12.5	0.8	1.67	98.0
Fumarole A8, June 28, 1947 gas-sampling tube[b]	0.58	0.33	a	a	77.6	20.5	0.96	1.76	. . . .

[a] none found

[b] analysis by mass spectrometer, National Bureau of Standards

Table 2--Estimation of water vapor, assuming saturation, in fumaroles A1 and A2, cone A

	Temperature	Vapor pressure of water	Barometric pressure	Volume per cent of water vapor
	°C	mm	mm	
Fumarole A1	96.5	670	703	95
Fumarole A2	97.0	682	706	96.5

Fair agreement of the $CO_2:SO_2$ ratios is indicated in three of the four samples. The three samples in fair agreement were from fumaroles A2 and A8, which were within 50 ft of each other in the same trench, probably the surface expression of an underlying fissure. Especially close agreement is found between the September 26, 1946 ratio (1.67) and the June 28, 1947 ratio (1.75) of samples taken in the gas-sampling tubes, suggesting little change in the ratios of the primary volcanic gases to each other during that period. The great differences in the percentages of atmospheric constituents can be explained in part by air contamination at the time of sampling and in part by actual differences in the proportion of those constituents coming at different times from the fumaroles. Thus on June 28, 1947, the pungency of the sulfur dioxide coming from A8 was noticeable, but not as annoying as on July 4. These and other similar primary fumaroles are probably inter-connected at slight depth with the main volcanic conduit and have received varying concentrations of the primary volcanic gases from time to time. In fact, the observed diminished activity of the extra-crater fumaroles in 1947 may possibly be explained by a process whereby most of the volcanic gases from the magma beneath Cone A were then expended through a single large orifice rather than retarded and dissipated through a breccia-filled pipe.

The estimation of steam in Table 2 is based on the ratio of composition to partial pressures, assuming the fumarole gases to be saturated with steam at the orifices. This assumption appears reasonable, considering the close agreement in temperature, 96° to 98°C, of approximately 20 primary fumaroles measured.

Incrustations collected from the surface of the ash in the vicinity of the primary fumaroles were examined optically by Jewell J. Glass of the Geochemistry and Petrology Branch, U. S. Geological Survey. White to yellow, and pale greenish gray to grayish green halotrichite ($FeAl_2(SO_4)_4 \cdot 22H_2O$) was the predominant mineral of the incrustations with minor gypsum ($CaSO_4 \cdot 2H_2O$). An isotropic sulfate with the index of soda alum ($NaAl(SO_4)_2 \cdot 12H_2O$) occurred as minute incrustations coating gypsum. The differences in color of the halotrichite may have been due to differences in degree of hydration, as on clear days yellow and grayish-green halotrichite predominated, whereas on rainy days the white and pale greenish gray varieties were noted. These incrustations are regarded as due to the reaction of fumarole gases and oxygen with the ash.

The fumaroles, A3-A7 (Fig. 2, upper inset), at the vent of the December 1945 lava flow were selected for temperature measurements, because at first they were thought to be primary on account of their high temperatures in the early part of the summer of 1946. The fumarole temperatures taken on different dates between July 19, 1946 and July 16, 1947 are presented in Table 3. The average temperatures of these fumaroles on the different dates is plotted against time in Figure 3.

Table 3--Temperatures in °C of fumaroles at vent of December 1945 lava flow

Date	A3	A4	A5	A6	A7	Average
July 19, 1946	300	325	306	332	337	320
July 27, 1946	326	272	312	276	258	289
August 22, 1946	128	101	(caved)	230	238	174
September 5, 1946	91	89	(caved)	90	89	90
September 26, 1946	93	93	(caved)	92	93	93
June 28, 1947	(caved)	(caved)	....	95	95	95
July 4, 1947	....	....	....	90[a]	94	94
July 16, 1947	....	....	....	(caved)	94	94
September 9, 1947	....	....	....	....	(caved)	....

[a] Partly caved, hence not included in average.

There is nearly a straight-line cooling trend indicated between July 19 and September 5, 1946. If a straight-line curve fitting these points is extrapolated backwards in time to December, 1945, when active lava was last observed flowing, a temperature approximating that of molten lava is indicated [ZIES, 1946, p. 179]. The small change in average temperature from September 5, 1946, to July 16, 1947, in contrast to temperatures taken on the earlier dates suggests control by the boiling point of water. Sometime between July 16 and September 9, 1947 the last of these lava fumaroles became extinct, indicating near-exhaustion of the excess heat in this part of the December 1945 lava flow after one year and eight months.

Cone C--Fumaroles on the rim of the principal crater of Cone C (see Fig. 2) were examined on July 1, 1946, and on September 10, 1948. There was no noticeable change in the character of the fumaroles between those dates. The temperatures of the fumaroles ranged from 95°C to 96°C and, like those of Cone A, are believed to have been maintained within this narrow range by the condensation of steam at or near the fumarole orifices. The fumaroles were similar in size to those on Cone A, but there the resemblance ended.

Two distinct areas of fumaroles, those without odor and those with a distinct odor of hydrogen sulfide, occurred in roughly concentric zones on the east, west, and south parts of the main crater rim. The odorless fumaroles were mainly on the east and west part of the rim of the main crater, and tended to occur outside the zone of hydrogen sulfide fumaroles with respect to the center of the crater. The odorless fumaroles apparently were emitting steam, and atmospheric gases. The hydrogen sulfide fumaroles were confined principally to a narrow zone about 200 ft long trending east-west along the south part of the crater rim, and were inside the zone of odorless fumaroles where the two types were adjacent.

The ash around the steam fumaroles had been decomposed to a gritty mud stained with red ferric oxide, suggesting an oxidizing environment. The ash around the hydrogen sulfide fumaroles had been altered to two types of clayey material, an outer zone of less altered, dark bluish-gray clay, and an inner zone of cream-colored material. Both were extremely slippery. The dark material contained aragonite, opaline silica, and minute crystals of pyrite, 0.001 to 0.02 mm in diameter, strewn through the matrix. The cream-colored clay mass contained orthorhombic sulfur, a ferric sulfate mineral, and aragonite crystals in a matrix of amorphous material. Crystobalite and anatase were identified by X-ray analysis as forming 10 to 15 per cent of the amorphous material, by Joseph M. Axelrod of the Geochemistry and Petrology Branch, U. S. Geological Survey. Apparently hydrogen sulfide had produced the pyrite by reaction with original magnetite, and also produced free sulfur by oxidation near the surface. Carbon dioxide apparently reacted with original calcium silicates to produce the aragonite. In the zone of more intense alteration, pyrite seems to have oxidized to a ferric sulfate mineral.

On geologic and geomorphic evidence, Cone C is considered older than Cone A. Cone C is believed to have been formed shortly after the formation of Okmok Caldera, before the Caldera had filled with water to its original outlet at the top of the present Crater Creek gorge. In addition a lava flow from Cone C underlies a lava flow from a nearby extinct cone and is therefore older. These two independent lines of evidence point to a considerable time lapse since the last activity of Cone C, which may have been several thousand years ago.

The presence of sulfur dioxide in the volcanic gases and of sulfate incrustations is associated with Cone A, the most active cone in Okmok Caldera, whereas hydrogen sulfide in the gases and either sulfur or pyrite incrustations is associated with Cone C, a long-quiescent cone.

Cone D--The volcanic activity of Cone D was manifested by the presence of many thermal springs along the north base of the cone. They are designated a through p from west to east (see Fig. 2, lower inset). On September 7, 1946, these springs ranged in temperature from 5° to 30°C. In summer, lush vegetation and swarms of insects make the area conspicuous, because it is surrounded by the barren ash- and lava-covered floor of the Caldera. Springs ℓ and p, and several others, were compound springs, each containing as many as 30 springlets. The warmer springlets generally had smaller discharges, and a thin siliceous sinter covered the rocks immediately below the orifices. Some of the cool springlets were precipitating hydrated iron oxide. There was a gradual decrease in temperature from 12.3°C to 6.1°C between spring a and the west springlet of ℓ, but no trend is apparent between the west springlet of ℓ and spring p. Spring q was a cold spring at a temperature of 3.9°C.

In order to calculate the heat loss of the springs it is necessary to define and arrive at a base-reference temperature. It might be defined as that temperature which would approach the average near-surface temperature of the surrounding area not affected by the volcanic heat. ALLEN and DAY [1935, p. 136] used the annual mean temperature as a base in calculating the heat loss of the thermal springs of Yellowstone National Park, but no air temperature records are available for Okmok Caldera.

To arrive at a base-reference temperature for use in calculating the heat given off by the springs of Cone C, it seems reasonable to assume that 3.9°C, the temperature of spring q is perhaps the closest approximation to such a base. Spring q emerged at the head of a steep-walled gulley about 25 ft deep and apparently included most of the subsurface drainage of the low area between Cone D and the east wall of Okmok Caldera. Thus, it appears reasonable that this spring derived little if any heat from the area beneath Cone D.

The discharge, temperature, and heat dissipation of the thermal springs, following, in part, methods of ALLEN and ZIES [1923, pp. 117-121] and ALLEN and DAY [1935, pp. 44-63, 136], are presented in Table 4. The total discharge of the springs was approximately 115 cfs and the heat loss was 21,000 kilogram calories/sec.

The ultimate source of nearly all the water discharged by these springs is believed to be the precipitation which falls on Cone D and that portion of the Caldera south of it and east of Cone C.

Table 4--Calculation of heat carried away by thermal springs north of Cone D based on observations of September 7, 1946

Spring	Discharge		Temp.	Temp. above base reference temp. (3.9°C)	Heat carried away	Remarks
	cfs	lit/sec	°C	°C	kcal/sec	
a	12.0	340	12.3	8.4	2850	Four springlets; all 12.3°C
b	6.7	190	12.3	8.4	1600	
c	6.0	170	12.3	8.4	1430	
d	4.0	113	12.3	8.4	950	West springlet
	3.5	99	11.7	7.8	770	East springlet; water sample no. 1
e	0.7	20	11.1	7.2	145	Three springlets; all 11.1°C
f	4.0	113	11.1	7.2	810	West springlet
	1.3	37	10.0	6.1	230	Middle springlet
	1.3	37	10.0	6.1	230	East springlet
g	5.3	150	10.0	6.1	910	West springlet
	4.0	113	10.0	6.1	690	Middle springlet
	4.0	113	9.2	5.3	600	East springlet
h	1.3	37	8.3	4.4	160	
i	0.1	3	8.9	5.0	15	
j	10.0	283	8.3	4.4	1250	
k	1.0	28	7.2	3.3	90	West springlet
	4.0	113	7.2	3.3	370	Middle springlet
	3.0	85	6.7	2.8	240	East springlet
ℓ	0.4	11	6.1	2.2	25	West springlet; water sample no. 2
	11.6	330	9.3[a]	5.4	1780	Two closely spaced springs, which have many springlets ranging from 6° to 22°C
	4.5	127	11.1[a]	7.2	910	
	1.0	28	6.7	2.8	75	East springlet
m	2.7	76	18.9	15.0	1140	
n	12.0	340	7.8	3.9	1330	
o	2.0	57	7.2	3.3	190	
p	8.0	227	15.6[a]	11.7	2660	Many small springlets ranging from 8° to 30°C
Totals	115	3250				
q	5.2	147	3.9	0.0	0	Cold spring used as base-reference temperature in above calculations

[a] Temperature of stream from springlets

This area including Cone D contains no surface streams and is roughly one-seventh of the watershed of Okmok Caldera.

The discharge of Crater Creek below the springs was calculated from approximate measurements at two points and found to be 720 and 910 cfs. Assuming an average of 815 cfs as the discharge of Crater Creek through Crater Creek Gorge, the discharge of the springs of Cone D (115 cfs) was about one-seventh (115/815) of the discharge from the entire Caldera. The relative agreement of watershed ratio and discharge ratio, although based on approximate measurements, is probably accurate within 25 per cent. Consequently part of the water coming from the springs must ultimately have come from precipitation on the area within the Caldera south of Cone D and must have passed through the base of the cone, where the meteoric water was slightly heated. We would have, in essence, a water-cooled volcano, which, were it not for its position astride the main drainage of the Caldera, might still be in the fumarolic stage of activity like Cone C. This appears all the more likely from the geologic evidence, which points to simultaneous origins of Cones C and D.

During September 1946 four water samples were collected from springs d, ℓ, and p. The analyses of these samples are given in Table 5. Analyses of samples 1 and 2 are almost identical except for the lower total dissolved solids of sample 2, which was collected at the west springlet of spring ℓ. This, considered with the gradual decrease in temperature along the springs from 11.7°C at the east springlet of spring d (sample 1) to 6.1°C at the west springlet of spring ℓ (sample 2) suggests a direct relationship of total dissolved solids to temperature for these springs and probably a common source (that is, from beneath Cone D). Samples 3 and 4 differ somewhat from each other and from samples 1 and 2, and hence are more difficult to interpret. Temperature variations from one spring to another were also more erratic between the warmest springlet of spring ℓ (sample 3) and the cool springlet of spring p where sample 4 was taken. Unfortunately, sample 3 was delayed several months in shipment from Alaska; hence, some solution of the sample bottle may have occurred.

All four samples contained a few parts per million of boron expressed as boric oxide, which is probably from a magmatic source. The Na:K molar ratios of the four samples are fairly constant and range from 14 to 16.

Table 5--Analyses of thermal spring waters from area north of Cone E

Constituent	Sample 1	Sample 2	Sample 3	Sample 4
	ppm	ppm	ppm	ppm
Cl	50	32	39	38
F	0.1	b	0.1	b
SO_4	128	94	69	116
CO_3	a	a	a	a
HCO_3	220[c]	168[c]	84[c]	334[c]
AsO_4	b	b	b	b
SbO_3	b	b	b	b
B_2O_3	3	2	9	4
Na	69	51	53	66
K	8	6	5.6	7
Ca	39	26	18	35
Mg	29	23	7.5	47
Fe	b	b	b	b
SiO_2	39	36	59	39
Total dissolved solids, (180°C)	480	349	303	499

Sample 1, East springlet of spring d, temperature, 11.7°C, September 25, 1946
Sample 2, West springlet of spring ℓ, temperature, 6.1°C, September 25, 1946
Sample 3, Warm springlet of spring ℓ, temperature, 22°C, September 7, 1946
Sample 4, Springlet on northernmost side of spring p, temperature, 8.9°C, September 25, 1946

---

[a] None found.
[b] Less than 0.1 ppm, if present.
[c] By direct titration; alkalinity due to silicate and borate included.

Thermal areas south of Inanudak Bay

Thermal springs and small geysers occur south of Inanudak Bay (see Fig. 2) in alluvium-floored valleys. These valleys are believed to be underlain by Tertiary (?) igneous rocks consisting of monzonite and minor aplite. On this basement, late Tertiary or early Quaternary basalt flows from Mt. Recheschnoi vents were poured out. The thermal springs are near sea level below the base of the late Tertiary and early Quaternary extrusives. Thermal springs were observed in three areas: south of Hot Springs Cove, southeast of Geyser Bight, and in the small unnamed valley that drains eastward across the narrowest part of Umnak (see Fig. 2). All these springs have been in existence more than a century and are similar to those in other thermal areas such as Yellowstone Park, where volcanic eruptions have long since ceased. Two steam fumaroles on the west slope of Geyser Creek valley draining into Geyser Bight have their vents in late Tertiary and early Quaternary basalt flows but are part of the Geyser Bight area of thermal activity.

These springs and geysers emerge chiefly from small boulder-filled basins two to six feet in width and less than three feet in depth, so there was no opportunity to measure change of temperature with depth [ALLEN and DAY, 1935, pp. 191-198; BARTH, 1947]. As long ago as the middle part of the Nineteenth Century it was reported by GREWINGK [1850, p. 205] that one geyser erupted every 15 min to a height of two feet. In 1946 and 1947 the geysers had changed little in appearance and behavior. Siliceous sinter was being deposited around the margins of their pools at that time.

The temperature, discharge, and pH of the accessible springs were measured mainly during the summer of 1947, and water and sinter samples of some were taken for analysis. The pH was measured using a set of test papers sensitive to within about 0.2.

Thermal springs in the vicinity of Hot Springs Cove occur at the beach and about 0.8 mi south of the beach (see Fig. 2 and 4). During periods of low tide the thermal springs at the beach are exposed along a half-mile linear zone. The thermal springs form small pools of shallow depth with negligible surface discharge. The maximum temperature obtained at a depth of six inches in the sand was 70°C. At high tide the springs are completely covered and there is nothing to suggest their presence. The explanation for the present coincidence of the shoreline and hot springs may be that groundwater heated by thermal springs inland is draining seaward and emerges above the strand line at low tide.

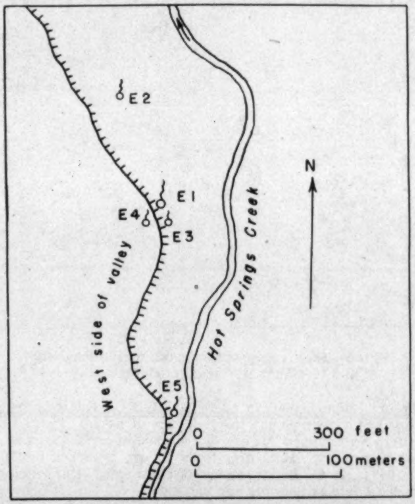

Fig. 4--Sketch map of thermal springs locality
0.8 mile south of Hot Springs Cove

The thermal springs 0.8 mi inland from Hot Springs Cove (see Fig. 2 and 4) are at the base of the west slope of the valley that drains northward into the cove and west of Hot Springs Creek. One large spring, E5, and four smaller ones, E1, E2, E3, and E4 were the only ones having a measureable discharge in 1946 and 1947. Their areal distribution is shown in Figure 4.

Several thermal areas occur in Geyser Creek Valley 2 1/2 to 4 1/2 mi southeast of Geyser Bight (see Fig. 2 and 5). The steam fumaroles F1 and F2 were situated on the west side of Geyser Creek Valley at altitudes of 950 and 800 ft respectively, whereas the other thermal areas were in the bottom of the valley 700 ft lower and were characterized by thermal springs and small geysers. The steam fumaroles emitted largely steam at a temperature of 99°C, essentially the boiling point of water at that altitude. Fumarole F1 was considerably larger than fumarole F2 and produced a condensation cloud 50 to several hundred feet in height depending on the relative atmospheric humidity.

Eight of the 22 thermal springs observed in Geyser Creek Valley were slightly superheated.

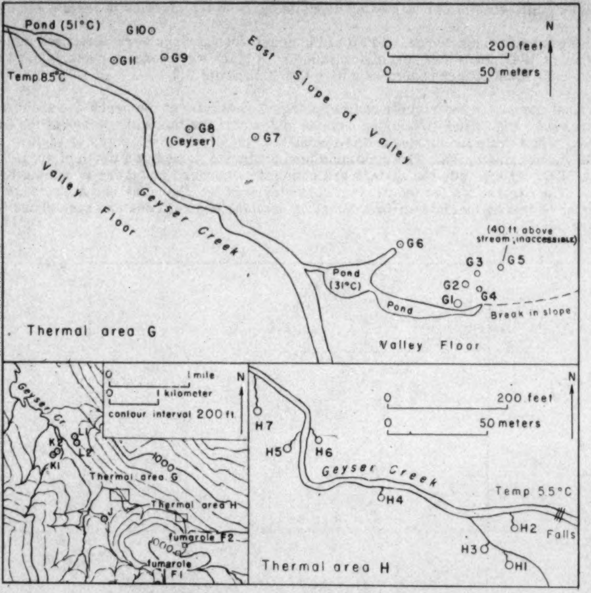
Pond (51°C)
Temp 85°C
G10
G11
G9
East Slope of Valley
0 200 feet
0 50 meters
N
G8 (Geyser)
G7
Valley Floor
Geyser Creek
G6
(40 ft above stream; inaccessible)
G3
G5
Pond (31°C)
G2
G4
G1
Pond
Break in slope
Thermal area G
Valley Floor
0 1 mile
0 1 kilometer
contour interval 200 ft
Geyser Cr.
K2
L1
L2
K1
1000
Thermal area G
Thermal area H
J
fumarole F2
1000
fumarole F1
H7
H5
H6
Geyser Creek
H4
Temp 5.5°C
H2
Falls
H3
H1
Thermal area H

Fig. 5--Sketch maps of thermal spring localities, 2.5 to 4.5 mi southeast of Geyser Bight

Four of these were geysers, superheated as much as 1 1/2°C. A few of the springs slightly under the boiling point of water had a continuous effervescence of gases. These observations suggest that the action of these geysers was caused largely by the exsolution of gases at depth with consequent lowering in the hydrostatic pressure according to the theory proposed by THORKELSSON [1940] and BARTH [1940 and 1947]. In the few instances of continuous effervescence the conduit was probably straight, so the gases could readily escape upward.

Heat loss of the thermal springs--The discharge, temperature, and heat loss of thermal springs south of Inanudak Bay are presented in Table 6. The heat losses of the thermal springs in the Hot Springs Cove and Geyser Bight areas were approximately 350 and 6000 kcal/sec, respectively. Inasmuch as these springs are near sea-level, the annual mean temperature (4.1°C) at Fort Glenn (unpublished data, U. S. Air Force) is used as a base reference temperature in making the heat calculations.

As a check against the heat liberated by the springs and geysers of the Geyser Bight area, the temperature of Geyser Creek was measured at the waterfall just above the thermal area and again just below the thermal area. At the former location the temperature was 5.5°C, at the latter, 8.5°C, a rise of 3°C. The discharge of the creek at the lower point was gaged and found to be 1400 lit/sec; therefore, approximately 4200 kcal/sec was being carried away by the stream. This value checks reasonably well with the total heat, 4600 kcal, obtained by measurement of individual springs. Probably the smaller quantity of heat calculated from stream measurements is due to heat loss owing to evaporation and radiation between the springs and the lower point on Geyser Creek.

Chemical character--The pH of the various thermal springs is presented in Table 6 and has been plotted against the corresponding temperatures of the springs in Figure 6. Data from similar

Table 6--Data on thermal springs south of Inanudak Bay

Thermal spring	pH	Average discharge	Temperature	Temperature above annual mean (4.1°C)	Heat carried away
		lit/sec	°C	°C	kcal/sec
E1	6.4	0.9	87	83	75
E2	5.7	0.9	47	43	39
E3	6.4	0.1	65	61	6
E4	5.0	0.6	35	31	19
E5	6.0	3.4	67	63	204
Totals,[a] Hot Springs Cove area		6			350
G1	7.5	4.3	101	97	417
G2	7.2	0.1	88	84	8
G3	6.8	0.3	100.5	96.5	29
G4	. . .	0.6	98	94	56
G5[b]	. . .	. . .	. . .	. . .	. . . .
G6	6.6	1.4	95	91	127
G7	7.0	1.4	82	78	109
G8[c]	7.5	2.8	100.5	96.5	270
G9	7.4	0.1	100.5	96.5	10
G10[d]	7.8	2.8	99	95	266
G11	. . .	2.8	77	73	204
H1[c]	6.9	11	101.5	97.5	1070
H2[c]	7.1	10	101	97	970
H3	6.6	none	53	. . .	. . .
H4	7.0	5.7	101	97	553
H5[c]	7.1	1.4	101	97	136
H6	7.4	1.1	100	96	106
H7	6.6	4.3	90	86	370
Totals,[a] C and D area		50			4600
J	6.8	12	88	84	1000
K1	. . .	2.8	58	54	152
K2	. . .	1.4	70	66	92
L1	. . .	1.4	69	65	91
L2	. . .	1.4	67	63	88
Totals,[a] Geyser Bight area		70			6000

[a] Totals are approximate. Those indicated for the Hot Springs Cove area are the results of measurements made on June 21, 1947; those indicated for the Geyser Bight area are those obtained on September 4, 1947.

[b] Vigorous, continuous bubbling of hot gases in natural well. No measurements made.

[c] Typical geyser; cycle, three to ten minutes of which 2 1/2 to 3 1/2 minutes consisted of vigorous ebullition to a height of two feet.

[d] Hot gases bubbling vigorously through water. In cycles of one to three minutes, bubbling increases, then decreases. This spring in believed midway in type between a thermal spring and a fumarole.

springs in the Tokaanu district of New Zealand [HEALY, 1942] are also shown. The maximum pH is 8.3 from the New Zealand area and 7.5 from the Geyser Bight area, but in both areas the pH roughly increases with temperature. The increase of pH with temperature is probably related to the loss of CO_2 from solution in the hotter springs.

Analyses of waters from thermal springs, E1, E5, G1, and H1 are presented in Table 7. Two samples of thermal spring E1 taken in successive years were almost identical, except that the sample taken on June 21, 1947 was slightly more dilute. The analysis of thermal spring E5 is similar to those of thermal spring E1. Presumably, the difference in concentration was the result of varying degrees of dilution of the parent magmatic fluid by meteoric water.

Table 7--Analyses of thermal spring waters from areas south of Inanudak Bay

Constituent	1a	1b	2	3	4
	ppm	ppm	ppm	ppm	ppm
Cl	1126	1104	782	569	482
F	0.6	0.9	0.5	1.9	1.2
SO_4	88	86	73	160	130
CO_3	a	a	a	33[b]	10[b]
HCO_3	67[b]	69[b]	65[b]	a	29[b]
NO_3	a	a	a	a	a
AsO_4	4.1	2.8	3.1	0.1	7.1
SbO_3	1.3	a	a	a	a
B_2O_3	92	88	64	159	157
Na	603	573	427	441	350
K	33	27	24	33	18
Li	3	2	2	3	2
NH_4	c	c	c	c	c
Ca	163	153	116	15	40
Mg	1.2	3.3	1.1	0.1	0.2
Fe	c	c	c	c	c
Al	d	d	d	d	d
SOi_2	88	99	65	303	150
Total dissolved solids (180°C)	2329	2208	1664	1741	1365
pH (1947) (at springs)	....	6.4	6.0	7.5	6.9

Sample 1a, Thermal spring E1, 4000 ft south of Hot Springs Cove, temperature 89°C, August 16, 1946.

Sample 1b, Thermal spring E1, temperature 87°C, June 21, 1947.

Sample 2, Thermal spring E5, 4500 ft south of Hot Springs Cove, temperature 68°C, August 16, 1946.

Sample 3, Thermal spring G1, 3 1/2 mi southeast of Geyser Bight, temperature 100°C, August 17, 1946.

Sample 4, Thermal spring H1, 4 1/2 mi southeast of Geyser Bight, temperature 101°C, August 17, 1946.

[a] None found.

[b] By direct titration, alkalinity due to silicate and borate included.

[c] Less than 0.1 ppm, if present.

[d] Less than 0.5 ppm, if present.

The presence of arsenic and boron in all the samples points to a magmatic source for part of the water of the springs. The large boron content of thermal springs C1 and H1 approaches that of certain types of alkaline thermal springs occurring throughout the world, such as The Tokaanu Hot Springs of New Zealand [HEALY, 1942, p. 6B] and Steamboat Springs, Nevada [BRANNOCK, FIX, GIANELLA, and WHITE, 1948, p. 221]. The boron content of the steam fumaroles and steam wells of Lardarello, Italy, averages about 500 ppm [KELLER and VALDUGA, 1946, p. 333], and has been demonstrated to be of magmatic origin.

The Na:K ratios in the five analyses are 31, 36, 30, 23, and 33. These ratios compare well with the average Na:K ratio of 34:1 found in the alkaline spring waters of the Upper Geyser Basin of Yellowstone National Park [ALLEN and DAY, 1935, p. 472]. FENNER [1936, pp. 300-301] has shown that at Yellowstone the high Na:K ratio of the waters can be related to the liberation of sodium by potassium in the feldspars of rhyolite at slight depth. In southwestern Umnak the monzonite of Tertiary (?) age has been replaced by pink aplite zones rich in potash feldspar. The surface on these rocks rises gently inland from 200 ft in the headlands bordering Geyser Bight (see Fig. 2) to about 500 ft in the central part of southwestern Umnak Island. These rocks probably form the bedrock underlying the thermal springs although no outcrops are visible. Hence, the thermal springs of southwestern Umnak Island may be emanations of a cooling, underlying intrusive similar to those exposed at the surface. If aplite masses which contain largely potash feldspar are still being formed at depth, they might account for the high Na:K ratios in the thermal springs at the surface.

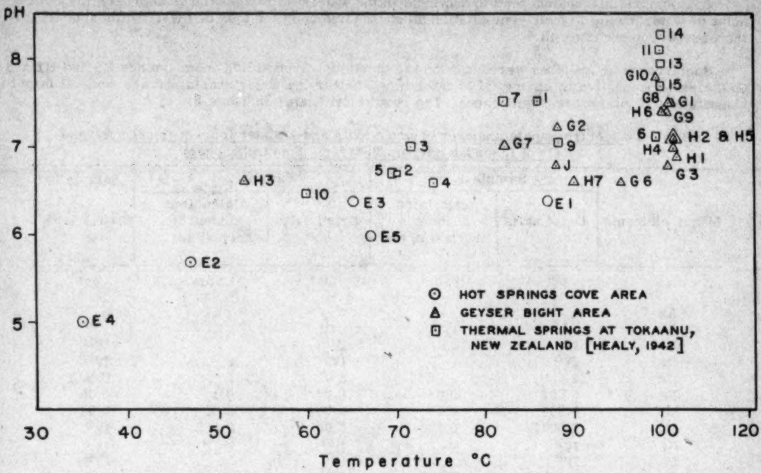

Fig. 6--Plot of pH against temperature for thermal springs south of Inanudak Bay

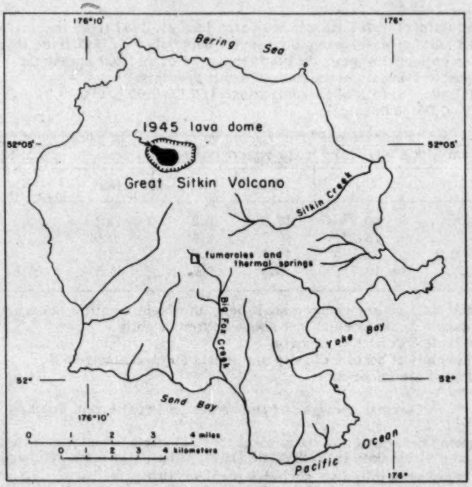
176°10'
176°
Bering Sea
1945 lava dome
52°05'
52°05'
Great Sitkin Volcano
Sitkin Creek
fumaroles and thermal springs
Big Fox Creek
Yoke Bay
52°
52°
Sand Bay
176°10'
0 1 2 3 4 miles
0 1 2 3 4 kilometers
Ocean
Pacific
176°

Fig. 7--Great Sitkin Island, showing areas of current volcanic activity

Calcium and magnesium tend to decrease in the waters as temperatures approach the boiling point of water, owing to their precipitation as carbonates upon the loss of CO_2. Silica appears to increase with increasing pH.

Spectrographic analyses were made on the dried dissolved solids from springs E1 and H1 and on the sinter deposited by spring G1 to determine whether the waters contained any unusual minor constituents of interest or significance. The results are shown in Table 8.

Table 8--Spectrographic analyses of dried salts and a sinter from thermal springs south of Inanudak Bay (A. T. Myers, Spectrographer)

Minor elements	Sample 1		Sample 2		Sample 3
	Dried salts	Calculated content in thermal spring	Dried salts	Calculated content in thermal spring	Dried salts
	pct	ppm	pct	ppm	pct
Ag	a	....	a	....	a
Au	I[b]	....	I[b]	....	I[b]
Bi	IV[b]	....	IV[b]	....	IV[b]
Cr	IV[b]	....	IV[b]	....	IV[b]
Cu	a	....	a	....	0.001
Fe	0.002	0.05	0.01	0.1	0.05
Mn	0.002	0.05	0.001	0.01	0.01
Mo	0.0002	0.005	0.0004	0.005	IV[b]
Ni	IV[b]	....	IV[b]	....	IV[b]
Co	IV[b]	....	IV[b]	....	IV[b]
Pb	0.0001	0.002	III[b]	....	III[b]
Sn	IV[b]	....	IV[b]	....	IV[b]
Sr	0.08	1.9	0.02	0.3	I[b]
Ti	a	....	a	....	a
V	a	....	a	....	a

Sample 1, Dried salts of water sample collected June 24, 1947 from thermal spring E1.
Sample 2, Dried salts of water sample collected September 4, 1947 from thermal spring H1.
Sample 3, Sinter collected August 18, 1946 from pool of thermal spring G1.

[a] Electrode impurity prevents estimation of small amounts.

[b] Not found at following levels of concentration: I, 0.05-0.02 pct; II, 0.01-0.006 pct; III, 0.005-0.002 pct; IV, 0.001-0.0005 pct.

Table 9--Analyses, in volume per cent, exclusive of water, of samples of fumarole gases from Great Sitkin Island, by mass spectrometer, National Bureau of Standards

Sample	H	N	O	A	CO_2	SO_2	total
1	.....	69.2[a]	17.8	0.8	12.1	0.1	100.0
2	....	78.2[a]	20.9	0.9	0.02	....	100.02
3	0.2	72.5	17.9	0.9	8.5	....	100.0
4	....	16.7	0.8	0.2	81.5[a]	0.8	100.0

Sample 1, Fumarole 1 on low rounded knoll beneath which is hollow shell and bubbling water.
Sample 2, Fumarole 2, six to eight feet above bottom of gully.
Sample 3, Fumarole 3 at bottom of gully.
Sample 4, Fumarole 4 at bottom of gully and within 50 ft of fumarole 3.

[a] The tenths figures are uncertain.

Thermal springs and fumaroles on Great Sitkin Volcano

The following description of the area of thermal springs and fumaroles on Great Sitkin Island (see Fig. 7 and 8) is taken from SIMONS [1947, p. 65], who made temperature measurements and collected gas samples in this area during September 1946.

"A group of hot springs, mud pots, and fumaroles occurs at an altitude of about 2000 ft near the head of the west fork of Big Fox Creek. On clear days a prominent cloud of condensed steam hangs over the largest of the springs. An area about 1000 ft long and 400 ft wide underlain by al-

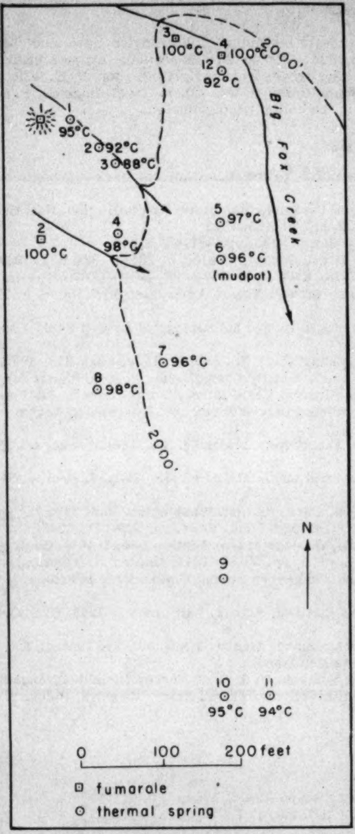

Fig. 8--Fumarole and thermal spring area on Great Sitkin Island

most completely decomposed rocks, brightly colored in red, pink, and yellow. Where any rock texture is preserved, the dominant rock is a breccia of porphyritic volcanics, and the area is probably an old vent-filling with its associated ejecta. The area is peppered with small thermal springs, mud pots, and tiny fumaroles, and the ground in the vicinity is warm. Lush grass and moss in an otherwise barren terrain, and the overflow channels of the springs are clogged with dark-green gelatinous algae.

"......The largest vent is a pool of hot muddy water six to eight feet across through which steam was bubbling with considerable violence when seen. Little was being discharged at the outlet, indicating that the boiling activity was due largely to passage of steam rather than to the influx of boiling water. In fact, most of the springs in the area have very small discharges and seem to be essentially fumarole craterlets in which surface water has collected. Many of the springs are muddy and several are mud pots containing viscous gray mud; pyrite was being deposited in one of them. Sublimates are rare, the bright color being due mainly to rock alteration."

Temperatures of 12 thermal springs ranged from 88° to 98°C, the upper values is the approximate boiling point of water at an altitude of 2000 ft. The springs ranged from neutral to acid (pH: 7 to 2). No simple relationship between pH, temperature, or the location of the springs, was apparent.

Analyses of gas samples from four fumaroles are presented in Table 9. All the fumaroles were emitting steam and other gases at or near a temperature of 100°C. All the samples contain nitrogen and argon in essentially the same ratio as in air and were probably contaminated at the time of collection. Sample 2 contained only air and water. Samples 1 and 4 had a CO_2:SO_2 ratio of approximately 100. Sample 3 contained 0.2 per cent of hydrogen, a primary volcanic gas that has been reported in gases from many volcanic regions.

No samples of gases were obtained from fumaroles on the spectacular crater dome of Great Sitkin Volcano (see Fig. 7). The dome is composed of black porphyritic basalt and is believed to have come into existence in March 1945, when Air Force pilots noted a red glow over the crater. The external aspect of the dome is that of a fractured blocky carapace. In the summer of 1946 a column of steam 4000 ft high rose from the center. According to R. R. Coats (personal communication), who visited the 1945 crater dome in June 1946, steam and strongly pungent gases were escaping from beneath the shattered carapace of the dome. He did not see the orifice of the main large fumarole near the center of the dome because of the great difficulty in traversing the blocky lava. According to Frank S. Simons (personal communication) the melting snow around the crater had a distinct sour taste late in the summer of 1946.

COATS (personal communication) also reported that no significant change had occurred in Great Sitkin Volcano during 1947 and up to the end of August 1948.

Acknowledgments

E. G. Zies of the Geophysical Laboratory, Carnegie Institution of Washington, gave much helpful advice on selection of equipment for use in the field. The writers also wish to express thanks to their colleagues on the United States Geological Survey, especially Earl Ingerson, R. E. Wilcox, H. A. Powers, and G. D. Robinson, for constructive criticism of this paper. D. M. Hopkins, F. S. Simons, and K. L. Wier gave valuable assistance in the collection of samples.

References

ALLEN, E. T. and DAY, ARTHUR L., Hot springs of the Yellowstone National Park, Carnegie Inst. Washington, Pub. 466, 525 pp., 1935.

ALLEN, E. T. and ZIES, E. G., A chemical study of the fumaroles of the Katmai region, Nat. Geogr. Soc., Contrib. Tech. Papers, Katmai ser. no. 2, pp. 77-155, 1923.

BARTH, TOM. F. W., Geysers in Iceland, Amer. J. Sci., v. 238, pp. 381-407, 1940.

BARTH, TOM. F. W., Geysers of Iceland, Trans. Amer. Geophys. Union, v. 28, pp. 882-887, 1947.

BRANNOCK, W. W., FIX, PHILIP F., GIANELLA, VINCENT P., and WHITE, DONALD E., Preliminary geochemical results at Steamboat Springs, Nevada, Trans. Amer. Geophys. Union, v. 29, pp. 211-226, 1948.

DAY, ARTHUR L., and ALLEN, E. T., The volcanic activity and hot springs of Lassen Peak, Carnegie Inst. Washington. Pub. 362, 190 pp., 1925.

FENNER, C. N., Bore-hole investigations in Yellowstone Park, J. Geol., v. 44, pp, 225-315, 1936.

GREWINGK, C., Beitrag zur Kentniss der orographischen und geognostischen Beschaffenheit der Nordwest Kuste Amerikas, mit den anliegenden Inseln, Verh. Russ.-K. min. Gesell., St. Petersburg, Jg. 1848-1849, pp. 76-432, 1850. (Also printed in book form: St. Petersburg, 351 pp., 1850.

HEALY, J., Boron in hot springs at Tokaanu, Lake Taupo, New Zealand J. Sci. Tech., v. 24, no. 1B, pp. 1B-17B, 1942.

KELLER, W. D., and VALDUGA, ADRIANO, The natural steam at Larderello, Italy, J. Geol. v. 54, pp. 327-334, 1946.

PERRET, FRANK A., The Vesuvius eruption of 1906, Carnegie Inst. Washington. Pub. 339, 151 pp., 1924.

ROBINSON, G. D., Exploring Aleutian volcanoes, Nat. Geogr. Mag., v. 94, pp. 509-528, 1948.

SIMONS, FRANK S., and MATHEWSON, DONALD E., Geology of Great Sitkin Island, U. S. Geol. Survey, Alaskan Volcano Investigations Rep. 2, pt. 4, pp. 55-69, 1947 (limited distribution).

THORKELSSON, TH., On thermal activity in Iceland and geyser action, Visindafelag Islendica, v. 25, 139 pp., 1940.

WILCOX, R. E., Report on activity of volcano, Umnak Island, Alaska, June and July 1945, U. S. Geol. Survey files, 1945 (unpublished).

WILCOX, R. E., Report on activity of volcano, Umnak Island, Alaska, 1 August, 1945 through 4 January, 1946: U. S. Geol. Survey files, 1946 (unpublished).

WILLIAMS, HOWEL, Notes on the eruption of Tulik Volcano, U. S. Geol. Survey files, 1945 (unpublished).

ZIES, E. G., Temperature measurements at Paricutin Volcano, Trans. Amer. Geophys. Union, v. 27, pp. 178-180, 1946.

U. S. Geological Survey,
Denver, Colorado

(Communicated manuscript received June 1, 1949;
open for formal discussion until March 1, 1950.)

Transactions, American Geophysical Union Volume 30, Number 5 October 1949

EFFECT OF RAINFALL ON MAGNITUDE AND FREQUENCY OF PEAK RATES OF SURFACE RUNOFF

W. D. Potter

Abstract--This study establishes a relationship between rainfall intensity and peak rates of surface runoff, and uses that relationship to estimate the peak rates of runoff that might be expected for various recurrence intervals. The procedures thus developed are utilized to determine the effect of intensity and amount of rainfall and number of excessive storms on the magnitude of peak rates of runoff for various frequencies. The relationships developed in the study are also utilized to adjust peak rates of runoff from watersheds of like physiography and land use for differences in rainfall.

Source of data

The data selected for analysis were those collected from two small agricultural watersheds located at the Central Great Plains Experimental Watershed near Hastings, Nebraska, operated by the Soil Conservation Service in cooperation with the Nebraska Agricultural Experiment Station. Watershed W-3 is a mixed-cover watershed of 481 acres. Watershed W-8 includes W-3, and has an area of 2,086 acres [U. S. DEPARTMENT OF AGRICULTURE, 1942]. Rainfall on and surface runoff from these two watersheds have been measured since July 1938. The rainfall is measured by both recording and standard rain gages, and the runoff by stage recorders with concrete broad crested weir controls (see Fig. 1). The eight-year period of record, 1939-1946, was selected for the study.

Normalcy tests for rainfall

The first step in the analysis of the data was to test the period of record to see if it was representative of a longer period with respect to the rainfall experienced. Probability curves were prepared to determine the rainfall intensity for various time intervals that might be expected for various frequencies [POTTER, 1948]. These were compared with similar curves prepared from a 27-year record (1920-1946) of the U. S. Weather Bureau for Lincoln, Nebraska. Probability curves of six-month (April-September) rainfall for the period of record were compared with similar curves for a 43-year record of the U. S. Weather Bureau for Hastings, Nebraska. The average annual number of excessive storms was compared with the 30-year average of YARNELL [1935]. Tables 1, 2, and 3 show these comparisons and indicate that the rainfall experienced during the period of record was a good sample of what might be expected over a longer period.

Table 1--Number of excessive storms at the Meteorological Station of the Experimental Watershed

Period	1939	1940	1941	1942	1943	1944	1945	1946	Total	Average	Yarnell's 30-year average
Apr.-Sep.	6	2	4	8	8	6	5	5	44	5.5	5.3
Calendar year	6	2	5	8	9	6	5	6	47	5.9	5.6

Rainfall intensity compared with peak rates of runoff

An examination of the hydrographs of surface runoff from W-3 for the principal storms indicated that the average time of concentration for the watershed was approximately 30 min. The maximum 30-min rainfall intensity was, therefore, determined for each of the 172 storms of record, and these were plotted against the corresponding peak rates of surface runoff from W-3 (see Fig. 2). An arbitrary minimum of 0.005 in/hr was set for the runoff peaks and all rates below this amount were considered to be zero. As might be expected, the plotted points showed a wide scatter, and the maximum peak rates of runoff for many rainfall intensities were 15 or 20 times the minimum values for the same intensities.

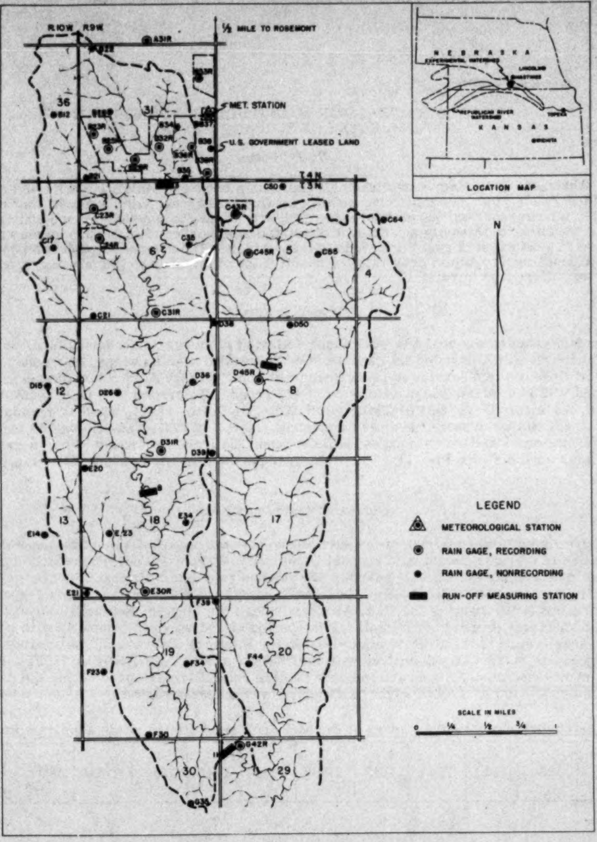
R10W R9W
½ MILE TO ROSEMONT
MET. STATION
U.S. GOVERNMENT LEASED LAND
T4N
T3N
LOCATION MAP
NEBRASKA
EXPERIMENTAL WATERSHED
LINCOLN
HASTINGS
REPUBLICAN RIVER WATERSHED
KANSAS
TOPEKA
WICHITA
N
LEGEND
METEOROLOGICAL STATION
RAIN GAGE, RECORDING
RAIN GAGE, NONRECORDING
RUN-OFF MEASURING STATION
SCALE IN MILES
0
¼
½
¾
1
36
31
6
5
4
12
7
8
13
18
17
19
20
30
29
A31R
B12
C17
C21
C23R
C31R
C35
C43R
C45R
C50
C55
C64
D15
D26
D31R
D36
D38
D39
D45R
D50
E14
E20
E21
E23
E30R
E34
F23
F30
F34
F38
F44
G35
G42R

Fig. 1--Central Great Plains experimental watershed, Hastings, Nebraska

Hydrologists have demonstrated that much of this difference may be accounted for by the condition of the watershed at the time of occurrence of the maximum rainfall intensity. Included in the term, "condition of the watershed," are such factors as soil moisture, tillage practices, and type and density of vegetative cover, all of which have been shown to materially affect the magnitude of peak rates of runoff.

Rather than attempt to assign values for each factor that may have affected the magnitude of the peak rate of runoff for each individual storm, the assumption was made that most of the variation in peak rates for any rainfall intensity could be explained by the consideration of only three watershed conditions. The first of these might be defined as one for which the net effect of all factors was such that maximum peak rates of runoff could be expected. The second was one for which minimum peak

Table 2--Rainfall Intensities

Station	Length of record	Interval	Recurrence interval				
			2 yr	5 yr	10 yr	25 yr	50 yr
	yr	min	in/hr	in/hr	in/hr	in/hr	in/hr
Experimental Watershed	8	15	3.20	4.18	4.95	6.20	7.65
Lincoln	27	15	3.06	3.77	4.27	5.05	6.00
Experimental Watershed	8	30	2.06	2.70	3.18	3.95	4.85
Lincoln	27	30	2.14	2.70	3.10	3.96	4.52
Experimental Watershed	8	60	1.28	1.57	1.80	2.12	2.50
Lincoln	27	60	1.28	1.59	1.83	2.18	2.59

Table 3--Amounts of rainfall for six-month period, April-September

Station	Period of record	Recurrence interval				
		2 yr	5 yr	10 yr	25 yr	50 yr
		in	in	in	in	in
Experimental Watershed	1939-1946	17	24	29	38	49
Lincoln	1895-1937	18	24	28	34	41

rates of runoff could be expected, and the third was an intermediate condition falling somewhere between these two extremes.

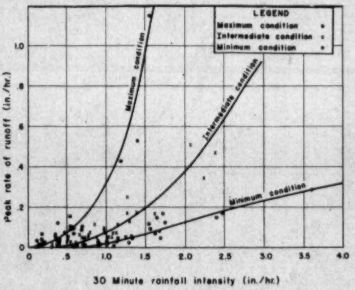

Fig. 2--Preliminary curves showing relationship between rainfall intensity and peak rates of runoff for W-3

The classification of each storm as to watershed condition was determined, not by an evaluation of each individual factor, but by the magnitude of the resulting peak rate of runoff. As shown in Figure 2, curves were drawn for the maximum and minimum values and a third curve for the remaining intermediate peaks. Each storm was then assumed to have occurred when the watershed condition was maximum, minimum, or intermediate, depending upon whether the resulting peak rate of runoff was closer to the maximum, minimum, or intermediate curve. To simplify computations, the storms in the maximum class were divided into 30-min rainfall intensity groups. Each group had a range of 0.1 in/hr, such as 0.1 - 0.2 in/hr and 0.2 - 0.3 in/hr. The rainfall intensities in each group were averaged as were the peak rates of runoff. The average 30-min intensity for each group was then plotted on semi-logarithmic paper against the corresponding average peak rate of runoff (see Fig. 3). This same procedure was followed in plotting average group values for the minimum and intermediate watershed conditions.

The relationship between 30-min rainfall intensities and peak rates of runoff for each of the three watershed conditions was determined by fitting a least-squares curve to each group of plotted points. Because of a lack of experimental data on peak rates of runoff for a maximum watershed condition that might be expected for rainfall intensities greater than 1.5 in/hr, an assumed runoff rate was assigned to correspond to a rainfall intensity of 5.0 in/hr. Since a rainfall intensity of this magnitude occurs only once in more than 100 years, it seemed reasonable to assume

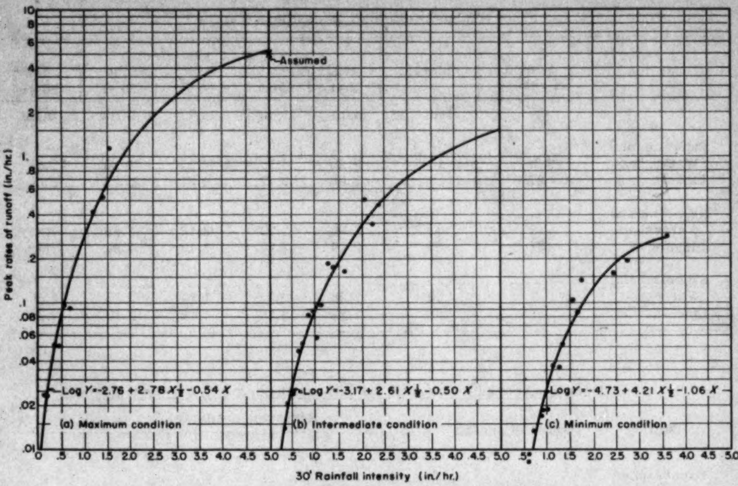

Fig. 3--Final curves showing relationship between rainfall intensity and peak rates of runoff for watershed W-3

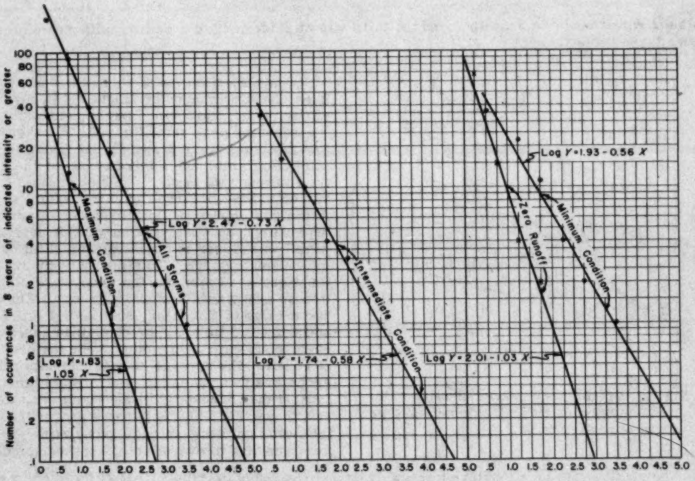

Fig. 4-- Frequency curves for various watershed conditions, W-3

that when such an occurrence coincided with a maximum watershed condition, the peak rate of runoff might be expected to closely approach the rainfall intensity. A peak runoff rate of 5.0 in/hr was, therefore, assumed for a 5.0 in/hr rainfall intensity and included with the experimental data in computing the least-squares curve.

Frequency of rainfall intensities for various watershed conditions--It has previously been shown that rainfall for the eight years of record was typical of a long time period. Since crops and tillage practices were also representative, it was assumed that the distribution of storms by intensity groups for the three watershed conditions would be a good sample of what might be expected over a longer period. Accordingly, the 172 storms were divided into intensity groups with a range of 0.5 in/hr for each group. The number of storms in each group that occurred when the watershed was in each of the three watershed conditions and those that produced zero runoff was tabulated. The number of storms with intensities that equalled or exceeded the intensities of each group was then tabulated for all storms and for each watershed condition. These values were plotted on semi-logarithmic paper with the number of occurrences as ordinates and rainfall intensities as abscissa (see Fig. 4). The midpoint of each intensity group was taken as the plotting position for the group. Average least-squares curves were then computed for the group of plotted points representing all storms, those that produced zero runoff, and those that occurred when the watershed was in maximum, minimum, and intermediate conditions.

Various values of intensity were substituted in the equations for these average curves to obtain the number of storms in an eight-year period that might be expected to have 30-min intensities that would equal or exceed each selected value. For each intensity, the number of occurrences that might be expected for the three watershed conditions and for storms of zero runoff was totaled. The number of occurrences was then expressed as a per cent of these totals (see Table 4).

Knowing the frequency of rainfall for the various 30-min intensities and the percentage of such storms that might be expected to occur for each watershed condition, it was possible to convert these percentages into frequency. The results of this conversion are shown in Table 5. The number of occurrences for the eight-year period of record, shown in the second column of this table, were obtained by substituting the first-column intensities in the equation of the curve (see Fig. 4) for which all storms were considered regardless of watershed condition or whether or not surface runoff resulted. The third column is obtained by dividing the period of record (eight years) by the number of occurences . The percentage columns for each watershed condition were taken from Table 4. The period of record was divided by the product of the total number of occurrences and the percentage to obtain the frequency for each watershed condition. Thus, for storms with maximum 30-min intensities equal to or greater than 0.5 in/hr, 126.9 occurrences could be expected in eight years, or an average of one storm every 0.063 year. The number of such storms that could be expected to occur when the watershed was in a maximum condition would be 126.9 × 0.163 in eight years. An average of one storm (for such condition) could then be expected in 8/126.9 × 0.163 or

Table 4--Proportion of total storms for various watershed conditions, for Watershed W-3

Maximum 30-min intensity	Watershed condition								Total	
	Maximum		Intermediate		Minimum		Zero runoff			
	Number of storms	Per cent of total	Number of storms	Per cent of total	Number of storms	Per cent of total	Number of storms	Per cent of total	Number of storms	Per cent
in/hr										
0.5	20.13	16.3	27.76	22.4	44.52	36.0	31.24	25.3	123.65	100
1.0	6.034	11.4	14.16	26.7	23.34	44.0	9.504	17.9	53.038	100
1.5	1.809	7.5	7.228	29.9	12.24	50.6	2.891	12.0	24.168	100
2.0	0.5425	4.7	3.689	32.0	6.415	55.7	0.8795	7.6	11.526	100
2.5	0.1626	2.9	1.882	33.2	3.363	59.2	0.2675	4.7	5.675	100
3.0	0.0488	1.7	0.9606	33.7	1.763	61.8	0.0814	2.8	2.854	100
3.5	0.0146	1.0	0.4903	33.7	0.9243	63.6	0.02475	1.7	1.454	100
4.0	0.0044	0.6	0.2502	33.5	0.4845	64.9	0.00753	1.0	0.747	100
4.5	0.0013	0.3	0.1277	33.6	0.2493	65.5	0.00229	0.6	0.381	100
5.0	0.0004	0.2	0.0651	32.7	0.1332	66.8	0.00070	0.3	0.199	100

Table 5--Frequency of rainfall intensities for various watershed conditions for Watershed W-3

Rainfall			Watershed Condition					
			Maximum		Intermediate		Minimum	
Maximum 30-min intensity	Storms in eight years[a]	Recurrence interval	Per cent of total storms	Recurrence interval	Per cent of total storms	Recurrence interval	Per cent of total storms	Recurrence interval
in/hr		yr		yr		yr		yr
0.5	126.9	0.063	16.3	0.386	22.4	0.281	36.0	0.175
1.0	54.95	0.146	11.4	1.28	26.7	0.547	44.0	0.332
1.5	23.80	0.336	7.5	4.48	29.9	1.12	50.6	0.664
2.0	10.31	0.776	4.7	16.51	32.0	2.42	55.7	1.39
2.5	4.464	1.79	2.9	61.72	33.2	5.39	59.2	3.02
3.0	1.934	4.14	1.7	243.53	33.7	12.28	61.8	6.70
3.5	0.8374	9.55	1.0	955.0	33.7	28.34	63.6	15.02
4.0	0.3627	22.06	0.6	3677.0	33.5	65.85	64.9	33.99
4.5	0.1571	50.92	0.3	16973.0	33.6	151.55	65.5	77.74
5.0	0.0680	117.58	0.2	58790.0	32.7	359.57	66.8	176.02

[a] As determined from the equation for all storms on Fig. 4.

0.386 year. Likewise, an average of one storm could be expected to occur in 8/126.9 × 0.224 or 0.281 year when the watershed was in an intermediate condition, and one storm in 8/126.9 × 0.360 or 0.175 year when the watershed condition was minimum.

These frequencies versus the corresponding 30-min rainfall intensities were plotted on graph paper for the three watershed conditions and smooth curves drawn through the points (see Fig. 5). These curves were used to determine for selected frequencies the 30-min intensity that might be expected to occur when the watershed was in each of the three conditions. For each of these frequencies, corresponding peak rates of runoff were determined from the rainfall intensity versus peak rate of runoff curves in Figure 3. A comparison of these values is shown in Table 6. Also included in this table are peak rates of runoff determined from a Gumbel probability curve, [GUMBEL, 1945; POTTER, 1948]. Since the Gumbel probability curve is based on the maximum peak rate for each year of record, frequencies applied to these curves are in terms of years rather than occurrences. For example, a frequency of once in five years, applied to the Gumbel curve would be one year in five years instead on one occurrence in five years. In spite of this difference the results indicate that, for the Hastings data, the peak rates computed for the maximum watershed condition and those derived from the Gumbel curve are nearly equal.

The data collected from the 2086-acre watershed W-8 were treated in a manner similar to that outlined for the 481-acre watershed W-3. For this watershed the average time of concentration was found to be approximately 90 min and the minimum peak rate of runoff considered was 0.001 in/hr. As was noted for W-3, a comparison of the peak rates of runoff for W-8 (see Table 7) shows little difference between the highest value computed for the watershed conditions.for each frequency and those derived from a Gumbel probability curve.

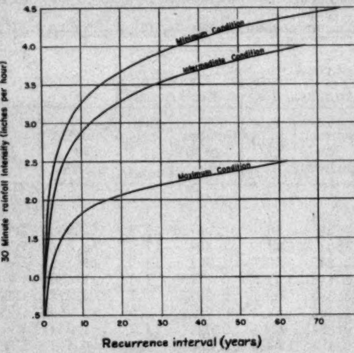

Fig. 5--Relationship between rainfall intensity and frequency for various watershed conditions W-3

Table 6--Peak rates of runoff for various frequencies and watershed conditions for Watershed W-3

Watershed condition	Recurrence interval in years					
	2	5	10	15	25	50
	in/hr	in/hr	in/hr	in/hr	in/hr	in/hr
Minimum	0.16	0.23	0.26	0.28	0.29	0.31
Intermediate	0.29	0.50	0.68	0.77	0.90	1.07
Maximum	0.38	0.70	0.99	1.18	1.35	1.70
Gumbel probability curve	0.41	0.77	1.01	1.15	1.33	1.55

Table 7--Peak rates of runoff for various frequencies and watershed conditions for Watershed W-8

Watershed condition	Recurrence interval in years					
	2	5	10	15	25	50
	in/hr	in/hr	in/hr	in/hr	in/hr	in/hr
Minimum	0.024	0.034	0.042	0.046	0.052	0.060
Intermediate	0.127	0.170	0.203	0.220	0.243	0.275
Maximum	0.105	0.157	0.200	0.230	0.270	0.327
Gumbel probability curve	0.107	0.180	0.232	0.260	0.292	0.341

The one other observation that will be made before passing on to the third objective concerns the difference between the frequency of a storm of given intensity and the frequency with which it might be expected to produce maximum peak rates of runoff. It has been observed by many hydrologists that storms of similar maximum intensities falling on the same watershed have produced radically different peak rates of runoff. Table 5 demonstrates numerically the wide difference that exists between the frequency of such a storm and the frequency of the maximum peak rate of runoff. For example, in Table 5, a storm having a maximum 30-min intensity that would equal or exceed 2.5 inches per hour might be expected to occur on an average of once every 1.79 years. Over a period of 1000 years, such a storm could be expected to occur approximately 560 times. Of these 560 storms, however, only one every 61.72 years or approximately 16 in 1000 years, could be expected to occur when the watershed was in a condition to give maximum peak rates of runoff. Likewise, 186 of the 560 storms could be expected to occur when the watershed was in an intermediate condition, and 332 when in a minimum condition. Twenty-six storms could be expected to produce peak rates of runoff less than 0.005 in/hr.

Effect of rainfall intensity, annual rainfall, and number of excessive storms on peak rates of runoff

The foregoing discussion has demonstrated that relationships may be established between rainfall intensity and peak rates of runoff by accounting for the variations in peak rates for any intensity by the consideration of three watershed conditions. If all of the factors included in the term, "watershed condition," had remained constant from year to year throughout the period of record, no difference would have been expected in the proportion of number of storms each year that would occur when the watershed was in each of the three conditions. An examination of the Hastings data for Watershed W-3, however, shows that this proportion, for a maximum condition, varied from six and eight per cent in 1940 and 1943 to 28 and 33 per cent in 1946 and 1942 (see Table 8). With the exception of rainfall, the annual variations in the major factors that affect surface runoff on the two Hastings watersheds were nearly constant for the period of record. Physiographic factors, such as soils, slopes, and drainage pattern were the same from year to year and may, therefore, be considered to have been constant. Farming practices varied only slightly during the period of record. Crops were planted and harvested at approximately the same time each year, the same crop rotations and tillage practices were applied, and approximately the same acreage was cultivated. When taken on a year to year basis, these factors, to a lesser degree, might also be considered to have been constant. Rainfall, however, is not a constant even when considered on a yearly basis. Such factors as annual amounts, annual number of excessive storms, and the magnitude of intensities for various time periods vary materially from year to year. It is this variation in rainfall that is believed to be primarily responsible for the observed variation in the proportion of annual number of storms for any watershed condition.

Annual rainfall and number of excessive storms compared with watershed condition--It would seem reasonable to assume that if the average number of excessive storms for any time period was double that of any other time period, then the chances would be greater for one such storm to occur when the watershed was in a condition to produce maximum runoff. Likewise, if the annual rainfall for any time period was double that for any other time period the chances for a storm to occur when the soil moisture in the watershed was high would also be greater. In other words, the percentage of storms that might be expected to occur when the watershed was in a maximum condition would vary with the number of excessive storms and with the annual rainfall.

The balance of this study is devoted to an attempt to verify the assumption that annual rainfall and number of excessive storms primarily determine watershed condition, whereas the magnitude of rainfall intensity primarily determines the magnitude of peak rates of runoff for a given watershed condition.

Table 8--Proportion of total storms for each watershed condition, annual rainfall and number of excessive storms by years for Watershed W-3

Year	Watershed condition								Total number of storms	Annual rainfall	Number of excessive storms	Annual rain x number of excessive storms
	Maximum		Intermediate		Minimum		Zero runoff					
	Number of storms	Per cent of total storms	Number of storms	Per cent of total storms	Number of storms	Per cent of total storms	Number of storms	Per cent of total storms				
										in		in
1939	3	13	2	9	6	26	12	52	23	14.11	6	85
1940	1	6	1	6	2	12	13	76	17	12.31	2	25
1941	9	21	4	10	6	14	23	55	42	25.76	5	129
1942	7	33	8	38	6	29	0	0	21	31.22	8	250
1943	1	8	5	42	3	25	3	25	12	15.48	9	139
1944	6	26	6	26	5	22	6	26	23	28.22	6	169
1945	2	13	5	31	4	25	5	31	16	20.67	5	103
1946	5	28	3	17	4	22	6	33	18	27.18	6	163
Total	34	..	34	..	36	..	68	..	172	....	..	...

For Watershed W-3, the storms for each year of record were classified as to the watershed condition that existed at the time of their occurrence and as to whether or not surface runoff resulted. The number of storms in each class was expressed as a per cent of the annual total (see Table 8), and plotted against corresponding values of the product of annual rainfall and number of excessive storms. Average least-squares curves were then computed for each group of plotted points (see Fig. 6). Similar relationships were computed from the W-8 data.

As would be expected, the relationship between the product of annual rainfall and number of excessive storms, and the per cent of storms, was found to be most pronounced for the two extreme conditions; that is, for those resulting in zero and maximum runoff. It is recognized that other rainfall factors, such as seasonal distribution of rainfall and individual storm pattern [SCHIFF; 1943] affect the watershed condition at the instant when peak rates of runoff occur. It is probable that for intermediate and minimum watershed conditions, these factors play a relatively more important part and thus account for the increased scatter of the plotted points for those conditions.

An analysis of variance showed the curves for maximum and zero watershed conditions for both W-3 and W-8 to be highly significant, the F factor falling between the 0.01 and 0.001 level. For intermediate watershed conditions, the F factor, for W-8, fell between the 0.05 and 0.01 level of significance, and for W-3 slightly below the 0.05 level. Neither of the curves for minimum watershed condition was found to be significant. It should be pointed out, in this connection, that in all

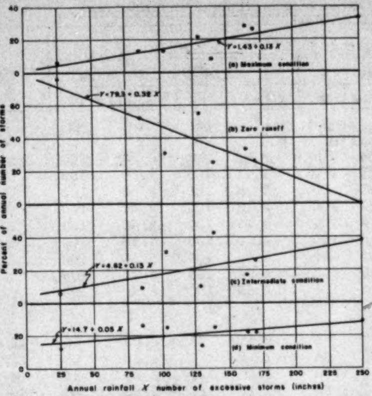

Fig. 6--Relationship between per cent of storms and product of annual rainfall and number of excessive storms for various watershed conditions for Watershed W-3

of the following computations in which these relationships were used, the maximum peak rates of runoff were found to occur on W03 when the watershed was in a condition for maximum runoff and on W-8 when the watershed was either in a maximum or intermediate condition. Since the relationship between the rainfall factors and the per cent of storms for those watershed conditions was significant, the lack of significance in the relationship for minimum conditions should not have materially affected the accuracy of the final results.

P-ratio--Before proceeding further in the study of the effect of rainfall intensity, amounts, and number of excessive storms on peak rates of runoff, a determination was made of the variation in these factors that might be expected within the area of application of the Hastings data. Eleven points were selected on the boundary lines of the States of Nebraska and Kansas. For each of these points and for Hastings the amounts of rainfall that might be expected for various time intervals and for various frequencies were determined from the isohyetal maps of YARNELL [1935]. These values were tabulated and expressed as a per cent of the corresponding value for the Experimental Watershed near Hastings. Table 9 shows a typical tabulation for one of these locations. The average of the percentages was then calculated for each time period. The deviation from the mean of these averages for each location was found to be no more than the error that was probably introduced by the necessity of interpolating between isohyetals. The mean values were, therefore, taken as the percentage ratio of the rainfall intensities at each of the locations to those near Hastings, the ratio being considered constant for all time intervals and for all frequencies. For the sake of simplicity this ratio was designated by P. The P ratio for each of the eleven locations was inscribed on a map and the location of lines of equal P ratios was determined by interpolating between these points (see Fig. 7). (The area of application was delineated from knowledge of physiographic and cultural features.)

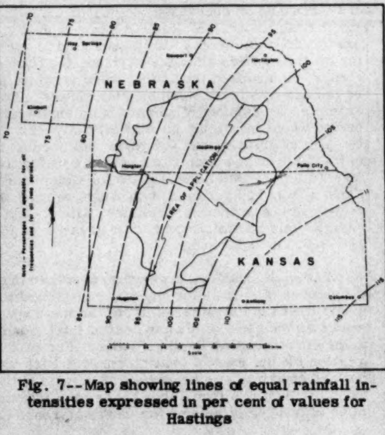

Fig. 7--Map showing lines of equal rainfall intensities expressed in per cent of values for Hastings

S-product--To determine the variation to be expected in the product of annual rainfall and number of excessive storms, nine locations in Kansas and Nebraska were selected. Eight of these locations had unbroken rainfall records for the period 1896-1930 and the ninth had a complete record between 1904 and 1930. Period of record, average annual rainfall, and Yarnell's 30-year average number of excessive storms were tabulated for each location (see Table 10). The products of annual rainfall and number of excessive storms, hereinafter referred to as the S product, were inscribed on a map and the position of lines of equal S products determined by interpolation (see Fig. 8).

Peak rates of runoff for various values of P and S--The next step was to apply these P and S values to the relationships derived from the Experimental Watershed data. Peak rates of runoff for various frequencies that would result from these new values of P and S could be determined and compared with those already calculated for W-3 and W-8. The difference would then be a measure of the effect of P and S on the magnitude

Table 9--Amounts of rainfall for various frequencies and time intervals

Time interval	Recurrence interval										Average
	2 years		5 years		10 years		25 years		50 years		
	Amount	P[a]	Amount	P[a]	Amount	P[a]	Amount	P[a]	Amount	P[a]	
hr min	in	pct	in	pct	in	pct	in	pct	in	pct	pct
Central Plains Experimental Watershed, Hastings (Loc. 1)											
5	0.41	100	0.50	100	0.57	100	0.68	100	0.73	100	. . .
15	0.88	100	1.07	100	1.25	100	1.47	100	1.60	100	. . .
30	1.26	100	1.53	100	1.85	100	2.20	100	2.50	100	. . .
1	1.50	100	1.95	100	2.30	100	2.75	100	3.07	100	. . .
2	1.75	100	2.25	100	2.75	100	3.45	100	4.00	100	. . .
4	. . .	. . .	2.75	100	3.25	100	4.00	100	4.50	100	. . .
8	. . .	. . .	3.00	100	3.50	100	4.40	100	5.10	100	. . .
16	. . .	. . .	3.25	100	4.00	100	4.60	100	5.20	100	. . .
24	. . .	. . .	3.50	100	4.10	100	4.80	100	5.50	100	. . .
Northwestern corner of Kansas (Loc. 2)											
5	0.35	86	0.45	90	0.48	84	0.56	82	0.65	89	86
15	0.69	79	0.92	86	1.05	84	1.19	81	1.38	86	83
30	1.00	80	1.32	86	1.62	88	1.80	82	2.06	82	84
1	1.15	77	1.43	74	1.83	80	2.20	80	2.63	86	79
2	1.30	75	1.63	73	2.10	76	2.80	81	3.25	81	77
4	. . .	. .	2.25	82	2.70	83	3.30	83	3.80	84	83
8	. . .	. .	2.50	83	2.95	85	3.70	84	4.20	82	84
16	. . .	. .	2.65	82	3.20	80	3.80	83	4.40	85	82
24	. . .	. .	2.80	80	3.25	79	4.00	83	4.50	82	81
										Mean	82

[a] P denotes the percentage ratio of the values determined, to the values for the Experimental Watershed near Hastings. The mean value, 82 for location 2 is the P value for the location as used in Figure 7.

of peak rates of surface runoff. Accordingly, the S values for each of the locations tabulated in Table 10 were substituted in the equations of the curves shown on Figure 6 to obtain percentages of total storms for watersheds similar to W-3. These percentages for watersheds similar to W-3 and W-8 are shown in Table 11.

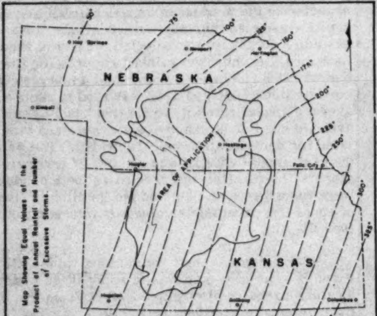

Fig. 8--Map showing equal values of products

The rainfall intensities tabulated in Table 5 were increased or decreased in accordance with the P ratio obtained for each location from Figure 7. Since the P ratio had been found to apply for all frequencies and time periods, the frequencies of the modified intensities were assumed to be the same as for the original intensities. For example, the number of storms in an eight-year period whose maximum 30-min intensity was equal to or greater than 0.5 in/hr had been found to be 126.9 or one such storm every 0.063 year (see Table 5). Since the P ratio for Columbus, Kansas, was 115 per cent, one storm every 0.063 year could be expected, therefore, with a maximum 30-min intensity equal to or greater than 1.15 × 0.5 or 0.58 in/hr.

For each location, it was then assumed that the number of storms for any watershed condition in any intensity class varied from the Hastings values as the ratio of the per cent of total storms to the corresponding Hastings value. For each location the per cent of total storms for each watershed condition was expressed as a ratio of those found for Hastings (see Table 11) and the Hastings value of number of storms for each watershed con-

Table 10--Annual rainfall, number of excessive storms, and S product for various locations

Location	Annual rainfall		30-year average number of excessive storms	S product
	Period	Average		
		in		in
Falls City, Nebr.	1895-1930	34.11	7.3	249.00
Kimbell, Nebr.	1896-1930	16.90	2.0	33.80
Hay Springs, Nebr.	1896-1930	21.21	2.2	46.66
Newport, Nebr.	1896-1930	23.83	3.6	85.79
Hartington, Nebr.	1896-1930	28.58	5.0	142.90
Columbus, Kans.	1896-1930	43.08	8.0	344.64
Anthony, Kans.	1896-1930	27.99	7.0	195.93
Hugoton, Kans.	1904-1930	18.71	3.4	63.61

dition and in each intensity class (see Table 4) was then multiplied by this ratio. These modified values were summed for each intensity class and the number of storms for each watershed condition expressed as a per cent of the total. For example, 45.72 per cent of the total storms at Columbus was found to occur when the watershed was in a maximum condition (see Table 11). This was 231.2 per cent of the corresponding value of 19.8 per cent found for W-3 at Hastings. Similarly, the per cent of total storms that would occur when the watershed was in intermediate, minimum or zero runoff condition was found to be 256.2 per cent, 17.2 per cent, and zero per cent respectively of the Hastings values. For storms with maximum 30-min intensity equal to or greater than 0.5 in/hr, 20.13 had been found to occur at Hastings, W-3, when the watershed was in maxmum condition (see Table 4). This value was multiplied by 2.312 to obtain the number of storms (46.54) with maximum 30-min intensities equal to or greater than 0.58 in/hr that might be expected to occur at Columbus for a maximum watershed condition and on watersheds similar to W-3 (see Table 12). Similarly, the number of storms when the watershed was in intermediate condition, was taken to be 27.76 × 2.562 or 71.12. For minimum watershed condition, the number was 44.52 × 0.172 or 7.66, and for zero runoff 31.24 × 0 or 0. The summation of the number of storms for each watershed condition was 125.32 and the value of this total was 37.1 per cent for maximum, 56.8 per cent for intermediate, 6.1 per cent for minimum, and 0 for zero runoff condition.

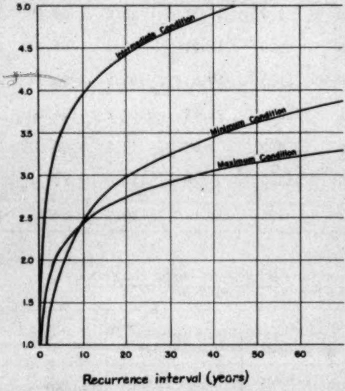

Fig. 9--Relationship between rainfall intensity and frequency for various watershed conditions, Columbus, Kansas, W-3

Having the per cent of storms in each intensity class that might be expected to occur for each watershed condition and the frequency of all storms in that class, it was possible to compute the frequency for each watershed condition following the procedure previously outlined. In a manner similar to that described for the Hastings data, frequency compared with rainfall intensity graphs were plotted. From these graphs, rainfall intensities corresponding to 2, 5, 10, 25, and 50-year frequenices were selected and peak rates of runoff were determined from the rainfall intensity versus peak rates of runoff graphs (see Fig. 3). These peak rates were then expressed as a percentage of similar values derived for Hastings. This procedure was followed for each of the nine locations for watersheds similar to W-3 and W-8. A sample of the intermediate and final results is shown for Columbus W-3, in Tables 12 to 14 and in Figure 9.

Q ratio--To separate the effects of P and S on peak rates of runoff, values of P equal to 70, 80, 90, 100, and 110 per cent were assumed for each of the nine locations and for watersheds similar to

Table 11--Proportion of total storms for each watershed condition for various locations

Location	S product	Watershed condition W-3							
		Maximum		Intermediate		Minimum		Zero runoff	
		Per cent of total storms	Per cent of Hastings	Per cent of total storms	Per cent of Hastings	Per cent of total storms	Per cent of Hastings	Per cent of total storms	Per cent of Hastings
	in								
Hastings, Nebraska	. . .	19.8	100	19.8	100	20.95	100	39.5	100
Falls City, Nebraska	249.0	33.43	168.8	37.88	191.8	28.16	134.4	0.53	1.3
Haigler, Nebraska	50.2	7.88	40.0	11.32	57.4	17.40	83.1	63.40	160.3
Kimball, Nebraska	33.8	5.77	29.1	9.13	46.2	16.51	78.9	68.59	173.5
Hay Springs, Nebraska	46.7	7.43	37.6	10.85	55.0	17.21	82.2	64.51	163.2
Newport, Nebraska	85.8	12.45	62.9	16.08	81.5	19.33	92.2	52.14	131.9
Hartington, Nebraska	142.9	19.79	100.0	23.71	120.0	22.42	107.2	34.08	86.2
Columbus, Kansas	344.6	45.72	231.2	50.66	256.2	3.62	17.2	0	0
Anthony, Kansas	195.9	26.61	134.7	30.80	155.9	25.28	120.8	17.31	43.8
Hugoton, Kansas	63.6	9.60	48.5	13.12	66.5	18.13	86.7	59.15	149.6

Table 12--Proportion of total storms for various watershed conditions, Columbus, Kansas, for Watershed W-3

Maximum 30-min intensity	Watershed condition								Total	
	Maximum		Intermediate		Minimum		Zero runoff			
	Number of storms	Per cent of total	Number of storms	Per cent of total	Number of storms	Per cent of total	Number of storms	Per cent of total	Number of storms	Per cent
in/hr										
0.58	46.54	37.1	71.12	56.8	7.66	6.1	0	0	125.32	100
1.15	13.95	25.7	36.28	66.9	4.01	7.4	0	0	54.24	100
1.73	4.18	16.8	18.52	74.7	2.10	8.5	0	0	24.80	100
2.30	1.25	10.6	9.45	80.1	1.10	9.3	0	0	11.80	100
2.88	0.376	6.5	4.82	83.5	0.578	10.0	0	0	5.774	100
3.45	0.113	3.9	2.46	85.6	0.303	10.5	0	0	2.876	100
4.02	0.0338	2.3	1.26	86.7	0.159	11.0	0	0	1.4528	100
4.60	0.0101	1.4	0.641	87.3	0.0833	11.3	0	0	0.7344	100
5.18	0.00304	0.82	0.327	87.7	0.0429	11.5	0	0	0.37294	100

W-3 and W-8. Peak rates of runoff were then determined for various frequencies for each value of P. Since the value of S at each location was not changed, this necessitated only the plotting of additional frequency versus intensity graphs using the same frequencies for any watershed condition but modifying the magnitude of the rainfall intensities by each of the assumed P ratios. When the peak rates of runoff were expressed as a percentage of the Hastings values, it was observed compared with those for the Experimental Watershed near Hastings, Nebraska

Watershed condition W-8							
Maximum		Intermediate		Minimum		Zero runoff	
Per cent of total storms	Per cent of Hastings	Per cent of total storms	Per cent of Hastings	Per cent of total storms	Per cent of Hastings	Per cent of total storms	Per cent of Hastings
13.2	100	23.0	100	17.85	100	46.0	100
30.40	230.3	43.59	189.5	25.64	143.9	0.37	0.8
0.34	2.5	8.85	38.5	12.78	71.6	78.03	169.8
0	0	3.85	26.0	11.72	65.8	84.43	179.0
0	0	8.04	35.8	12.55	70.3	79.41	172.2
5.72	43.5	15.07	65.5	15.08	84.5	64.13	139.5
14.36	108.7	25.05	109.0	18.78	105.5	41.81	90.9
44.86	339.6	55.14	239.8	0	0	0	0
22.38	169.1	34.32	149.2	22.21	124.5	21.09	45.9
2.37	17.8	11.20	48.8	13.65	76.8	72.78	158.2

Table 13--Frequency of rainfall intensities for various watershed conditions, Columbus, Kansas, W-3

Rainfall		Watershed condition					
Maximum 30-min intensity	Recurrence interval	Maximum		Intermediate		Minimum	
		Per cent of total storms	Recurrence interval	Per cent of total storms	Recurrence interval	Per cent of total storms	Recurrence interval
in/hr	yr		yr		yr		yr
0.58	0.063	37.1	0.170	56.8	0.111	6.1	1.03
1.15	.146	25.7	0.568	66.9	0.218	7.4	1.97
1.73	.336	16.8	2.00	74.7	0.450	8.5	3.95
2.30	.776	10.6	7.32	80.1	0.969	9.3	8.34
2.88	1.79	6.5	27.5	83.5	2.14	10.0	17.9
3.45	4.14	3.9	106.2	85.6	4.84	10.5	39.4
4.02	9.55	2.3	....	86.7	11.0	11.0	86.8
4.60	22.06	1.4	....	87.3	25.3	11.3	....
5.18	50.92	0.82	....	87.7	58.1	11.5	....

that there was little variation for the 10, 25, and 50-year frequencies for any one location and set of S and P values. The average of the percentages corresponding to these frequencies was, therefore, taken as a measure of the effect of P and S on peak rates of runoff. This average percentage is is referred to as the Q ratio.

Relationships between S, P and Q--For like P ratios, values of the Q ratio were plotted against the corresponding S value for each location and a least squares curve computed for each value of P. One such curve was computed for each value of P for both W-3 and W-8 type watersheds (see Fig. 10).

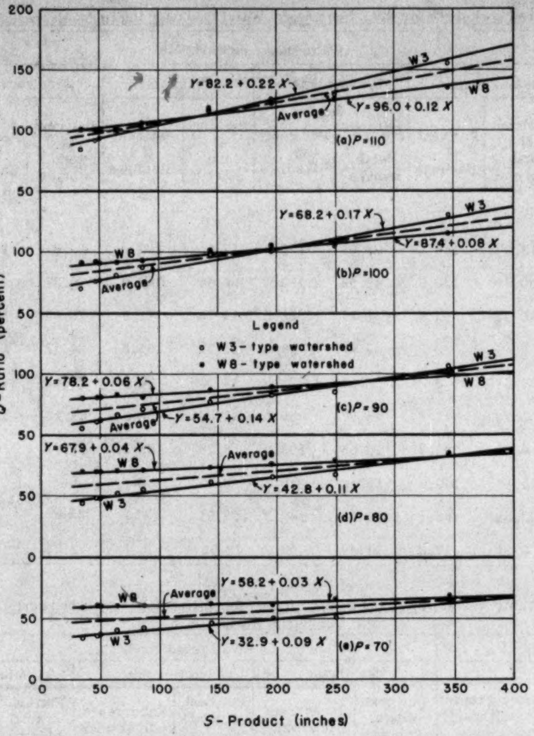

Fig. 10--Relationship between Q ratio and S product for W-3 and W-8 type watersheds for various values of P

Table 14--Peak rates of runoff for various frequencies and watershed conditions, Columbus, Kansas, for Watershed W-3

Watershed condition	Recurrence interval in years				
	2	5	10	25	50
	in/hr	in/hr	in/hr	in/hr	in/hr
Minimum	0.04	0.12	0.18	0.25	0.28
Intermediate	0.67	0.92	1.12	1.36	1.55
Maximum	0.89	1.35	1.75	2.38	2.85

It will be noted that for each value of P the curves for the two type watersheds cross and for extreme values of S the divergence becomes considerable. It is believed that much of this divergence may be due to the inexactness of assumptions and relationships used in the development of the curves rather than to the difference in size of watersheds, although future tests on a wide range of watershed sizes may prove otherwise. Within the range of values of S and P to be found within the area of application for the Hastings data, the deviation of either curve from an average curve is not excessive. This deviation varies from approximately two per cent in the vicinity of Hastings to approximately ten per cent at the extreme westerly limits of the area.

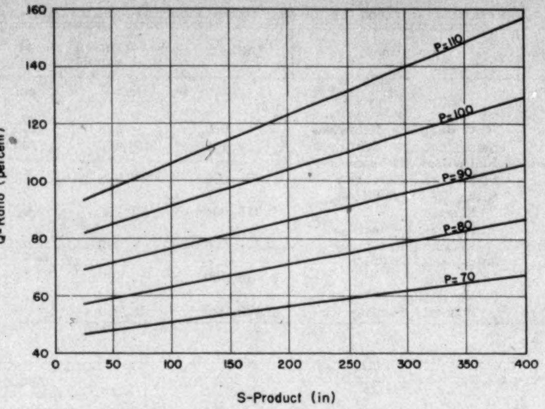

Fig. 11--Average curves showing relationship between Q ratio and S product for various values of P

An examination of these average S - Q curves (see Fig. 11) indicate that for a given value of P there is a variation in the Q ratio of from 20 to 59 per cent that may be ascribed to the effect of annual rainfall and number of excessive storms on peak rates of runoff. Likewise, for a given value of S, there is a variation in the Q ratio of from 50 to 89 per cent that may be ascribed to the effect of the magnitude of rainfall intensity.

To determine the variation in the Q ratio that might be expected within the limits of the area of application for the Hastings data, values of the Q ratio were selected from the average S - Q ratio curves (see Fig. 11) for each of the nine locations, and inscribed on a map. Lines of equal values of the Q ratio were then determined by interpolation (see Fig. 12).

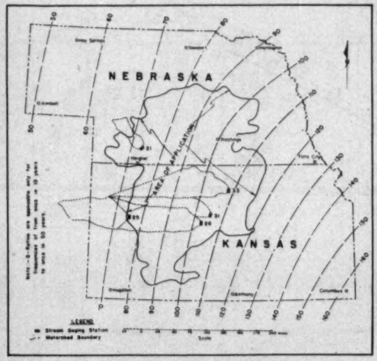

Fig. 12--Map showing lines of equal Q ratio

Peak rates of runoff adjusted to compensate for rainfall differences

The Q ratio map may be used to adjust peak rates of runoff derived from the Hastings data to compensate for rainfall differences at other locations. The following example illustrates that such a map may also be used to advantage in determining area versus peak rate relationships. Gumbel probability curves were computed for the peak rates of runoff from two of the Hastings watersheds, W-8 and W-11, and from five watersheds measured by the United States Geological Survey for the period 1939 to 1946 (see Table 15). The five USGS watersheds were outlined on the Q ratio map. The value of the Q ratio corresponding to the center of gravity of each watershed was then tabulated and the peak rate of runoff for a ten-year recurrence interval divided by this ratio. This correction was made to compensate for the differences in rainfall from that experienced at Hastings. In other words, the corrected peak rates were those that might have been expected if the rainfall on all of the watersheds had been similar to that at Hastings.

Table 15--Peak rates of runoff for ten-year frequencies corrected for rainfall differences

Watershed	Location	Size	Uncorrected peak rates	Q Ratio	Corrected peak rates
		ac	cfs	pct	cfs
W-8	Near Hastings, Nebraska	2,086	488	100	488
W-11	Near Hastings, Nebraska	3,490	442	100	442
21	Red Willow Cr. near McCook, Nebraska	366,000	3,930	68	5,780
31	Saline R. near Wilson, Kansas	1,215,000	12,990	90	14,400
25	Smoky Hill R. near Elkader, Kansas	2,280,000	9,940	64	15,500
33	Solomon R. at Beloit, Kansas	3,480,000	28,630	92	31,100
26	Smoky Hill R. near Russell, Kansas	4,460,000	23,950	76	31,500

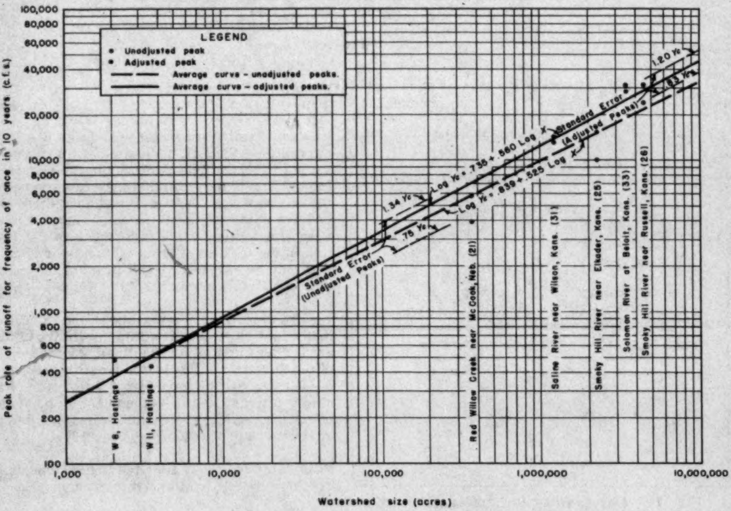

Fig. 13--Relationship between adjusted and unadjusted peak rates of runoff, and size of watershed

Both the corrected and uncorrected peak rates were plotted against the watershed area on logarithmic paper (see Fig. 13). Even a casual examination of this graph would indicate that the scatter of the points had been materially reduced by the correction for rainfall differences. To measure this reduction in scatter more accurately, an average least-squares curve was computed for both corrected and uncorrected values (see Fig. 13). A comparison of the standard error bands computed for the two curves shows that the upper limit of error, expressed as a per cent difference from the theoretical or curve value, had been reduced from 34 to 20 per cent or by slightly less than 1/2 and the lower limit from 25 to 17 per cent or by approximately 1/3. It was not expected that all of the deviations from an average curve could be explained by differences in rainfall, as some of the watersheds are partially or wholly outside of the area of application and at least one of them has diversions above the measuring station. The material reduction in these deviations, however, and the resulting increased reliability of the area - peak rate relationship would seem to to justify the use of the rainfall correction.

Conclusions

(1) The variations in peak rates of runoff that result from any maximum rainfall intensity may be explained by defining the watershed condition at the beginning of the high intensity period.

(2) Workable relationships may be established between maximum rainfall intensities for a given time period and resulting peak rates of runoff by the consideration of three watershed conditions.

(3) The proportion of the annual number of storms that may be expected to occur when a watershed is in a maximum or intermediate condition is primarily dependent upon the amount of rainfall and the number of excessive storms and varies as some function of their product.

(4) There is a wide difference between the frequency of a storm of given intensity and the frequency with which it produces maximum peak rates of runoff. The magnitude of this difference depends upon the frequency with which the storm may be expected to occur when the watershed is in each of several conditions.

(5) Rainfall intensity, amounts of rainfall, and the number of excessive storms all have a material effect on the magnitude of peak rates of runoff that may be expected for any given frequency. For a storm that may be expected to occur with a given frequency when the watershed is in any given condition, the magnitude of the rainfall intensity determines the magnitude of the peak rate of runoff. The amount of rainfall and the number of excessive storms determine the number of times that a storm of a given frequency may be expected to occur when the watershed is in any given condition.

(6) Peak rates of runoff determined from measurements made at one location should be modified to compensate for rainfall differences before being applied to another locality. Rainfall corrections should also be made when peak rates of runoff from watersheds in different localities or from the same watershed but for different time periods are to be compared to determine the effect of factors other than rainfall.

References

GUMBEL, E. J., Simplified plotting of statistical observations, Trans. Amer. Geophys. Union, v. 26, pp. 69-82, 1945.
POTTER, W. D., Analytical procudures for determining the effect of landuse on surface runoff, Agric. Eng., v. 29, pp. 64-71, 1948.
SCHIFF, LEONARD, Classes and patterns of rainfall with reference to surface runoff, Trans. Amer. Geophys. Union, pt. 2, pp. 438-451, 1943.
U. S. DEPARTMENT OF AGRICULTURE, Hydrologic data, Central Great Plains Experimental Watershed, Hastings, Nebr., 1938-1940, U. S. Dept. of Agric. Hydrologic Bull. 3, 1942.
YARNELL, D. L., Rainfall intensity-frequency data, U. S. Department of Agriculture, Misc. Pub. 204, 1935.

Soil Conservation Service,
Washington 25, D. C.

(Manuscript received, September 29, 1948, and as modified, April 7, 1949; presented at the Thirtieth Annual Meeting, Washington, D. C., April 21, 1949; open for formal discussion until March 1, 1950.)

Transactions, American Geophysical Union   Volume 30, Number 5   October 1949

NATURAL WATER LOSSES IN MOUNTAIN DRAINAGE AREAS OF SOUTHERN CALIFORNIA

Harold C. Troxell and Harlowe M. Stafford

(Published with the approval of the Director, U. S. Geological Survey)

Abstract--For twenty-five small mountain drainage areas of Southern California, natural water losses are shown to vary with basin altitude, and with estimated absorptive and retentive characteristics of the drainage areas. Among other relationships demonstrated is the increase of the annual natural water loss with increased annual precipitatiom to an optimum, beyond which the loss is about uniform regardless of increased precipitation.

It has long been recognized that a substantial portion of the season's precipitation is consumed by natural water losses. These losses, which vary from area to area with altitude, latitude, precipitation, absorptive and retentive qualities of the mantle rock, and many other influences, are principally the results of transpiration from plant life, evaporation from soil and snow, and interception and subsequent evaporation of precipitation retained by the foliage of plant life during periods of rainfall. Current and past literature contains many references to and discussions of these natural water losses. KITTREDGE [1938] prepared a map showing their general distribution throughout the United States. WILLIAMS [1940] determined the basin-wide water losses for numerous semi-arid and humid areas east of the Rocky Mountains. Other investigators have undertaken to analyze the many factors influencing these losses and to determine the relationship among those factors.

In regions which are essentially semi-arid, such as Southern California, the natural water losses in the mountain drainage areas range from about 50 to 95 per cent of the precipitation. From the standpoint of water supply, therefore, they are of extreme importance; it is only by a reduction of these losses that the usable water from the mountain drainage area can be increased in any substantial measure. As can be observed from data presented in this paper, the reduction of natural water losses by a few inches could, under certain conditions, almost double the recoverable water in some drainage areas.

As a part of studies of the hydrology of the San Bernardino and eastern San Gabriel Mountains and of western Riverside County made by the United States Geological Survey in cooperation with San Bernardino and Riverside Counties, data on the natural water losses in the several mountain drainage areas were developed. It is the purpose of this paper briefly to present those data and the indicated relationships among the factors influencing the water losses.

Mean seasonal natural water losses--Derived as the residual quantity after the recoverable water has been subtracted from the basin-wide precipitation, the mean seasonal natural water losses are given in Table 1 for 25 mountain drainage areas in Southern California, together with the size and average altitude. The mean values are for the 50-year period 1896 to 1946. Those for seasonal precipitation were derived from isohyetal maps prepared in connection with the other hydrologic studies of these areas.

In principle, mean seasonal recoverable water is the mean seasonal runoff, plus or minus the change in mountain ground-water storage during the 50-year period, plus the natural subsurface leakage from the drainage area. The mean seasonal runoff is based on the records at gaging stations and of surface or subsurface diversions above the gaging stations. The runoff given by these records varying in length from 15 to more than 50 years was, where necessary, extended to include the 50-year period.

The change in mountain ground-water storage can be evaluated from the relation between storage and the recession curves of daily discharge, the equations for which were introduced by BARNES [1942]. When this method was applied for the 50-year period in the Lytle Creek drainage area, the average daily discharge during the month of September 1896 was 22 cfs, indicating a basin-wide ground-water storage of 22,300 ac ft. In September 1946 the average daily discharge was 33 cfs, representing a basin-wide storage of 33,500 ac ft. The net gain in storage during the 50-year

Table 1--Mean seasonal precipitation, recoverable water, and natural water losses, in mountain drainage areas of Southern California, 1896 to 1946

Drainage area	Size	Average altitude	Mean seasonal precipitation	Mean seasonal recoverable water	Mean seasonal natural water losses
	sq mi	ft	in	in	in
Mojave River Basin					
Deep Creek below Green Valley Creek	15.8	6600	37.5	19.1	18.4
Crab Creek near Green Valley	3.92	6400	30.6	12.0	18.6
Deep Creek near Hesperia	137	5800	21.6	7.1	14.5
West Fork of Mojave River near Hesperia	74.8	4000	27.1	8.1	19.0
Santa Ana River Basin					
San Antonio Creek near Claremont	16.9	6700	41.8	18.9	22.9
Cucamonga Creek near Upland	10.1	5100	38.0	11.8	26.2
Day Creek near Etiwanda	4.8	5100	37.9	17.4	20.5
Lytle Creek near Fontana	47.9	5400	39.3	11.8	27.5
Lone Pine Creek near Keenbrook	15.3	4700	26.2	1.6	24.6
Cajon Creek near Keenbrook	40.9	3900	18.2	3.4	14.8
Waterman Canyon Creek near Arrowhead Springs	4.55	3600	32.9	8.8	24.1
Strawberry Creek near Arrowhead Springs	8.6	3500	32.3	8.4	23.9
City Creek near Highland	19.8	3800	34.8	7.8	27.0
Santa Ana River near Mentone	200	7000	29.3	6.5	22.8
Mill Creek near Craftonville	42.9	6600	39.4	13.4	26.0
San Jacinto River at Lake Hemet	67.3	5300	22.7	2.3	20.4
Strawberry Creek near San Jacinto	28.0	5500	29.5	5.8	23.7
North Fork San Jacinto River near San Jacinto	27.2	6100	34.1	8.8	25.3
Santa Margarita River Basin					
Temecula Creek at Nigger Canyon, near Temecula	319	3500	18.2	0.7	17.5
Murrieta Creek at Temecula	220	1700	14.9	0.8	14.1
Temecula Creek at Railroad Canyon, near Temecula	592	2700	16.9	0.7	16.2
San Luis Rey River Basin					
San Luis Rey River at Lake Henshaw, near Mesa Grande	209	....	21.9	2.6	19.3
San Dieguito River Basin					
Santa Ysabel Creek near Mesa Grande	58	3400	29.8	4.7	25.1
Whitewater River Basin					
Snow Creek near Whitewater	11.5	6200	33.3	12.2	21.1
Palm Canyon Creek near Palm Springs	94	3900	14.1	1.2	12.9

period was thus indicated to be 11,200 ac ft, giving a mean seasonal increment of 0.09 inch over the drainage area, a value very much smaller than the errors normally expected in the determination of the mean seasonal runoff. Similarly, the Santa Ana River drainage area above the gaging station near Mentone showed no difference in mountain ground-water storage as computed for the first and last months of the 50-year period. From these and similar determinations for other drainage areas, it was concluded that the mean seasonal change in storage over this particular 50-year period could be considered as negligible. No adjustment for such a change in storage was made, therefore, in determining the values for recoverable water given in Table 1.

Natural subsurface leakage from the individual drainage areas is largely unknown. It is believed that over much of the mountain area the piezometric surface of ground-water bodies is closely associated with the topographic features and that if these piezometric surfaces could be mapped, they would show considerable similarity to the contours of the land surfaces. Under these conditions the subsurface movement will be closely parallel to the surface drainage, with most of the subsurfac escape from the area confined to the debris fill at the mouth of the canyon. If, then, as is true of mos of the gaging stations in these drainage areas, the runoff from the area is measured where geologic barriers cross the channel or in narrow canyon sections in which there is little or no alluvial fill, the subsurface escape is likely to be negligible. In deriving the recoverable water, therefore, the subsurface leakage during the 50-year period was assumed to have been zero.

As shown in Table 1, the mean seasonal natural water losses in these mountain drainage areas range from 14.1 inches in Murrieta Creek to 27.5 inches in Lytle Creek.

Table 2--Seasonal precipitation, recoverable water and natural water losses in San Antonio Creek drainage area, 1921 to 1941

Season	Precipitation	Recoverable water			Natural water losses
		Runoff	Change in ground-water storage	Total	
	in	in	in	in	in
1921-1922	86.1	59.1	+4.3	63.4	22.7
1922-1923	37.6	16.3	-6.5	9.8	27.8
1923-1924	26.5	8.2	-5.1	3.1	23.4
1924-1925	28.9	6.0	-1.4	4.6	24.3
1925-1926	50.2	16.6	+5.9	22.5	27.7
1926-1927	47.7	24.6	+2.8	27.4	20.3
1927-1928	28.3	9.3	-6.8	2.5	25.8
1928-1929	32.5	8.4	-0.2	8.2	24.3
1929-1930	33.8	10.6	+3.3	13.9	19.9
1930-1931	31.9	9.5	-2.0	7.5	24.4
1931-1932	56.8	23.0	+3.8	26.8	30.0
1932-1933	27.4	9.0	-5.9	3.1	24.3
1933-1934	25.1	7.3	-2.7	4.6	20.5
1934-1935	54.9	21.4	+7.5	28.9	26.0
1935-1936	31.3	11.7	-2.9	8.8	22.5
1936-1937	64.8	34.3	+5.9	40.2	24.6
1937-1938	71.2	48.7	+3.3	52.0	19.2
1938-1939	27.3	13.0	-7.0	6.0	21.3
1939-1940	44.2	16.5	+0.4	16.9	27.3
1940-1941	78.6	43.1	+9.8	52.9	25.7

Individual seasonal natural water losses--The similar determination of seasonal natural water losses for individual years is illustrated in Table 2.

As indicated, the recoverable water represents the combination of the seasonal runoff as measured at the gaging station and the net seasonal change in ground-water storage. First in Table 2 are the data for the very wet season of 1921-1922. During this season the basin-wide precipitation was 86.1 inches, the observed runoff 59.1 inches, and the mountain ground-water storage was substantially recharged in the winter and spring months. On October 1, 1921, at the beginning of the season, the runoff from ground-water storage amounted to 13 cfs, indicating, on the basis of normal ground-water runoff recession curves, a ground-water storage over the entire drainage area of 14.1 inches. On October 1, 1922, at the end of the season, the ground-water runoff amounted to 17 cfs, indicating a storage of 18.4 inches, a net gain in ground-water storage during the season of 4.3 inches as shown in Table 2. Added to the seasonal runoff, the recoverable water is thus indicated to have been 63.4 inches, and the subtraction of the latter from the seasonal precipitation of 86.1 inches gives the natural water losses amounting to 22.7 inches.

During the season of 1922-1923 in which the precipitation and observed runoff were, respectively, 37.6 and 16.3 inches, analysis of the ground-water runoff indicated that there was a net loss in ground-water storage and that 6.5 inches of the observed runoff came from storage developed by antecedent precipitation. Therefore, crediting only 9.8 inches of recoverable water to the season's precipitation, the computed natural water losses were 27.8 inches.

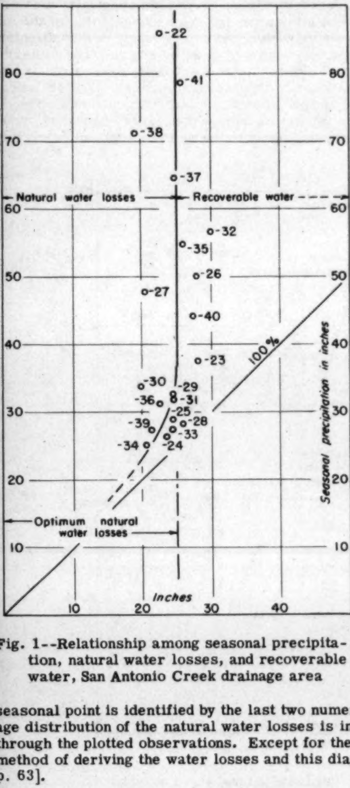

Fig. 1--Relationship among seasonal precipitation, natural water losses, and recoverable water, San Antonio Creek drainage area

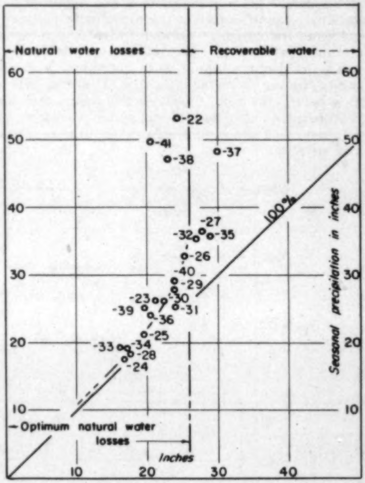

Fig. 2--Relationship among seasonal precipitation, natural water losses, and recoverable water, Strawberry Creek drainage area

In order best to indicate the relationship among seasonal precipitation, water losses, and recoverable water, the data of Table 2 were plotted (see Fig. 1) with identical vertical and horizontal scales, and the seasonal precipitation given by the vertical scale. Consequently, the straight line drawn at a 45° angle from the point of origin represents complete disposal of the seasonal precipitation. Each seasonal point is identified by the last two numerals of the year in which the season ended. The average distribution of the natural water losses is indicated by the single curve of relationship drawn through the plotted observations. Except for the adjustment for changes in ground-water storage, the method of deriving the water losses and this diagram are quite similar to those used by LEE [1941, p. 63].

From the curve of Figure 1, it may be noted that the natural water losses tend to remain fairly constant as long as the seasonal precipitation exceeds 30 to 35 inches; and that below this precipitation they gradually diminish in magnitude.

Limiting values of the water losses are shown at the upper extreme where the curve becomes asymptotic to the vertical, and at the lower extreme by the value at which there is complete disposal of the precipitation. On Figure 1 this lower limit is not well defined by the observational data, but the upper limit is represented by a seasonal water loss of about 25 inches. This limiting value may be designated as the "optimum natural water losses," the average losses experienced under conditions of maximum availability throughout the season of soil moisture derived entirely from precipi-

tation. The optimum losses as thus defined and derived differ somewhat from THORNTHWAITE'S [1944 and 1945] potential evapotranspiration; they are generally smaller.

Relation of optimum natural water losses to altitude and absorptive and retentive qualities of the drainage area--One of the principal objects of the studies from which the data of this paper have been drawn was to point out the hydrologic characteristics of the individual drainage areas and to correlate them with geologic and physiographic characteristics. Stressed particularly was a general classification of the areas with respect to the absorptive and retentive qualities of the mantl rock, as indicated by various hydrologic criteria. Of the latter, the most consistent classification a to most, moderately, and least absorptive and retentive areas was given by analysis and compariso of (1) the distribution of daily and monthly discharge, (2) accumulated precipitation and runoff from the beginning of the season, and (3) storm precipitation-flood runoff relationships. With these crite as a basis, the San Antonio Creek drainage area is classified as most absorptive and retentive; and it is believed that the natural water losses as given in Table 2 may be considered typical of mountain drainage areas of Southern California of like physiographic features and comparable precipitati and altitude.

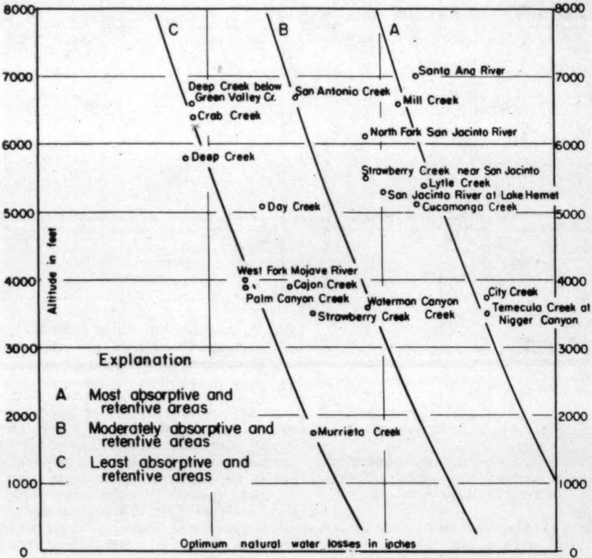

Fig. 3--Relationship between the optimum natural water losses and altitude in mountain areas of Southern California

The Strawberry Creek drainage area fell in the classification of moderately absorptive and retentive, with precipitation somewhat less than in the San Antonio Creek area (see Table 3). This

stream drains a steep frontal mountain area of 8.6 sq mi above the gaging station near Arrowhead Springs. The average altitude is 3500 ft and the 50-year mean seasonal precipitation is 32.3 inches. In the 20-year period presented in Table 3, the seasonal precipitation ranged from 17.5 to 53.3 inches, and the seasonal natural water losses are indicated to have ranged from 16.2 to 30.0 inches.

Table 3--Seasonal precipitation, recoverable water, and natural water losses in Strawberry Creek drainage area, 1921 to 1941

Season	Precipitation	Recoverable water			Natural water losses
		Runoff	Change in ground-water storage	Total	
	in	in	in	in	in
1921-1922	53.3	24.0	+4.9	28.9	24.4
1922-1923	26.2	8.0	-3.0	5.0	21.2
1923-1924	17.5	3.5	-2.8	0.7	16.8
1924-1925	21.3	3.1	-1.5	1.6	19.7
1925-1926	32.8	5.5	+2.1	7.6	25.2
1926-1927	36.4	8.1	+0.6	8.7	27.7
1927-1928	18.2	2.9	-2.4	0.5	17.7
1928-1929	27.8	3.6	+0.3	3.9	23.9
1929-1930	26.4	4.0	0	4.0	22.4
1930-1931	25.3	2.4	-1.2	1.2	24.1
1931-1932	35.3	6.8	+1.5	8.3	27.0
1932-1933	19.3	2.8	+0.3	3.1	16.2
1933-1934	19.1	3.0	-1.2	1.8	17.3
1934-1935	35.8	5.5	+1.5	7.0	28.8
1935-1936	24.1	4.5	-0.7	3.8	20.3
1936-1937	48.3	15.4	+2.9	18.3	30.0
1937-1938	47.1	22.3	+1.8	24.1	23.0
1938-1939	25.1	8.6	-3.1	5.5	19.6
1939-1940	29.2	7.1	-1.8	5.3	23.9
1940-1941	49.7	21.8	+7.3	29.1	20.6

In Figure 2, the curve indicates that the optimum natural water losses in the Strawberry Creek drainage area amount to about 26 inches; that they tend to remain fairly constant as long as the seasonal precipitation exceeds 30 to 35 inches; and that for a seasonal precipitation of 20 inches the loss is about 18 inches and represents 90 per cent of the season's precipitation.

Values of the optimum natural water losses as similarly determined for 19 mountain drainage areas of Southern California have been plotted on Figure 3 to indicate the relationship between these losses and altitude. The observations show considerable scattering, with the losses varying as much as 13 inches or more for the same altitude. However, when analyzed with respect to absorptive and retentive qualities of the drainage areas, the spread shown by the plotted data largely indicates the effects of these watershed characteristics. The greatest losses are shown for the most absorptive and retentive areas such as Mill, Lytle, and Temecula Creeks and Santa Ana River; and the smallest losses are shown by the least absorptive and retentive areas such as the Mojave River basin streams and Palm Canyon and Murrieta Creeks.

This correlation has been indicated on Figure 3 by three curves representing the most, moderately, and least absorptive and retentive areas. As also shown by these curves, the optimum natural water losses tend to decrease with increase in altitude. In the least absorptive and retentive areas they decrease from about 29 inches at sea level to 18 inches at an altitude of 7000 ft; and this same decrease of about 11 inches in indicated by the moderately and most absorptive and retentive drainage areas.

References

BARNES, BERTRAM S., Discussion of rainfall-runoff prediction, Trans. Am. Soc. Civ. Eng., v. 107, p. 838, 1942.

KITTREDGE, JOSEPH, JR., The magnitude and regional distribution of water losses influenced by vegetation, J. Forest., v. 36, p. 776, 1938.

LEE, CHARLES H., Total evaporation for Sierra Nevada watersheds by the method of precipitation and runoff differences, Trans. Amer. Geophys. Union, pt. 1, pp. 50-66, 1941.

THORNTHWAITE, C. W., in Report of Committee on Transpiration and Evaporation, Trans. Amer. Geophys. Union, pt. 5, pp. 686-693, 1944; v. 26, no. 3, pp. 451-455, 1945.

WILLIAMS, G. R., and Others, Natural water losses in selected drainage basins, U. S. Geol. Surv., Water-Supply Paper 846, 1940.

U. S. Geological Survey,
Los Angeles, California

(Manuscript received March 1, 1949; presented at the Twenty-Third Regional Meeting, Los Angeles, California, February 5, 1949; open for formal discussion until March 1, 1950.)

Transactions, American Geophysical Union   Volume 30, Number 5   October 1949

PRELIMINARY STUDIES ON SOIL PERMEABILITY AND ITS APPLICATION

Leonard Schiff and F. R. Dreibelbis

Abstract--The procedure of a preliminary study on soil permeability is described. Water was applied to soil cores at their initial field soil moisture content in such a way as to simulate natural conditions. Data are presented showing variation of transmission rates and percolation rates with initial field soil moisture content for the topsoil and subsoil of Muskingum silt loam and Keene silt loam. Some comparisons were made with transmission rates and percolation rates obtained by hydrograph analysis and soil moisture changes of small watersheds under natural conditions. The data indicate considerable replication appears necessary to obtain average representative values by the core method. Even when sufficient replication establishes significant values, core data must be applied with caution and preferably in the light of watershed performance. Potential infiltration rate curves are established based on transmission rates and soil moisture changes. The use of such curves for estimating surface supplies to runoff is indicated.

Introduction--A knowledge of soil permeability is essential in evaluating hydrologic characteristics of soil. This paper presents preliminary data on laboratory determinations of soil permeability primarily as a measure of rates of soil-water movement. Most permeability studies have been concerned with percolation rates of soil-water movement after saturation as a hydrologic basis for classifying soils. This study considers transmission rates as well as percolation rates obtained for soils at different initial soil moisture contents. A few relationships between results obtained in the laboratory and on watersheds under natural conditions are indicated. Such a study should be valuable in studies of runoff, flood control, and other hydrologic phenomena as a basis for evaluating the hydrologic performance of watersheds. A rapid method that gives a reasonably close approximation of actual field performance would be very useful where expensive measuring installations are not practical and where there is immediate need for information on permeability.

Experimental procedure--Soil cores were obtained by a special sampler in which a cylindrical aluminum tube three inches long and three inches in diameter was used as a means of holding the core. A jack sampler was used to minimize structural disturbances in the sampling of the core. In the laboratory the cores were weighed and set on a ring stand supporting a 100 cc burette. The core was supported by a wire screen covered with cheese cloth. A 100 cc graduate cylinder supporting a ten cm diameter funnel was used to collect the percolate beneath the core. The procedure was designed to simulate, as nearly as possible, natural conditions. Water was added from a burette, in drop form close to the surface to minimize soil disturbance. A small constant head was maintained, sufficient to cover the core. A stop watch was used to obtain the time it took for the water to move through the core. From the time required, the linear velocity of the water was determined and referred to as a transmission rate. The application of water was continued and simultaneous readings were made of both the burette and graduate cylinder at periodic intervals. The percolation rate was considered to be the rate of application of water when the volume of percolate equalled the volume of water applied to the surface over a given period of time. This occurred when the soil was at or near saturation. The degree of saturation was determined by the extent to which the pore space was filled.

With sampling tubes of known volume the determinations of volume weight, total pore space, field soil moisture, and maximum saturation values were obtained. In the data obtained from the first samples it was found that water, at times, ran along the inner wall of the tube rather than through the core. To overcome this objection, the inner walls of the tubes were lined with a thin coating of vaseline.

Some methods in use do not seem to simulate natural conditions because cores are frequently saturated for some time prior to the determination of percolation rates, and heads are maintained. Even the manner of saturating cores is different from that which occurs in nature. A saturated condition in the field is the exception rather than the rule. Insofar as results are concerned, comparisons with other methods could be made in the saturated range for percolation rates.

An example will help to clarify the terms used. Assume that the average rate of infiltration for a period of time is four inches per hour and at the start of this period there is 0.20 inch of unfilled pore space in the top inch of soil. An infiltration rate of four inches per hour would supply 0.20 inch of water within the soil in three minutes. Water would have had to move at least one inch, the depth of soil with 0.20 inch of pore space, in three minutes. This is equivalent to a linear veloci or transmission rate of at least 20 in/hr. The transmission rate multiplied by the pore space per in of soil through which water moves is equal to the percolation rate. The percolation rate at a given level within the soil is equal to the infiltration rate if the soil is saturated above that level. Prior to saturation the percolation rate is equal to the infiltration rate minus the rate of exhaustion of pore space above the level considered.

The transmission and percolation rates of individual cores vary considerably due to a number of factors. The most important of these factors are soil heterogeneity, influence of plant roots and residues, worm holes and other biological channels, particle size and parent material fragments, pore space and its continuity, stability of the soil structure, and entrapped air.

Infiltration and percolation rates are functions of the space through which water may move downward and the velocity or transmission rate of water through this space. This space consists of natural structural cleavage lines as well as biological channels including old root channels, worm holes, and the like. Upon swelling of the soil colloids these openings between structural aggregates become smaller.

The wide variation of percolation rates even for the same soil type has been mentioned by numerous investigators. In spite of precautions to eliminate samples having cracks or leaks, considerabl replication is necessary to obtain representative values. During the course of this investigation it wa observed that permeability rates seemed to vary with initial soil moisture content. Consequently, all data have been plotted showing variation of such rates with initial field soil moisture content.

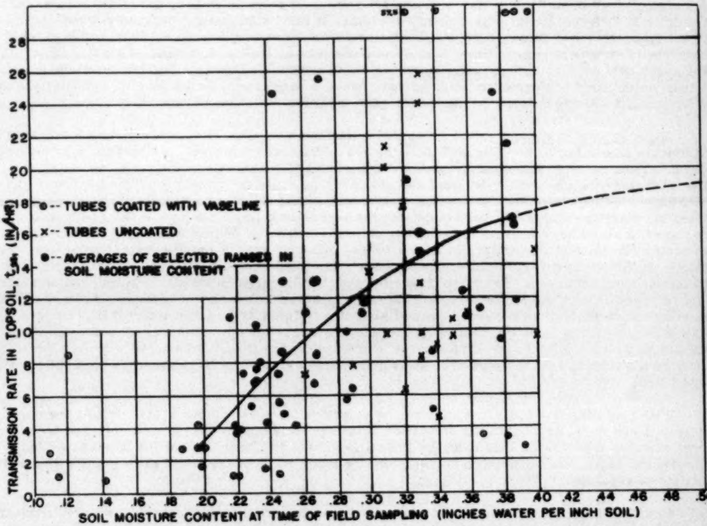

Fig. 1--Transmission rates of topsoil (0 - 7") of Keene silt loam from Watershed 123

Transmission rates obtained from core samples of the topsoil of Keene silt loam are shown in Figure 1. The transmission rate curve was fitted among points representing averages of selected ranges in initial field soil moisture content. The points from which averages were obtained show a wide scatter for each selected 0.02-inch range in soil moisture content. A considerable number of replicates are necessary in any soil moisture range to establish an average point reasonably near the true transmission rate. The location of the portion of the transmission rate curve above a soil moisture content of 0.39 inch of water per inch of soul was based on the shape of the pore size distribution curve for Keene silt loam topsoil, [SCHIFF and DREIBELBIS, 1949a]. For wetter conditions it is difficult to bring a core in from the field without appreciable change from its initial soil moisture content.

Percolation rates obtained for the subsoil of Keene silt loam are shown in Figure 2. The curve was established in a manner similar to that for the transmission rate curve. The portion of the curve beyond a soil moisture content of 0.39 inch of water per inch of soil was drawn down to a value of 0.04 in/hr. This value is the minimum constant infiltration rate that has been found by hydrograph analysis for the subsoil of Keene silt loam, [SCHIFF and DREIBELBIS, 1949a and b]. Other values obtained by hydrograph analysis are also shown in Figure 2.

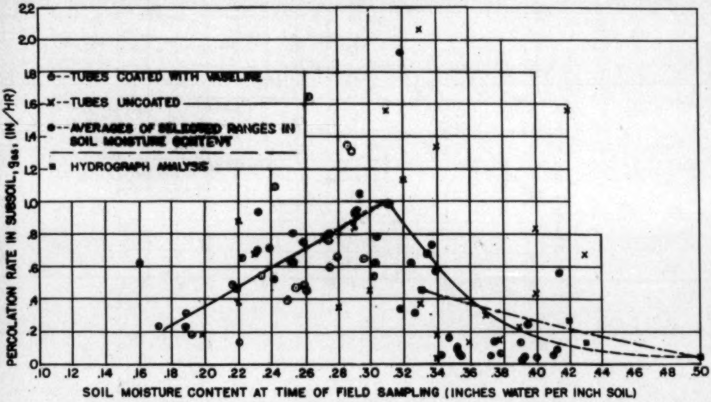

Fig. 2--Percolation rates for subsoil (7 - 14") of Keene silt loam from Watershed 123

Transmission rate curves and percolation rate curves for the topsoil and subsoil of Muskingum silt loam and Keene silt loam are shown in Figure 3. They were established using the procedure mentioned above. Extensions of the various curves are shown by dashed lines as indicated in Figures 1 and 2.

Based on the scatter of points there is no complete justification for drawing the curves in the manner shown in Figures 1, 2, and 3. However, they were drawn in this fashion as the usual field procedure is to take the average of several samples. The major movement of water downward is through the non-capillary pores, particularly after field capacity is reached. Field capacity is approximately 0.30 inch of water per inch of soil for the topsoil and subsoil of Muskingum silt loam and the topsoil of Keene silt loam, and 0.36 for the subsoil of Keene silt loam. With soil moisture above field capacity, transmission- and percolation-rate curves may approximate straight lines, with or without slope. Such lines would probably reach a minimum when swelling is complete. Additional information is needed to establish the curves more definitely. The shape of the infiltration curve or percolation-rate curve at any horizon would then be more nearly a combined function of the exhaustion of pore space and an approximately constant transmission rate. The horizontal dashed lines shown in Figure 3 at transmission rates of 6.7 and 5.0 in/hr were obtained by taking the average of points, excluding a few exceptionally high values, between field capacity and 0.40 inch of water per inch of subsoil for Muskingum silt loam and Keene silt loam, respectively.

The shapes of the curves as drawn in Figure 3 are of considerable interest. With the exception of the transmission-rate curves for the topsoils, the highest average transmission and percolation rates were obtained when core samples were taken at a field moisture content in the vicinity of field capacity. Capillary suction, the high volume of pore space, and the tendency for air to escape more readily when soil is relatively dry at the time of water application, are factors which may influence the shape of the rate curves when samples were taken below field capacity. Above field capacity the swelling effect of soil colloids, and the greater difficulty in removing entrapped air may be important factors in decreasing rates.

In this study the major effort was directed in the attempt to establish a method of determining soil permeability and to compare the results on two soil types of distinctly different hydrologic characteristics. Some data have also been obtained to make a land use comparison involving watersheds in woodland, meadow, wheat, and corn. Because of the replication necessary sufficient data have not yet been obtained. Preliminary data indicate much more rapid rates on woodland soils. Transmission rates in the vicinity of 40 in/hr have been obtained in the top horizon of woodland soils

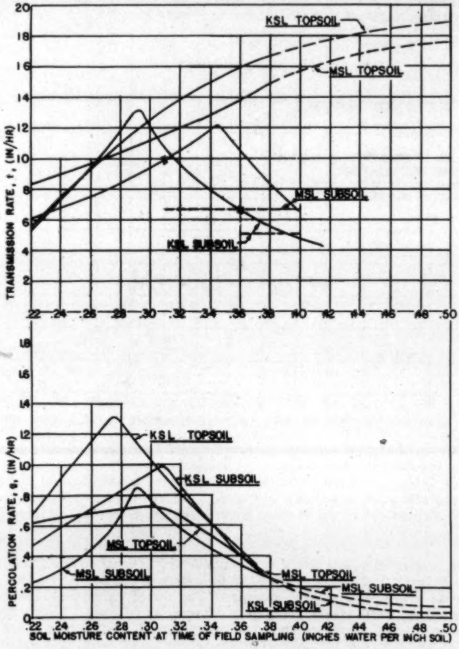

Fig. 3--(A) Transmission and (B) percolation rates for topsoil and subsoil of Keene silt loam (KSL) and Muskingum silt loam (MSL)

Transmission rates and percolation rates for Muskingum silt loam and Keene silt loam have been obtained from soil moisture changes and hydrograph analysis of the field performance of small watersheds, [SCHIFF and DREIBELBIS, 1949a and b]. Although small watersheds in a four-year rotation of corn, wheat, and two years of meadow were used, results from only the wheat and meadow will be considered. Sealing of the soil surface occurs in corn watersheds and further study is neede for such conditions.

For the present, results obtained from core samples and analyses of field performance will be compared only in a general way. Transmission rates shown in Figure 3 for the topsoil of Muskingum silt loam and Keene silt loam are approximately 14 in/hr at field capacity and 18 in/hr at saturation. Analyses of field performance indicate a transmission rate of about 20 in/hr for the topsoil of both Muskingum silt loam and Keene silt loam for a wide soil moisture range from below field capacity to saturation. Figure 3 also indicates transmission rate values as low as six in/hr for an initial field moisture content of 0.22 inch of water per inch of soil. Under such conditions runoff would occur at rainfall intensities of less than two in/hr. Actually, under such conditions, soil will absorb a rainfall intensity of about 5.6 in/hr; at 5.6 in/hr the transmission rate would be about 20 rather than six in/hr. As shown in Figure 3, in the range from field capacity to 0.40 inch of water per inch of soil, the average transmission rate in the subsoil of Muskingum silt loam is 6.7 in/hr and for Keene silt loam 5.0 in/hr. Field performance indicates values less than these. However, only a few storms on natural watersheds during the period studied to date provide sufficient water for the subsoil to perform at capacity rates. Further study of subsoil performance is needed. Percolation rates obtained by analyses of the field performance of the subsoils indicate consistently low values of 0.08 in/hr for Muskingum silt loam in the vicinity of saturation and 0.04 in/hr for Keene silt loam. A number of cores indicate values of this magnitude, although not as consistently, as may be seen in Figure 2 for Keene silt loam. In Figure 2 for the initial soil moisture range between 0.33 and 0.42 inch of water per inch of soil for Keene silt loam, the average percolation rates obtained by cores decreased from 0.73 to 0.11 in/hr compared to a decrease of from 0.46 to 0.21 in/hr by hydrograph analysis. Differences between results obtained by soil cores and analysis of watershed performance present important considerations and a challenge to experimental procedure. Cores introduce such errors as disturbance of soil structure during sampling, particularly on heavy soils; water may move between the soil and tube; the soil has more freedom to expand in the tube under the influence of swelling colloids; and air may escape from the bottom of the core.

Relationships between the available storage space at any time, the transmission rate, and the infiltration rate were indicated in previous work [SCHIFF and DREIBELBIS, 1949a and b]. The shape of the infiltration curve also indicates the operation of laws within the soil profile. The percolation rate at any time at any plane within the soil is the infiltration rate minus the storage space depletion rate above this plane. When the soil is saturated above this plane and the storage space depletion rate is zero, the infiltration rate is equal to the percolation rate. This indicates relationships that may be established between the percolation rate and infiltration rate. However, in the remainder of this paper the application of this type of information will be limited to the use of transmission rates and infiltration rates.

Application--The method of application is a working tool which has been developed in detail [SCHIFF, in preparation]. Briefly, a part of this method is discussed in the following to illustrate the application of permeability data. The relationships between infiltration rates and transmission rates were based on the volume of unfilled pore space or available storage space at any time. The difference between the soil moisture content at any time and saturated value of the soil was taken to be the available storage space yet to be exhausted. Actually, the soils studied herein approach, although do not reach, saturation under capacity infiltration rates and the downward movement of the wet front. Saturation is reached somewhat after water reaches the subsoil control horizon or bottleneck. The available storage space for various soil moisture contents is shown in Table 1.

Table 1 also shows the constant transmission rates or velocities used for the topsoil and subsoil of Muskingum silt loam and Keene silt loam. The potential infiltration rate that can exist for any given soil moisture content or available storage space is also shown in Table 1, for the soil moisture range from field capacity to saturation; it is obtained by multiplying the storage space per inch of soil by the transmission rate. Plotting potential infiltration rates against soil moisture results in straight lines of different slope, one for the topsoil, one while storage space is being exhausted in the topsoil as water moves through the subsoil, and one for the subsoil after the topsoil is saturated, as shown by the straight dashed lines in Figure 4. The high transmission rates in the topsoil permit rapid use of the storage space in the topsoil. Runoff is generally low while storage space remains in the topsoil. However, as moisture content increases, infiltration rates drop rapidly even though gravitational water has not reached the subsoil. This is shown by the straight line section marked MSL and KSL topsoil. The pores seem to "clog" with water containing variable amounts of soil colloids, the greater the colloidal content the greater the restriction. This clogging seems to reduce the effective cross-sectional area through which water flows downward, although transmission rates or velocities may remain approximately uniform and fairly high. Diminishing effective areas of cross-section multiplied by the fairly-constant velocity of flow result in diminishing rates of flow through the soil and consequently diminishing infiltration rates.

After water begins to move slowly into a subsoil of lower transmission rates, the remaining storage space fills in the topsoil and the topsoil approaches saturation. The lower rates of exhaustion of this remaining, and generally small volume of storage space in the topsoil, and lower transmission rates in the subsoil usually are reflected by the section of greatest curvature in the infil-

Table 1--Potential infiltration rates for various transmission rates, soil moisture contents, and available storage space

Soil moisture content per inch of soil	Available storage space per inch of soil	Potential infiltration rates for transmission rates of		
		5.0 in/hr KSL[a] subsoil	6.7 in/hr MSL[b] subsoil	20 in/hr KSL and MSL topsoil
in	in	in/hr	in/hr	in/hr
0.30	0.20	1.00	1.34	4.00
0.31	0.19	0.95	1.27	3.80
0.32	0.18	0.90	1.21	3.60
0.33	0.17	0.85	1.14	3.40
0.34	0.16	0.80	1.07	3.20
0.35	0.15	0.75	1.00	3.00
0.36	0.14	0.70	0.94	2.80
0.37	0.13	0.65	0.87	2.60
0.38	0.12	0.60	0.80	2.40
0.39	0.11	0.55	0.74	2.20
0.40	0.10	0.50	0.67	2.00
0.41	0.09	0.45	0.60	1.80
0.42	0.08	0.40	0.54	1.60
0.43	0.07	0.35	0.47	1.40
0.44	0.06	0.30	0.40	1.20
0.45	0.05	0.25	0.33	1.00
0.46	0.04	0.20	0.27	0.80
0.47	0.03	0.15	0.20	0.60
0.48	0.02	0.10	0.13	0.40
0.49	0.01	0.05	0.07	0.20

[a] Keene silt loam
[b] Muskingum silt loam

tration capacity-rate curve when plotted against time. In Figure 4 the section where water is depleting storage space in the topsoil and subsoil is represented by the straight dashed line marked MSL topsoil-subsoil and KSL topsoil-subsoil. Values for this section were obtained from the subsoil columns of Table 1. The infiltration curve, after the topsoil is saturated, is mainly a function of water movement rates in the subsoil. The infiltration rate is further reduced as storage space is exhausted in the subsoil and probably approaches a minimum as the swelling of colloids becomes complete. This section for each soil is represented by the straight dashed line marked MSL subsoil, and KSL subsoil.

Each section would not be a straight line if transmission rates varied with progressive changes in soil moisture. However, transmission rates could be constant for a given horizon and storage space exhausted in such a fashion as to result in the curvature of various sections of the infiltration rate curve. Further investigation is needed in this respect. Potential infiltration rate curves of smooth curvature marked MSL adjusted and KSL adjusted, were also drawn in Figure 4 as guided by the series of straight lines. The positions of these curves were governed mostly by the positions of the topsoil and subsoil lines as these were more definitely defined by the field and laboratory data.

It is to be noted that for either the topsoil(0 - 7") or subsoil(7 - 14") each unit on the horizontal scale in Figure 4 represents an increment of 0.02 inch of water per inch of soil. For the section of this scale where exhaustion of the remaining storage space takes place in the topsoil as water is moving into the subsoil, each horizontal unit represents a gain of 0.01 inch of water per inch of soil in the topsoil and 0.01 gain in the subsoil, or 0.02 in total. For this section of overlap the division of the total gain would be more accurate if based on the ratio of the storage space depletion rate of the topsoil to the subsoil. Such refinetment may not be necessary for many practical solutions.

Differences in transmission rates do not appear great between the subsoils of Muskingum silt loam and Keene silt loam. However, the differences that do exist as well as the greater swelling of colloids in the subsoil of Keene silt loam, seem to cause considerable differences in hydrologic per-

formance. This is evidenced by the higher moisture content of Keene silt loam antecedent to a storm, a major reason for greater runoff from Keene silt loam.

Potential infiltration curves may be made up similarly for a number of important combinations of antecedent topsoil and subsoil moisture contents. It is to be noted that such infiltration curves are functions of soil moisture, and not of time when capacity rates exist under an adequate supply of water. Such curves may be used when the antecedent soil moisture content is known. Two methods called T_1 and T_2 have been developed to apply these infiltration curves, [SCHIFF, in preparation]. Method T_1 is more rapid but not as accurate as Method T_2. Method T_1 assumes that all of the ground rainfall enters the soil, is uniformly distributed in the topsoil until the moisture content of the topsoil is 0.46 inch, is then equally divided between the topsoil and subsoil until the topsoil is saturated, and is then uniformly distributed in the subsoil. When the subsoil becomes saturated the minimum infiltration rate occurs. Potential infiltration rate points for corresponding soil moisture gains based on the amounts of ground rainfall are plotted on graphs showing intensities of ground rainfall against time. These points establish the potential infiltration-rate curve. Intensities of ground rainfall in excess of this curve yield water-supply increments available for surface runoff. Method T_2 accounts for the water entering the soil, by subtracting the total increments of estimated surface runoff at any given time from the accumulated ground rainfall up to the same time. Also, the distribution of water within the topsoil and subsoil is based on the ratio of the storage space

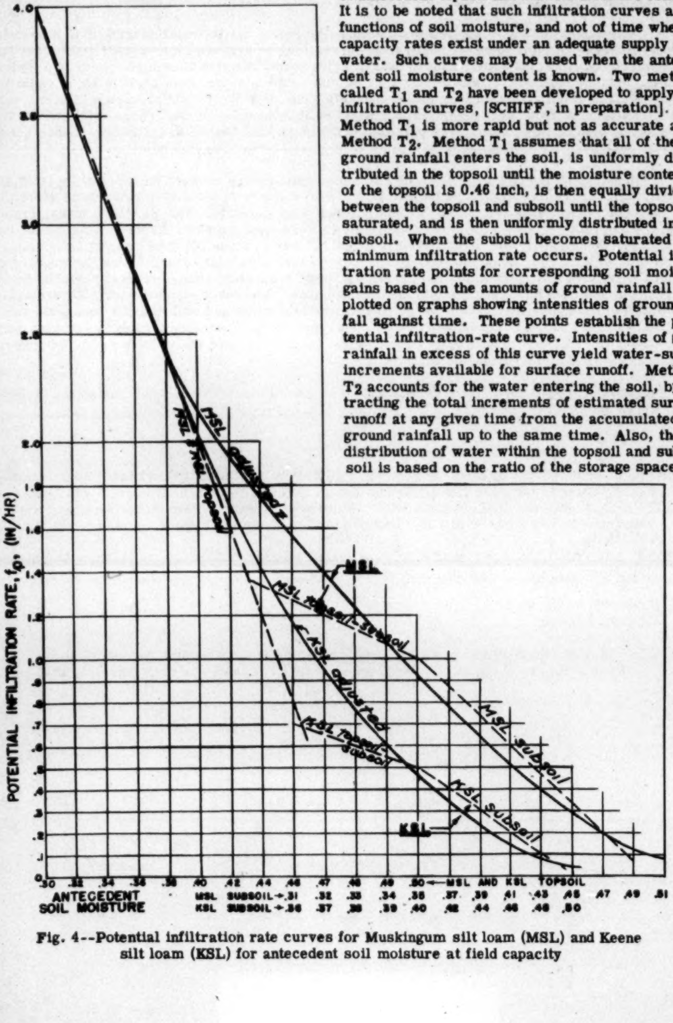

Fig. 4--Potential infiltration rate curves for Muskingum silt loam (MSL) and Keene silt loam (KSL) for antecedent soil moisture at field capacity

depletion rate of the topsoil to the subsoil. If there are long periods during a storm in which no rain falls there will be a decrease in the soil moisture content which may be estimated from percolation rates. Storage space and the potential infiltration rate are thus increased. When rain begins to fall again the infiltration rate will be based on the actual storage space at the time and will show the recovery that seems somewhat difficult to establish at the present.

These methods may be applied to an anticipated storm, a particular storm, or to a specific storm pattern. In fact, potential infiltration curves may be prepared for various antecedent soil moisture conditions and superimposed over various storm patterns that might occur in a given locality. Surface supplies for runoff may thus be estimated in advance for a given set of conditions. Total surface runoff may be estimated reasonably well. For hydrologic problems involving appreciable subsurface flow, such contributions must be accounted for as part of the total stream flow. The actual rate of flow at any given point in the drainage basin would be a function of the excess rainfall on each field and the physical watershed characteristics above this point.

Summary and conclusions--Data on soil permeability were obtained on two soil types of distinctly different hydrologic characteristics. Transmission and percolation rates were determined by the core method at different initial field soil moisture contents. The maximum transmission rates, except for the topsoil, and percolation rates were obtained when the soil was at or near field capacity. These results were compared in a general way to those obtained by hydrograph analysis of natural watersheds. Data obtained by the core method apparently are variable and require considerable replication. Such information can be more accurately applied to field performance in the light of its relationship to results obtained from natural watersheds whenever such data are available. Potential infiltration-rate curves, based on transmission rates and soil moisture changes, can be used to estimate surface supplies to runoff. However, this is not the only objective of such studies. Such an approach leads to knowledge of soil-water movements and the influence of soil properties and land use, a major hydrologic objective.

Acknowledgment--Grateful acknowledgment is made to R. E. Youker for assistance in obtaining soil cores and making laboratory determinations of transmission and percolation rates.

References

SCHIFF, LEONARD, and DREIBELBIS, F. R., Infiltration, soil moisture and land-use relationships with reference to surface runoff, Trans. Amer. Geophys. Union, v. 30, pp. 75-88, 1949a.
SCHIFF, LEONARD, and DREIBELBIS, F. R., Movement of water within the soil and surface runoff with reference to land use and soil properties, Trans. Amer. Geophys. Union, v. 30, pp. 401-411, 1949b.
SCHIFF, LEONARD, Surface runoff supply estimates based on soil-water movements and precipitation patterns, SCS-Tech. Pub., in preparation.

Soil Conservation Service,
Coshocton, Ohio

(Manuscript received April 25, 1949; presented at the Thirtieth Annual Meeting, Washington, D. C., April 21, 1949; open for formal discussion until March 1, 1950.)

Transactions, American Geophysical Union Volume 30, Number 5 October 1949

STUDIES OF CLEAVAGE IN THE METASEDIMENTARY ROCKS OF THE NORTHWEST ADIRONDACK MOUNTAINS, NEW YORK

A. E. J. Engel

(Published by permission of the Director, U. S. Geological Survey)

Abstract--The pre-Cambrian gneisses, schists, and marbles of the Grenville series, in the northwest Adirondack Mountains, have been complexly sheared and in part refoliated during metamorphism. The principal directions of shear that may be inferred from inspection of foliations and associated lineations are (1) northeast-southwest (couple near horizontal) and (2) southeast-northwest (vertical couple). These directions are roughly subparallel respectively to the directions of gross lithologic trend and average dips.

The lithologic trend and average dips are patterns imparted by the metasedimentary formations and rudely accordant orthogneisses. Some large-scale shear at appreciable angles to the lithologic patterns appears in features of thick, mobile units such as marble, and in relatively brittle gneissic units which have ruptured and floated apart, as well as where large, discordant intrusives, or basement nodes seem to have obstructed or complicated the evolving, conventional pattern.

If, instead of the gross process or patterns of shear, the details of the shear patterns are studied, the rock motions as reflected by foliations and lineations are more complex and commonly along surfaces at variance with individual beds. Thus, secondary foliations (cleavages) evolve only in part along or subparallel to bedding, and in considerable part across and at the expense of beds. Examples are discussed in which either key layers or folds appear in the rocks and seem to be directly associated with the shearing movements. These examples are used on the assumption that the form of the folds or the key layer contributes valuable data on the stage or degree of shear involved.

The many other exposures of subparallel rock surfaces, in which no fold or key layer is apparent, are believed to have a common origin with, and fit within the limits of, types described. All prominent foliations of metamorphic origin (cleavages) are inferred to have evolved during successive, closely related stages of what was clearly a triaxial-type deformation.

Introduction--The northwest Adirondack Mountains furnish an excellent example of an area of variously deformed and chemically modified sedimentary rocks in which sets of foliation surfaces of diverse origin are well developed and well exposed. In large part because these rocks have been studied extensively by numerous geologists with quite different backgrounds, considerable divergence exists, both in published descriptions and in opinions of origin of these foliations. A necessarily brief and accordingly generalized attempt at evaluation of the form, relations, and origin of some of these surfaces is presented.

General geology of the region--In the northwest Adirondack Mountains a great sequence of pre-Cambrian metasedimentary rocks, now referred to the Grenville series [VAN HISE, 1892], has been mashed and shortened from the southeast and northwest into an elongate belt rudely wedge-shaped in cross-section (see Fig. 1). The deformed metasedimentary rocks are bounded on the southeast by a large complex of anorthosites, gabbros, syenites, and granites which forms the prominent Andirondack Upland [BUDDINGTON, 1939]. The northwest flank of this dominantly igneous complex is plated with folded sheets and more irregularly shaped masses of syenite and granite which are inferred to form a shelf of irregular relief dipping at moderate angles to the northwest under the metasedimentary belt [BUDDINGTON, 1939, pp. 238-243, Figure 25].

The opposite (northwest) side of the metasedimentary belt seems to be bounded by a somewhat complementary shelf of intrusive granitic rocks of the Frontenac axis. This shelf and the foliation in the granitic rocks dip, in general, steeply southeastward.

Within the belt of metasedimentary rocks thus outlined, herein called the Grenville Belt, are many bodies of gabbro, syenite, and granite, presumably satelitic to the larger igneous complex of the Adirondack Upland. These three rock types comprise about one-fourth of the surface area of

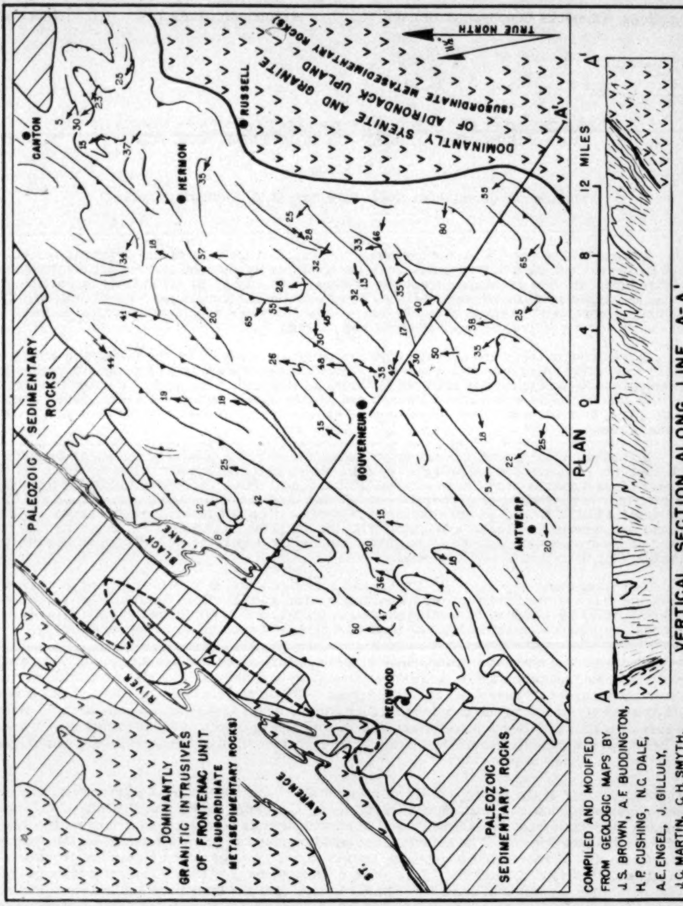
PALEOZOIC SEDIMENTARY ROCKS
CANTON
HERMON
RUSSELL
DOMINANTLY SYENITE AND GRANITE OF ADIRONDACK UPLAND (SUBORDINATE METASEDIMENTARY ROCKS)
TRUE NORTH
GOUVERNEUR
ANTWERP
REDWOOD
BLACK LAKE
RIVER
LAWRENCE
DOMINANTLY GRANITIC INTRUSIVES OF FRONTENAC UNIT (SUBORDINATE METASEDIMENTARY ROCKS)
PALEOZOIC SEDIMENTARY ROCKS
A
A'
PLAN
0 4 8 12 MILES
VERTICAL SECTION ALONG LINE A-A'
COMPILED AND MODIFIED FROM GEOLOGIC MAPS BY J.S. BROWN, A.F. BUDDINGTON, H.P. CUSHING, N.C. DALE, A.E. ENGEL, J. GILLULY, J.C. MARTIN, C.H. SMYTH.

Fig. 1--Map and vertical section of some prominent structural features in the northwest Adirondack Mountains, N. Y.; the broad central area which is devoid of pattern and outlined by heavy lines, is composed largely of metasedimentary rocks of the Grenville series; the strike and dip symbols within this area indicate the general northeast trend and direction of dip of lithologic units and dominant foliations in the Grenville series; the lines also tend to indicate the orientation of the axes of major northeast-trending folds in the Grenville series; the hook- and S-shaped curvatures in the trend lines southeast of Canton and Gouverneur, indicate a general southeasterly zone of cross folds within the rocks of the Grenville series; the direction and amount of plunge of large folds throughout the rocks of the Grenville series are indicated by the arrows with plunge values the belt of metasedimentary rocks. The enclosing metasedimentary rocks of the Grenville series form the remaining three-fourths of the area. This exposed segment of the Grenville series is composed largely of thick zones of (1) marble, (2) migmatitic quartz-biotite-feldspar gneisses in part garnetiferous, (3) pyritic, graphitic, and sillimanitic schists, and (4) biotitic, feldspathic, and micacious quartzites. These rocks represent what was formerly a group of carbonate, clastic, and perhaps pyroclastic sediments.

The emplacement of the igneous-like rocks in part preceded and in part coincided with the more severe regional deformation of the sediments. The oldest intrusives are gabbroic rocks which, with the sediments, were subsequently intruded by syenites, prior to significant deformation. At a later time, during stages of profound folding and flowage of these solidified igneous-like rocks and enclosing metasedimentary rocks, granitic magmas, and what definitely seem to be fluids derived apparently from these magmas, permeated most of the sediments, adding to and complementing changes effected by the synchronous dynamic metamorphism. Bodies of granite were emplaced, and the accompanying contact-metamorphic effects were compounded with the dynamic metamorphism and migmatization. Feldspathization, tourmalinization, scapolitization, and magnesia metasomatism were common processes in reconstitution of many layers in the marble as well as in the clastic sediments.

Throughout the Grenville belt the metasedimentary rocks have a prevailing northeast trend (see Fig. 1). Along the southeast margin of the belt, dips are commonly northwest at moderate angles. Average dips steepen and pass through the vertical as the metasedimentary belt is crossed from southeast to northwest, and most layers on the northwest side of the belt dip steeply southeast. The prevailing northeast trend and fanlike pattern of dips are in large part reflections of the orientation of many large folds within the belt. These folds clearly have major segments that trend northeast. In general, their axes plunge gently northeast or southwest and their axial planes tend to converge downward in accordance with the downward convergence of dips of the rock layers, which form the flanks of the folds (see Fig. 1).

Along the southeast side of the belt, and to a somewhat comparable degree along its northwest side, major deviations appear in the regional northeast surface trends of rock units. Thus, in the southeasterly zone, southeast of the villages of Canton, Gouverneur, and Antwerp, expecially marked hooklike and S-shaped curves complicate the regional trends [see especially MARTIN, 1916, the quadrangle map]. Many of these hook and S-shaped flexures are surficial reflections of folds which, at the surface, trend athwart the regional trend. The axes of these folds plunge north to northwest at angles approaching or conforming to the northwest dip of the rock layers. As these crossfolds are carefully traced out, some are found to merge abruptly into the gently plunging folds which define the regional northeast trends. Thus the axes of many northeast-trending folds appear, as the sites of cross folds are approached, to be sharply inverted through 90° or more by solid rock flow. Although the most pronounced development of fold axes that plunge approximately northwest occurs along the southeast and apparently the northwest sides of the belt, some segments of folds plunging at intermediate angles between the regional trend and the dip occur within the central part of the belt. In general, however, the southeast zone containing cross or inverted folds passes abruptly to the northwest into a more central zone of the metasedimentary belt, in which most folds plunge at angles less than 30° to the northeast or southwest; and many folds in the central zone plunge at angles of only 5° to 20°, in conformity with the trend of the rock layering.

Earlier studies of foliation--In the numerous earlier geological studies that have been made of the rocks of the Grenville series within the belt described above, it commonly has been noted or implied that much of the layering within the paragneisses, schists, and marble represents bedding. The most prominent surfaces of cleavage which commonly involve strong dimensional parallelism of constituent minerals are widely described as "closely parallel to the bedding," [CUSHING, 1916, p. 22] or "everywhere parallel to the bedding" [BUDDINGTON, 1929, p. 81; CUSHING and NEWLAND, 1925, p. 52]. The region has long been cited as a classic example of the occurrence of bedding cleavage or bedding schistosity. [VAN HISE, 1895, pp. 661-662; DALY, 1917, p. 403].

Actually, from reading published studies of the Grenville series in the belt and from discussions with geologists who have used the term bedding foliation in the northwest Adirondacks, it seems that the degree of parallelism implied between bedding and prominent cleavage varies greatly with the different geologists, and with the same geologists in different reports on comparable types of rocks and structural features. Thus CUSHING [1905, p. 400] states that "sometimes this new structure (cleavage) is parallel to the old bedding planes and sometimes it is not." In later reports, however, CUSHING [1916, p. 22] and CUSHING and NEWLAND [1925, p. 52] concluded that in the Adirondack region the cleavage is "everywhere parallel to the bedding." The belief in widespread and rigorous parallelism between bedding and secondary foliation in the rocks of the Grenville series is especially manifest in some of the genetic concepts offered to explain the bedding foliation. Thus VAN HISE [1895], LÖWL [1906], DALY [1917], MILLER [1916], CUSHING and NEWLAND [1925], and others endorsed the concept of load metamorphism or "Belastungsmetamorphismus" [LÖWL, 1906, p. 50] to explain the bedding schistosity of the Adirondacks and elsewhere. Daly championed the idea of load metamorphism in large part presumably because he reasoned that the parallelism of schistosity and bedding to the degree and areal extent conceived of by himself and others in the Adirondacks is "truly inexplicable by pure dynamic metamorphism" [1917, pp. 403-404]. The reasoning that rigorous bedding foliation cannot be a product of severe dynamic metamorphism seems sound enough. Certainly no worker has satisfactorily demonstrated, theoretically, experimentally, or in the field, that a pronounced secondary foliation can evolve rigorously parallel to closely folded bedding, during folding especially in the axial areas of genetically related, close folds.

One wonders why these workers did not re-examine more carefully the basis for their conclusio that the foliation was a rigorous bedding foliation. MILLER, [1916, p. 588] after years of field work in the Adirondack region, stated that "a more or less well-developed foliation is always parallel to the stratification surfaces, which are usually distinctly preserved in spite of the crystallization" and was led to the necessary and amazing conclusion that "there is no known evidence within the Adirondack region that the Grenville strata have ever been highly folded or severly compressed . . . . ," [1916, p. 595].

Subsequent studies, especially those of MARTIN [1916], BUDDINGTON [1929], and BROWN [1936], have clearly established the presence of complex fold and flowage phenomena in the rocks of the Grenville series in the northwest Adirondacks. These workers assert or imply one very striking and important feature, which is the strong accordance of lithologic trends and the trends of most prominant secondary foliation. There is little discussion, however, of rock surfaces, their interrelations or origin, except by BUDDINGTON [1929, p. 81] who states that "the foliation of the Grenville formations is everywhere parallel to the bedding in the Northwest Adirondacks." This statement is misleading in that Buddington clearly recognized at this date that the "Grenville formations were to some extent split into thin leaves, kneaded and torn into shreds, or disintegrated . . . . " [1929, p. 92-93].

Marked discordances between bedding and secondary foliation in the marble of Grenville series have been discribed by GILLULY [1945], but the detailed text of this excellent, thought provoking work is unpublished. GILLULY [1945, map] mapped and described tremolite-talc schists and other layers as "marking shear zones" which he concluded commonly bear little or no relation to the original bedding (unpublished manuscript). It is interesting to note that SMYTH [1896] had previously described the same rocks as "bedded" and "interstratified" in the marble.

Occurrence and interrelations of lithologic layers and bedding--In rocks as thoroughly metamorphosed as the Grenville series of the northwest Adirondacks, the use of the terms "beds" and "bedding" for many of the lithologic layers involves some assumptions that are unwarranted and misleading. Many of the sedimentary rocks are so thoroughly sheared, recrystallized and reconstituted that well-defined, clearly demonstrable sedimentary features are rare. The rounded clastic particle shapes have been obliterated by secondary crushing and recrystallization. There are no existent crossbedding, ripple marks, mud cracks, or other minor sedimentary features which would be helpful in structural and stratigraphic studies. Gradations in grain size and lithology exist in some layers which appear to be relict beds, but these rocks are completely recrystallized, and modified in mineral composition, apparently due in large part to reactions between the initial sedimentary constituents. For example, some diopside-quartz laminae show well-defined gradations in grain size, but the gradation is reversed at intervals of only a few feet along the strike. It is inferred that the diopside has formed by reaction between silt-sized quartz grains and finer-grained dolomite with the release of CO_2. These reaction and recrystallization processes seem to have resulted locally in diopside grains as large as, or larger than the quartz grains in the adjoining quartzite laminae. Accordingly the gradation as it now exists is reversed in some places from that originally formed by sedimentatio Layers of this type, and others of uniform and appropriate compositional differences probably indicate well-defined, relict beds. These "beds" vary up to several inches in thickness, and cannot reasonabl be interpreted as secondary segregation layers formed by processes of metamorphic differentiation [ESKOLA, 1935].

Few of even the least-deformed relict beds in the siliceous and silicated gneisses, schists, and quartzites are devoid of surfaces of flow or fracture cleavage for more than a few tens or hundreds of feet along the strike or down dip. Prominent cleavages appear in these harder rocks where they occur in thick zones or lithologic units, as well as in thin interlayers in the marble.

In general, rock cleavage indicative of more intense, penetrative deformation, cataclasis, and flow appear more commonly in the metasedimentary rocks and associated intrusive rocks that lie along the margins of the Grenville Belt, and are less common and pronounced within the central zone of the Belt. But there is no uniform appearance of different types of cleavage suggestive of less intense, or less prolonged deformation as the belt is traversed northwest or southeast from margin to core. Nor can specific types of cleavage be ascribed to any single rock type. On the contrary, highly contrasting types of rock cleavage, reflecting both gradual and abrupt variations in degree and type of deformation, appear from place to place within the Grenville Belt.

The occurrence of these contrasting types of cleavages seems largely attributable to a pronounced anisotropism during metamorphism of adjoining formations, and parts of formations or layers within the major rock types. Contrasts in strength and mobility were developed in interbeds and zones of initially similar composition by textural variations along and especially across beds, and by differential permeation and injection of metasedimentary rocks by magma and magmatic fluids. Physical anisotropism was also induced by metamorphic textural and compositional variations consequent upon the reconstitution, reaction, and recrystallization of sedimentary and introduced constituents, both along and across original bedding.

Extreme contrasts in rock competence during deformation are also apparent where sedimentary rocks of quite different composition and mobility under given dynamothermal conditions are intimately interlayered. Perhaps the most striking examples appear where quartzitic beds are interlayered in carbonate-rich marble.

In a few scattered beds in all rock types, and expecially in these quartzose and silicated beds in the marble, the surfaces defined by sedimentary variations in texture and composition seem to have been little disturbed by recrystallization and reaction of components, (see Fig. 2A). No strongly defined dimensional or lattice mineral parallelism of planar or linear types has been developed along these beds. Such incipient or poorly defined planar fabrics as do exist appear to have evolved largely by mimetic recrystallization of minerals with their longest axis or axes along or very close to the bedding. The absence of visible, divergent surfaces, lineations, and pronounced planar fabrics suggests that these relict beds have been sheltered from the dynamic metamorphism in an environment of comparatively little stress. They clearly cannot have been "geared" to the intense rock motions indicated by many of the structural features in the northwest Adirondacks. These relict beds seem to be fragments "floated along" in a more mobile protective rock medium throughout the major stages of dynamic metamorphism, when major differential stresses were operative.

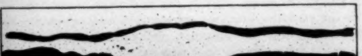

Fig. 2A--Quartz-feldspar granulite layers (solid pattern) intercalated with highly feldspathized and injected quartz-pyroxene layers (stippled); the granulite layers are interpreted as relict beds, highly recrystallized and reconstituted, but not greatly disturbed by dynamic metamorphism; 2B--Layers similar in composition to those in Figure 2A, but partly folded, sheared, and dispersed; secondary shear surfaces essentially parallel with the axial planes of the folds are plainly visible and tend to blur bedding

In other layers, less confidently interpreted as relict beds, the layering tends toward gneissic banding as defined by LEITH [1923] and SWANSON [1941, p. 1247]. Some of these layers are probably altered considerably from their initial sedimentary composition by introduction of magmatic or other foreign components. Layering, and incipient to well-defined cleavages parallel to layering, are not as sharply accentuated in hand specimens and thin sections as in the outcrop. Feldspars, quartz, diopside, and stubby amphiboles dominate the layers, although micas and other platy minerals occur locally. The various mineral components are separated in less uniform and more diffuse layers than those defined by clear-cut bedding.

In many of these gneissic layers, statistical measurements with a Wentworth stage indicate a slight dimensional elongation of grains roughly parallel to the layering. Commonly, divergences from parallelism of longest axes of component minerals are in no preferred direction athwart the layering. No sharply defined parallelism of platy and prismatic minerals and no lineations are visible in the outcrop. The layers are thoroughly recrystallized to medium- or coarse-grained size.

Gneissic layers of this type are thrown into open and close folds, and blurred or obscured by younger, prominently developed cleavages formed during severe stages of deformation. The occurrence of structural features of this type in layers not readily susceptible to flow and shearing out, suggests that the gneissic layering may be a fairly rigorous "bedding foliation" developed by mimetic recrystallization of primary and introduced constituents in layers accordant with the bedding. It seems more reasonable to me, however, that most of these gneissic layers represent beds in part (axial areas of evolving isoclines) sheared out and refoliated during severe stages of metamorphism, after emplacement of the syenites, and thus more comparable to prominent cleavages described in a later section of this paper.

Gneissic layers of this type are not as common in the marbles as in the carbonate-poor migmatitic gneisses which are interpreted as widely permeated by magmatic fluids, which follow in general, the gneissic layering.

Within the Gouverneur Quadrangle, and at the scattered other places in the Grenville series that have been studied intensively outcrop by outcrop, and in mines, the sharply defined layers, described herein with some assurance as relict beds relatively unblurred by younger cleavage surfaces comprise less than one-tenth of the metasedimentary layers exposed. The gneissic banding, which may reflect bedding accurately, and in which sedimentary constituents are clearly dominant, is more abundant, probably appearing in at least a third of the quartzose and silicate gneisses. The remainde of the layers of dominantly sedimentary composition throughout the rocks of the Grenville series exhibit cleavages which blur the bedding to various degrees or completely obscure it. Examples of various types and stages of development of secondary foliation surfaces, and their relations to the beds in the silicated and siliceous gneisses and schists in the Gouverneur Quadrangle and in other areas throughout the northwest Adirondacks are described below. These examples are taken from outcrops and thin sections where various stages of folding of beds are visible. Outcrops that exemplify variou stages of folding are common enough, although in many rocks where bedding is interpreted as being in part or wholly sheared out, folds are absent and the extent of the process is difficult if not impossible to evaluate. Commonly, as in folded rocks from other terranes, the types and prominence of secondary surfaces and their orientation in relation to the bedding can be correlated with the stage of development of the associated fold formed during the same rock movements, and with the position of the secondary surface on the fold. The assumption is made, therefore, that wherever bedding is sufficiently distinctive and visible to define folds, and parts of associated folds, there is more tangible evidence of the degree and nature of the rock motion at this point, and thus the nature of the associate secondary surfaces is better evaluated.

Occurrence and interrelations of bedding and secondary foliations in more competent rocks--Commonly, the well-defined folds in the siliceous and harder silicated beds, where opposite flanks of the folds subtend angles somewhat less than 80° or 90°, are accompanied, at least in the axial regions of the folds, by incipient to clearly visible surfaces of fracture and slip (see Fig. 2B and 3, point A). These surfaces, designated S_2 in these rocks, tend to parallel the axial planes of folds to which they are genetically related. Thus they have the geometrical relation to bedding of "fracture" and "shear" or "slip" cleavage, although, in general, they lack the uniformity and sharp definition characteristic of the features commonly described as fracture and slip cleavage. In some folds, or in some beds in folds, the stratification is displaced slightly along the S_2 surfaces, which appear as parallel or subparallel thrust faults, or slip cleavage. In other folds, and along some interlayers between displaced beds, little or no displacement is visible. Commonly the trace in the outcrop of the S_2 surfaces is defined by faint corrugations in the rock. In general, in these relatively open folds (see Fig. 2B and 4), only a minority of the mineral components are grown, rotated, or flattened distinctly parallel to the plane of the S_2 surfaces. In these examples bedding is still visible, and constitutes the most prominent lithologic layering. Commonly however, in the axial areas of the fold a faint sheeting or grain exists in the beds parallel to the S_2 surfaces. This grain may be observed in outcrops, although it is rarely visible in hand specimens or thin sections (see Fig. 5), and no distinctive elongation of grains between the cleavages can be found by statistical microscopic measurements of oriented grain outlines. No statistical analyses of crystallographic orientations have been made in these rocks as yet.

Beds along the flanks of these relatively open folds commonly show very little disturbance, or only a general tendency or planar orientation of mineral grains parallel or subparallel to bedding. Slight en-echelon development of amphiboles, micas, and slightly elongate quartz grains can be detected in some beds. The grains along bedding have their longest axes somewhat athwart the bedding, and roughly parallel to the axial plane of the fold.

In these open folds in the visible bedding that plunge at low angles, essentially parallel to the regional trends, the dips of existing S_2 surfaces and, necessarily, the dips of associated axial planes

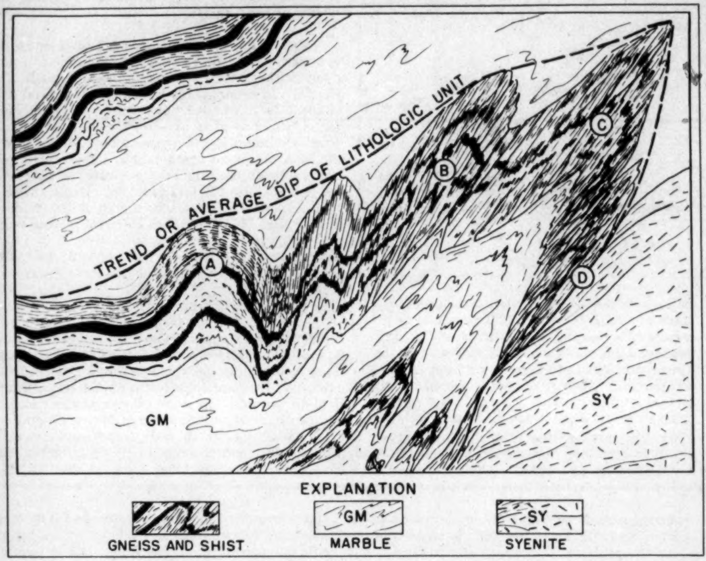

Fig. 3--Schematic examples of the development of cleavages in the metasedimentary rocks of the Grenville series and in associated syenite; points (A), (B), (C), and (D) indicate successive stages in the shearing out of bedding and the evolution of prominent secondary surfaces of shear and related lithologic layers; the diagram may be considered as a cross section of areas where folds plunge gently or a plan where folds plunge near the average dip of layers

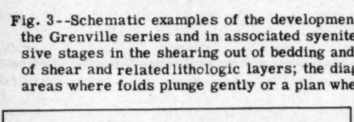

Fig. 4--Asymmetric folds in what is probably bedding in a quartz-biotite-microcline gneiss; the beds are sliced by numerous small thrusts whose surfaces are essentially parallel to the axial planes of the folds

of the cleaved folds, commonly diverge as much as 60° to 90° from the average dip of the beds and from the enclosing lithologic zones. In the outer zones of the Grenville Belt, and locally within the core of the belt are essentially similar types of open folds which plunge athwart the regional trends. These exhibit a comparable divergence of strikes of their axial planes and associated S_2 surfaces from the regional trends. The relationships of these features are illustrated schematically in Figure 3, at point A.

It is especially notable that within a particular area of cross folds, all the visible fold axes in bedding are essentially parallel. No incipient or well-defined folds of diverse orientation or relict refolded folds which when "unrolled" approach or parallel regional trends, appear in the relict beds. Similarly, in these areas of cross folds, all intersections of bedding and S_2 are essentially accordant with the plunge of the cross folds. There seems to be no superposition of cross folding and shearing motions upon a previously developed system or framework of close folds, foliations, and lineations related to and

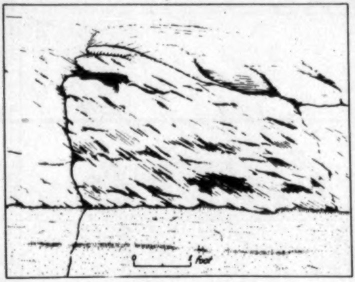

Fig. 5--A segment of silicated layers on the flank of a fold; the horizontal filiation is interpreted as largely relict bedding; the diagonal foliation visible in the upper part of the figure developed after the horizontal layering, and parallel to the axial plane of the fold; the lowermost layers have flowed almost parallel to bedding and exhibit no axial plane foliation

accordant with the major northeast regional trends of rock units.

Examples of greater degrees of rock motion are manifest by more closely compressed folds in many of the harder, siliceous beds (point B of Fig. 3). In general, the bedding in the axial areas of these folds is cut by prominent cleavage surfaces, which tend to parallel the axial planes of the fold. Commonly, the more closely compressed the fold, the more prominent are these cross-cutting surfaces, and the less definite the outlines of the bedding and the fold (see Fig. 3). In these folds or relict folds, whose flanks delimit angles of less than 60°, numerous mineral grains composing the beds have rotated, flattened, or grown with their longest axis or axes roughly or quite parallel to the axial plane of the fold, Figure 3, points B and C.

Actually, transitions in type and form, from the descriptive point of view, exist between the S_2 type of surfaces, which appear in some open folds in beds and the strongly developed, more schistose types of foliation surfaces associated with close folds. In some places where beds of contrasting composition and different competence are involved, the S_2 "fracture cleavage" types cutting one bed merge abruptly into "flow cleavage" types in an adjoining bed of quite different composition and different susceptibility to shearing and recrystallization processes. These features have been described from other localities by BALK [1936, p. 706], BROUGHTON [1946, p. 7], and others.

The nature of the axial-plane cleavages in the axial areas of the moderate to close folds varies considerably in different beds of the same fold, and even in different folds in rocks of essentially similar composition. So-called slip folding is a conspicuous process in a few folds, and in parts of many folds, although by no means a dominant process. Shearing is apparent along many axial-plane surfaces of varying degrees of definition in one or more beds, whereas beds adjacent to these were deformed by penetrative flow which may not be reflected in distinctive shear surfaces, Figure 5. Many of the visible shear surfaces evolve from tiny asymmetric crumples in bedding, comparable to classic examples described from other terranes. The visible displacements on most surfaces associated with asymmetric, small folds are thrusts ranging from microscopic ruptures to obvious faults with several or many inches or even several to tens of feet net slip, Figure 4. In very large folds, displacements along associated surfaces may reach thousands of feet.

In general, even in the stronger rocks, however, discontinuous displacements caused by rupture of the material are masked and possibly subordinate to continuous displacements resulting from flow and recrystallization of the components. Presumably both continuous and discontinuous shears were contemporaneous and complementary during the more severe stages of dynamothermal metamorphism, similar to the way in which rock components are reported to react under high pressure and shearing stress in the laboratory [GRIGGS, 1936; BRIDGMAN, 1936].

In examples of rocks more closely folded, where the folds approach isoclines in form, the associated axial plane surfaces are much more distinctly developed. The degree of asymmetry of these folds and their orientation with respect to major lithologic trends are in strong contrast with those of open folds (in Fig. 3 compare A and D). In areas where groups of beds, each of about the same competence, were folded, their form and orientation are determined largely by the position of the fold in relation to associated major structures. For example, movements of beds along flanks of other folds, or along major shear zones between rocks of different competence, are commonly manifest in asymmetrical drag and flowage folds, some of which approach isoclinal form (see Fig. 3, B and D). Movements of thick beds in the apex areas of major folds, which are commonly areas of marked convergence of rock components, usually result in symmetrical folds with saw-toothed, fan, and other forms, Figure 6. Obviously in these apex areas, shear couples were much less dominant than in flank areas, and along shear zones.

As the folds become more closely compressed, their axial planes, and the essentially accordant shear surfaces, tend to form successively smaller angles with the average lithologic dip and trend of

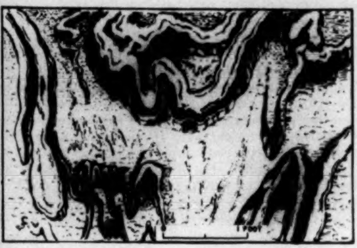

Fig. 6--Relict beds of quartz-pyroxene and quartz-microcline granulite (weathered out in relief) enveloped in carbonate rich marble and deformed into roughly svmmetrical folds in an area of convergence of marble on the crest of a much larger fold

the Grenville Belt. Commonly at the stage of deformation wherein these axial-plane surfaces are prominently defined as surfaces of schistosity, with clearly defined accordant cleavage banding, the still visible parts of the sheared fold, as defined by bedding, approach isoclinal form. Accordingly, the shear surfaces tend to converge toward parallelism with bed fragments, if they are still detectable, along both flanks of the more nearly symmetrical folds, and especially along the long flanks of the asymmetrical folds. At this stage of shearing out of bedding indicated above, the shear surfaces and the cleavage banding have a maximum divergence of less than 30°, and in many places less than 15° from the gross trend and average dip of the enclosing lithologic unit (see Fig. 3, points C and D).

An important and synchronous effect produced by the increased growth, alignment, or flattening of minerals along the well-defined shear surfaces is a progressive slicing, shearing out, and obliteration of bedding and of any essentially accordant, interbed slip surfaces which outlined the original fold, Figure 3, points C and D. In the described examples of more coherent and stronger beds, the initial and most thorough effacement of bedding, and of any foliation parallel with bedding, commonly occurs in the axial or short flank areas of folds. This very common destruction of folds in bedding in their axial areas is in marked contrast to the quoted [LAHEE, 1941, p. 280] statement of Van Hise that axial regions of folds in highly deformed metasedimentary rocks are the best places to search for relict beds [VAN HISE, 1895].

These relations seem to offer one answer to the conclusions of earlier workers, previously cited, that secondary foliation is "everywhere parallel to bedding." The most prominant discordances between very distinct cleavage and bedding appear in apex areas of isoclinal folds. If extensive interbed flow and slip have been possible along flanks of these isoclines, there is no appreciable discordance of bedding and cleavage in their flank areas; and in many parts of the northwest Adirondacks, as in other terranes, the apical areas of isoclines--where discordance of beds and prominant secondary surfaces is profound--comprise some fifth or less of the total surface area. Commonly the area of outcrop of these sheared out apices is only one tenth or even less of the total outcrop. Accordingly, most exposures are of flank areas where, true enough, there is superficial if not actual parallelism or near accordance of the prominant cleavage with bedding.

Where the folding and refoliation process has continued, the flank areas of the isoclines are subsequently folded, commonly along the same axes or axes only slightly askew from those of the initial folding. In these younger, essentially accordant folds, the cleavage which had its inception with the evolution of the initial isoclines clearly wraps around the nose of the younger fold. In some instances the closely spaced, prominant earlier cleavages near bedding facilitate interlayer slip and no strong axial plane cleavage evolves in the younger folds until they too approach isoclinal form.

In many places where the shearing-out is profound, however, no fragments indicative of true beds remain at any position in the "ghost" of what was originally a fold. In other places vestiges of beds appear along the flanks of folds as lenticles and sheetlike fragments overlapping somewhat similar remnants on the opposite flank. These bedding shards and streaks, overturned in respect to each other, are duplicated and triplicated in some places, and almost invariably a pronounced foliation, divergent from the initial horizons, permeates the relict bed fragments.

In still other examples along flank areas, the relict beds are rolled, or refolded, sheared out, and dispersed along succeeding, dominant shear surfaces. Relicts of relatively competent bed fragments, which seem to have been protected from strong differential stresses by a more fluid envelope during the early stages of deformation, appear frozen in various positions near or in contact with enclosing hard rocks. The effect of more pronounced differential stresses introduced by this juxtaposition of hard fragments is reflected in the more advanced stage of shearing out, and refoliation of these fragments along younger generations of prominent shear surfaces. Many visible, lenticular relicts of succeeding generations of lithologic layers, such as vein or injection materials, or planar sheets formed along previously developed but somewhat comparable shear surfaces, tend to be aligned slightly en-echelon, or in the slightly askew patterns of logs in a stream. Rocks of pronounced lenticular fabric evolve most commonly where cataclasis is dominant, or where the layers are of contrasting competence, and contain differently shaped mineral components.

In some of these rocks, especially where micas, chlorite, amphiboles, and other minerals of inequidimensional form are associated with quartzose and feldspathic granulites, no single set of surfaces is well-defined and dominant. Refoliation is expressed in two or even more slightly divergent surfaces whose composite trend may define the grain of the rock. Less well developed surfaces in these rocks tend to diverge at larger angles from the trend and average dip of the enclosing lithologic unit. These surfaces are the homologues of the incipient S_2 surfaces in open folds in bedding. The fabric diagram of mica poles in these rocks is a girdle with two or more maxima. Figure 7 shows a tremolite schist from a tremolite-talc mine, in which two sets of shear surfaces, intersecting at angles less than 15° are visible in the underground exposures and in thin section.

Refoliation processes in mobile rocks--In rocks dominated by a single mineral constituent, or rocks composed of groups of minerals having similar crystal habits, the dominant shears evolved in any stage of refoliation are much more uniform. Where these minerals are types which readily become mobile during deformation, such as clay minerals and carbonates, the shearing out of bedding and refoliation of the rock is a less definitive and apparently a more rapid process than in the siliceous and silicated rocks already described. Actually it seems difficult if not impossible to evaluate accurately the proportions of prominent foliations that have formed at the expense of the bedding. As with other metamorphic processes [GROUT, 1941, p. 1528], the more thorough and complete the shearing out of beds and refoliation of rocks, the more difficult it becomes to reconstruct this sequence of events. In many areas of poorly exposed rocks, or in well-exposed but highly recrystallized and reconstitute rocks, an outcrop may contain only one well-defined set of uniform surfaces, but there is little or no evidence to indicate whether this foliation is relict or accentuated bedding, or secondary shear surfaces. The gneissic layering described in an early section of this paper is a good example of such foliation whose origin is obscure.

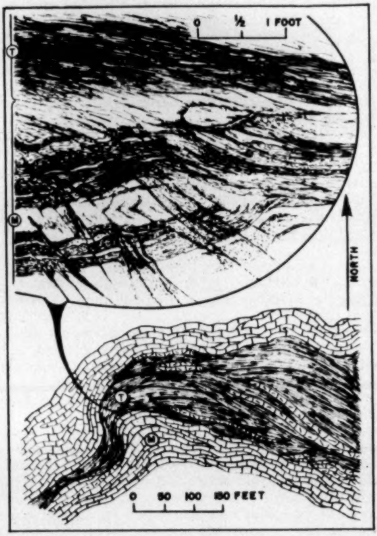

Fig. 7--An example of quartzose marble (M) which is partly sheared out into tremolite-talc schist (T) near the crest of a steeply plunging cross-fold in the marble; the oldest visible foliation in the marble (inset) is probably bedding, somewhat disturbed by interbed slip; note the deviation in angle between the divergent secondary shears in the quartzose marble and those in the tremolite-talc schist where bedding is completely obliterated.

In other outcrops, two or more intersecting sets of foliation exist, but even if one is clearly older than the other, there is no certainty that it is bedding. In the more obscure examples, reasoning by analogy with features and relations from more definite outcrops of the types described, it is estimated that in about one-fourth to one-third of the outcrops of hard siliceous and silicated gneisses, the dominant foliation is of secondary shear origin.

Bedding in the initially argillaceous and carbonate-rich rocks is even more extensively and strikingly sheared out. Probably less than one-third of the prominent layering in the marble represents bedding. These more mobile layers have been deformed "ahead" of the gneisses, with resulting internal and contact foliations of distinctive types (see Fig. 8).

The differential rate and degree of deformation between different rocks are well illustrated by examples described below from zones within the marble and at the contacts of marble with the harde rocks previously described.

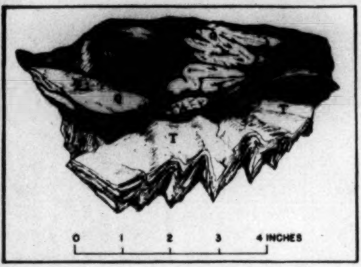

Fig. 8--Lenticles and knotted fragments of quartzite beds (Q) sheared and rolled out in phlogopite schist (dark) at contact with crumpled talc schist (T); bedding is completely obliterated in the phlogopite and talc schits ; the axes of the folds in the talc schist are parallel to the longest dimemsion of the quartzite relicts above, and both features are clearly the product of the same rock motion

The marble is recrystallized, largely to a medium- or coarse-grained rock in which calcite and dolomite are the dominant constituents. Where the marble layers contain little else than calcite or dolomite, primary and secondary foliation surfaces, folds, and other lineations are in general obscured by the complete recrystallization of the carbonates. Even where shear surfaces do appear in these pure carbonate masses, it is commonly impossible to find suitable criteria by which to distinguish bedding from shear surfaces.

Layers, streaks, and irregular masses of quartz, calcium- and magnesium-bearing silicates, carbonaceous matter, graphite, and other constituents are present, however, in many areas of marble. These constituents delineate numerous surfaces of cleavage. Relict bedding seems to be especially well indicated by certain interlayered quartzitic laminae, quartz-calcite beds, quartz-diopside and quartz-feldspar garnulites, and thin, micaceous layers. Various micaceous, siliceous, or silicated masses composed of these "beds" and other layers are continuous for hundreds or thousands of feet along the strike and down dip. These layers are interpreted with some confidence to be stratigraphic zones.

In general, the form and interrelations of visible patterns and structural features of the marble are the result of its initial thickness, and its mobility during deformation as determined by composition, by position of the layers relative to other, commonly more competent rocks, and by the major structures of the enclosing or adjoining competent rocks.

Thin siliceous beds intercalated between carbonate-rich layers had little stiffening effect during metamorphism. They are in large part broken and "floated apart" but they may still serve as excellent markers by which the various motion patterns of the enclosing marble may be traced.

Deformation of the marbles commonly is reflected in various degrees of thinning and squeezing out of carbonate rock at one point, and its convergence and thickening at another. Features indicative of these opposing processes may be apparent both within a thin section, or on regional maps. As VAN HISE [1895] and many other workers have noted, the marble tends to accommodate its form, within limits, to that of the enclosing and adjoining harder rocks.

The marble zones are especially constricted and thinned on flanks of major folds in the Grenville series, whereas convergence, thickening, and duplication of marble are characteristic features of axial areas of folds, Figures 6 and 9. Some marble belts, such as those formerly interlayered with the quartz-oligoclase-garnet gneiss south of Edwards, N. Y. (see Fig. 9), are completely separated by constriction of the enclosing, hard gneisses on the flanks of folds, and squeezed into enormously thickened "eddies" of convergence in axial areas of folds (see Fig. 9, point A).

The thrusting forces of igneous masses during or subsequent to intrusion and solidification produced somewhat similarly disrupted, or distorted bodies of marble, which have flowed away from the "prow" of the intrusive node, into pressure shadows along its sides and its wake. Just west of the area indicated in Figure 9, the marble interlayered with the feldspathic gneiss and biotite-oligoclase-garnet gneiss has been almost severed by the constricting motions of granite and gneisses.

Where zones of carbonate-rich marble are constricted and greatly thinned between relatively straight or smooth-surfaced harder rocks, remarkably uniform relations are introduced between the surfaces of flow in the marble and the marginal foliation in the harder rocks. In general, an approach toward accordance of the shear surfaces in the marble, and the lithologic surface of the adjoining or included harder rocks increases as the contact between the two is approached. Most of the folds in the bedding or in secondary surfaces in the carbonate-rich marble near smooth surfaced harder rocks

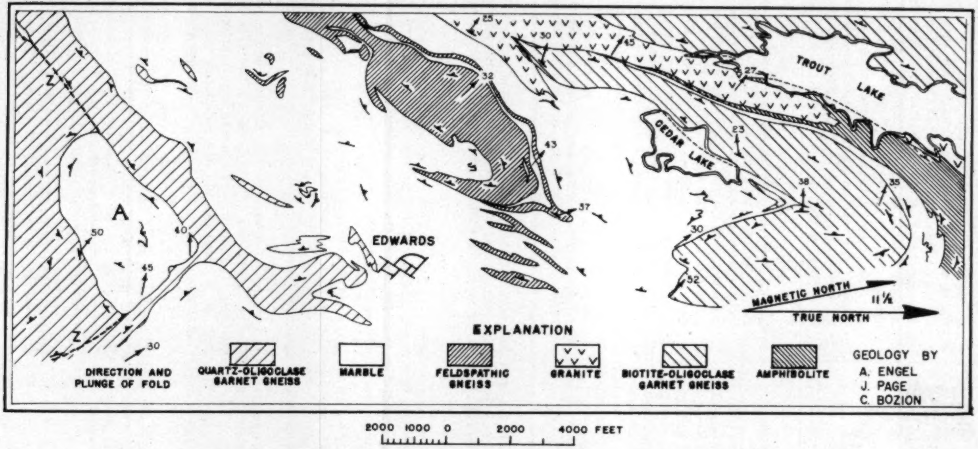
TROUT LAKE
CEDAR LAKE
EDWARDS
A
Z
Z
25
30
45
27
32
43
23
37
38
35
30
52
50
40
45
30
MAGNETIC NORTH
11½
TRUE NORTH
EXPLANATION
DIRECTION AND PLUNGE OF FOLD
QUARTZ-OLIGOCLASE GARNET GNEISS
MARBLE
FELDSPATHIC GNEISS
GRANITE
BIOTITE-OLIGOCLASE GARNET GNEISS
AMPHIBOLITE
GEOLOGY BY
A. ENGEL
J. PAGE
C. BOZION
2000 1000 0 2000 4000 FEET

Fig. 9--Geologic map of highly deformed rocks of the Grenville series near Edwards, N. Y.; two closely associated major folded structures, whose axes are essentially parallel, are present in the area; one is reflected in the hook-shaped outlines of the feldspathic gneiss and biotite-oligoclase-garnet gneiss; this fold plunges northwest (see arrows) at about 35° and is interpreted as a large subsidiary drag fold on the northern nose of a large dome which is outlined in the external form of the quartz-oligoclase-garnet gneiss at the south side of the map; the form of the easterly, short flank of the drag fold is largely obliterated, especially in the marble; the slivers of feldspathic gneiss north of Edwards are presumably remnants, however, of this short flank; the marble at (A) represents a former interlayer in the gneiss, whose former stratigraphic position is indicated by the dotted lines (Z); the marble is interpreted as having flowed between the bounding surfaces of the gneiss, largely northeastward into the apex of the dome in the garnet gneiss; less extreme examples of flow of marble in the apex of the subsidiary drag fold are visible in the thickened marble zones east of Cedar and Trout Lakes; strike and dip symbols in the gneisses represent local attitudes of larger remnants of beds; these same symbols in the marble represent attitudes of prominant surfaces of flow are asymmetric, almost from their inception. Whenever folds are recognizable in examples of extensive movement and shear, they appear as isoclines, commonly recumbent, with flanks essentially parallel to the shear surfaces. In some outcrops these recumbent isoclines or blurred relicts of isoclines in the marble reflect the profound shearing out of the carbonate-rich beds, even before pronounced folding is apparent in adjoining harder beds.

The deformation of the marble well "ahead" of the adjoining harder beds, and the uniformity of shear surfaces within the marble, result locally in what may appear to be unconformable stratigraphic relations between carbonate rocks. Thus, at a stage where beds in a quartzite or quartzose zone are strongly folded, but still clearly recognizable, the bedding in adjoining marble may have been completely obliterated by the flow of carbonate material. The forms of isoclines visible in the carbonate rock actually may be defined by bedding, by secondary or tertiary shear surfaces formed during the shearing out of either bedding or subsequently formed cleavage bands. Figure 10 shows an outcrop wherein such relations are believed to have evolved between marble and a thinly layered (bedded) quartzose zone during dynamic metamorphism. The folded and crumpled surfaces in the quartzite undoubtedly are relict bedding. The prominent uniform surfaces in the marble are secondary shears that simulate the sheared-out bedding. The relict isoclines in the marble at (A) and (B), Figure 10, are either folds in bedding, or folds, in younger, secondary surfaces. The essential parallelism of the shear surfaces in the marble at and near the quartzite with the trend of the quartzite persists for thousands of feet along the strike.

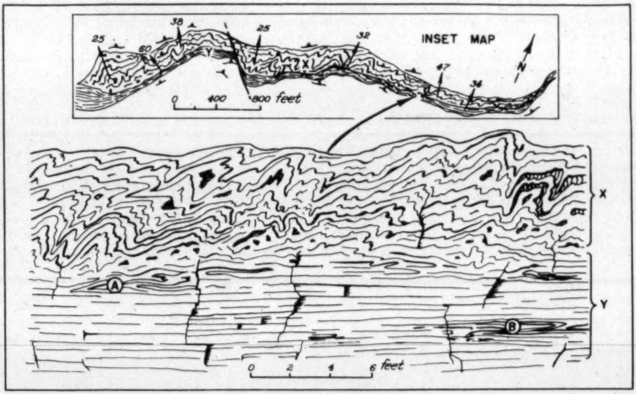

Fig. 10--Sketch of an outcrop showing relations of quartz schist (X) to underlying, pyritic silicated marble (Y); the plicated foliation in the quartz schist is probably bedding, but the uniform layers in the underlying marble are clearly defined by surfaces of flow; relict apices of isoclinal folds in the marble are visible at (A) and (B), and less clearly elsewhere; the axes of these folds are essentially parallel to the axes of the folds in the quartz-schist; most or all primary beds in the marble have been obliterated by extensive flow which has followed the margin of the stiffer quartz schist and produced flow surfaces which simulate uniform bedding

Quite obviously differential response to deformation of this type produces features which simulate stratigraphic unconformities. In contrast, the shearing out of bedding in more mobile layers, with the development of secondary surfaces essentially parallel to the trend of the adjoining harder rocks in which the foliation is not visibly folded, can completely mask stratigraphic unconformities. In such places the tectonic contacts between contrasting lithologic units, zones of displacement probably measurable in tens or hundreds of feet, appear superficially to be as conformable and undisturbed as bedding in a conformable sequence of sedimentary rocks. In general, the shearing-out processes tend to prodece many more pseudo-conformable than discordant relations.

In most of the marble, the existing, essentially "conformable" contacts of marble and gneisses or schists are rarely undisturbed sedimentary contacts. Many siliceous interbeds in the marble served as rigid partitions during much of the deformation, and the shearing of mobile carbonate rock along these more competent sheets involved marked differential stress. Directions of shearing moti are recorded in the form and orientation of folds and genetically associated planar and linear fabrics. The growth of prismatic and platy minerals, especailly tremolite, anthophyllite, and mica, by metamorphic processes, seems to have been greatly facilitated along these highly stressed zones. Carbonate layers and grains intercalated between those of quartz and other silicate minerals have served as efficient lubricants during the shearing out of the harder rocks.

Locally in these zones, some hard, distinctive bed or other unit which can be used as a datum plane, such as a sill emplaced prior to severe deformation, is not completely obliterated by the shearing processes. The form and distribution of these relicts, and their relations to shear surfaces of secondary origin offer some quantitative data as to the minimum displacement and shearing out of the marble. They also help to determine the relations of the present lithologic contacts to preexisting stratigraphic horizons.

The amphibolite enclosed in the tremolite schist, (see Fig. 11), is one of a group of distinctive rock layers that are interpreted as either relict, reconstituted beds in the marble, or as possible camafic sills. Where least altered, the mineral components of the amphibolites, diopside, hornblende, and oligoclase feldspar, and their bulk chemical composition are consistent with metasedimentary or igneous rocks. Where amphibolitic layers of the type shown in Figure 11 are exposed with more definite beds, they are accordant with bedding; and almost invariably the amphibolites have been involved in all the stages of severe dynamothermal deformation reflected in the enclosing beds. Most of the amphibolite fragments of Figure 11 are converted to phlogopite mica schist. The syenitic rocks, clearly emplaced before the onset of severe dynamic metamorphism, intrude the amphibolites.

Accordingly, if the amphibolites are not beds, they are probably igneous sheets emplaced along bedding prior to the major stages of dynamothermal metamorphism. Interpreted as either sill or bed, the smeared-out amphibolite fragments would seem to outline rudely the relict form of a highly disturbed and displaced stratigraphic horizon. If this is a valid interpretation, the relations of the present lithologic zones and layers of metamorphic origin may be contrasted with the trace of the sheared-out horizons as reflected by the amphibolite fragments. The general agreement in the trend of both these primary and secondary features is striking. The greatest departure from parallelism, at F-E-C, Figure 11, seems to reflect an infolding and a reconversion of marble to tremolite schist, comparable to a somewhat similar reconversion indicated in a less advanced stage at B, Figure 11.

The influence of the anisotropy produced by bedding, a type of stratigraphic control, is obvious i the form and orientation of the secondary shear surfaces and zones as defined by the tremolite schist. The rude coincidence in trend between the amphibolite and the belt of tremolite schist is especially impressive in view of the extent of the rock movements, as indicated especially by the dispersed and folded pattern outlined by the amphibolite fragments.

Obviously those displacements in and along the amphibolite, which have occurred without visible loss of continuity in the rocks, cannot be calculated with any accuracy, although they are undoubtedly large. Solid flow is indicated, however, by the fact that much of the amphibole in Figure 11 is thinne by shear to less than one-fourth the thickness found where deformation is least pronounced, Figure 11 point A.

Discontinuous displacements, that is, rupture of the amphibolite along shear surfaces and zones in the tremolite schist, however, can be calculated. Inasmuch as there is no evidence of divergent axes of rotation and of crossed strain, the movements along these ruptures were probably genetically related to and closely associated with those movements on the surfaces of flow that did not cause obvious rupture in the amphibolite. The direction of maximum net slip of the formerly continuous amphibolite fragments along cross-cutting ruptures, lies about normal to the axes of the plunging folds in the rocks. This displacement of the amphibolite, along some 15 prominent shears between C and E, Figure 11, where the amphibolite angles across the tremolite schist, was carefully measured. The total, measurable displacement of micaceous amphibolite fragments is 168 ft. If the displacement of the fragments between E and D are included, the displacement is increased to 243 ft of measurable net slip between C and D, Figure 11. The additional continuous displacements along and in the amphibolite cannot be measured but are presumably equal to this amount.

The areas of convergence into which marble has flowed, such as axial regions of folds, are frequently characterized by intricate crenulations in the surfaces of flow, and in the included, harder

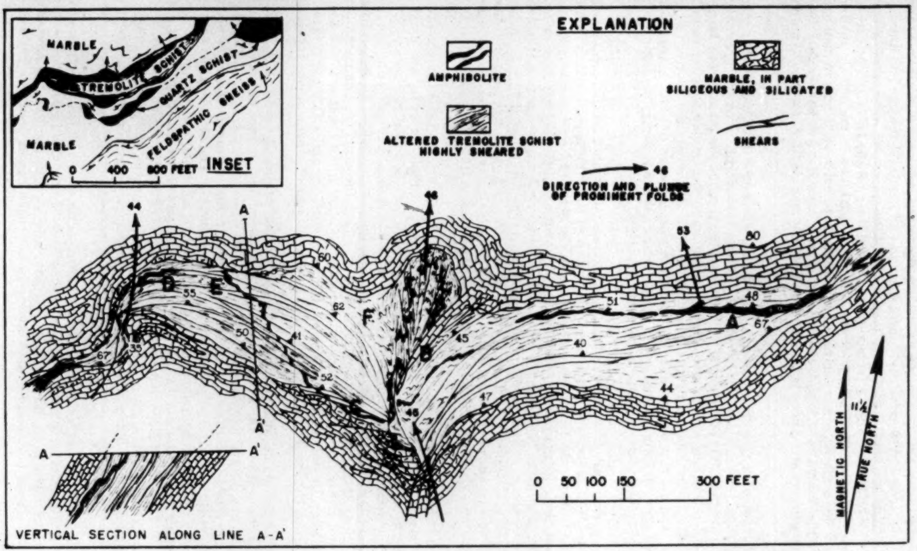
EXPLANATION
AMPHIBOLITE
MARBLE, IN PART SILICEOUS AND SILICATED
ALTERED TREMOLITE SCHIST HIGHLY SHEARED
SHEARS
46
DIRECTION AND PLUNGE OF PROMINENT FOLDS
MARBLE
TREMOLITE SCHIST
QUARTZ SCHIST
FELDSPATHIC GNEISS
MARBLE
0 400 800 FEET
INSET
44
A
46
53
80
60
55
62
51
48
67
50
41
45
40
67
35
52
47
44
46
A'
A
A'
D
E
F
B
C
0 50 100 150 300 FEET
MAGNETIC NORTH
TRUE NORTH
11¼°
VERTICAL SECTION ALONG LINE A-A'

Fig. 11--Simplified geologic map of the seventh level of a talc mine, Talcville, N. Y., showing types of shearing out of marble, amphibolite, and tremolite-talc schist; the general pattern indicated in the distribution of amphibolite fragments is interpreted as a reflection of a relict stratigraphic horizon; the inset indicates the relations of the tremolite-talc schist and marble to nearby lithologic units which are interpreted as deformed remnants of stratigraphic zones; strike and dip symbols represent attitudes of secondary surfaces of shear, in most places rudely accordant with the trends of relict beds layers and beds in the marble. The swirled patterns in some areas onconvergence of marble are comparable to patterns of foam on quiet pools below turbulent stretches in mountain streams. The sinuous, but essentially parallel surfaces of shear, and the associated recumbent isoclines which characterize the areas of thinning and divergence described above are replaced in the convergent areas by swirled shear surfaces and by intricately involuted fan and isoclinal folds. The axial planes of these intricate folds are curved surfaces, (especially when examined in sections normal to fold axes) which diverge at greater angles from regional trend lines as the folds are traces into the nearby harder layers. Almost invariably, however, the shear surfaces in the marble tend to approach conformity with the surfaces of harder rocks as the contacts between them are approached. Conversely, the greater the thickness of the marble without guiding partitions of harder interbeds, the more common the shears and structures within the cores of the marble that diverge from those in adjoining gneisses.

Many of the folds and complex flowage surfaces within thick, carbonate-rich marble have little or no reflection in the structure of the adjoining gneisses. Almost invariably, however, a traverse across the rock trend, from the heart of an "eddy" in the marble, into the gneiss or other hard adjoining rock, indicates the increasing accordance of shear surfaces in the marble with the bounding surface of the harder rock, as the lithologic contact is approcached. Commonly the contact is a "conformable" tectonic type, and the fact that rock flowage imparts what appears to be an essential transition in type between the structures in marble and in gneiss may cause the unwary geologist to underestimate the degree of deformation and rock movements involved.

Summary--The pronounced anisotropism which has so obviously persisted throughout deformation and controlled to a marked degree the evolution of cleavages in many metasedimentary rocks in areas of the northwest Adirondacks is largely a reflection of the layered fabric originating from, or controlled by sedimentation. Large parts of the thicker siliceous and silicated para-gneisses, as well as thinner, harder zones and beds clearly remained as semi-continuous sheets throughout the various stages of deformation. These sheets acted as guides to the direction of flow in the more mobile interlayers and zones. Prominent sills and lenses of syenite, and older more mafic igneous rocks emplaced prior to severe stages of deformation, served similarly, as baffles which prevented the development of widespread prominant shears at large angles to the major lithologic units.

A significant direction of tectonic motion within the rocks of the Grenville series apparently has been northwest-southeast, as reflected by the prominent trends of lithologic units, and most major folds, since the folds are by no means solely products of slip folding in the conventional sense. As the regional northeast-trending folds evolved from gentle undulations into near isoclines lengthening or elongation of layers toward the axial areas of the folds was equaled by sideward motions of rock especially along the margins of the Grenville Belt. Thus the more mobile rocks of the Grenville Belt flowed not only in the directions of regional dips, but in the zones now occupied by cross folds, flow was laterally northeast-southwest along the surfaces and within the folded structures defined by harder lithologic units. Thus the deformation was of a pronounced triaxial type.

It seems clear that, as the major and minor folds were formed, incipient surfaces of shear (cleavage) developed nearly parallel to the axial planes of associated folds, commonly at stages when respectively, strikes and dips of the axial planes of the folds diverged as much as 90° from regional trends or average dips of the lithologic units. Accordingly, the incipient cleavages may lie almost athwart the average dip or the trend of bedding and of rock units. The tendency, however, for the more mobile layers to flow along the surfaces of less mobile adjoining beds or layers, or along surfaces at low angles to the beds during the more severe stages of deformation, is reflected in the approach toward parallelism of secondary shears with relict beds and lithologic zones as the shears become increasingly dominant. This dominance of shear surfaces is, of course, possible only through the development of associated planar fabrics and lithologic layers at the expense of much bedding.

The intersections of cleavages and bedding, as well as intersections of younger surfaces of cleavage, appear to be essentially parallel to each other and to the axes of all folds in both bedding, and in cleavages at any one point. There are no relict minor folds, or intersections of foliation distinctly discordant with the axes of cross folds where these appear in the rocks of the Grenville series.

Presumably no strong shearing and torsional motions occurred in these rocks along divergent axes or at appreciable angles to the cross-folding motions, either well before or after the development of the cross folds.

The incipient to moderate rock motions and rotation along a northeast-southwest direction, which are inferred to have occurred in some part prior to stages of cross-folding, do not seem to have been of sufficient intensity or magnitude to produce well-defined cleavages. This conclusion is based largely upon the fact that in areas of cross folding no visible, relict, secondary surfaces intersect the many widely scattered relict beds along lines trending northeast-southwest; nor have folded cleavages, or folded intersections of cleavage and bedding been observed in areas of cross folding which might be "unrolled" into lines paralleling the axes of the gently plunging, northeast or southwest trending folds.

There is little doubt that in many areas of the northwest Adirondacks a map drawn with the strikes and dips of the diverse, major rock surfaces and layers plotted under a single symbol does little practical violence to the facts, or to gross structural and stratigraphic reconstructions. The thick units of gneiss and marble remain as distinctive masses which outline roughly most major structures. But the evolution of existing features, which include this tendency toward parallelism of many prominant primary and secondary rock surfaces must be appreciated in unraveling the complex deformational history of these rocks, and in precluding marked oversimplifications of their metamorphic history.

Some of the most serious errors of interpretation and generalization involving even gross regional features are possible where two or more major lithologic units are closely interfolded and sheared out to the extent that the original forms of these units are repeated and blended together. This process of infolding, presumably represented at a final stage at F, Figure 11, and at an intermediate stage at B, Figure 11, may cause two quite different gneisses to be sheared and fused together into an apparently continuous and correlative unit.

Such shearing processes, and many others, complicated by dispersal and granitization of units, makes an assured correlation and structural synthesis of these rocks seem possible only to the incorrigible optimist.

Acknowledgments--During the field work and preparation of this paper, the writer has derived invaluable help and pleasure from stimulating comments proffered by numerous individuals. H. M. Bannerman, C. N. Bozion, A. F. Buddington, B. F. Leonard, and Walter S. White have read the manuscript and contributed much to the writer's thinking in the course of vigorous discussions.

The many published studies on the subject of rock cleavage, and previous studies of the geology of the northwest Adirondack Mountains, including an excellent, unpublished manuscript by James Gilluly, have furnished a crystallized pattern of data and ideas drawn upon with great profit, pleasure, and appreciation by the author.

References

BALK, ROBERT, Structural and petrologic studies in Dutchess County, New York, Bull. Geol. Soc. Amer., v. 47, pp. 685-774, 1936.

BRIDGMAN, P. W., Shearing phenomena at high pressure of possible importance for geology, J. Geol., v. 44, pp. 653-669, 1936.

BROUGHTON, JOHN G., An example of the development of cleavages, J. Geol,, v. 54, pp. 1-18, 1946.

BROWN, J. S., Structure and primary mineralization of the zinc mine at Balmat, New York, Econ. Geol., v. 31, pp. 233-258, 1936.

BUDDINGTON, A. F., Granite phacoliths and their contact zones in the Northwest Adirondacks, Bull. N. Y. State Mus., no. 281, pp. 51-107, 1929.

BUDDINGTON, A. F., Geology and mineral resources of the Hammond, Antwerp, and Lowville quadrangles, Bull. N. Y. State Mus., no. 296, 1934.

BUDDINGTON, A. F., Adirondack igneous rocks and their metamorphism, Geol. Soc. Amer., Mem. 7, 1939.

BUDDINGTON, A. F., Origin of the granitic rocks of the northwest Adirondacks, Geol. Soc. Amer., Symposium on granite, 1948.

CUSHING, H. P., Geology of the northern Adirondack region, Bull. N. Y. State Mus., no. 191, 1905.

CUSHING, H. P., Geology in the vicinity of Ogdensburg, Bull. N. Y. State Mus., no. 191, 1916.

CUSHING, H. P., and NEWLAND, D. H., Geology of the Gouverneur quadrangle, Bull. N. Y. State Mus., no. 259, 1925.

DALY, R. A., Metamorphism and its phases, Bull. Geol. Soc. Amer., v. 29, pp. 375-418, 1917.

ESKOLA, PENTTI, On the principles of metamorphic differentiation, Bull., Comm. Geol. Finlande, pp. 68-77, 1935.

GILLULY, JAMES, Geologic map of the Gouverneur talc district, New York, U. S. Geol. Survey map, preliminary edition, 1945.

GRIGGS, DAVID, Deformation of rocks under high confining pressures, J. Geol., v. 44, pp. 541-577, 1936.

GROUT, F. F., The formation of igneous looking rocks by metasomatism, Bull. Geol. Soc. Amer., v. 52, pp. 1526-1576, 1941.

LAHEE, F. H., Field geology, McGraw-Hill, 4th ed., 1941.

LEITH, C. K., Structural geology, Henry Holt and Company, 1923.

LOGAN, WILLIAM, Geology of Canada, 1863,

LÖWL, F., Geologie, Leipzig and Vienna, 1906.

MARTIN, J. C., The pre-Cambrian rocks of the Canton Quadrangle, Bull. N. Y. State Mus., no. 185, 1916.

MILLER, W. J., Origin of foliation in the pre-Cambrian rocks of northern New York, J. Geol., v. 24, pp. 587-620, 1916.

SMYTH, C. H., JR., Genesis of the talc deposits of St. Lawrence County, New York, School of Mines Q., Columbia Univ., v. 17, pp. 333-341, 1896.

SMYTH, C. H., JR., and BUDDINGTON, A. F., Geology of the Lake Bonaparte Quadrangle, Bull. N. Y. State Mus., no. 269, 1926.

SWANSON, C. O., Flow cleavage in folded beds, Bull. Geol. Soc. Amer., v. 52, pp. 1245-1264, 1941.

VAN HISE, C. R., Correlation papers, Archean and Algonkian, U. S. Geol. Surv. Bull. 86, 1892.

VAN HISE, C. R., Principles of North American pre-Cambrian geology, U. S. Geol. Surv., 16th An. rep., part 1, 1894-1895.

California Institute of Technology,
Pasadena, California

(Manuscript received March 28, 1949; presented as a part of the Symposium on Slaty Cleavage and Related Phenomena at the Twenty-Ninth Annual Meeting, Washington, D. C., April 22, 1948; open for formal discussion until March 1, 1950.)

Transactions, American Geophysical Union Volume 30, Number 5 October 1949

REVIEWS, ABSTRACTS, AND BIBLIOGRAPHY

REVIEWS AND ABSTRACTS

WILSON, M.E. (Chairman), Structural geology of Canadian ore deposits, a symposium, Can. Inst. Min. and Metal, Montreal, 948 pp., 1948.

This attractive volume might almost be called "The Geology of Canada." The descriptions of mining districts and individual mines cover all of the types of structures and geology of the various regions of Canada, except those of the Great Plains.

The arrangement is geographic. Chapter I contains three papers giving the general geologic and structural setting in the Cordilleran Region, the Pre-Cambrian Shield, and the Appalachian Region, respectively. Chapters II, III and IV treat these three regions in detail. In each region arrangement is by belts, areas, or districts, with individual detailed papers on single mines, groups of mines, or districts. Altogether, 123 authors contributed to the symposium.

The volume is well illustrated with line drawings, both cross sections and geologic and structural maps. Most of the sections and maps were redrawn by the Draughting and Reproduction Division of the Mines and Geology Branch, Department of Mines and Resources. The resulting uniformity of illustration gives a very pleasing effect and makes far easier reading and interpretation. There are also some well chosen photographs and a few colored plates.

The index appears to be complete for authors' names, mine names, and for geograpnic divisions. Therefore, it is easy from the table of contents and index to locate a paper about a particular mine or district. It is very difficult, however, to locate a structural or genetic type of deposit unless one is already familiar enough with the various mines and districts to know which ones illustrate the features he is seeking. It appears to the reviewer that the usefulness of the volume would have been enhanced considerably if these features had been included in the index and an appendix had been included fitting all of the mines and districts into a classification like that in "Ore Deposits as Related to Structural Features."

EARL INGERSON

BIBLIOGRAPHY

BIBLIOGRAPHY: GENERAL

AMT FÜR BODENFORSCHUNG, Bodenkundliche Übersichts Karte, Grossblatt 94b, Düsseldorf-Köln, scale 1:100,000, 1 map, 33" x 25", Celle, British Zone, Germany, 1949.

AMT FÜR BODENFORSCHUNG, Geophysikalische Karte von Nordwestdeutschland, scale 1:500,000, 3 maps, each 28" x 26", magnetic gravimetric, and seismic, Celle, British Zone, Germany, 1949.

FREIESLEBEN, HANS CHRISTIAN, Geophysical conclusions from observations on the dip of the horizon, Deutsche Hydrographische Zs., Hamburg, v. 2, pp. 78-82, 1949 (in German with summary in English).

HARVARD UNIVERSITY OBSERVATORY, Centennial symposia, December, 1946, Contributions on interstellar matter, electronic and computational devices, eclipsing binaries and the gaseous envelope of the Earth, Cambridge, 385 pp., 1948.

LAHAYE, EDMOND, Le Centre de physique du globe à Dourbes, Inst. R. Mét. Belg., Mém., v. 31, 24 pp., 1949.

MICHIGAN COLLEGE OF MINING AND TECHNOLOGY, Conference on radioactive ores (seven papers), May 6, 1949, Mich. Col. Min. Tech., 31 pp., 1949.

MORGAN, JOHN D. JR., The domestic mining industry of the United States in World War II, Nat. Sec. Res. Bd., 500 pp., 1949.

NATIONAL RESEARCH COUNCIL, Report of the committee on the measurement of geologic time 1947-1948, Div. of Geology and Geography, Nat. Res. Coun., 77 pp., 1949.

SHULEIKIN, V. V., The development of Soviet Geophysics, Akad Nauk USSR, v. 12, no. 4, pp. 289-305, 1948 (in Russian).

BIBLIOGRAPHY: GEODESY

BERROTH, A., Ueber ein allgemeines Kartenwerk der Schwere, Part 2, Riv. Geomineraria, v. 10, pp. 3-11, 1949.

BOAGA, G., Trigonometria geodetica sopra una superficie qualunque, Boll. Geod. Ist. Geogr. Mil., Firenze, v. 8, pp. 49-54, 1949.

DANILOV, V. V., On the use of a control base-line in precise linear measurement, Sbornik Nauchno-Tekhnicheskikh i Proizvodstvennykh Statey po Geodezii, Kartografii, Topografii, Aeros yemke i Gravimetrii, v. 4, pp. 12-17, 1944.

DELMONTE, R., Geodesia di pozione; determinazione di tempi e metodi a coincidenza, Boll. Geod. Ist. Geogr. Mil., Firenze, v. 8, pp. 79-86, 1949.

INTERNATIONAL ASSOCIATION OF GEODESY, Proceedings of the meeting of the Eighth General Assembly in Oslo in August 1948, Bull. Geod., 94 pp., April 1949 (in French except for Schermerhorn's paper especially listed).

KAZINSKIY, V. A., Elastic level, Sbornik Nauchno-Tekhnicheskikh i Proizvodstvennykh Statey po Geodezii, Kartografii, Topografii, Aeros yemke i Gravimetrii, v. 1, pp. 43-46, 1941.

KRASOVSKIY, F. N., On the measurement of angles in the triangulation of I-Class by Schreiber's method, Sbornik Nauchno-Tekhnicheskikh i Proizvodstvennykh Statey po Geodezii, Kartegrafii, Topografii, Aeros yemke i Gravimetrii, v. 1, pp. 25-27, 1941.

KRASOVSKIY, F. N., Main geodetic foundation in the USSR, Sbornik Nauchno-Tekhnicheskikh i Proizvodstvennykh Statey po Geodezii, Kartografii, Topografii, Aeros yemke i Gravimetrii, v. 2, pp. 26-43, 1943.

KRASHENINNIKOV, G. D., Construction of space photogrammetric network, Sbornik Nauchno-Tekhnicneskikh i Proizvodstvennykh Statey po Geodezii, Kartografii, Topografii, Aeros yemke i Gravimetrii, v. 2, pp. 54-68, 1943.

KREYFETS, M. E., First experience of organizing work with elastic pendulums, Sbornik Nauchno-Tekhnicheskikh i Proizvodstvennykh Statey po Geodezii, Kartografii, Topografii, Aeros yemke i Gravimetrii, v. 1, pp. 119-131, 1941.

LAGERQVIST, PER-AXEL, Kurze Zusammenfassung von gravimetrischen Experimentaluntersuchungen Geophys. Lab., Djursholm, 11 pp., 1948.

LEJAY, R. P. PIERRE, The modern development of the science of gravity measurement (Développements modernes de la gravimetrie), Gauthier-Villars, Paris, 243 pp. + 75 fig., 1947 [abstr. in Appl. Mech. Rev., v. 2, p. 191, 1949].

MARCANTONI, A., Sopra una condizione di massima pricisione nello sviluppe delle basi geodetiche, Boll. Geod. Ist. Geogr. Mil., Firenze, v. 8, pp. 55-64, 1949.

MARUSSI, D. A., La nuova triangolazione di I e II ordine della Sicilia, Boll. Geod. Ist. Geogr. Mil., Firenze, v. 8, pp. 69-78, 1949.

MIKHAYLOV, A. A., Gravimetric work in the USSR, Sbornik Nauchno-Tekhnicheskikh i Proizvodstvennykh Statey po Geodezii, Kartografii, Topografii, Aeros yemke i Gravimetrii, v. 5, pp. 49-59, 1944.

MORELLI, C., On a correction of gravity values, Atti. Accad. Naz. Lincei (R. C. Cl. Sci. Fis. Mat. Nat.) v. 2, pp. 780-782, June 1947 (in Italian), [abstr. in Phys. Abstr., v. 52, p. 442, 1949].

OLCZAK, TADEUSZ, The measurements with the Eötvös torsion balance and the problem of determining the higher normal derivatives of the external gravity potential, Geol. Inst., Poland, Bull. 45, pp. 5-44, 1948 (in Polish with summary in English).

PACELLA, G. B., Intorno al significato fisico delle leggi di variazione della densita di legendre e di roche nell'interno terrestre, Boll. Geod. Ist. Geogr. Mil., Firenze, v. 8, pp. 87-90, 1949.

PACELLA, G. B., Un nuovo motivo per preferire la teoria dinamica alla teoria ortometrica della livellazione geometrica, Boll. Geod. Ist. Geogr. Mil., Firenze, v. 8, pp. 65-68, 1949.

RYTOV, A. V., State network of high precision and of precision leveling, Sbornik Nauchno-Tekhnicheskikh i Proizvodstvennykh Statey po Geodezii, Kartografii, Topografii, Aeros yemke i Gravimetrii, v. 5, pp. 38-49, 1944.

SCHERMERHORN, W., The relation between photogrametry and geodesy today, Bull. Géod., pp. 48-58, 1949.

SUDAKOV, S. G., Fundamental problems of the reorganization of the main geodetic network in the USSR, Sbornik Nauchno-Tekhnicheskikh i Proizvodstvennykh Statey po Geodezii, Kartografii, Topografii, Aeros yemke i Gravimetrii, v. 2, pp. 12-25, 1943.

SUDAKOV, S. G., Development of the State Geodetic Service in the USSR during 25 years, Sbornik Nauchno-Tekhnicheskikh i Prozvodstvennykh Statey po Geodezii, Kartografii, Topografii, Aeros yemke i Gravimetrii, v. 5, pp. 3-24, 1944.

URMAYEV, N. A., Reduced length of a geodetic line, Sbornik Nauchno-Tekhnicheskikh i Proizvodstvennykh Statey po Geodezii, Kartografii, Topografii, Aeros yemke i Gravimetrii, v. 1, pp. 19-25, 1941.

VIROVETS, A. M., Allowance for the influence of short-period errors in the division of the limb in the triangulation work of I class, Sbornik Nauchno-Tekhnicheskikh i Proizvodstvennykh Statey po Geodizii, Kartografii, Topografii, Aeros yemke i Gravimetrii, v. 2, pp. 43-53, 1943.

VIROVETS, A. M., Astronomic and geodetic network of the USSR, Sbornik Nauchno-Tekhnicheskikh i Proizvodstvennykh Statey po Geodezii, Kartografii, Topografii Aeros yemke i Gravimetrii, v. 5, pp. 24-38, 1944.

VYDRIN, F. I., Geodesy and the markscheider scheme, Moscow, Coal Techn. Pub., 1948.

BIBLIOGRAPHY: SEISMOLOGY

BECKER, FERDINAND, Sea waves and microseisms, Deutsche Hydrographische Zs., Hamburg, v. 2, pp. 67-78, 1949 (in German with summary in English).

BULLEN, K. E., Introduction to the theory of seismology, Cambridge Univ. Press, 276 pp. + 43 figs., 1947 [abstr. in Appl. Mech. Rev., v. 2, p. 191, 1949].

KORIDALIN, E. A., A study of the structure of the Earth's crust by seismic methods, Akad. Nauk SSSR, Moscow, 75 pp. + illus., 1939.

LANGFORS, U., Diminution of the Earth tremors caused by explosion, Tekn. Tidskr., v. 79, pp. 141-148, February 1949 (in Swedish) [abstr. in Phys. Abstr., v. 52, p. 352, 1949].

MILNE, W. G., Bibliography of seismology, items 6858-7003, July to December, 1948, Pub. Dominion Obs., Ottawa, v. 14, no. 4, pp. 70-95, 1949.

PENDSE, C. G., On the theory of seismometers, Part II, Phil. Mag., v. 39, pp. 985-988, December 1948 [abstr. in Phys. Abstr., v. 52, p. 352, 1949].

BIBLIOGRAPHY: METEOROLOGY

BAATARD, FRANÇOIS, La mécanique aléatoire et le problème de la turbulence, Bull. Tech. Suisse Romande, Stat. Centrale Suisse Mét., Zurich, 35 pp., 1948.

BLEEKER, W.; HEIERMAN, J. H.; and SCHMIDT, F. H., De meteorologische grondslagen van het zweefvliegen, "Bibliotheek van de zweefvlieger" (deel V), N. V. Leidse Vitgeversmaatschappij, 1948 (On the meteorological problems in soaring), Abstract in Ciel et Terre, v. 65, p. 123, 1949.

BOFFI, JORGE A., Efecto de la Cordillera de los Andes en la circulación general del aire sobre la República, Argentina, An. Soc. Cient., Argentina, v. 147, pp. 126-140, 1949 (summary in English).

BOSSOLASCO, MARIO, Le precipitazioni nevose nell'Italia settentrionale, Geofis. Pura e Applicata, Milano, v. 13, ... , 28 pp., 1948.

BOSSOLASCO, MARIO, Le correnti dell'alta troposfera e della stratosfera inferiore sulle regioni equatoriali, Geofis. Pura e Applicata, Milano, v. 14, fasc. 1-2, 12 pp., 1949.

CHU, COCHING, LEE, JOHN and CHANG, PAOKUN, The temperature of China, Inst. Met. Acad. Sinica, Nanking, 934 pp., 1940.

COURT, ARNOLD, Refractive temperature, J. Franklin Inst., v. 247, pp. 583-595, 1939.

DAMMANN, W., Witterungsgeschichte Mitteleuropas seit 1881, An. Met., Hamburg, v. 1, pp. 268-277, 1948.

FOLEY, JAMES C., Frost in the Australian region, Govt. Printer, Melbourne, pp. 15-142, 1945.

FRANKENBERGER, E., Uber den Austauschmechanismus der Bodenschicht und die Abhängigkeit des vertikalen Massenaustausches vom Temperaturgefälle nach Untersuchungen an den 70 m hohen Funkmasten in Quickborn, Holstein, An. Met., Hamburg, pp. 3-23, 1948 (summary in English).

GEORGE, P. A., Low stratus clouds over Bangalore, India Met. Dept., Sci. Notes, v. 10, pp. 119-132 + 12 fig., 1946.

GEORGI, J., Bemerkungen zur glazialen Antizyklone, An. Met., Hamburg, v. 1, pp. 277-283, 1948.

GLADWIN, HAROLD STERLING, Tree-ring analysis; tree-rings and droughts, Priv. print. for Gila Pueblo, Globe, Ariz., 36 pp., 1947.

HAUDE, W., Verdunstung und Wasseranspruch von Kulturpflanzen, An. Met., Hamburg, v. 1, pp. 283-288, 1948.

HESSE, W., Über die Ergebnisse der Lebensgeschichte von Kaltlufttropfen, An. Met., Hamburg, v. 1, pp. 289-290, 1948.

JORGENSEN, DONALD, L., An objective method of forecasting rain in Central California during the raisin-drying season, Mon. Wea. Rev., v. 77, pp. 31-46, 1949.

KOPPE, H., Kalendermässige Bindung im Witterungsablauf und kosmische Steuerung, An. Met., Hamburg, v. 1, pp. 294-306, 1948.

KOSIBA, ALEKSANDER, Klimat ziem Slaskich, Wydawnictwa Inst. Slaskiego, Zagadnienia Gospodarcze Slaska, Katowice-Wroclaw, Poland, ser. 2, no. 9, 125 pp., 1948.

KRUHL, H., Zur Anwendung der Raethjun'schen Zyklonentheorie, An. Met., Hamburg, v. 1, pp. 301-307, 1948.

MIDDLETON, WILLIAM EDGAR KNOWLES, Meteorological instruments, 2d ed. rev., Toronto, Univ. of Toronto Press, 227 pp., 1947.

MILLER, JAMES, E., Studies of large scale vertical motions of the atmosphere, prepared from reports by Eugene Aubert, Alfred K. Blackadar, and others, Dept. Met., New York Univ., 109 pp., 1948.

MONTGOMERY, RAYMOND BRAISLIN; ARMSTRONG, JOHN C.; BYERS, HORACE R.; and OTHERS, Convection patterns in the atmosphere and ocean, New York Acad. Sci., pp. 705-844, 1947.

NEWMAN, B. W., and McCANN, A., Weather conditions affecting aviation over the Tasman Sea, part IV: Flying conditions over the Tasman Sea (1940-1944), Govt. Printer, Melbourne, 20 pp., 1946.

PIERY, MARIUS, Le climat de Lyon et de la région lyonnaise, Cartier Lyon, 389 pp., 1946.

POLLI, SILVIO, Su di un microbarografo modificato, An. Geofis., Ist. Talassografico, Trieste, v. 2, pp. 103-112, 1949.

PRIESTLEY, C. H. B., Atmospheric pressure changes: the importance of deviations from the balanced (gradient) wind, Australian J. Sci. Res., ser. A, v. 1, pp. 41-57, 1948.

RAETHJEN, P., Die Bedeutung atmosphärischer Austauschvorgänge für die Entstehung der Zyklonen, An. Met., Hamburg, v. 1, pp. 340-345, 1948.

REGENER, E., Das atmosphärische Ozon, Geophys., Dieterich'sche Verlagsbuchandlung, Wiesbaden, pt. 2, v. 18, pp. 297-307, 1948.

REIDAT, R., Der Jahresgang des Nebels in Deutschland, An. Met., Hamburg, v. 1, pp. 307-312, 1948.

ROLL, H. U., Über die vertikale Temperaturverteilung in der wassernahen Luftschicht, An. Met., Hamburg, v. 1, pp. 353-360, 1948 (summary in English).

ROSHARDT, AURELIAN P., Der Winter in der Innerschweiz, eine vergleichende Studie auf Grund zwanzigjähriger Beobachtung, Mitt. Natur. Gesellschaft, Luzern, v. 15, 143 pp. 1946.

SAWYER, J. S., Cooling of air by rain as a factor in convection, Met. Off., Air ministry, Prof. Notes no. 96, pp. 2-11, 1949.

SEILKOPF, H., Spezielle Grosszirkulation und Witterung, An. Met., Hamburg, v. 1, pp. 312-326, 1948

THAMS, CHR., Mittelwerte der Globalstrahlung in Zürich, Natur. Gesellschaft, Zürich, v. 90, pp. 26 35, 1945.

THAMS, J. C., Erfahrungen mit einem Kompensationspyrheliometer, Jahresbericht der Naturforschen den Gesellschaft Graubündens, Mitt. Schweiz. Met. Zentralanstalt, Zürich, v. 81, pp. 74-84, 194

VANDENPLAS, A., La temperature au Congo belge, Bruxelles, 189 pp., 1947.

VENHO, S. N., A study of meteorological phenomena connected with the outflow of polar air masses over Western Europe, Mitt. Met. Zentralanst., Zürich, no. 33, 75 pp., 1949.

WAGNER F., Mammatusform als Anzeichen für Absinkbewegung in Wolkenluft, An. Met., Hamburg, v. 1, pp. 336-340, 1948.

WALDEN, H., 25-tägiger Temperaturzyklus im Sommerhalbjahr 1947, An. Met., Hamburg, v. 1, pp. 172-181, 1948.

WALKER, GILBERT, T., Some correlation coefficients between certain upper air data, Met. Off., Air ministry, Prof. Notes no. 97, pp. 2-7, 1949.

YAKUBOV, T. F., Deserts and their study, Union Geogr. Soc., v. 80, p. 179, 1948.

YERKES OBSERVATORY, Symposium, the atmospheres of the Earth and planets; papers presented at the Fiftieth Anniversary of the Observatory, Sep., 1947, Chicago Univ. Press, 366 pp., 1949.

YUDIN, M. I., Daily course of temperature of the air and convective heat exchange, Izv. Akad. Nauk SSSR, Ser. Geog. Geofiz., Moscow, v. 12, no. 4, 307 pp., 1948 (in Russian).

BIBLIOGRAPHY: TERRESTRIAL MAGNETISM AND ELECTRICITY

BAILEY, R., Canadian aerial magnetic surveys (M. A. D.), Canadian J. Res. F., v. 26, pp. 523-539, 1948 [abstr. in Phys. Abstr., v. 52, pp. 444, 1949].

EIGENSON, BORIS S., Solar activity and its terrestrial effects, Moscow, Govt. pub. techn. theor. lit., 323 pp.,+ diagrs., 1948.

ERRULAT, FRITZ, Measurement of the horizontal intensity of the Earth's magnetic field in the Baltic 1938 and 1939 with the plunged double-compass, Deutsche Hydrographische Zs., Hamburg, v. 2, pp. 1-21, 1949 (in German with summary in English).

LAHAYE, EDMOND, Les perturbations de la déclinaison magnétique enregistrées à Uccle pendant la période 1939-1943, Inst. R. Mét. Belg., Mém., v. 21, pp. 3-47, 1946.

LOEB, L. B., The mechanism of lightning discharge, J. Franklin Inst., v. 246, pp. 123-148, 1948 [abstr. in Phys. Abstr., v. 52, p. 353, 1949].

MACHT, HANS G., On the physical representation of the geomagnetic residual field, Deutsche Hydrographische Zs., Hamburg, v. 2, pp. 35-43, 1949 (in German with summary in English).

MALMFORS, KARL GUSTAV, Determination of orbits in the field of a magnetic dipole with applications to the theory of the diurnal variation of cosmic radiation, Arkiv Matematik, Astronomi Och Fysik, K. Svenska Vetenskapsakademien, v. 32, no. 8, 64 pp., 1945.

MEYER, OTTO, Measuring of the vertical intensity of the Earth's magnetic field at sea with the magnetron, Deutsche Hydrographische Zs., Hamburg, v. 2, pp. 22-34, 1949 (in German with summary in English).

MITKEVICH, VLADIMIR F., The magnetic field and its changes, pub. Academy of Sciences USSR, Moscow, 354 pp. + diagrs., 1946.

ROMAÑA, PUJÓ, ANTONIO, and TORROJA, MENÉNDEZ, JOSÉ, M., El predominio de las manchas solares al este del meridiano central y la inclinación de sus ejes hacia el oeste, Publ. Observatorio del ebro, Tarrangona, Misc. 3, no. 218, 23 pp., 1948.

SIMPSON, GEORGE, Atmospheric electricity during disturbed weather, Met. Off. Geophys. Mem. no. 84, v. 10, 51 pp.,+ 18 pl., 1949.

SLAUCITAJS, L., Some notes on secularvariation, Contributions of Baltic Univ., Pinneberg, no. 63, 4 pp., 1948.

STOFFREGEN, W., Ionosphere reflections recorded mechanically by means of a repetition frequency converter, Forsvarets Forskn Inst. Arb., pp. 178-183, 1947 (in English) [abstr. in Phys. Abstr v. 52, no. 618, p. 352, 1949].

WALÉN, CLAËS, On the theory of sun-spots, Arkiv för Matematik, Astronomi och Fysik, Stockholm, v. 30, no. 15, 85 pp., 1944.

ZABOROVSKY, ALEXANDER I., Electric prospecting, Govt. fuel tech. lit, Moscow, 443 pp. + illus. + diagrs., 1943.

BIBLIOGRAPHY: OCEANOGRAPHY

ARTHUR, R. S., Forecasting Hawaiian swell from January 2 to 5, 1947, Bull. Amer. Met. Soc., v. 29, pp. 395-440, 1948.

BOEHNECKE, G. and NEUMANN, G., Allgemeine Ozeanographie, Geophys., Dieterich'sche Verlagsbuchhandlung, Wiesbaden, pt. 2, v. 18, pp. 76-107, 1948.

BUCH, KURT, Amnesomsättingen i Skärgårdsvattnen, Skärgårdsboken, pp. 134-146, Helsingfors, 1948.

CARLOTTI, P. L., Études d'obstacles immergés produisant un changement de fréquence de la houle océanique et destinés à supprimer la barre en certains points du littoral africain, Bull. Assn. Tech. Marit. Aéronaut., no. 47, pp. 275-296, 1948.

CUBILLIOS MOYA, R., Determinación del oxigeno en el agua de mar, Rev. Biol. Mar., Chile, v. 1, pp. 46-56, 1948.

DARMOIS, R., and DARMOIS, J., Déterminations physicochimiques sur l'eau méditerranéenne dans la region de Monaco, C.-R., v. 228, pp. 417-418, 1949 [abstr. in Chem. Abstr., p. 4058, 1949].

DURST, C. S., Slope of the ocean, Nature, v. 163, pp. 993-994, 1949.

EWING, M., and WORZEL, J. L., Propagation of sound in the ocean, long-range sound transmission, Mem. Geol. Soc. Amer., no. 27, v. + 35 pp., 4 pl., 1948.

FRANKCOM, C. E. N., Variation of temperature in a free-water surface, Met. Mag., v. 77, pp. 281-282, 1948.

GHEORGIU, V., and CALINECENCO, N., The pH value and silinity of the water of the Black Sea, Rev. Stiintifica "V. Adamachi," v. 32, pp. 43-45, 127-129, 1946 (in Roumanian) [abstr. in Chem. Abstr. 5763e, 1947].

GRANQVIST, GUNNAR, Den Finländska Skargårdens hydrografi, Skårgardsboken, pp. 104-133, Helsingfors, 1948.

GROEN, P., Two fundamental theorems on gravity waves in inhomogeneous incompressible fluids, Physica, v. 14, pp. 294-300, 1948.

HANSEN, W., Bewegungsvorgänge in Meere, Geophys., Dieterich'sche Verlagsbuchhandlung, Wiesbaden, pt. 2, v. 18, pp. 108-131, 1948.

HARDENBERG J. D. F., Onderzoek en problemen der Indische zeeën, Chron. Nat., v. 104, pp. 337-344, 1948.

HARNWELL, G. P., Submarine physics, Amer. J. Phys., v. 16, pp. 127-139, 1948.

HELA, I., Ueber die Schwankungen des Wasserstandes in der Ostsee mit besonderer Berücksichtigung des Wasseraustausches durch die dänischen Gewässer, An. Acad. Sci. Fennicae, Ser. A, no. 23-28, pp. 1-108, 1944.

HORN, W., Gezeiten des Meeres, Geophys., Dieterich'sche Verlagsbuchhandlung, Wiesbaden, pt. 2, v. 18, pp. 132-163, 1948.

INMAN, DOUGLAS L., Sorting of sediments in the light of fluid mechanics, J. Sed. Petrol., v. 19, pp. 51-70, 1949.

JOSEPH, J., Meereskundliche Messgerate, Geophys., Dieterich'sche Verlagsbuchhandlung, Wiesbaden, pt. 2, v. 18, pp. 178-214, 1948.

KALLE, K., Physik und Chemie des Meeres, Geophys., Dieterich'sche Verlagsbuchhandlung, Wiesbaden, pt. 2, v. 18, pp. 164-177, 1948.

KELLER, W. O., and FOLEY, R., Missouri River sediments in river water, ocean water, and sodium oxalate solution, J. Sed. Petrol., v. 19, pp. 78-81, 1949.

KING, C. A. M., and WILLIAMS, W. W., The formation and movement of sand bars by wave action, Geogr. J., v. 103, pp. 70-85, 1949.

KRICK, IRVING P., Study of oceanographic factors for Texas offshore drilling site, Oil and Gas J., v. 48, pp. 261-275, 1949.

LABAYE, G., Note sur le débit solide des cours d'eau, Houille Blanche, v. 3, no. spécial, pp. 600-627, 1948.

LEGENDRE, R., Les industries chemiques de la mer, Bull. Inst. Océan. Monaco, no. 922, 15 pp., 1947.

MERCANTON, P-L, Marées du lac Leman, Bull. Soc. Vaudoise Sci. Nat., v. 64, pp. 73-75, 1948.

NIZERY, A., Étude des déformations de la houle au voisinage d'une jetée, Houille Blanche, Fr., v. 3, no. spécial, pp. 628-633, 1948.

PEKERIS, C. L., Propagation of sound in the ocean. Theory of propagation of explosive sound in shallow water, Mem. Geol. Soc. Amer., no. 27, vii + 117 pp., 1948.

ROMBAKIS, S., Der Einfluss meteorologischer Faktoren auf die Topographie des physikaliscnen Meeresniveaus. Zs. Met., v. 2, pp. 300-305, 1948.

SAMALEA, JUAN A., Exploración del "banco del Xauen", accidente topografico descubierto frente al Peñón de Vélez de la Gomera, Bol. Inst. Españ. Oceánogr., no. 16, 7 pp., 1949.

SHEPARD, F. P., Dangerous currents in the surf, Phys. Today, v. 2, pp. 20-29, 1949.

SHEPARD, F. P., and EMERY, K. O., Bottom-sediment charts of the Asiatic continental shelves, Bull. Geol. Soc. Amer., v. 57, pp. 1229-1230, 1946.

STROBAND, H. J., Ein bijdrage tot de kennis van de getijberekening op benedenrivieren en zeearmen, Ingenieur, v. 59, no. 36, pp. B89-B95, 1947.

TRASK, PARKER D.; PHLEGER, FRED B.; and STETSON, HENRY C., Recent changes in sedimentation in the Gulf of Mexico, Science, v. 106, pp. 460-461, 1947.

UPSON, J. E., Late Pleistocene and Recent changes of sea level along the coast of Santa Barbara County, California, Amer. J. Sci., v. 247, pp. 95-115, 1949.

VERLOOY, J., Over de invloed van de neerslag op de waterstenden in het Scheldebekken, An. Trav. Publ. Belg., v. 48, pp. 349-359, 1947.

WORZEL, J. L. and EWING, M., Propagation of sound in the ocean, explosion sounds in shallow water, Mem. Geol. Soc. Amer., no. 27, vi + 53 pp, 1948.

BIBLIOGRAPHY: VOLCANOLOGY

AFANASEV, G. D., Phenomena of the microclinization of granodioritic batholithic intrusions of the western caucasus type, Isvest. Akad. Nauk, SSSR, Ser. Geol., no. 3, pp. 27-44, 1949.

ANDREATTA, CIRO, Appunti sopra l'origine dei graniti, Rend. soc. mine al. Ital., v. 3, pp. 43-48, 1946.

BER, A. G., On the exposed effusive rocks in the Mesozoic of the central part of the Turgaisk depression, Dok. Akad. Nauk SSSR, v. 67, pp. 121-124, 1949.

BRUNO, MARIA, Un caratteristico filone basico zonato a noduletti quarzosi del M. Frerone (Amadello meridionale), Rend. soc. mineral. Ital., v. 3, pp. 87-106, 1946.

CLEGG, E. L. G., Notes on tin and Wolfram in Burma and India, Rec. Geol. Surv. India, Calcutta, v. 76, 168 pp., 1948.

COTELO NEIVA, J. M., Ovbasalto da Nazaré, Pub. Mus. Lab. Min. Geol. Fac. Sci. Porto, no. 49 (2), 12 pp., 1948.

COTELO NEIVA, J. M., Filão de microsientito augítico no monte de S. Bartolomeu (Nazaré), Pub. Mus. Lab. Min. Geol. Fac. Sci. Porto, no. 50 (2), 9 pp., 1948.

DOS SANTOS PEREIRA, JUDITE, Rochas ígneas provenientes do Torrão (alcacer do Sal), Pub. Mus. Lab. Min. Geol. Fac. Sci. Porto, no. 52 (3), 11 pp., 1948.

D'ZOTSENIDZE, G. S., and SKIRTLADZE, N. I., On the presence of the fundamental phase in the older effusive volcanic (rocks of) Gruz, Dok. Akad. Nauk SSSR, v. 66, pp. 689-692, 1949.

EINARSSON, TRAUSTI, Über das Wesen der heissen Quellen Islands Vísindafélag, Íslendinga, v. 26, 1942.

FONG, K. L., Field evidences of supergene enrichment of the copper deposits of Szechuan, Sikang and Yunnan, Bull. Geol. Soc. China, v. 27, pp. 347-358, 1947.

GUIMARÃES, DJALMA, Jazidas minerais de origem magmática, Anais. Segundo Cong. Pomam. Eng. Min. and Geol., v. 2, pp. 9-22, 1946.

HOLMES, ARTHUR, Monazite as a geological timekeeper, Proc. R. Soc. Edinb., v. 63, pp. 115-124, 19

JAHN, WILLIAM F. and PESONEN, PAUL E., Investigation of the tin-bearing pegmatites in the Tinton Area, South Dakota, U. S. Bur. Mines, Rep. of Invest. No. 4484, 25 pp., 1949.

JÉRÉMINE, E., Sur quelques roches provenant du Maroc Oriental aiounite et mestigmérite, Notes et Mém., Morocco, no. 71, Notes Ser. Géol., v. 1, pp. 67-71, 1948.

JUGOVICS, L., Beiträge zur Kenntniss der Gesteine von Ost-Celebes, Geol. Hung., Budapest, v. 8, pp. 1-124, 1944. (Rocks are intrusive, range from aplite and quartz porphyry to harzburgite and peridotite, but most of those described are ultrabasic.)

KATKOVA, N. C., The role of potash metasomatism in the generation of (some) caledonian granitic intrusives (Tyan-Shan), Dok. Akad. Nauk SSSR, v. 66, pp. 467-470, 1949.

LEGRAND, R. and MORTELMANS, G., Un contact de la diorite quartzifère de Lessines et de l'Ordovicien, Bull. Soc. Belge Géol., v. 57, pp. 642-673, 1948.

LOBANOVA, V. V., On the petrography of the potassic rocks of the Eastern Pre-Carpathians, Dok. Akad. Nauk SSSR, v. 66, pp. 1161-1164, 1949.

MARCET RIBA, J., Mudanzas magmaticas (de Gerona), Estudios Geól., Inst. Invest. Geól. "Lucas Mallada," Madrid, no. 9, pp. 211-218, 1948.

MARCET RIBA, J., Períodos eruptivos de la provincia de Gerona, Estudios Geól., Inst. Invest. Geól. "Lucas Mallada," no. 9, pp. 189-204, Madrid, 1948.

MARCET RIBA, J., Provincias petrográficas (de Gerona), Estudios Geól., Inst. Invest. Geól. "Lucas Mallada," Madrid, no. 9, pp. 205-209, 1948.

MORIN, PH., Note préliminaire sur le Massif de Microgranite de Boujada (Région de Taza), Notes et Mém., Morocco, no. 71, Notes Ser. Géol., v. 1, pp. 73-80, 1948.

MORTELMANS, G., Le granite de Noqui et ses phénoménes de contact, Bull. Soc. Belge Géol., v. 57, pp. 519-540, 1948.

NADIRADZE, V. P., and ABAMELIK, E. M., On the petrography of neo-intrusions of the Tkemlovan region of the Georgian SSR, Dok. Akad. Nauk SSSR, v. 64, pp. 121-124, 1949.

NICKEL, ERWIN, Beiträge zur Petrographie des Odenwaldes, IV, Wechselbeziehungen zwischen Diortien, Graniten und Schiefern in Wesltichen Odenwald, Heidelberger Beitr. Min Petr., v. 1, pp. 427-470, 1948.

NICKEL, ERWIN, Plagioklaseinschlüsse in Sanidineinsprenglingen der Nevadite von den Cerros Alifragas, Heidelberger Beitr. Min. Petr., v. 1, pp. 403-406, 1948.

NYSTRÖM, T., Some alkaline rocks of Shansi Province, Bull. Geol. Soc. China, v. 27, pp. 55-83, 1947.

OFTEDAHL, CHRISTOFFER, Studies on the igneous rock complex of the Oslo region, IX, the feldspars, Skript. Norsk. Vidensk.-Akad. Oslo, Math.-Nat. Kl., pp. 77, 1948.

PÉREZ MATEOS, JOSEFINA and T. GÁRATE COPPA, MARÍA, Estudio geoquímico de sulfuros de cobre, Estudios Geól., Inst. Invest, Geól. "Lucas Mallada," Madrid, no. 9, pp. 159-176, 1948.

POLDERVAART, ARIE, Three methods of graphic representation of chemical analyses of igneous rocks, Trans. R. Soc. S. Africa, v. 32, pp. 177-188, 1949.

READ, H. H., Metamorfismo e actividade ignea, Pub. Mus. Lab. Min. Geol. Fac. Sci. Porto, no. 51, (3), 45 pp., 1948.

RODOLICO, F., and PIERUCCINI, R., Il berillio nella differenziazione del magma selagitico. Rend. soc. mineral. Ital., v. 2, pp. 41-46, 1942.

SAN MIGUAL ARRIBAS, ALFREDO, Sobre unas erupciones volcanicas en la zona Prat de compte-Pauls (Tarragona), Estudios Geól., Inst. Invest. Geól. "Lucas Mallada," Madrid, no. 9, pp. 51-84, 1948.

SAN MIGUEL ARRIBAS, ALFREDO and SAN MIGUEL DE LA CAMARA, M., Las rocas eruptivas y metamórficas de las comarcas del Priorato y Campo de Tarragona, Estudios Geól., Inst. Invest. Geól. "Lucas Mallada," Madrid, no. 9, pp. 107-132, 1948.

SCHIAVINATO, GIUSEPPE, Ricerche chimicopetrographiche sui Monti Berici, Rend. soc. mineral. Ital., v. 3, pp. 241-263, 1946.

SMALES, A. A., Analysis of Bodimin Moor Monazite for lead, thorium and uranium, Proc. R. Soc. Edinburgh, v. 63, pp. 125-129, 1948.

STARK, M., Basische Gesteine der Euganeen, IV, Min. Petr. Mitt., v. 55, pp. 213-270, 1943.

SUESS, H. E., Die kosmische Häufigkeit der chemischen Elemente, Experientia, v. 5, pp. 266-270, 1949

TERMIER, HENRI; TERMIER, GENEVIÈVE; and JOURAVSKY, G., Une roche volcanique à gros grain de la famille des ijolítes: La Talzastite: Notes et Mém., Morocco, no. 71, Notes Ser. Géol. v. 1, pp. 81-120, 1948.

VASSOEVICH, H. B., Stratification (by) settling-differentiation, Dok. Akad. Nauk SSSR, v. 66, pp. 685-688, 1949.

WALKER, FREDERICK, The paragenesis of a hornblende lamprophyre from Bellville, near Cape

Town Trans. R. Soc. S. Africa, v. 32, pp. 189-194, 1949.

WANG, C. C., On the magmatic differentiation of the Tzuchinshan alkaline rocks, Linhsien, Shansi, Bull. Geol. Soc. China, v. 27, pp. 227-242, 1947.

WINKLER, HELMUT G. F., Zuzammenhand zwischen Kristallgrösse und Salbandabstand bei magmatischen Gang-Intrusionen, Heidelberger Beitr. Min. Petr. v. 1, pp. 251-268, 1949.

BIBLIOGRAPHY: HYDROLOGY

ABD-EL-AL, IBRAHIM, L'aridité et l'écoulement dans les pays du Moyen-Orient, Pub. Tech. Scien., École Franc. Ingin., Beyrouth, no. 14, 1948.

ASSOCIATION INTERNATIONALE D'HYDROLOGIE SCIENTIFIQUE, Réunion de Washington, General Assembly in Washington in 1939, v. 1 and 2, Intern. Assc. Hydrology, IUGG, Each about 400 pp., including a number of papers, pages not numbered in series.

BARROWS, H. K., Floods, their hydrology and control, McGraw-Hill, 432 pp., 1948.

BERG, L. S., Hydrometeorological Station Imeni V. K. Davydov, Union Geogr. Soc., v. 80, p. 182, 1948.

DEBENHAM, FRANK, Report on the water resources of Bechuanaland Protectorate, Northern Rhodesia, Nyasaland Protectorate, Tanganyika, Kenya, and Uganda, Colonial office, (London) Col. Res. Pub., no. 2, 85 pp., 1948.

DEVROEY, E. J., À propos de la stabilisation du niveau du Lac Tanganika et de l'amélioration de la navigabilité du Fleuve Congo, Inst. R. Col. Belge, Brussels, v. 5, no. 3, 135 pp. + 18 pl. + 6 pl., 1949.

FRIEDRICH, W., Hydrographie, Geophysik, Pt. II, Naturforschung und Medizin in Deutschland, 1939-1946, v. 18, pp. 215-249, Dietrich'sche Verlagsbuchhandlung, (no date).

GOLAB, JOŹEF, Short characteristics of the springs in the Krzeszowice region near Cracow, Geol. Inst., Poland, Bull. 28, pp. 26-38, 1947 (in Polish, with summary in English).

GOLAB, JÓZEF, Hydrogeological characteristics of the Gubalówka Range near Zakopane, Geol. Inst. Poland, Bull. 32, pp. 39-46, 1947 (in Polish, with summary in English).

FISHEL, V. C., Ground-water resources of Republic County and northern Cloud County, Kansas, State Geol. Surv. Kan., Bull. 73, 194 pp., 1948.

FORSCHUNGSANSTALT FUR GEWÄSSERKUNDE, Abfluss-Messregeln für Flügel, Bielefeld, v. 3, 40 pp., 1948.

IMHOFF, KARL, Die Abwasserlast der deutschen Flüsse, Zs. Gesundheitsingenieur, v. 4, 6 pp., 1947.

IMHOFF, KARL, and WAGNER, HUBERT, Zur Reinhaltung der deutschen Flüsse, Arbeitsbereich der Forschungsanstalt fur Gewässerkunde, Bielefeld, 5 pp., 1949.

JOHNSSON, O. HARALD, Thermichydrological studies of Lake Klämmingen, Med. Geog. Inst. Stockholms Hogskola, no. 70, 154 pp., 1946 (in Swedish with summary in English).

KITTRELL, F. W., and QUINN, J. J., Multipurpose reservoirs and downstream water supply, Eng. News Rec., pp. 42-45, May 26, 1949.

LANSFORD, W. M., and MITCHELL, W. D., An investigation of the backwater profile for steady flow in prismatic channels, Univ. Ill., Engr. Exp. Sta. Bull., no. 381, 94 pp., 1949.

LATTA, BRUCE F., Ground-water supplies at Hays, Victoria, Walker, Gorham, and Russell, Kansas, with special reference to future needs, State Geol. Surv. of Kansas, Bull. 76, pp. 121-196, 1948.

PENMAN, H. L., Evaporation in nature, Rep. Phys. Soc. Progr. Phys., v. 11, pp. 366-388, 1946-1947 [abstr. in Phys. Abstr., v. 52, no. 618, p. 352, 1949].

REBINDER, PETER A., Making soils impermeable to water and mechanically erosion resistant, Akad. Nauk SSSR, Moscow, 20 pp. + illus., 1942.

SCHROEDER, G., Die wasserwirtschaftliche Generalplanung, Veröffentlichung der Forschungsanstalt für Gewässerkunde, Windelsbleiche bei Bielefeld, 186 pp., 1948.

SOBOLEV, S. S., Development of erosion processes in the European territory of the USSR, and how to combat them, Academy of Sciences USSR, Moscow, 305 pp. (?), 1948.

THOMPSON, HENRY D., Drainage evolution in the Appalachians of Pennsylvania, An. N. Y. Acad. Sci. v. 52, art. 2, pp. 31-62, 1949.

TRUPAK, N. G., Frozen soil in the construction industry, Govt. pub. constr. liter., Moscow, 320 pp., (?), 1948.

VISCHER, S. S., American dry seasons, Ecology, v. 30, pp. 365-370, 1949.

WALLÉN, CARL CHRISTIAN, Glacial-Meteorological investigations on the Kårsa Glacier in Swedish Lappland 1942-1948, Geogr. An. Stockholm, 240 pp., 1948-1949.

WILLIAMS, CHARLES C., Contamination of deep water wells in southeastern Kansas, State Geol. Surv. of Kan. Bull. 76, pp. 13-28, 1948.

ZINGG, TH; in der GAND, H.; SCHILD, M.; and BUCHER, E., Schnee und Lawinen im Winter 1946-1947, Winterberichte des Eidg. Inst. für Schnee-und Lawinenforschung, Davos-Weissfluhjoch, no. 11, 83 pp., 1949.

BIBLIOGRAPHY: TECTONOPHYSICS

ANDEREGG, HANS, Géologie des Isentals, Comm. Géol. Soc. Helv. Sci. Nat., Mat. Cart. Géol. Suisse, Berne, v. 77, 64 pp., 1940.

ANDREATTA, CIRO, La regola di orientazione die cristalli di ilivina nelle tettoni, Rend. soc. mineral. Ital., v. 3, pp. 41-42, 1946.

AUBERT, D., Monographie géologique de la Vallée de Joux, Comm. Géol. Soc. Helv. Sci. Nat., Mat. Cart. Géol. Suisse, Berne, v. 78, 134 pp., 1943.

BELYAEVSKII, N. A., Alpine tectonics of Western Kuen-Lunya, Izvest. Akad. Nauk SSSR, Ser. Geol., no. 2, pp. 29-42, 1949.

BOGDANOV, A. A., Unconformities; types, meaning and (methods of) investigation, Izvest. Akad. Nauk SSSR, Ser. Geol., no. 2, pp. 43-60, 1949.

BONI, A., and **BALCONI, M.,** Le formazioni scistoso-cristalline ed eruttive dell' Alta Val Prompia, Rend. soc. mineral. Ital., v. 2, pp. 25-27, 1942.

BRÜCKNER, WERNER, Tektonik des oberen Schächentals (Kanton Uri), Beiträge Geol. Karte Schweiz, 80 pp., 1943.

BÜRGL, HANS, Zur Stratigraphie und Tektonik des oberöstereichischen Schliers, Verhandlungen Geol. Bundesanstalt, Vienna, pp. 122-172, 1946, pp. 123-163, 1949.

CAMPANA, BURNO, Géologie des nappes préalpines au Nordest de Château-d' Oex, Comm. Géol. Soc. Helv. Sci. Nat., Mat. Cart. Géol. Suisse, Berne, v. 82, 63 pp., 1943.

CHIA-YIN, WANG, A segment of Nanlin Range from Kianghua to Lanshan Districts, southwest Hunan, Bull. Geol. Soc. China, v. 27, pp. 359-365, 1947. (Account of structure with geologic map, with descriptions of feather joints, veins, and slickensides. Attitudes of all structures are given, and a stereographic projection of the slickensides, with inferred directions of motion is included.)

CHRISTA, E., Über Gefügekunde als neuen Forschungszweig der Petrographie, Sitz. Phys.-Med. Societät Erlangen, v. 72, pp. 229-256, 1942.

DEMAY, ANDRÉ, Tectonique antéstephanienne (Upper Carboniferous) du Massif Central, Mém. Carte Géol. Det. France, Paris, 259 pp., 1948.

ESKOLA, P. E., The problem of mantled gneiss domes, Q. J. Geol. Soc. London, v. 104, pp. 461-476, 1949.

FRASSON, BRUNO ANTONIO, Geologie der Umgebung von Schwarzenburg, Comm. Géol. Soc. Helv. Sci. Nat., Mat. Cart. Géol. Suisse, Berne, v. 88, 62 pp., 1947.

HO, T. L., Petrofabric analysis by means of X-rays, Bull. Geol. Soc. China, v. 27, pp. 389-398, 1947. (Discusses theory and techniques and gives three examples, (1) quartz fabric in a quartzite, (2) quartz fabric in a quartz-mica schist, and (3) the fine structure of agate.)

HOU, T. F., Outline of the diastrophic history of Szechuan and its relation to mineral deposits, Bull. Geol. Soc, China, v. 27, pp. 253-263, 1947.

HUME, W. F., Terrestrial theories; a digest of various views as to the origin and development of the Earth and their bearing on the geology of Egypt, Geological Survey of Egypt, Cairo, 522 pp.,+ 160 pp. index, 1948.

KENT, P. E., A structure contour map of the buried Pre-Permian rocks of England and Wales, Proc. Geol. Assoc., v. 60, pp. 87-104, 1949.

KOLBIN, M. F., New data on the geomorphology, tectonics, and gravitation of the dome-like elevations in the Stalingrad region, Bull. Mosk. Obshchest. Ispytat. Prirody, Otdel Geol., v. 23, pp. 83-91, 1948.

KORIN, I. Z., On the question of recent faulting in the southern Urals, Bull. Mosk. Obshchest. Ispytat Prirody, Otdel Geol., v. 23, pp. 79-82, 1948.

KOSYZIN, V. A., On the application of the principle of vertical crushing to the shallow tectonic structures of the Russian Platform, Bull. Mosk. Obshchest. Ispytat. Prirody, Otdel. Geol., v. 23, pp. 61-68, 1948.

KRONOMKIN, P. H., On certain fundamental questions of tectonics, Bull. Mosk. Obschest Isphytat. Prirody, Otdel Geol., v. 23, pp. 103-110, 1948.

KUZNETSOV, E. A., Tectonics of the central Ural, Akad. Nauk SSSR, Inst. Geol. Nauk, Moscow, 139 pp. + illus. maps + profiles, 1941.

KUZNETSAB, B. A., Tectonic framework of Tuva and its relation to the structure of the altai-Sayan range, Dok. Akad. Nauk SSSR, v. 64, pp. 553-556, 1949.

LEBEDEV, A. P., On the inner tectonics of the Yalping-ner gabbroic intrusion of the northern Urals, Dok. Akad. Nauk SSSR, v. 63, pp. 721-724, 1948.

LIV, K. C., An outline of the geological structure in the Weining-Shueicheng area, Kweichow, Bull. Geol. Soc. China, v. 27, pp. 373-388, 194. (Outline of the tectonic history of the area is included

MAGNANI, M., Su di un presunto giacimento di minerali di stagno nelle Alpi Carniche Rend. soc. mineral. Ital., v. 3, pp. 139-149, 1946.

MALEVANNYI, E. T., On the question of the Nikolaev fold, Dok. Akad. Nauk SSSR, v. 64, pp. 101-104, 1949.

RICHTER, G., Bedeutung der historischen Tektonik, Zs. Deut. Geol. Gesell., v. 98, pp. 188-193, 1946.

SCHÜLLER, A., Zur tektonischen Analyse der Münchberger Gneismasse, Zs., Deut. Geol. Gesell,, v. 97, pp. 66-94, 1945,

SEIDEL, GERHARD, Eine anschauliche Darstellung tektonischer Flächen im Diagramm, Glückauf, v. 85, pp. 337-342, 1949.

SHAKVARSTOVA, K. A., New data on the geology of the southwestern part of the Vitim Uplands, Bull. Mosk. Olshchestvo, v. 53, pp. 29-42, 1948 (in Russian; gives the stratigraphic and tectonic setting of the area and discusses its tectonic and magmatic cycles).

SMAKULA, ALEXANDER, and **KLEIN, M. W.,** The plastic deformation and crystal orientation of thallium halides, J. Optical Soc. Amer., v. 39, pp. 445-453, 1949,

USSR, ACADEMY OF SCIENCES, Tectonics of the U. S. S. R., Volume I, Tectonics of Central Kazakstan, 302 pp., 1948 (in Russian).

UMBGROVE, J. H. F., The root of the Alps, Kon. Ned., Akad. Weten., Proc., v. 51, pp. 761-775, 1948.

UMBGROVE, J. H. F., Origin of the Jura Mountains, Kon. Ned., Akad. Weten., Proc., v. 51, pp. 1049-1062, 1948.

VENING MEINESZ, F. A., About mountain-formation on the Earth, Proc. Kon. Ned. Akad. Weten., v. 51, pp. 929-938, 1948.

VOLFSON, F. I., Relation of endogenetic mineral deposits to megascopic tectonic brecciation, Izv. Akad. Nauk SSSR, Ser. Geol., no. 6, pp. 21-30, 1948 (in Russian).

VON WOLFF, F., Zur Probelmatik des pazifischen Erdraums, Zs., Deut. Geol. Gesell., v. 98, pp. 166-171, 1946.

NOTES AND PERSONALIA

NOTES

Corrigendum--The following correction is noted in the Transactions: Vol. 30, June 1949, in the paper by Gunnar M. Brune, pp. 398 and 399, Figures 2 and 3 are interchanged.

U. S. Geological Survey issues new index map of aerial photography of the United States--The fourth edition of the index map showing the status of aerial photography of the United States, with a related explanatory statement, has recently been issued by the Survey. Copies may be obtained by writing to the Survey in Washington, D. C.

New German publications in meteorology--The German publication, Die Grosswetterlagen Mitteleuropas, reviewing Northern Hemisphere weather month by month, began publication by the Deutscher Wetterdienst in der US-Zone, Bad Kissingen with data for the month of January, 1948. In 1948, this was an 8-page leaflet about 8" x 12". In 1949, the presentation of maps has been considerably improved, and the size is about 11 1/2" x 16 1/2". The same Service is also publishing Zugänge der Wetterdienstbibliotek, beginning in January 1949, covering many publications over the whole world. Deutsches Meteorologisches Jahrbuch, US-Zone, 1945, has also been published.

Continuation of geophysical seminars at the Cambridge Field Station of the United States Air Force--The series of seminars noted in the August issue of the Transactions [p. 615] at the Cambridge, Massachusetts, Field Station of the Air Force is continuing. The seminar of October 21, 1949, will relate to observational aspects of the general circulation under the leadership of Victor P. Starr; that of October 28 will relate to laboratory studies of de-ionization processes at ionospheric pressures, and will be lead by Osmund T. Fundingsland.

PERSONALIA

Charles C. Bates of the U. S. Navy Hydrographic Office spent July and August, 1949, at the Arctic Research Laboratory, Point Barrow, Alaska.

Wayne V. Burt of Scripps Institution of Oceanography has joined the staff of the Chesapeake Bay Institute of The Johns Hopkins University.

Luis R. Capurro has been appointed Commanding Officer of an Argentine survey ship.

J. W. E. Edmonson, until recently with the Shell Oil Co. in Houston, Texas, has resumed his studies as a graduate student at Texas College of Arts and Industries.

Thomas Alexander Gleeson has been appointed Assistant Professor of Meteorology at The Florida State University.

S. T. Harding, Professor of Irrigation at the University of California in Berkeley, has retired after 35 years of service.

Hector V. Iglesias has been appointed officer in charge of the Department of Hydrography and Meteorology of the Direccion General de Navagacion y Hidrografia, Buenos Aires, Argentina.

Dale F. Leipper of Scripps Institution of Oceanography has been appointed acting head of the newly-established Department of Oceanography at the Agricultural and Mechanical College of Texas.

Luna B. Leopold, Head, Department of Meteorology of the Pineapple Research Institute of Hawaii has resigned his position to return to his graduate studies at Harvard University.

John Lyman has been appointed Deputy Director of the Division of Oceanography in the U. S. Navy Hydrographic Office.

Samuel B. Morris, General Manager and Chief Engineer of the Department of Water and Power of Los Angeles, has been elected President of the Public Power Association.

Rodolfo N. Panzarini has been appointed Executive Officer of the Argentine cruiser Almirante Brown, and Hector Etchebehere is a Gunnery Officer on the same vessel.

Ernest J. Parkin has resigned as Assistant Professor of Civil Engineering at Ohio State University and accepted a position as Mathematician in the Leveling Section, Division of Geodesy, U. S. Coast and Geodetic Survey in Washington, D. C.

Asrar A. Qureshy has completed two years of graduate study at the University of Iowa, and returned to Pakistan where he has been appointed design engineer in the Irrigation Branch of the West Punjab Provinces.

Thorndike Saville, Dean of the College of Engineering, New York University, has been elected President of the American Society for Engineering Education.

Gersham K. Greening, meteorologist of the U. S. Weather Bureau in Salt Lake City, died July 31, 1948 at the age of 62. He was born at Cornland, Illinois, and as a young man, entered upon a career as a meteorologist, making a study of floods and hailstorms in Iowa, and climatic conditions in the days of Lewis and Clarke. He had been with the Weather Bureau since 1921, and a member of AGU since 1934.

Lawrence F. Hanks, hydraulic engineer for the U. S. Geological Survey, died at Kemmerer, Wyoming on June 20, 1949. He was born at Monte Vista, Colorado in 1907, and received his baccalaureate degree from Colorado Agricultural and Mechanical College in 1929. In 1930, he entered the services of the Geological Survey on water resources investigations.

Martin Knudsen, professor at the University of Copenhagen, died May 27, 1949, at the age of 78. Long an investigator in many phases of physical oceanography, he probably will be best remembered for his method of determining the chlorinity, salinity, and density of sea water. He devised the pipette and burette bearing his name; compiled the Hydrographical Tables, first published in 1901; and until his death supervised the preparation of "Copenhagen Normal Water," which is recognized as the international standard of reference for sea water chlorinity.

Harry Leypoldt, civil engineer with the Harbor Department of the City of Los Angeles died February 6, 1949 at the age of 60. He was born in Philadephia and secured his baccalaureate degree from the University of Pennsylvania in 1911. He entered service with the U. S. Coast and Geodetic Survey in 1912 continuing until 1919. Since 1923 he had been with the Los Angeles Harbor Department, making special studies of variations in tide datum and their relationship to Earth movements.

Arthur M. Morgan, ground-water consultant of Fargo, North Dakota, died February 5, 1949 at the age of forty. He was born in Sheridan, Wyoming and received his baccalaureate degree from the University of Wyoming in 1931. He received a master's degree in 1932, and a doctorate in 1941 from Columbia University. His early professional work was with the Geological Survey of Wyoming. In 1935, he entered the service of the U. S. Geological Survey which continued until 1947, at which time he established himself as a consultant on ground-water problems.

Edwin L. Moseley, Professor Emeritus of Biology and Curator of the University Museum, Bowling Green State University, died June 6, 1948 at the age of 83. He was born at Union City, Michigan and received his master's degree from the University of Michigan in 1885. He was awarded an honorary doctorate by Bowling Green State University in 1943 which he served as Head of the Department of Biology from 1914 until his retirement. The early part of his professional career was spent in teaching in high schools in Michigan and Ohio. His broad interests in biology brought him into touch with various facets of the geophysical field, especially in the changes in the level of Lake Erie, and cyclic tendencies in precipitation.

William J. Rooney, physicist with the Department of Terrestrial Magnetism, Carnegie Institution of Washington died August 31, 1949, following an automobile accident in Utah. He was born in Waltham, Massachusetts April 20, 1890, received a baccalaureate degree (BA) from Boston College in 1912, and another (BS) from Massachusetts Institute of Technology in 1915. The first years of his professional career were with the E. I. du Pont de Nemours and Company and the National Bureau of Standards. He entered the service of the Carnegie Institution in 1924. His outstanding work was in the fields of ballistics, Earth currents, and electrical resistivity of the Earth.

Twenty-Fifth Regional Meeting, Davis, California, February 3 to 4, 1950--The Sections of Meteorology and Hydrology will hold the Twenty-Fifth Regional Meeting of AGU at Davis, California, February 3 to 4, 1950. F. J. Veihmeyer, Division of Irrigation, University of California, Davis, California has been designated as Chairman of the Union Committee arranging the meeting. J. C. Marr, 520 C Street, Davis, California is Chairman of the Committee arranging the program in Hydrology. R. Corday Counts, Jr., E. M. Vernon, and E. H. Fletcher of the Forecast Center, U. S. Weather Bureau, San Bruno, California are the Committee arranging the program for Meteorology. Correspondence relative to the meeting should be addressed to one of these.

Thirty-First Annual Meeting, Washington, D. C., May 1 to 3 (or 4), 1950--Pursuant to the earlier preliminary announcement of the Thirty-First Annual Meeting of the American Geophysical Union on May 1 to 3 (or 4), 1950, Monday to Wednesday (or Thursday), arrangements are progressing to provide sessions for all Sections, a general session of the Union, and several joint sessions of two or more Sections. Place this meeting on your agenda and make plans to come.

This announcement is also an invitation for members and others to communicate plans for preparation and presentation of papers. Titles of papers with three copies of the abstract should be sent in at the earliest possible date, and not later than February 20, 1950, advising of the time required (most papers are allowed from ten to 20 minutes) and projection equipment needed. Send abstracts to the office of AGU at 1530 P Street, N. W., Washington, D. C., or to the Secretary of the appropriate section, as follows:

Geodesy	Frank L. Culley	U. S. Coast and Geodetic Survey, Washington 25, D. C.
Seismology	Florence Robertson	4349 Forest Park Blvd., St. Louis 8, Missouri
Meteorology	Woodrow C. Jacobs	4302 Kentbury Drive, Bethesda 14, Maryland
Terrestrial Magnetism and Electricity	David G. Knapp	3827 W. Street, S. E., Washington 20, D. C.
Oceanography	Richard H. Fleming	Division of Oceanography, Hydrographic Office, Navy Dept., Washington 25, D. C.
Volcanology	Francis G. Wells	U. S. Geological Survey, Washington 25, D. C.
Hydrology	Ray K. Linsley, Jr. or	5517 Glenwood Road, Bethesda 14, Maryland
	Ralph N. Wilson (Program Chairman)	3900 Hamilton St., Apt. E-101, Hyattsville, Maryland
Tectonophysics	Wilbur S. Burbank	3346 Runnymede Place, N. W., Washington, D. C.

Complete manuscripts of papers should be forwarded in triplicate by March 31, 1950, in order that news releases may be prepared. If a paper is written in collaboration, please indicate by whom it will be presented. Arrangements can be made for presentation of papers by authors who are unable to attend the meetings. Advise also whether the paper is being submitted for the program only or whether it is also desired that it be given consideration for publication. (Papers for publication only are also welcome for consideration for the *Transactions*.)

The Chairman of the Committee on Meetings (J. P. Marble, U. S. National Museum, Washington 25, D. C.) invites suggestions and comments that will be helpful in planning the proposed meeting. Especially invited are comments relating to papers and symposia bearing on more than one section.

Make hotel or room reservations directly with the hotel of your choice as soon as possible. Failing on the first attempt, bear in mind that advance bookings not taken up are cancelled two weeks in advance, so a follow-up request in mid-April may bring the desired response, Our meeting is scheduled for the same week as the U. S. Chamber of Commerce in Washington. During the last two years we have met at the same time as the D.A.R. Convention in Washington which is a worse situation, but at no time yet, to our knowledge, has it not been possible to find quarters. Even though no advance reservation has been made, it has been possible to arrange for quarters after arrival in Washington through the Greater National Capital Committee (204 Evening Star Building, Washington 4, D. C., telephone STerling 3535) but they may find it necessary to direct you to a tourist home. Also we are block-booking rooms at certain hotels that will be listed in a Special Announcement in December.

John Putnam Marble, Chairman,
Committee on Meetings

CORPORATION MEMBERS

GEOPHYSICAL RESEARCH CORPORATION

Geophysical Prospecting
Application of Geophysical Methods in the Petroleum Industry

2607 North Boston Place
Tulsa 6, Oklahoma

KEUFFEL AND ESSER COMPANY

Drafting, Reproduction, and Surveying Equipment and Materials
Slide Rules Measuring Tapes

300 Adams Street
Hoboken, New Jersey

RANNEY METHOD WATER SUPPLIES, INC.

Ground Water Exploration and Development

841 Alton Avenue
Columbus 3, Ohio

RUSKA INSTRUMENT CORPORATION

Developers, Designers, and Manufacturers of Instruments for Field and Observatory Use
Magnetic, Geodetic, Seismic, and Meteorological Work

4607 Montrose, Boulevard
Houston 6, Texas